

III.

RESULTS

AND

DISCUSSION

III RESULTS AND DISCUSSION

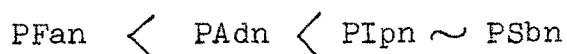
A. Preliminary Studies

III.1 Addition polymerization of monomers

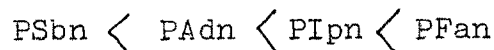
Before proceeding with the studies on copolymers with ionic character, it was considered worthwhile to carry out homopolymerization of some of the monomers used e.g. maleic anhydride, fumaric acid, vinyl acetate, etc. (82). It has been reported that homopolymerization of maleic anhydride yielded poly (maleic anhydride) having M_n ranging between 625 and 710 (83). It is observed in the present studies that low yield of poly (maleic anhydride) is obtained by the homopolymerization of maleic anhydride from benzene solution with benzoyl peroxide as initiator. The product melts at 125-27°C and is soluble in alcohol, acetone, DMF etc. Low yields are also obtained on the homopolymerization of vinyl acetate and fumaric acid (83). The products are soluble in alcohol, acetone, DMF, etc. No product was obtained when toluene was used as a solvent. Similarly, poly(maleic anhydride) with lower yield and melting point of 155-60°C was reported to be obtained when polymerization was carried out in acetic anhydride (84,85). Poly (fumaric acid) shows a melting range of 210-70°C and is more crystalline and melts at a higher temperature than poly (maleic anhydride).

III.2 Condensation Polymerization

Polyanhydrides of various dibasic acids are reported in literature. Thus poly(adipic anhydride) (86), poly(suberic anhydride) (87), poly(sebacic anhydride) (88), poly(azelaic anhydride) (89), and their higher homologues (90-92), poly(isophthalic anhydride) and poly(terephthalic anhydride) (93,94) were prepared and used in epoxy compositions, paints, adhesives, etc (87, 95-102). Polyanhydrides are prepared (Table II.4) by the condensation polymerization of dibasic and polybasic acids, such as adipic acid, fumaric acid, sebacic acid, isophthalic acid and EDTA using acetic anhydride as a condensing agent. It is observed that the yield increases in order



Low yields are obtained mainly due to side reactions and reverse reactions. Thus adipic acid can get transformed into cyclopentanone and fumaric acid into maleic anhydride (103). The cyclic monomer can be obtained by distilling poly(adipic anhydride) in vacuum (104). All the products are soluble in DMF. PFan, PAdn and PSbn get hydrolyzed by water. The melting points of these products are increasing in order



The determination of free acid content (AVI) and acid content after hydrolysis (AVS) of PSbn indicates that the degree of polymerization of PSbn is twenty. (Acetyl end groups are not assumed).

The polycondensation of tetrabasic acid EDTA was also carried out. The product is insoluble in all solvents except DMF and melts at 100°C. It is affected by acids and alkalies. The determination of AVI and AVS indicates that (i) in the polydianhydride, one of the two anhydride groups of the dianhydride unit is quite stable, (ii) the second anhydride group is unstable and (iii) 33 % of the second anhydride group is in free-acid form.

The polymerization of p-hydroxybenzoic acid and p-amino benzoic acid in presence of acetic anhydride yields oligomers with acetyl end groups and degree of polymerization of 5 and 4 respectively as evidenced by AVI and AVS studies.

Attempt was made to modify the properties of PFan to increase its stability to hydrolysis by copolymerization of fumaric and terephthalic acids. The product is stable to hydrolysis by water and exhibits melting behaviour. Co-condensation seems to be better than mixing or blending of polymers in this case.

Reduced viscosity of solutions of PSbn, PAb and POB in DMF is calculated and plotted against % concentration

in fig.III.1. Intrinsic viscosity of PSbn, PAb and POB has been obtained by extrapolation as 0.031, 0.009 and 0.005 dL/g respectively. Use of the molecular wt (M) obtained from AVS studies and of the relation

$$[\eta] = K \sqrt{M}$$

has been made to calculate K. The values of K are 5.1×10^{-4} , 3.9×10^{-4} and 2.0×10^{-4} respectively.

III.3 Addition Copolymerization

The copolymers from the following monomer pairs have been prepared: (a) styrene + vinyl acetate, (b) styrene+ maleic anhydride, (c) styrene+fumaric acid, (d) styrene + acrylic acid, (e) styrene + methyl methacrylate, (f) divinyl benzene + acrylic acid and (g) divinyl benzene + fumaric acid. Literature study has shown that (1) styrene-maleic anhydride copolymers have been prepared and studied by Tso (62), Cho (63), Seymour and Garner (105), Miskarli and coworkers (106), Chow (107), Kurakov and coworkers (108), Cutter and Nunn (109), Evani and Raymonds (110), Chiao and Ray Chaudhari (111), Barton and Vaskova (112), Raetzsch and Nguyen (113) Kudrna and coworkers (114), Vainer and coworkers (115), Miller (116), Maxim and coworkers (117), Kurbanov and coworkers (118), etc, (2) styrene- acrylic acid copolymers by Price (56) Lee (119), Nyquist, Platt and Priddy (52), Panov (64,120), Priddy (121), Mirkamilov and coworkers (69), Kaemmerer and

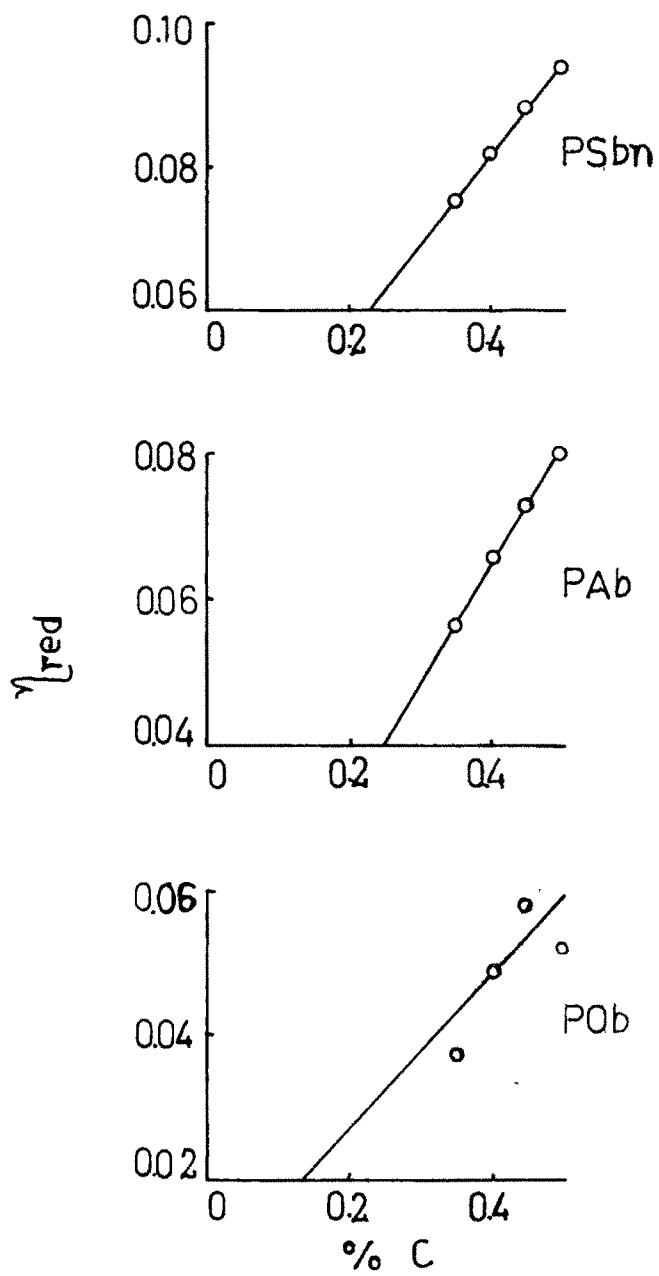


fig. III 1 Plot of η_{red} vs % C
for PSbn, PAb & POB

Petzny (122), Toppet and coworkers (54), Smets and van Gorp (123), etc., (3) styrene-fumaric acid copolymers by Lordi and Triplett (58); Takahara (124), etc., (4) styrene-methyl methacrylate copolymers by Zubov and coworkers (125), Balaraman (126), Kuo and Chen (127), Hirai, Tenabe and Koinuma (128), Bonta and coworkers (129, 130), Kucharikova (131), Brown and White (132), etc.

Copolymerization of styrene with vinyl acetate was carried out from benzene solution. The product was found to be soluble in acetone, benzene, carbon tetrachloride, DMF, etc.

Copolymerization of styrene with maleic anhydride was carried out in acetone solution and in absence of solvent. The products are insoluble in water, alcohol, carbon tetrachloride, etc, partly soluble in benzene and soluble in acetone, DMF, etc.

Copolymerization of styrene with fumaric acid was carried out in ethanol solution. The product melts at 245°C and is insoluble in alcohol, benzene, carbon tetrachloride, etc, soluble in acetone, DMF, hot water, etc.

Copolymerization of styrene with acrylic acid was carried out in THF solution and in absence of solvent. The products are insoluble in water, partly soluble in benzene, carbon

tetrachloride, etc. and soluble in alcohol, acetone, DMF, etc. The analysis of the two products indicates the ratio of styrene to acrylic acid as 1:1 in the copolymer. Reduced viscosity of these products is plotted vs % concentration in fig.III.2. Intrinsic viscosity (dL/g) has been obtained by extrapolation as 0.55 for PSA (B), 0.17 for PSA(S)T and 0.16 for PSA(S)T'.

Copolymerization of styrene with methyl methacrylate was carried out in ethanol solution. The products are insoluble in water, alcohol, acetone and soluble in benzene, carbon tetrachloride, DMF, etc. The analysis of the products indicates the ratio of styrene to methyl methacrylate in the product as 1:1. Literature survey showed that styrene-methyl methacrylate was hydrolysed by acid by refluxing for one week (132). AVS-h values of the products indicate 10 % hydrolysis of the copolymers on heating with sodium hydroxide on water-bath for 4 hr.

Sets of copolymers were prepared by copolymerizing divinyl benzene with acrylic acid or fumaric acid using different mole ratios of the monomers. The products were not melting upto 280°C and were insoluble in all solvents used. The increased insolubility can be attributed to the crosslinking of the chains.

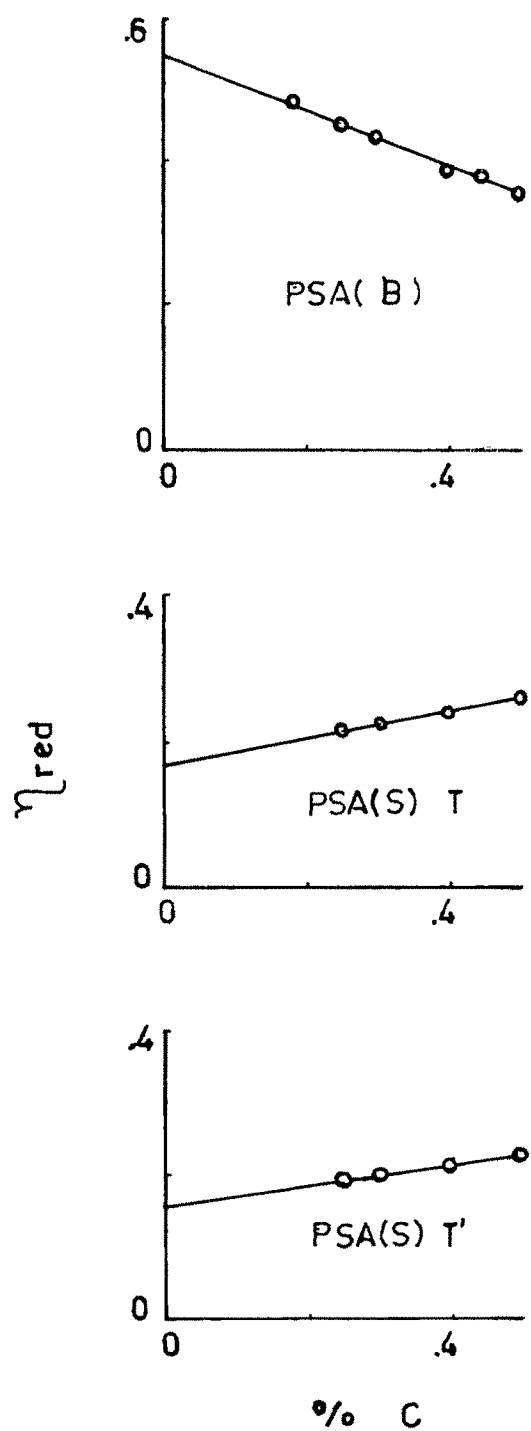


fig.III. 2 Plot of η_{red} vs % C

The copolymers of styrene with maleic anhydride, fumaric acid and acrylic acid were prepared by varying the mole ratios of the monomer pairs and the sets of products obtained were studied in details.

B. Detailed Studies

III.4 Copolymers

(Solution polymerization)

4.(a) Styrene-maleic anhydride Copolymers:

A set of nine copolymers of styrene with maleic anhydride with varying mole proportions was prepared at 60°C. The yield increased from 40 % to 89 % as the mole % of maleic anhydride in the feed increased from 5 % to 66 %. The products are pale yellow in colour and they are insoluble in alcohol, carbon tetrachloride, etc. but soluble in acetone DMF, etc. The mole fractions of maleic anhydride in the products, calculated on the basis of the formulae suggested from analytical results, vary from 0.3 to 0.83. If the mole fraction of maleic anhydride in the product is plotted versus the mole fraction of maleic anhydride in the feed (Fig.III.3), a straight line is obtained. If the literature data (133) were introduced into the plot, a part of the line can be better represented by a parabolic curve. The cross point of the parabola with the straight

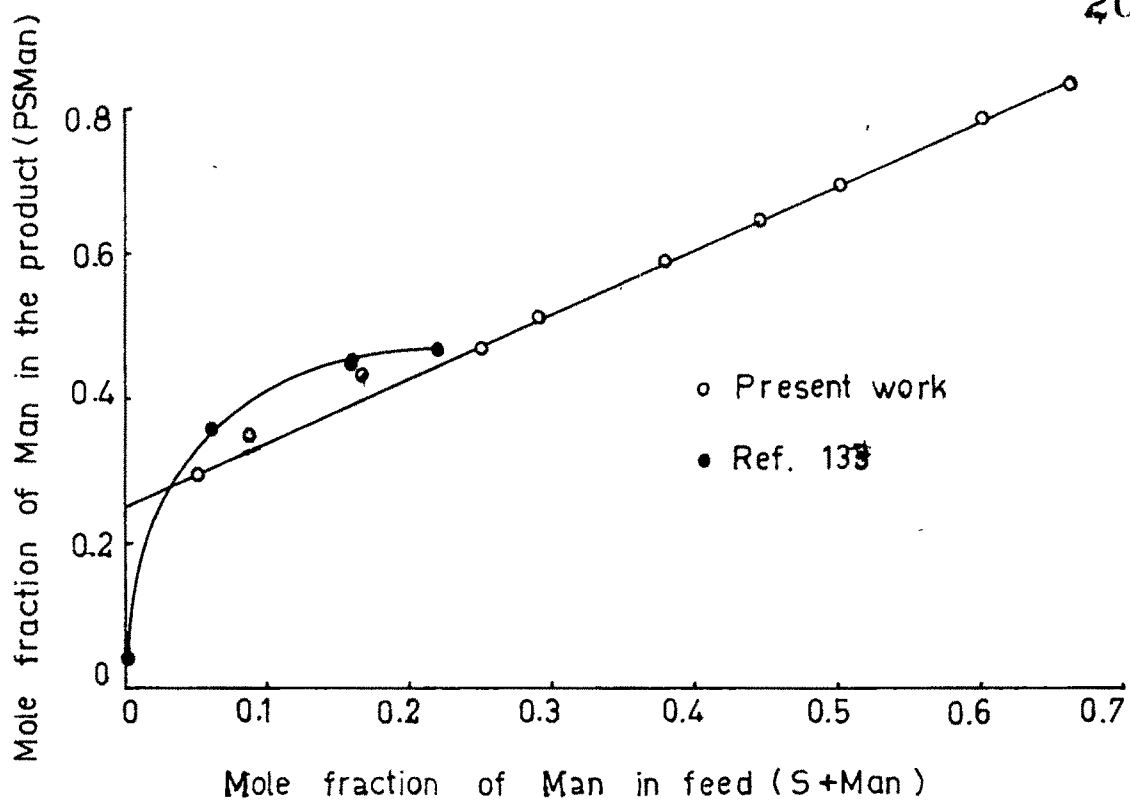


fig. III.3

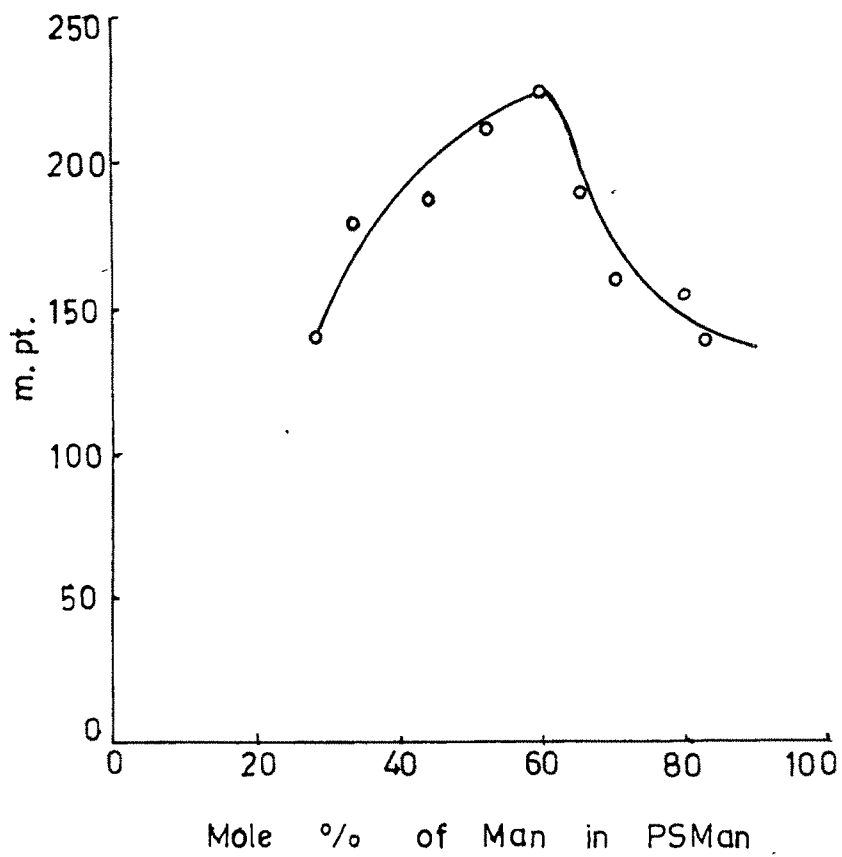


fig. III.4

line is at the mole fraction of 0.25 of maleic anhydride in the feed and of 0.48 of maleic anhydride in the product.

It has been reported in literature that (i) the copolymer is alternating if prepared at 80°C and random if prepared at 130°C (105) (ii) the copolymer is alternating if prepared at 80°C, bulky if prepared at 110°C and random if prepared at 130°C (134). The products prepared for the present studies are considered to be alternating.

The products show a variation in the melting point along the series. If the melting point is plotted versus mole % of maleic anhydride in the product (Fig.III.4), a curve is obtained with a maximum at about 60 mole % of maleic anhydride in the product.

Studies on IR spectra of such copolymers have been reported (62,63,118) and absorption bands at 1850, 1780, 1720-10 and 700 cm^{-1} have been identified. The IR spectra of PSMAn-1,5 and 9 are presented in Fig.II.2. It is observed that the band at 700 cm^{-1} decreases in intensity and that at 1720 cm^{-1} increases in intensity with the increase in mole fraction of maleic anhydride in the product.

It is considered that all the anhydride groups are not available and hence 70% to 80% of the anhydride is identified as acid in AVS studies. Neutralization of the acid is

carried out for the preparation of salts on the basis of available acid groups under comparable conditions.

Intrinsic viscosity can be obtained by the use of various equations. Thus, use can be made of (i) Huggins equation

$$\eta_{\text{red}} = [\eta] + kC = [\eta] (1 + k' C [\eta])$$

(2) Martin equation

$$\text{Log } \eta_{\text{rel}} = [\eta'] (1 + k'' C [\eta'])$$

(3) Kreaemer equation

$$\frac{\text{Log } \eta_{\text{rel}}}{C} = [\eta''] (1 + k''' C [\eta''])$$

η_{red} vs % C is plotted in fig.III.5

Log η_{rel} vs % C is plotted in fig.III.6

$\frac{\text{Log } \eta_{\text{rel}}}{C}$ vs % C is plotted in fig.III.7

It is observed that $[\eta]$ (also $[\eta']$ and $[\eta'']$) varies with mole fraction of maleic anhydride in the product (fig.III.8). The value of $[\eta]$, $[\eta']$ and $[\eta'']$ lie in the range of 0.34 to 0.97, 0.016 to 0.027 and 0.13 to 0.40 respectively. Thus

$$[\eta'] < [\eta''] < [\eta]$$

Intrinsic viscosity of PSMa has been reported in literature as 0.3 dL/g (110).

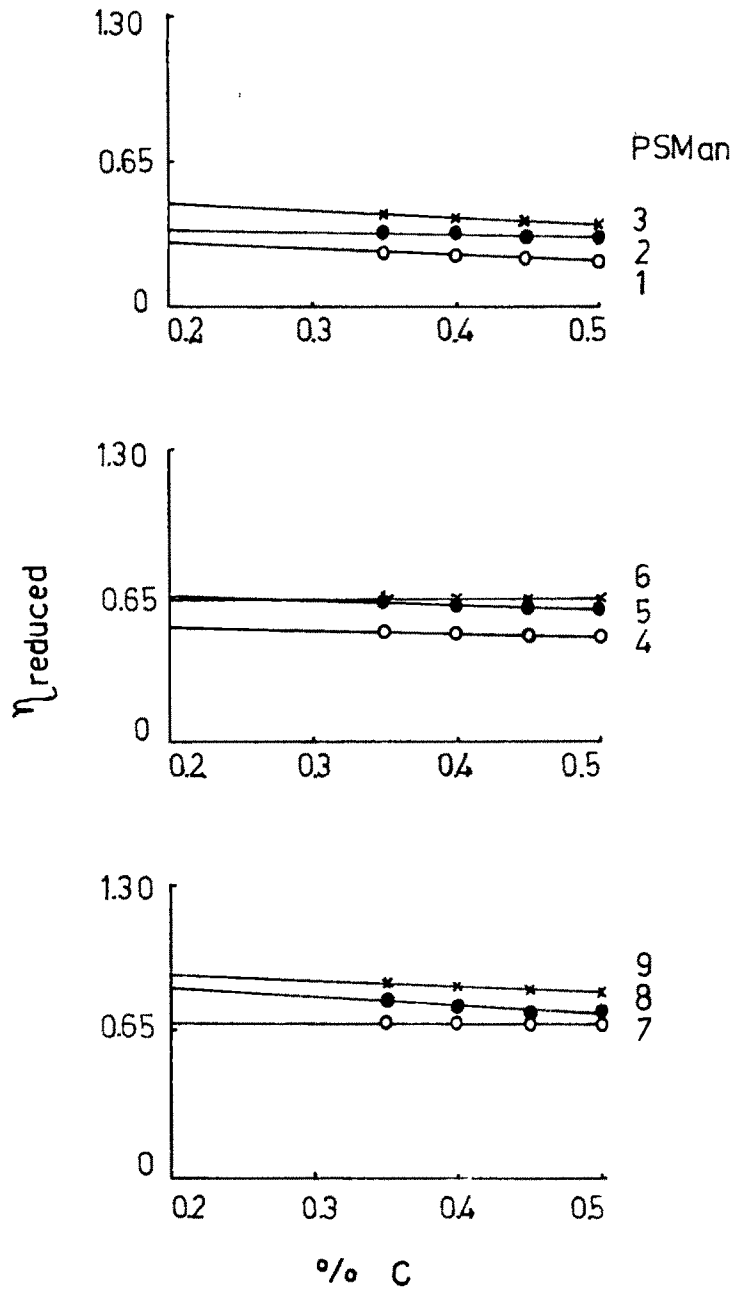


fig. III. 5 Plots of η_{reduced} vs % C
for the set of PSMAN (H form)

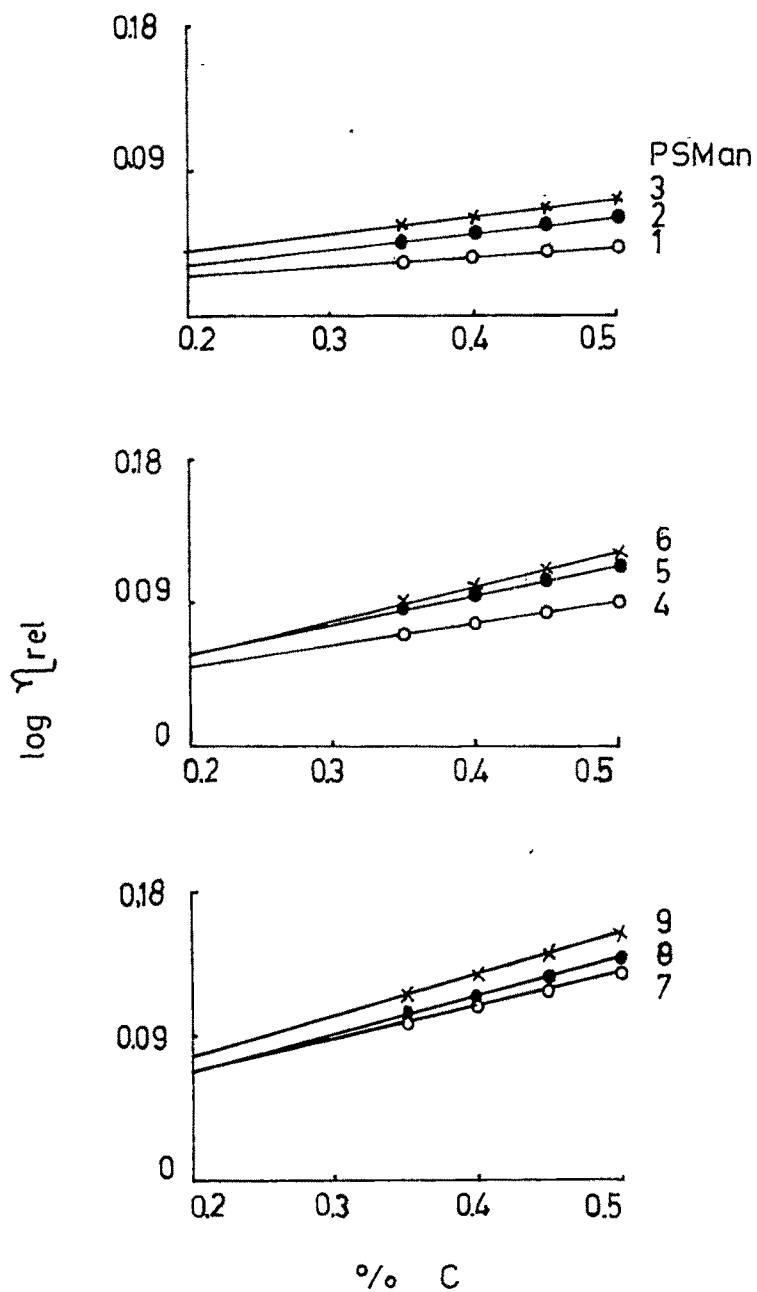


fig. III.6 Plot of $\log \eta_{rel}$ vs $\% C$
for the set of PSMAN (H form)

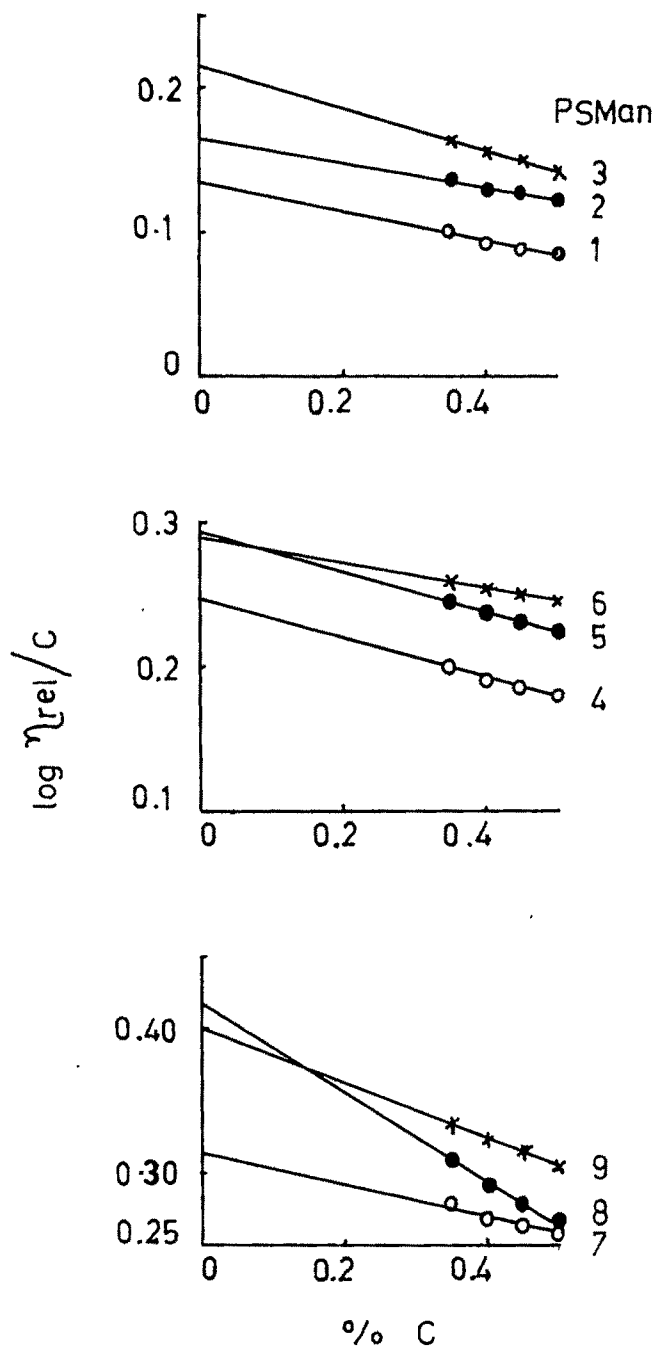


fig. III.7 Plot of $\log \eta_{rel}/C$ vs $\% C$
for the set of PSMAN (H form)

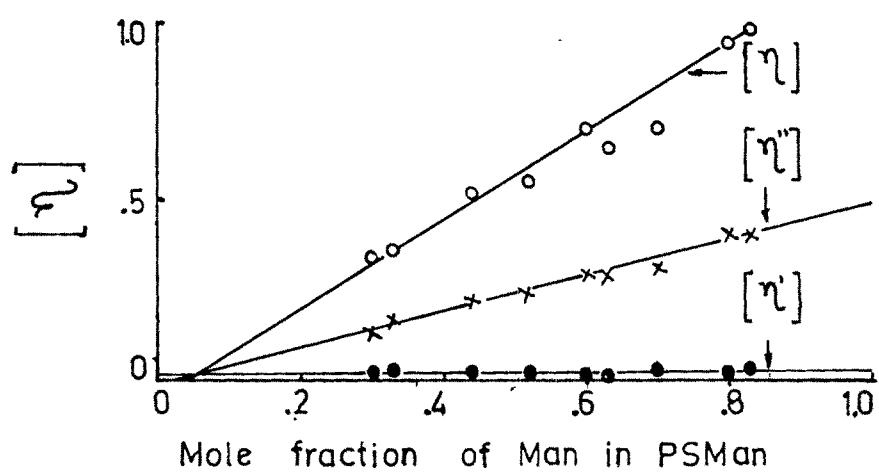


fig.III.8

The slopes of the lines are negative for the plots in figs.III.5 and 7, while positive in fig.III.6. From the values of slopes and intercepts the values of the constants k' , k'' and k''' are evaluated and are presented in table III.1. It is observed that the values of k' and k''' are negative and vary over a small range, while those of k'' are positive and vary over a very wide range.

4(b) Styrene-fumaric acid copolymers

Two sets (one of eight and the other of nine) copolymers of styrene with fumaric acid with varying mole proportions were prepared at 79°C. The yield increased from 51 % to 98 % as the mole fraction of fumaric acid increased. The copolymers are insoluble in benzene, carbon tetrachloride etc and soluble in alcohol, acetone, DMF etc. The mole fractions of fumaric acid in the copolymers, calculated on the basis of the formulae suggested from AVS data analytical results vary from 0.13 to 0.78. If the mole fraction of fumaric acid in PSFa is plotted against the mole fraction of fumaric acid in the feed a curve is obtained (fig.III.9).

IR spectra (fig.II.3) of PSFa-1,5 and 9 have an absorption band at about 1700 cm^{-1} increasing in intensity as the mole fraction of Fa in PSFa increases.

Table III.1

No	Product	constant		
		k'	k''	k'''
1	PSMan-1	-2.34	2.34	-5.42
2	PSMan-2	-1.02	3.82	-3.06
3	PSMan-3	-1.23	2.43	-3.11
4	PSMan-4	-0.56	313.11	-2.05
5	PSMan-5	-0.51	458.74	-1.68
6	PSMan-6	0.00	8.00	-1.08
7	PSMan-7	0.00	274.30	-1.04
8	PSMan-8	-0.50	546.10	-1.83
9	PSMan-9	-0.33	352.50	-1.19

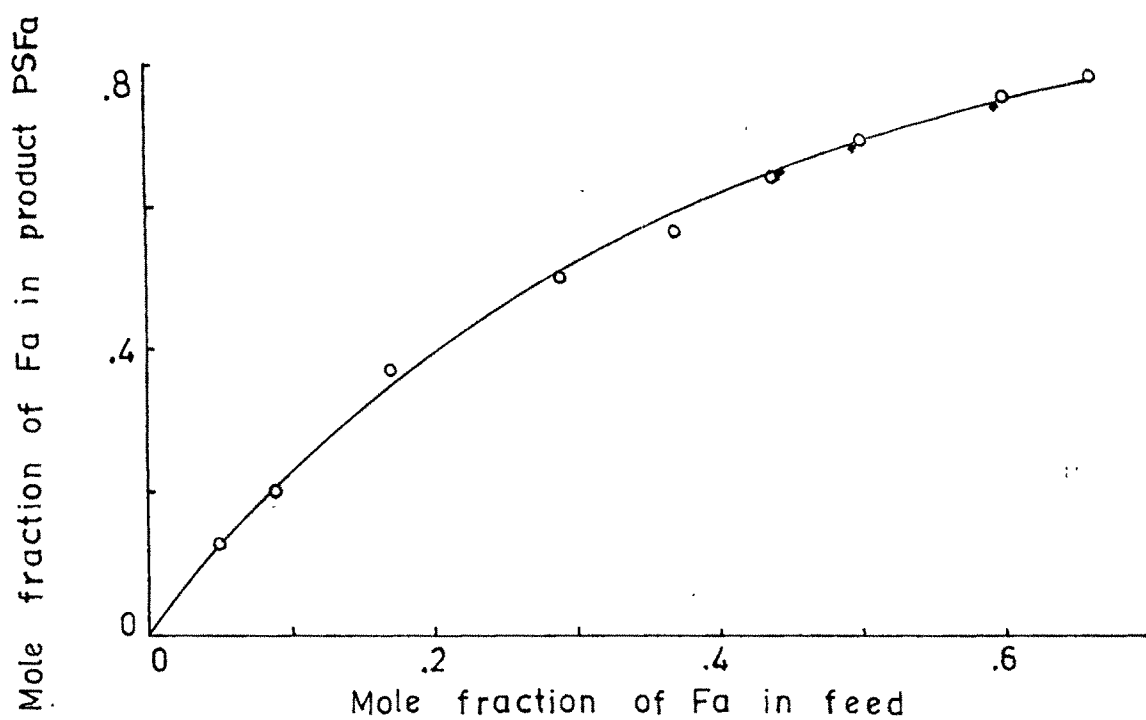


fig.III.9

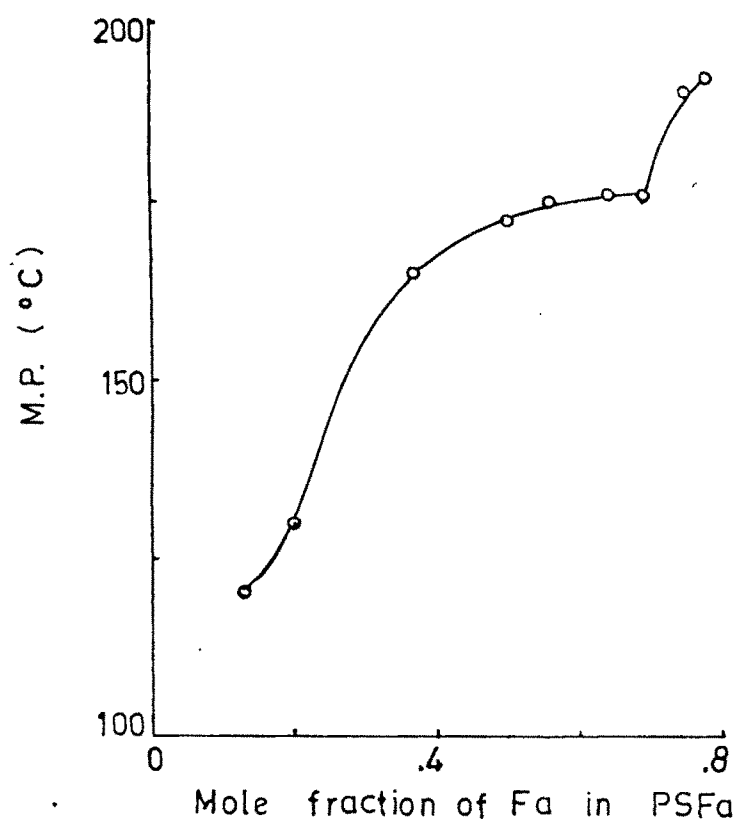


fig.III.10

The products show a variation in melting point along the series. If the melting point is plotted vs mole fraction of fumaric acid in the product a curve is obtained. (Fig.III.10) The melting point has two sudden jumps in the curve corresponding to the values of 0.25 and 0.125 mole fraction of fumaric acid in PSFa.

Intrinsic viscosity has been evaluated by plotting η_{red} vs % C in Fig.III.11, $\text{Log } \eta_{rel}$ vs % C in fig.III.12 and $\text{Log } \frac{\eta_{rel}}{C}$ vs % C in fig. III.13. η_{red} vs % C for less dilute solution is plotted in fig.III.14. It is observed that slopes of the curves gradually become increasingly positive as the mole fraction of fumaric acid in PSFa increases.

η_{red} vs % C in 10 % fumaric acid and in 0.1 N Na_2SO_4 are plotted in figs.III.15 and 16. Addition of fumaric acid lowers $[\eta]$ of PSFa, by possibly reducing the dissociation of PSFa in DMF; while addition of Na_2SO_4 increases $[\eta]$ of PSFa, possibly by imparting ions atmosphere for PSFa.

It is observed that $[\eta]$ (also $[\eta']$ and $[\eta'']$) varies with mole fraction of fumaric acid in general (fig.III.17) The values of $[\eta]$, $[\eta']$ and $[\eta'']$ are increasing in order.

$$[\eta'] < [\eta''] < [\eta]$$

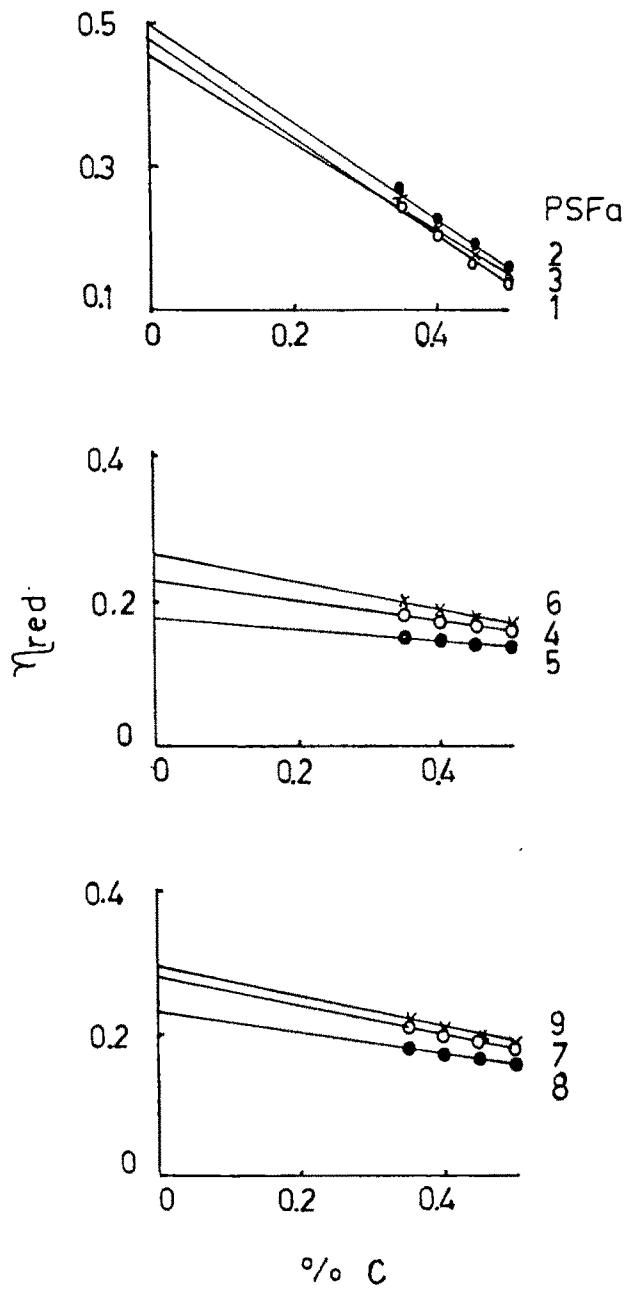


fig. III.11 Plot of η_{red} vs % C
 for the set of PSFa (H form)
 (from table 21-c)

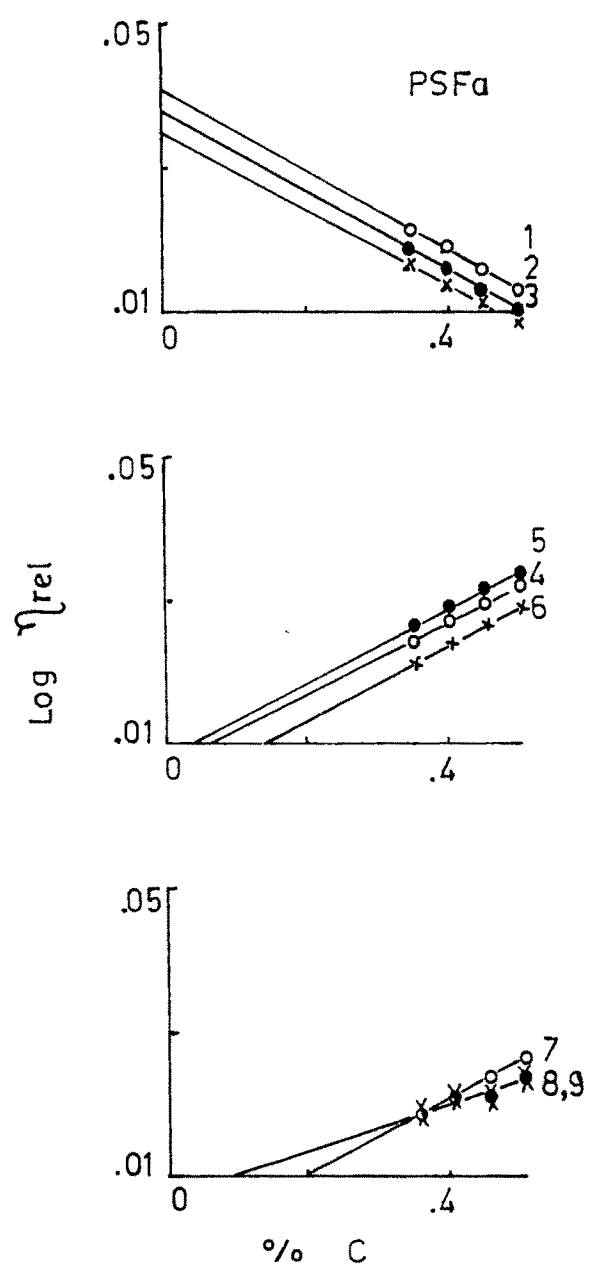


fig.III.12 Plot of $\text{Log } \eta_{\text{rel}}$ vs % C
for PSFa set
(from table 21-c)

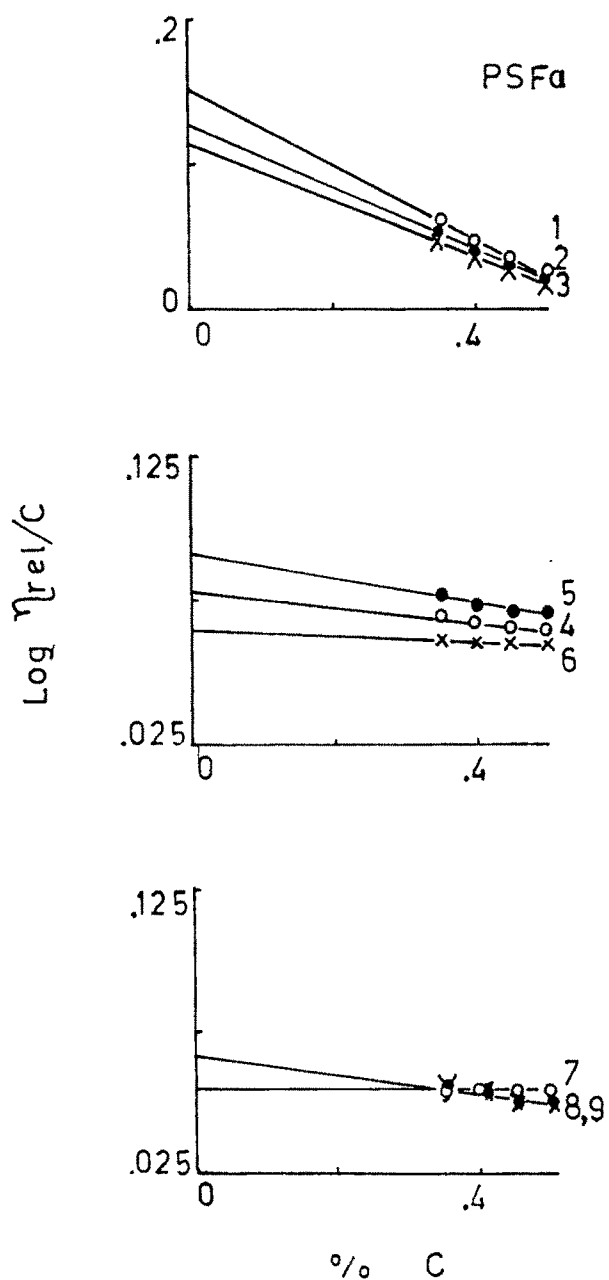


fig.III.13 Plot of $\text{Log } \eta_{rel}/C$ vs $\% C$
for PSFa set
(from table 21-c)

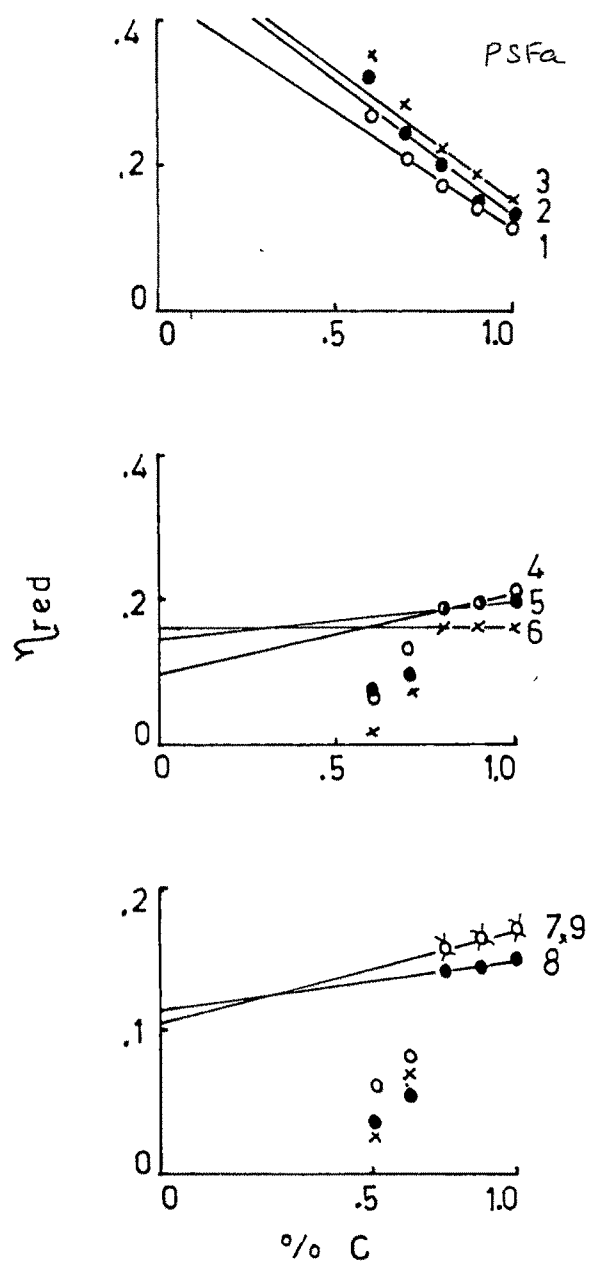


fig.III.14 Plot of η_{red} vs % C
for PSFa (H form) set
(from table 21-b)

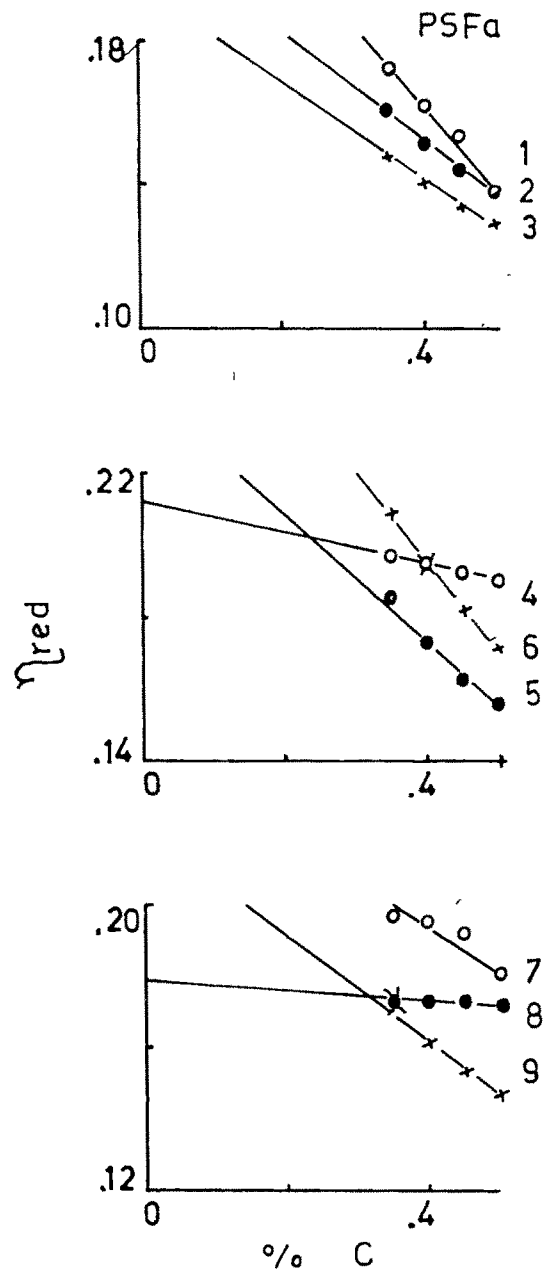


fig. III.15 Plot of η_{red} vs % C
for PSFa (H form)
(from table 21 e)

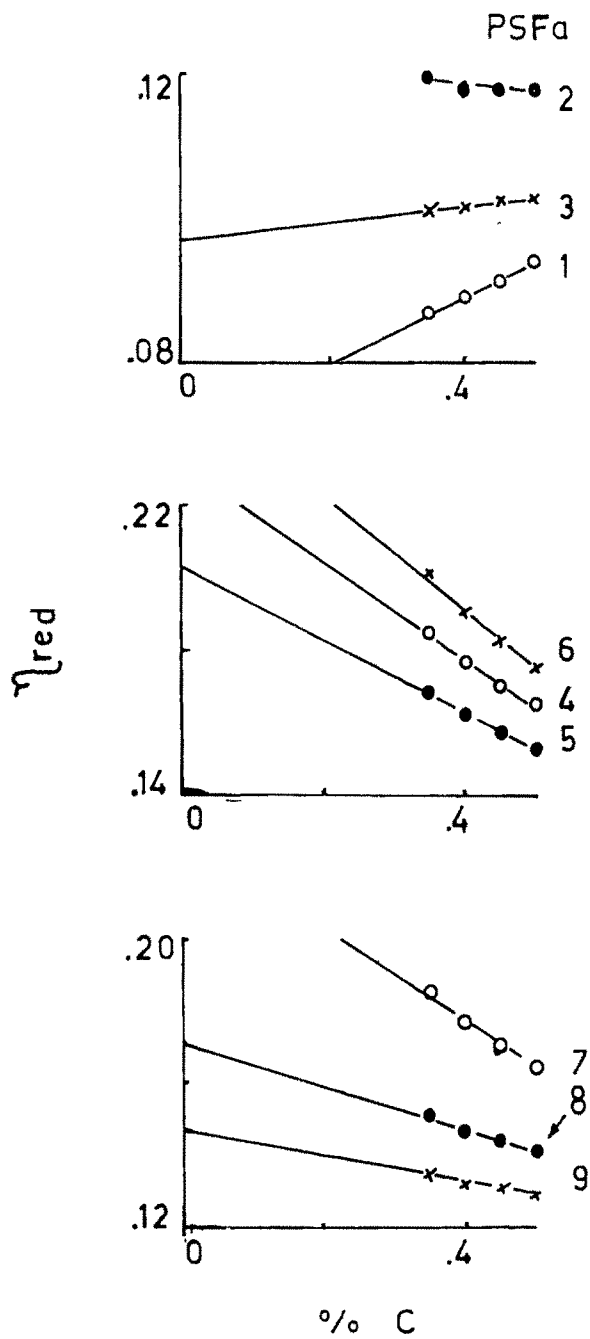


fig III 16 Plot of η_{red} vs % C
for PSFa (H form)
(from table 21-f)

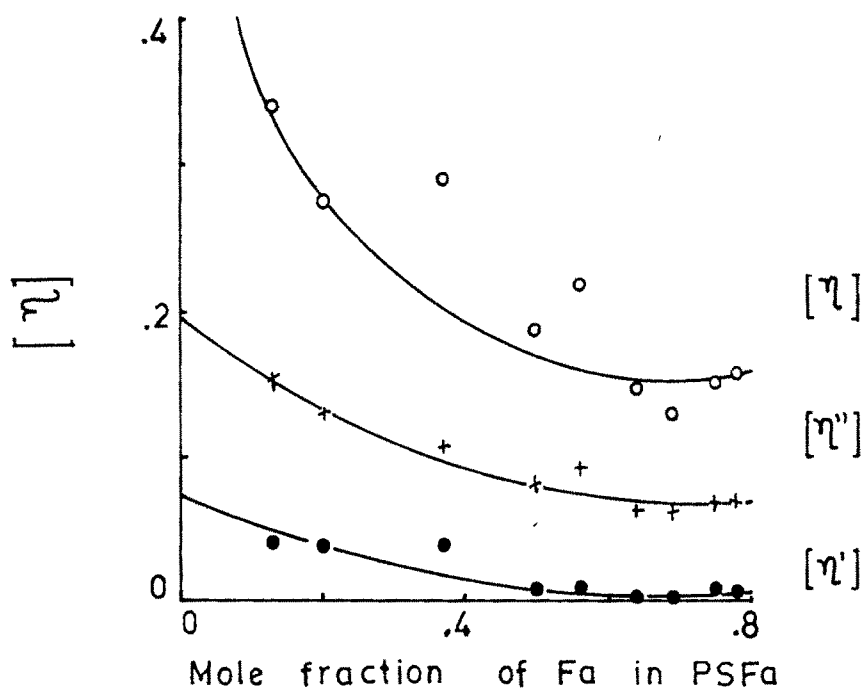


fig. III.17

It is also observed that values of $[\eta]$ in relation to those of $[\eta']$ or $[\eta'']$ are more scattered in the plots.

The slopes of the lines are negative in fig.III.11 and 13, while negative or positive in fig.III.12. From the values of slopes and intercepts, the values of constants k' , k'' and k''' are calculated and are presented in table III.2. It is observed that the values of k' and k''' vary over a small range, while those of k'' vary over a very wide range. It is suggested that Huggins or Kraemer equation is better than Martin's equation for a set of copolymers.

4(c) Styrene-acrylic acid copolymers

A set of nine copolymers of styrene with acrylic acid with varying mole ratios was prepared at 75°C. The yield increased from 69 % to 98 % as the mole % of acrylic acid in the feed increased from 5 % to 66 %. The products are white in colour and soluble in alcohol, acetone, DMF, etc. The mole fractions of acrylic acid in the products as calculated on the basis of the formulae suggested from the analytical results and AVS data vary from 0.09 to 0.66. If the mole fraction of acrylic acid in the product is plotted against the mole fraction of acrylic acid in the feed (fig.III.18), a straight line is obtained in the upper region of the plot, while the lower region can be better

Table III.2

No	Product	constant		
		k'	k''	k'''
1	PSFa-1	-4.94	-33.9	-11.50
2	PSFa-2	-5.87	-38.60	-13.17
3	PSFa-3	-5.95	-44.3	-17.10
4	PSFa-4	-2.04	1182.0	- 4.76
5	PSFa-5	-2.12	717.8	- 5.00
6	PSFa-6	-	1978.7	-
7	PSFa-7	0.00	5585.6	0.00
8	PSFa-8	-3.17	679.6	- 7.60
9	PSFa-9	-	624.8	- 7.90

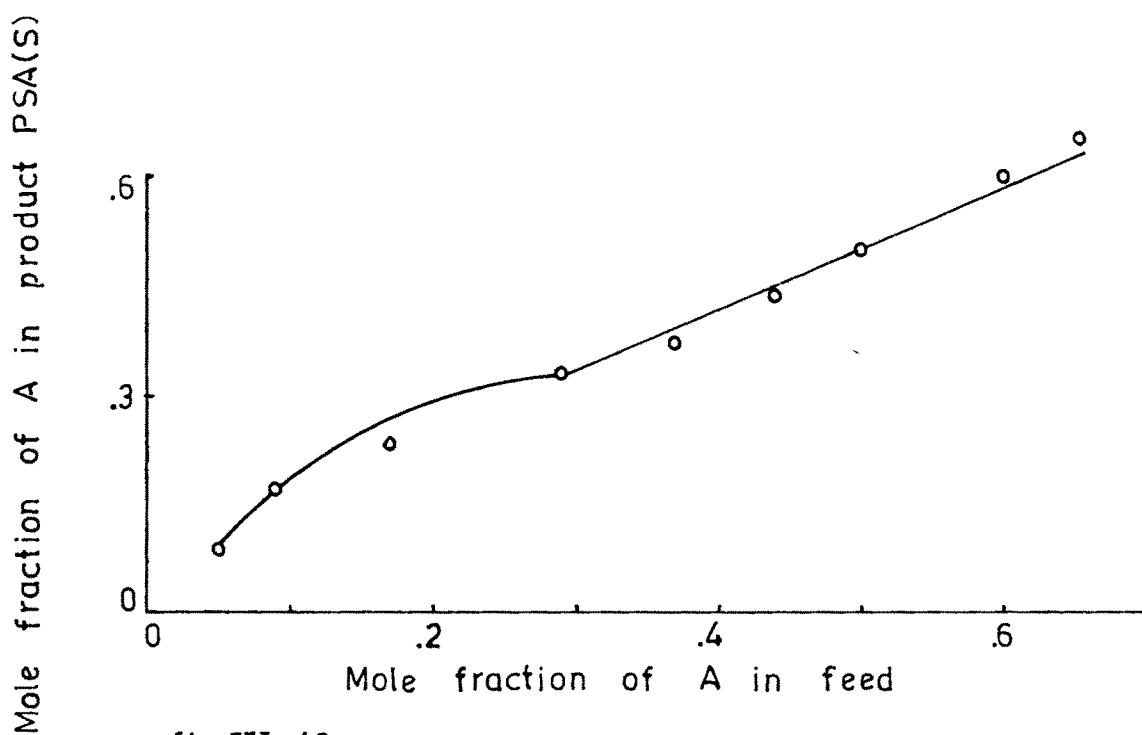


fig.III. 18

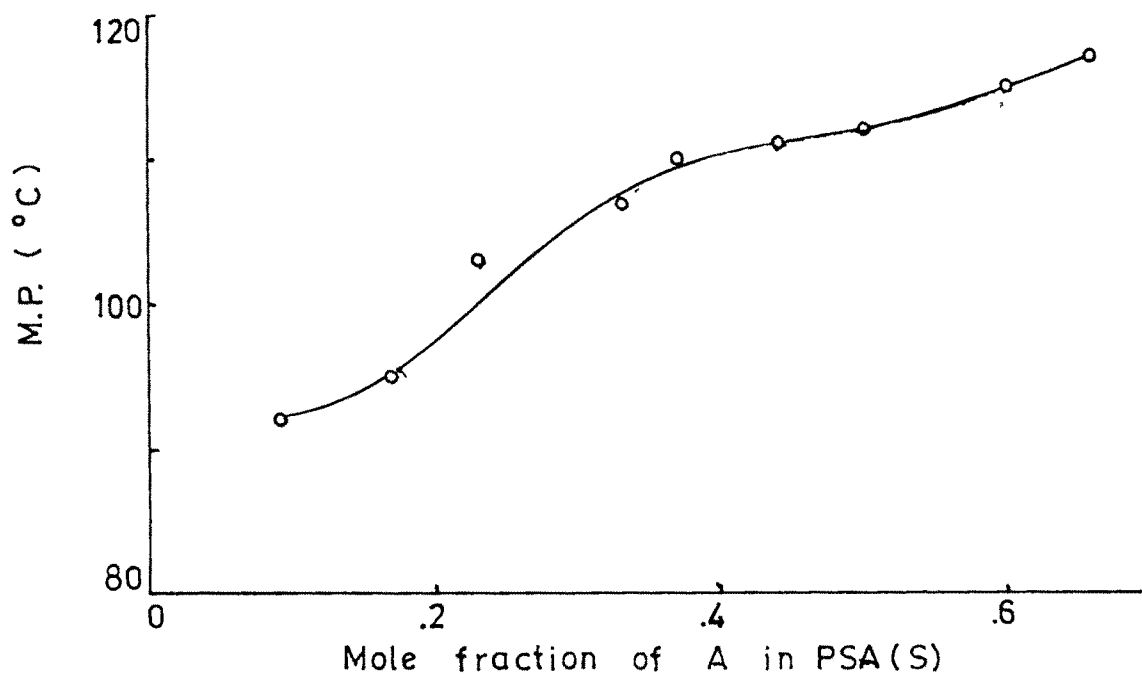


fig. III. 19

represented by a parabolic curve. The crosspoint of the parabola and straight line is at 0.29 mole fraction of acrylic acid in the feed and at 0.34 mole fraction of acrylic acid in PSA(S).

IR spectra of PSA(s)-1, 5 and 9 (Fig.II.4) have an absorption band at about 1700 cm^{-1} increasing in intensity and the absorption band at 695 cm^{-1} decreasing in intensity as the mole fraction of acrylic acid in PSA(s) increases (52, 56).

The products show a variation in melting point along the series. If the melting point is plotted versus mole fraction of acrylic acid in the product (fig.III.19), the values are not increasing linearly.

η_{red} vs % C is plotted in fig.III.20, $\text{Log } \eta_{\text{rel}}$ vs % C is plotted vs % C in fig. III.21, and $\text{Log } \frac{\eta_{\text{rel}}}{c}$ is plotted vs % C in fig. III.22.

The values of $[\eta]$, $[\eta']$ and $[\eta'']$ are increasing in order

$$[\eta'] < [\eta''] < [\eta]$$

$[\eta]$ vs mole fraction of acrylic acid in PSA(s) is plotted in Fig. III.23. The scatter of points with reference to curves for $[\eta]_{,n}^{[\eta]}$ and $[\eta'']$ increases in order.

$$[\eta'] < [\eta''] < [\eta]$$

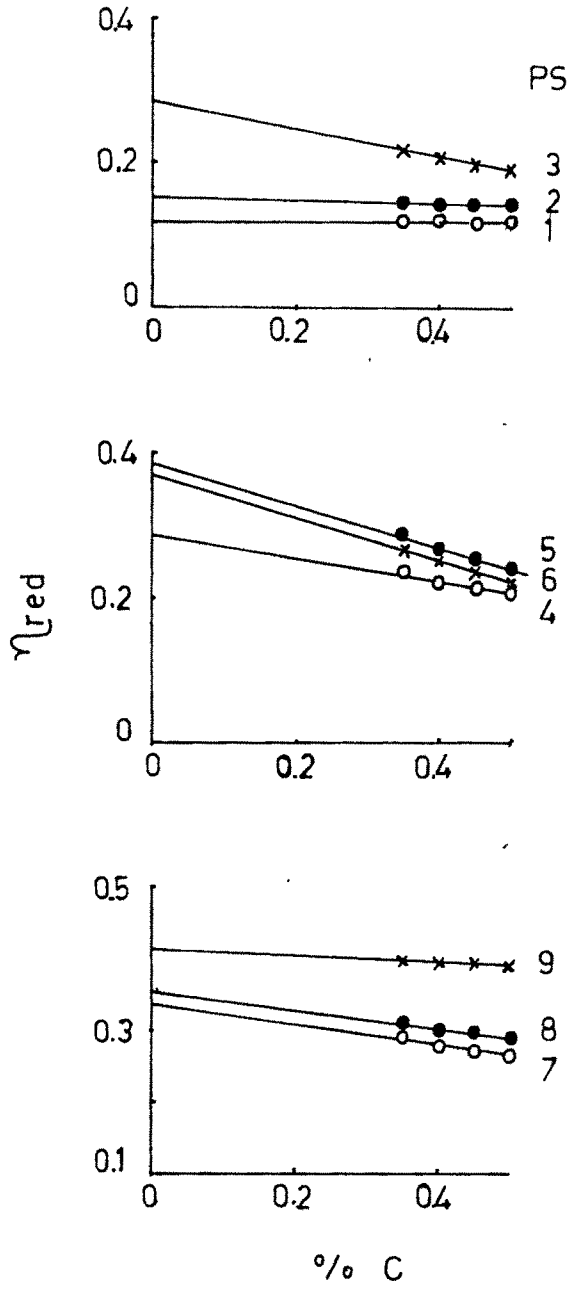


fig. III.20. Plot of η_{red} vs % C for the set of PSA(S) (H form)

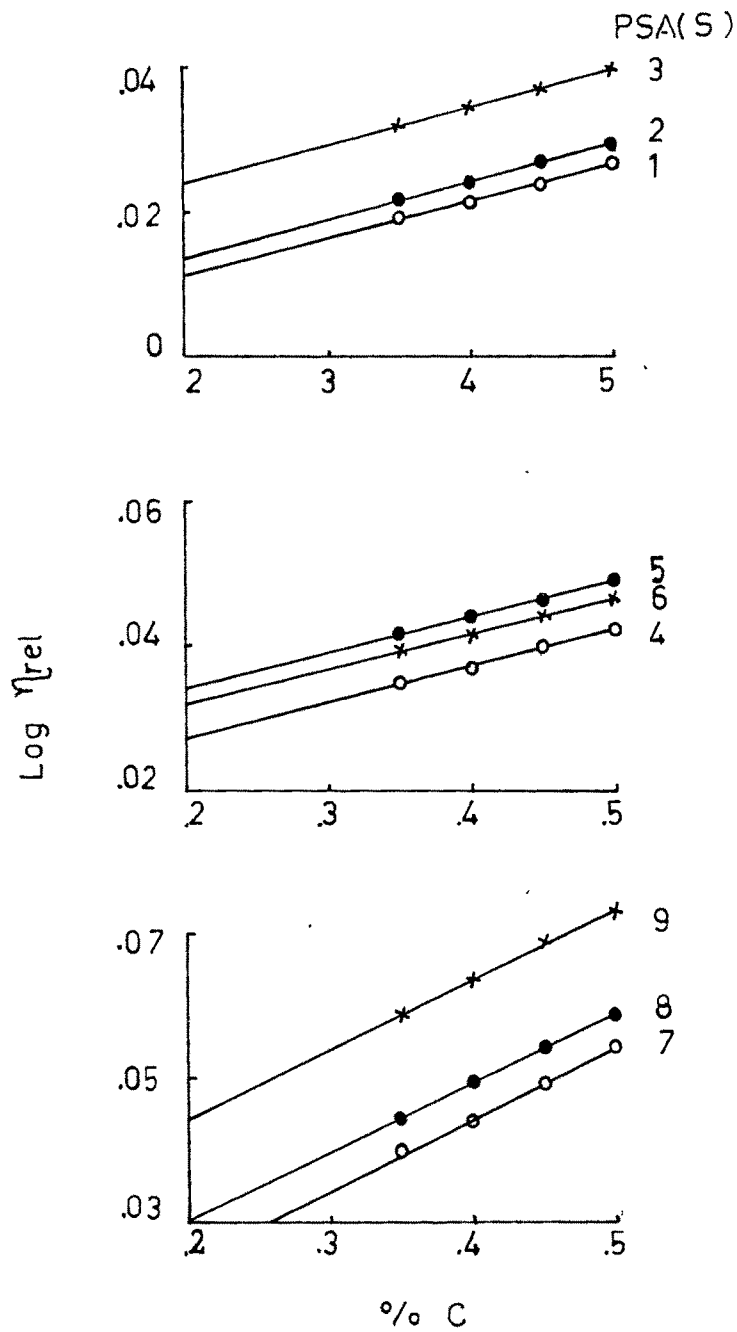


fig. III, 21. Plot of $\text{Log } \eta_{\text{rel}}$ vs $\% \text{ C}$
for the set of PSA(S) (H form)

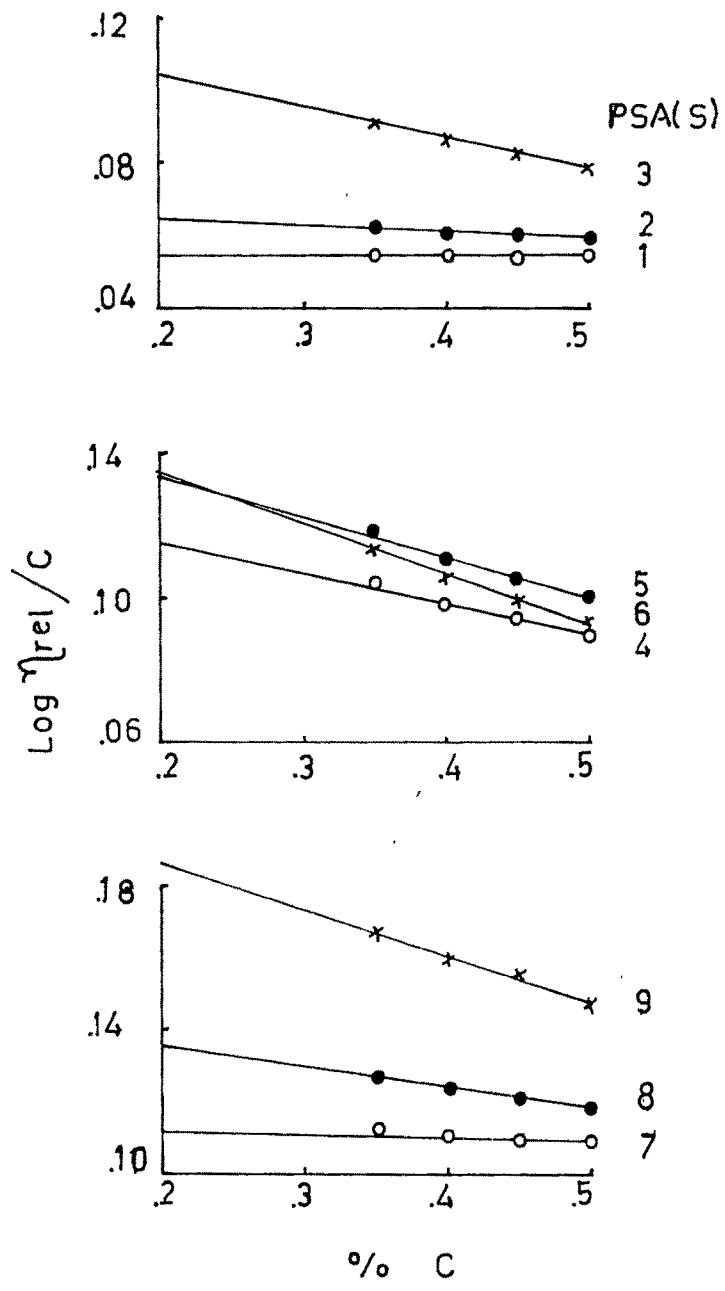


fig. III.22 Plot of $\text{Log } \eta_{\text{rel}}/C$ vs $\% C$ for the set of $\text{PSA}(S)$ (H form)

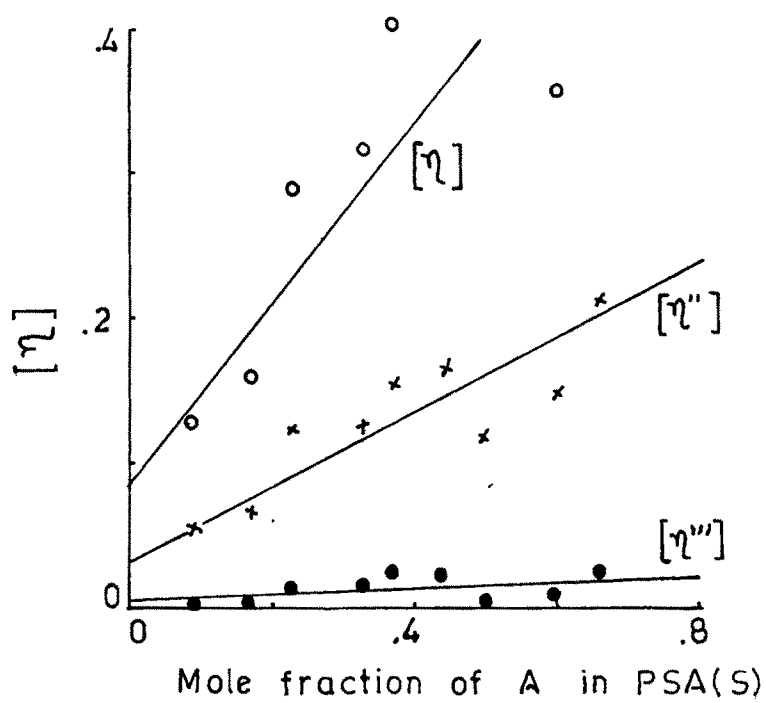


fig.III. 23

The slopes of the plots are negative in fig.III.20 and positive in figs. III.21 and 22. From the values of the slopes and intercepts the values of constants k' , k'' and k''' are evaluated and are presented in table III.3. It is observed that the values of k'' and k''' vary over a small range, while those of k' vary over a very wide range.

4(d) General

Some of the observations regarding the sets of copolymers of styrene with unsaturated acid or acid anhydride can be generalised. The mole fraction of the acid in the products is presented in table III.4.

If the mole fraction of acid in the product is correlated with the mole fraction of acid in the feed, the lower region of the plot is a curve, while the upper may usually be a straight line.

In the IR spectra of the products, the band at about 1720 cm^{-1} is increasing in intensity and the band at 695 cm^{-1} is decreasing as the mole fraction of the acid in the product is increasing. The band at 695 cm^{-1} can be attributed to styrene, whereas the band at 1720 cm^{-1} can be attributed to the acid.

Table- III.3

No	Product	K'	K''	K'''
1	PSA(S)-1	0	5385.0	0
2	PSA(S)-2	-1.6	6222.2	- 3.8
3	PSA(S)-3	-2.0	268.4	- 5.7
4	PSA(S)-4	-2.2	168.6	- 5.3
5	PSA(S)-5	-1.9	80.0	- 4.5
6	PSA(S)-6	-	98.8	- 5.3
7	PSA(S)-7	-	4938.3	0
8	PSA(S)-8	-0.8	771.1	- 2.8
9	PSA(S)-9	-	151.6	- 2.8

Table III.4

No.	Product	mole fraction of acid or acid anhydride in the product								
		x = 1	2	3	4	5	6	7	8	9
1	PSMan (x)	0.30	0.33	0.44	0.52	0.60	0.63	0.70	0.80	0.83
2	PSFa (x)	0.13	0.20	0.37	0.50	0.56	0.64	0.69	0.75	0.78
3	PSA(S)(x)	0.09	0.17	0.23	0.33	0.37	0.44	0.50	0.60	0.66

237

The melting points of the products do not show a linear relation with the mole fraction of acid in the product.

Huggin's equation, Martins equation and Kraemer equation have been used to evaluate intrinsic viscosity. It has been generally observed that

$$[\eta'] < [\eta''] < [\eta]$$

The slopes are generally negative for Huggins plots and positive for Martins plots.

III.5 Salts of copolymers

Sets of copolymers of styrene with maleic anhydride, fumaric acid and acrylic acid were prepared and their nature and formulae were established on the basis of analytical data, AVS results, IR spectra, melting and solubility behaviour, etc. Their relative viscosity in DMF solution was determined and intrinsic viscosity was evaluated.

To prepare partial salts available acid content on reaction for 24 hrs was determined. Hence 20 % and 50 % of the available acidic proton was replaced by Na(I), Cu(II), Zn(II), Ba (II) or Ca (II). The products were studied for their viscosity in solution.

Literature survey reveals certain important studies. Viscosity of Na salts varied exponentially with the degree of neutralization (64). Log of the viscosity varied with the log of the degree of neutralization at fixed concentration in solution (69). When metal ion replaces acidic proton, η_{max}/η_0 represents the degree of coil compression (53). Effects of the degree of substitution in Na, K, Li, and Cs salts on the activation energy of viscous flow were studied (44, 47). Viscosity of partially neutralized styrene-acrylic acid copolymer salts decreased initially on successive dilution, reached a minimum and then increased (135). Viscosity of Na, Rb, Ca and Zn salts of styrene-methacrylic acid copolymers was studied with reference to degree of substitution, solvent polarity, addition of pyridine etc. (136). Li, Na, Rb, Cs, Mg, Ca, Ba, Fe, Pb, Cu, Mn and Zn salts of styrene-methacrylic acid copolymers were studied for thermal stability at various degrees of substitution (137). Na, Rb, K, Zn, Ca and Co salts of styrene-methacrylic acid were studied for thermo-mechanical properties (138). Addition of alkali increases the viscosity of the solution of styrene-methacrylic acid copolymer upto pH 10 (139).

Reduced viscosity has been calculated from relative viscosity determined for the salts in solution. Plots of η_{red} vs % C are presented in figs. III. 24, 25, 26 and 27

for the salts of PSMAN, in figs. III 37, 38, 39, 40 and 41 for the salts of PSFa and in figs. III 53, 54, 55, 56 and 57 for the salts of PSA(s). Plots of $\log \eta_{rel}$ vs % C are presented in figs. III 28, 29, 30 and 31 for the salts of PSMAN, in figs. III. 42, 43, 44, 45 and 46 for the salts of PSFa and in figs. III. 58, 59, 60, 61 and 62 for the salts of PSA(s). Plots of $\log \eta_{rel}$ vs % C are presented in figs. III. 32, 33, 34 and 35 for the salts of PSMAN, in figs. III 47, 48, 49, 50 and 51 for the salts of PSFa and in figs. III.63, 64, 65, 66 and 67 for the salts of PSA(s).

Salts of PSMAN

Intrinsic viscosity $[\eta]$ or $[\eta']$ for all the salts with two degrees of substitution increases with increase in the mole fraction of maleic anhydride in PSMAN and the values of $[\eta]$ are generally higher than the corresponding values of $[\eta']$. However, the values of $[\eta']$ show small variation with the change in the mole fraction of maleic anhydride in PSMAN increase in the values of $[\eta]$ with the increase in the mole fraction of maleic anhydride (fig. III.36) can be attributed to the formation of ion pairs or ion aggregates or ion-cross links in increasing amount. If the values of $[\eta]$ for the H form of PSMAN are compared with the corresponding values of $[\eta]$ for the metal salt

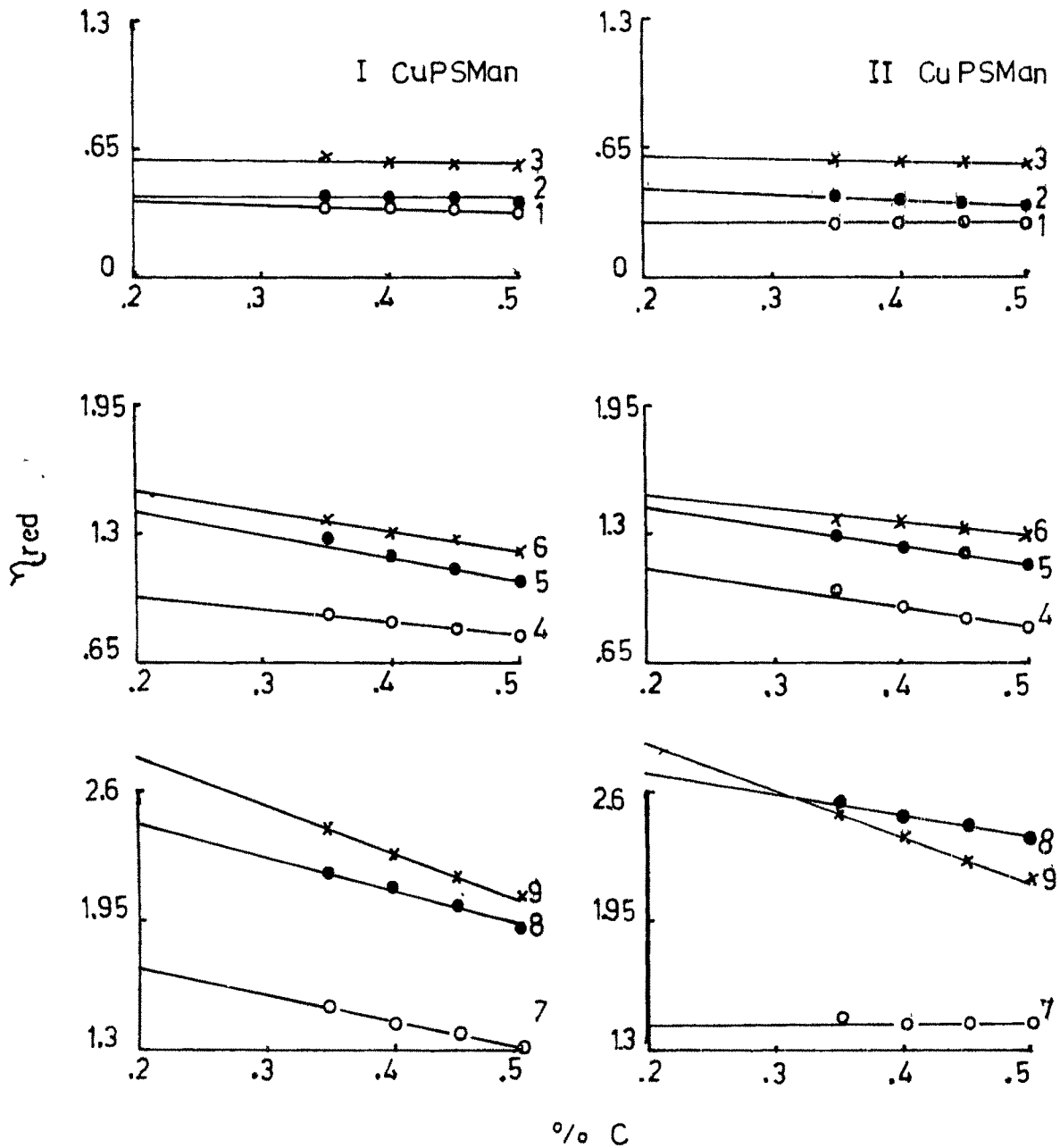


fig.III.24 Plot of η_{red} vs % C
for the sets of CuPSMan

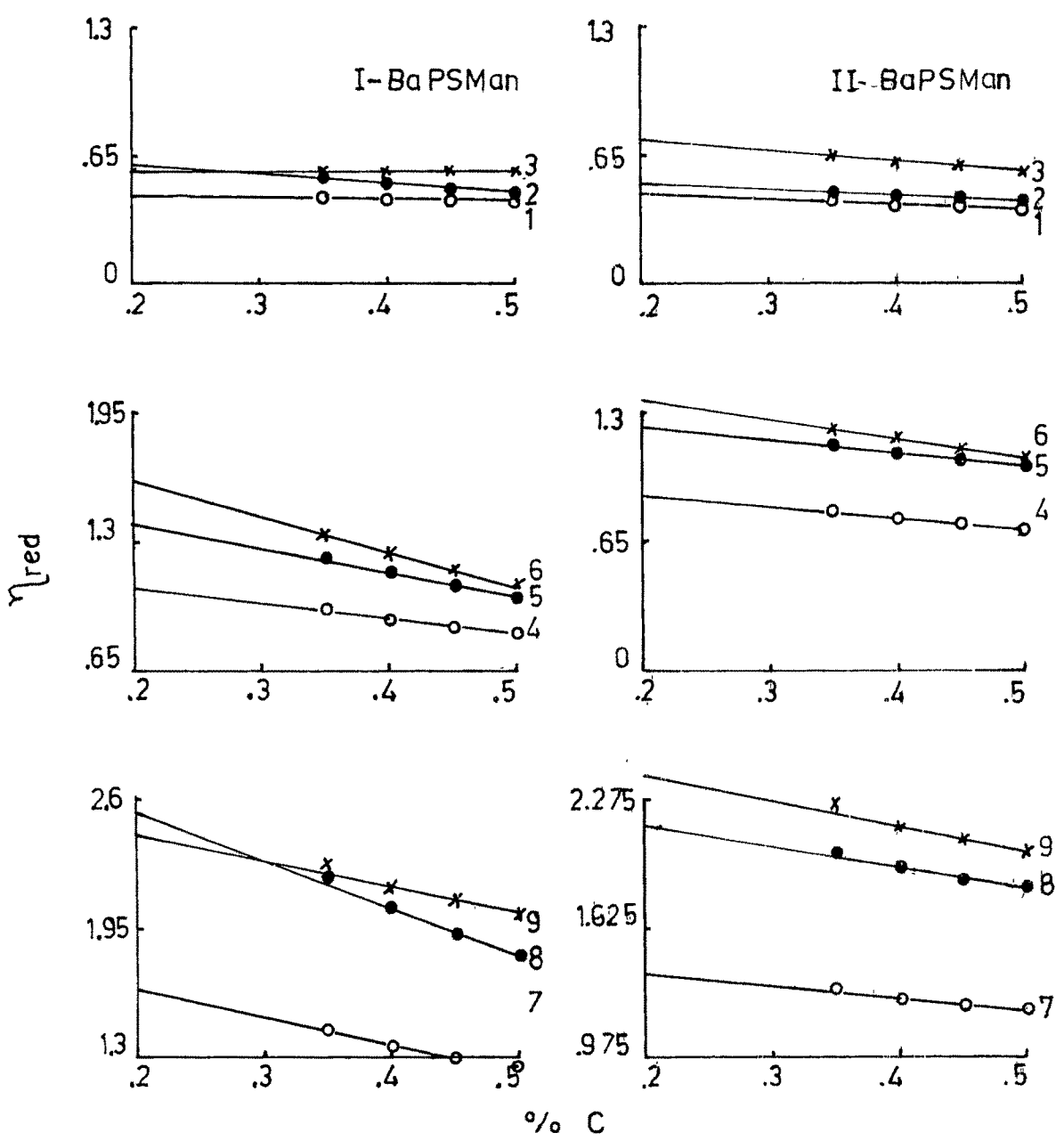


fig. III.25 Plot of η_{red} vs % C for the sets of BaPSMan

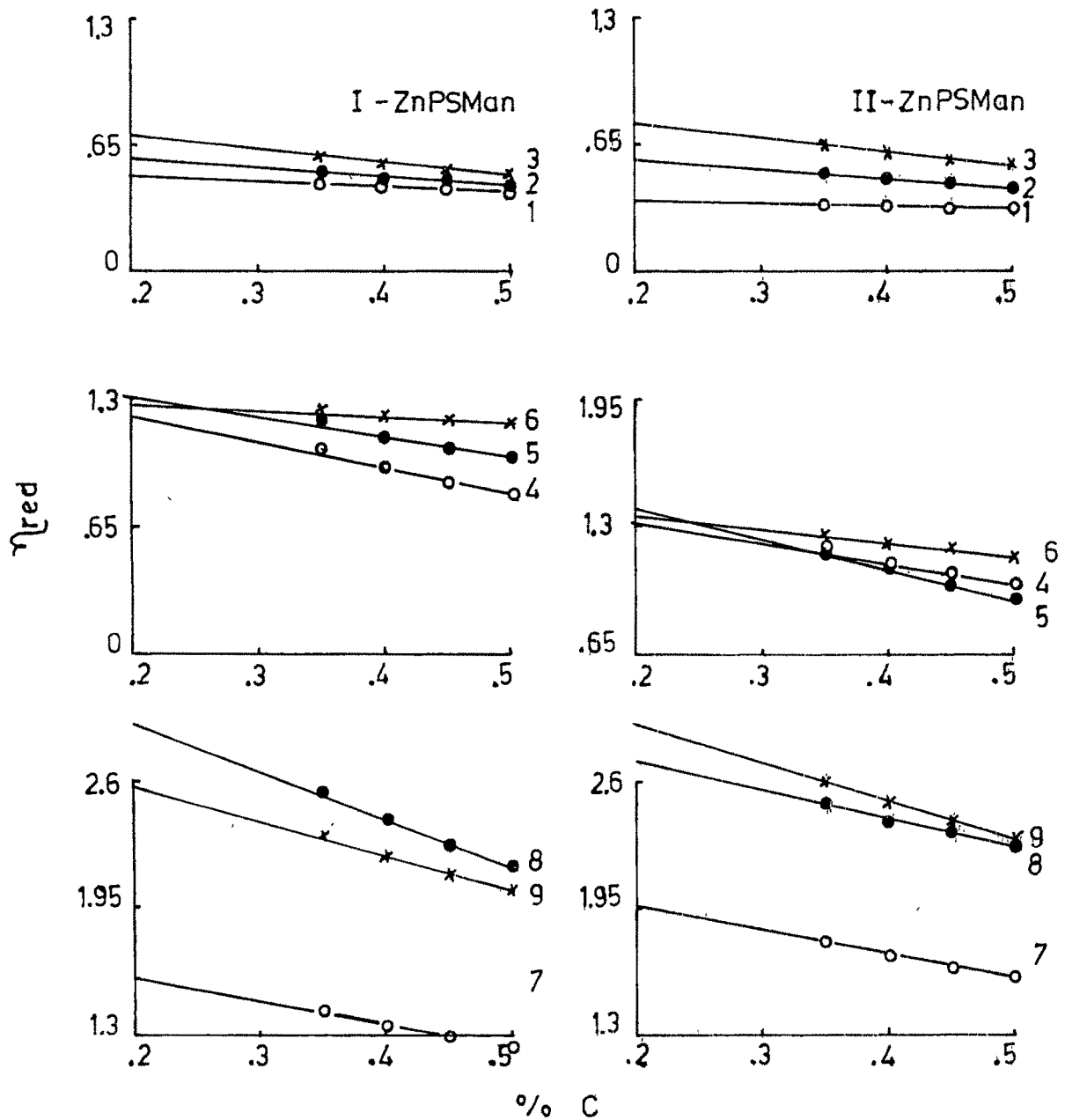


fig.III 26 Plot of η_{red} vs % C
for the sets of ZnPSMan

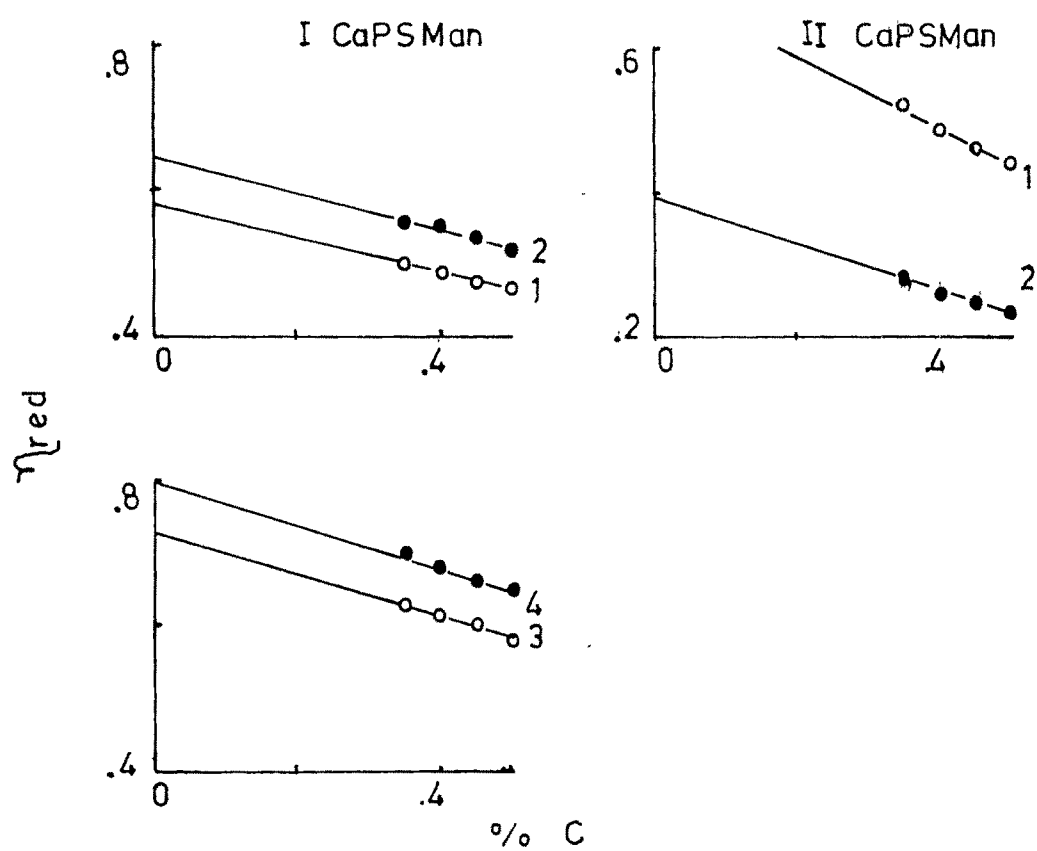


fig.III.27 Plot of η_{red} vs % C
for CaPSMan sets

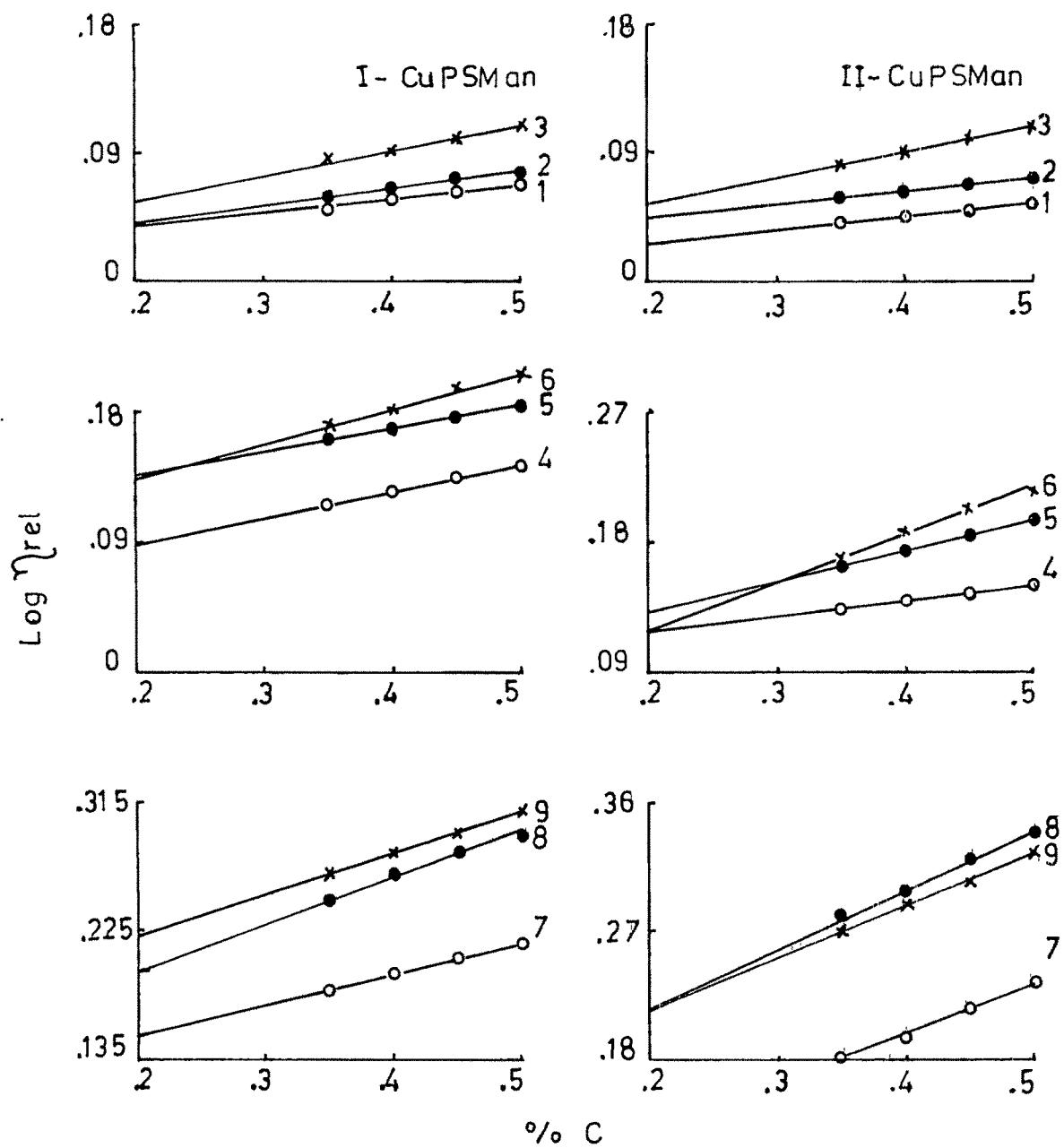


fig.III.28 Plot of $\text{Log } \eta_{\text{rel}}$ vs $\% \text{ C}$
for the sets of CuPSMan

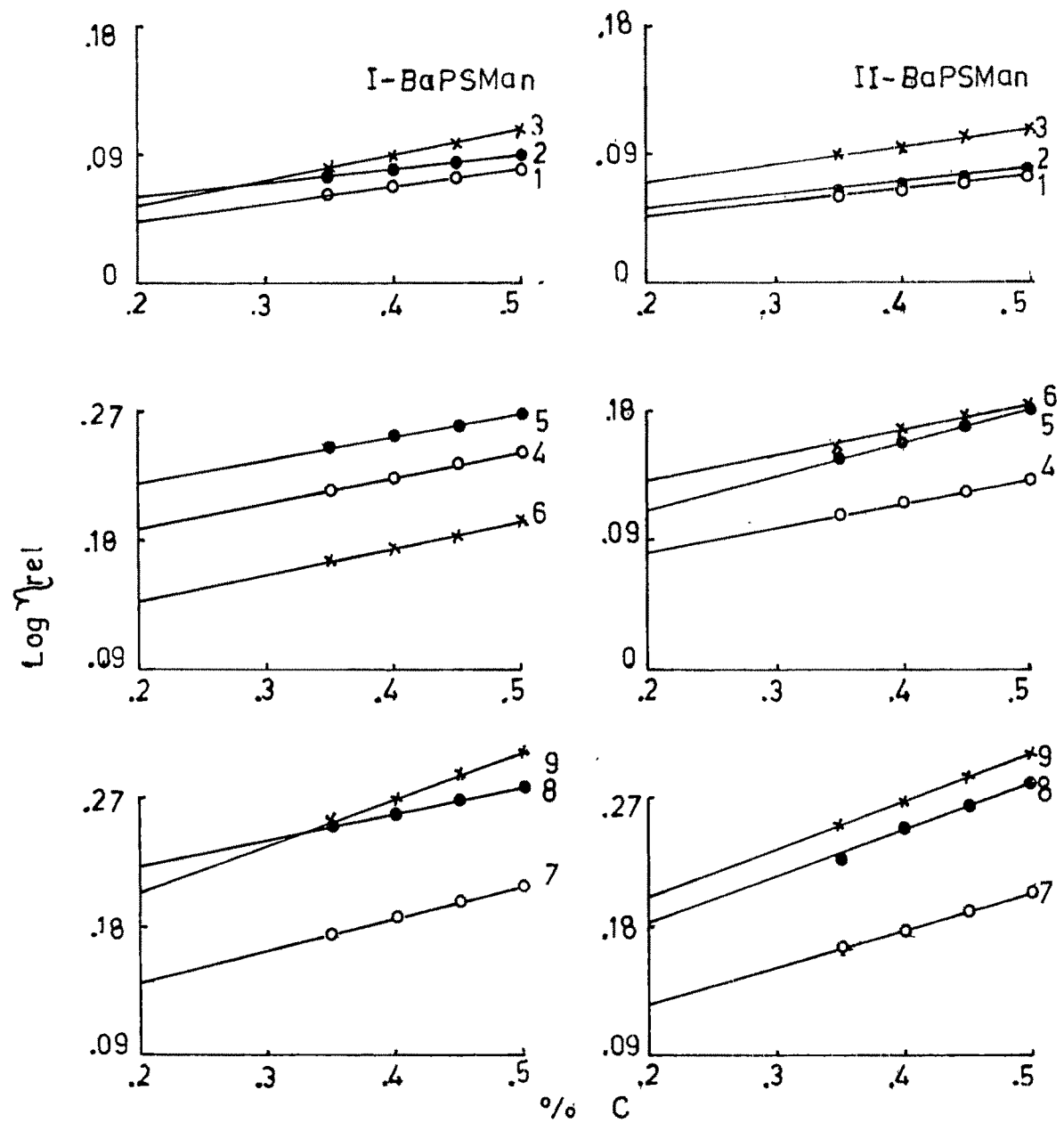


fig.III.29 Plot of $\text{Log } \eta_{\text{rel}}$ vs % C
for the sets of BaPSMan

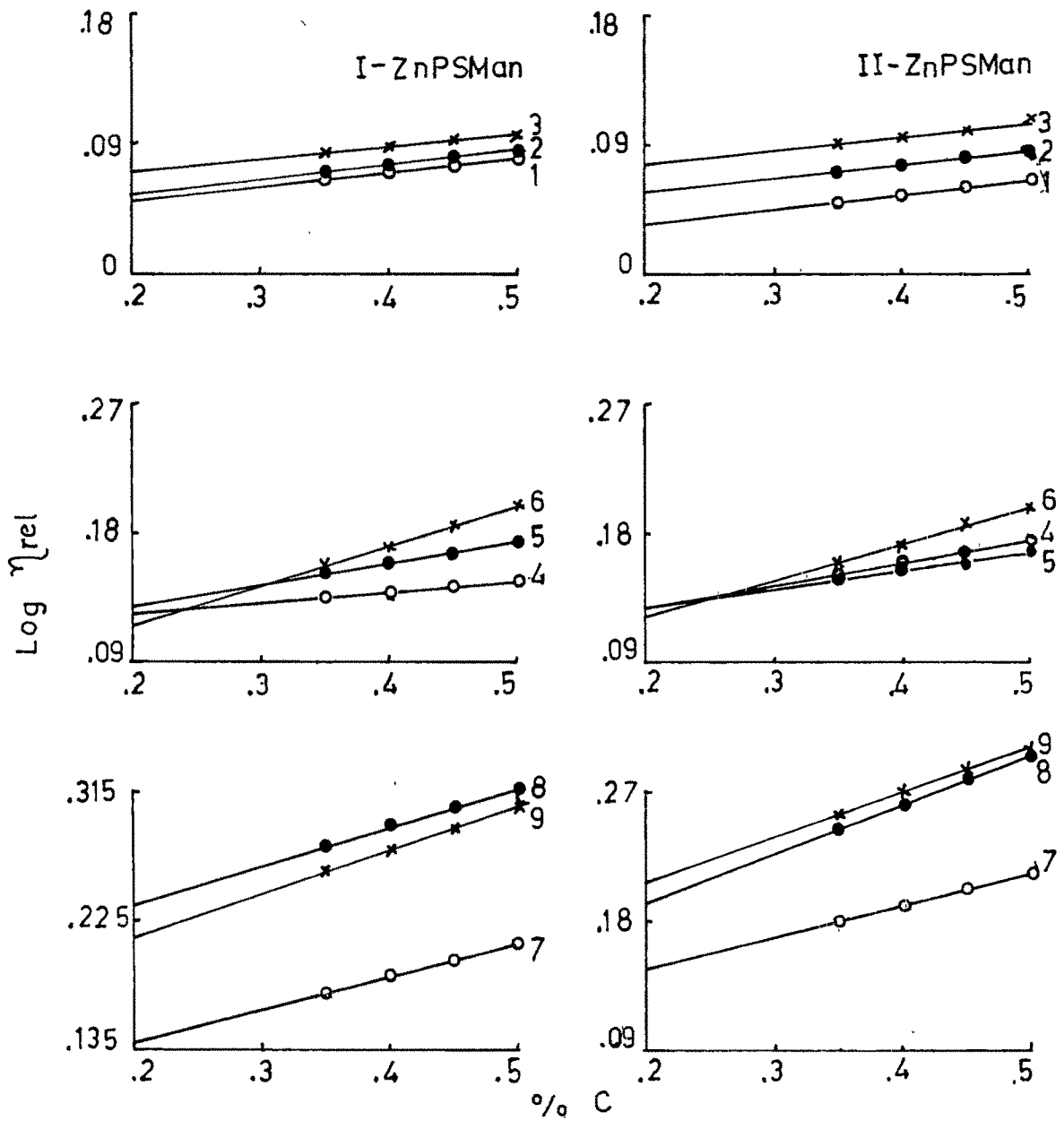


fig.III.30 Plot of $\text{Log } \eta_{\text{rel}}$ vs % C
for the sets of ZnPSMan

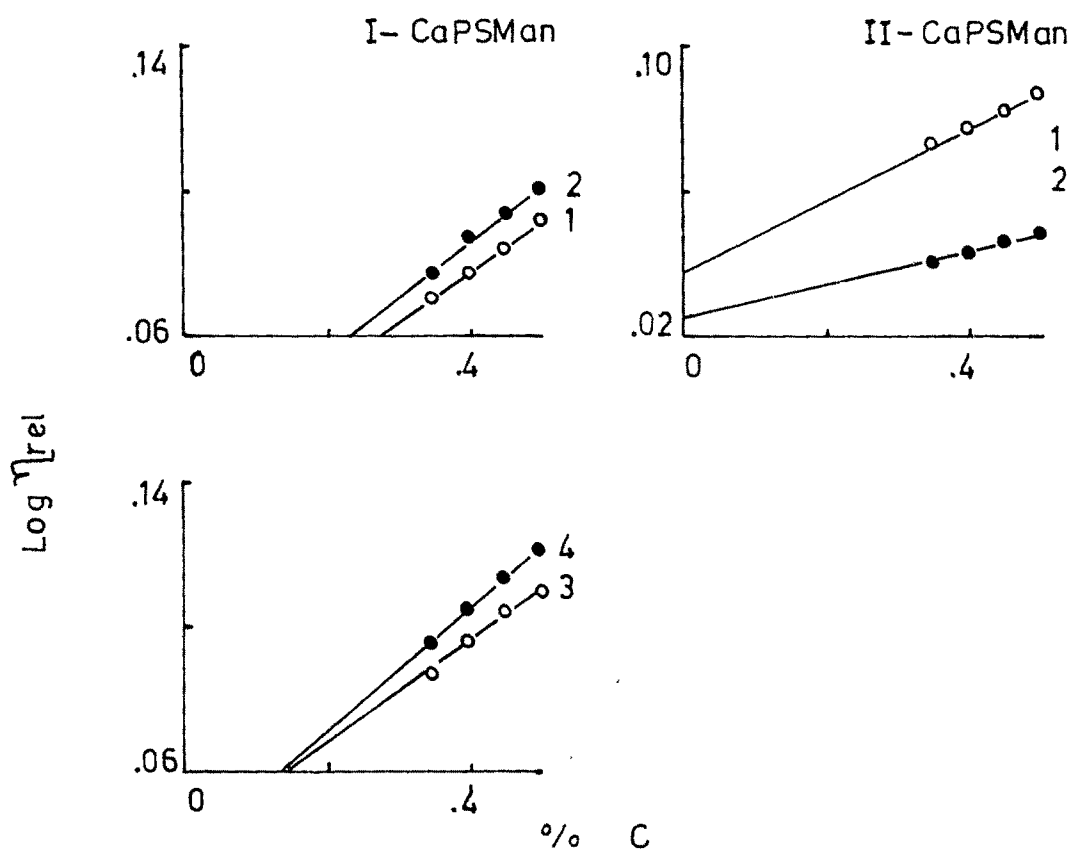


fig.III.31 Plot of $\text{Log } \eta_{\text{rel}}$ vs $\% \text{ C}$
for CaPSMan sets

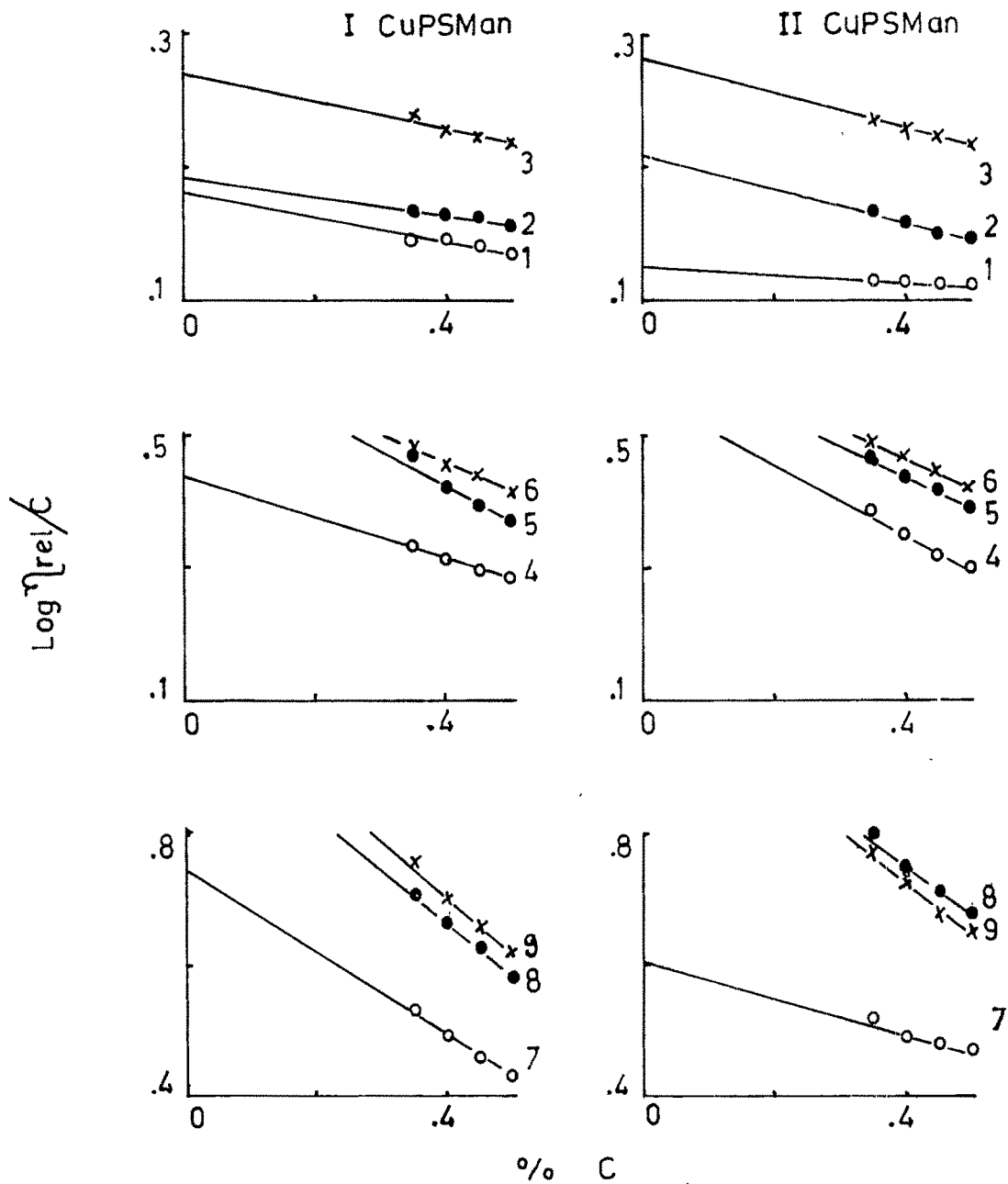


fig.III.32 Plot of $\text{Log } \eta_{rel}/C$ vs $\% C$ for CuPSMan sets

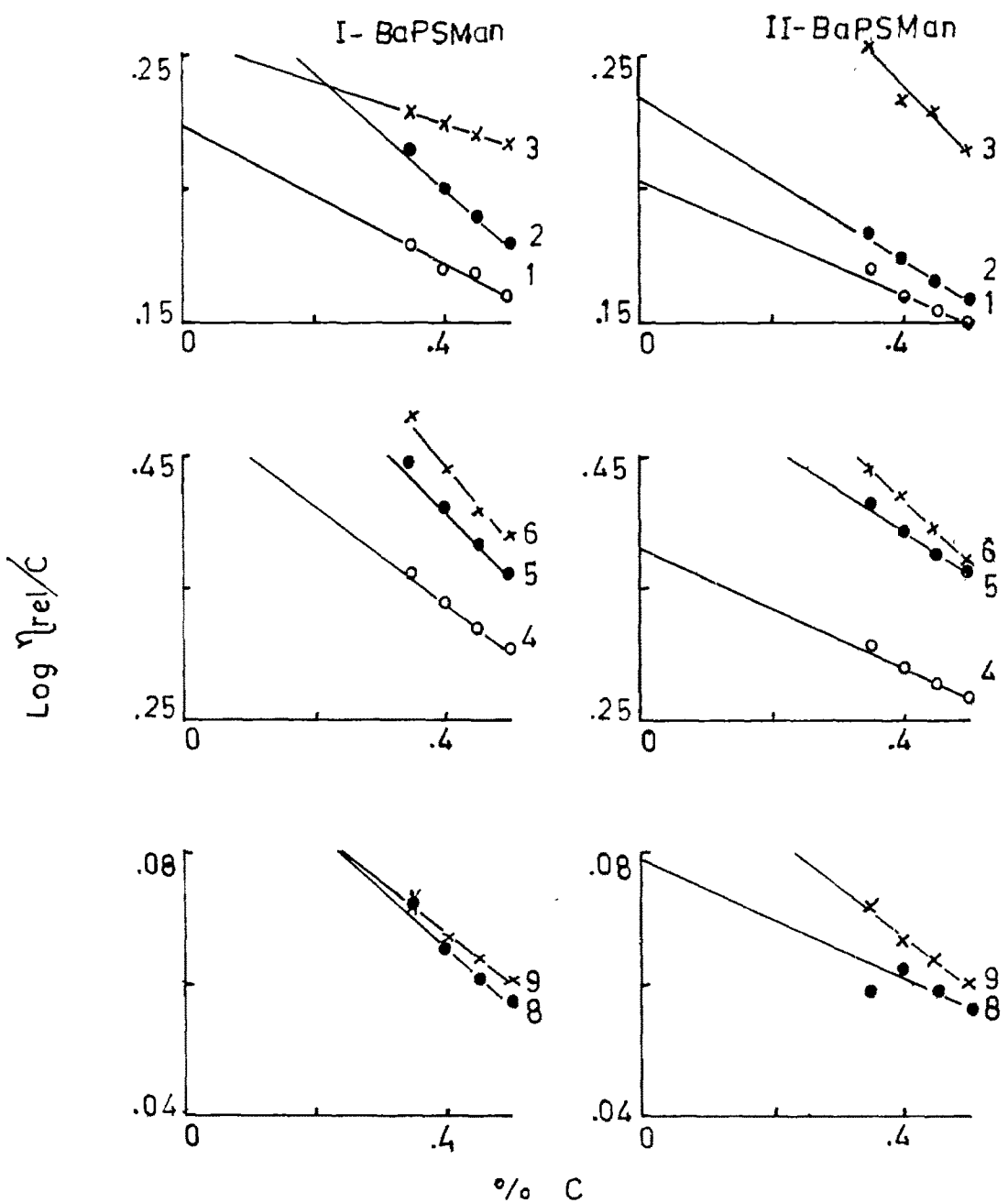


fig.III.33 Plot of $\text{Log } \eta_{rel}/C$ vs % C for BaPSMan sets

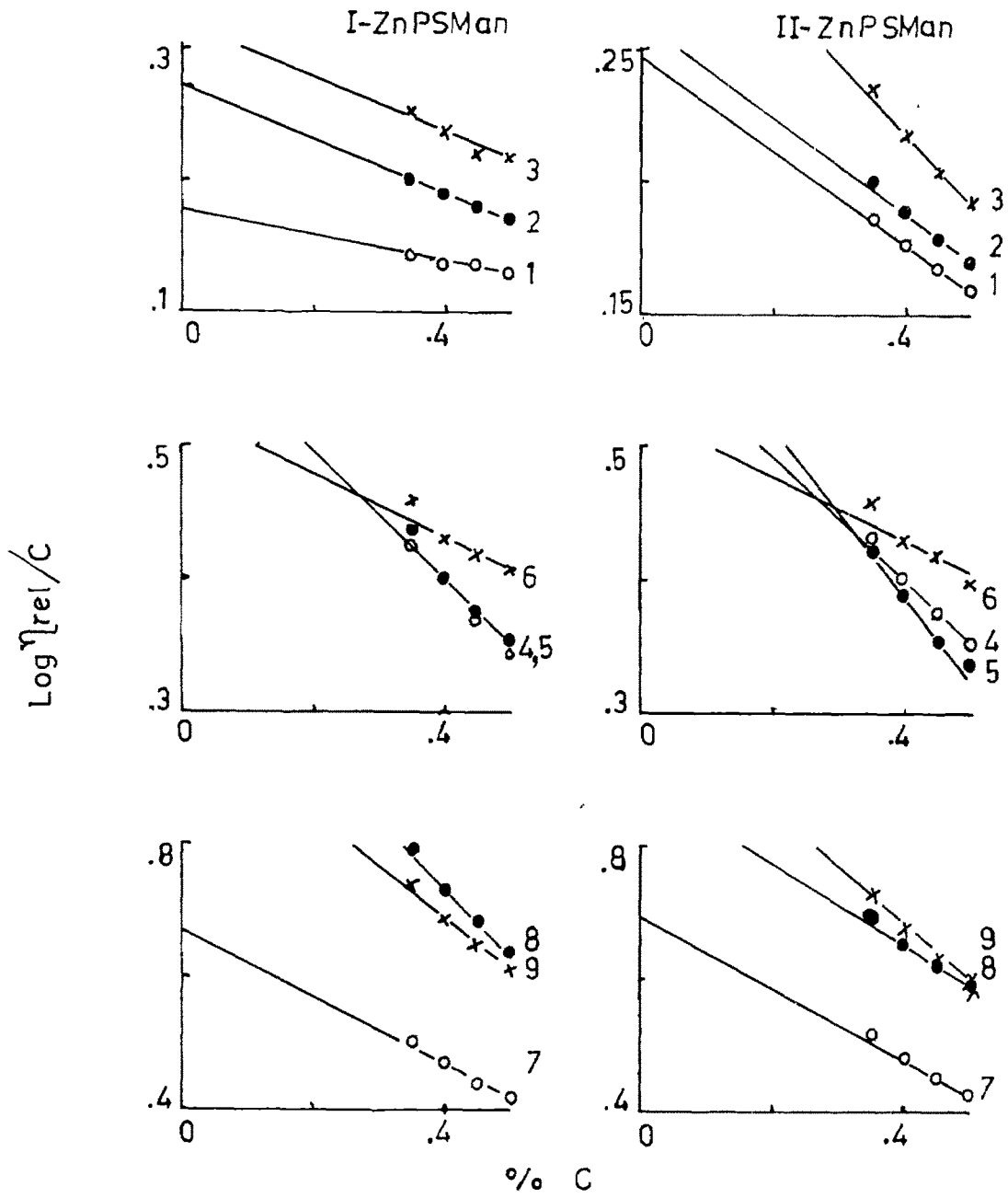


fig.III.34 Plot of $\text{Log } \eta_{\text{rel}}/C$ vs % C for ZnPSMan sets

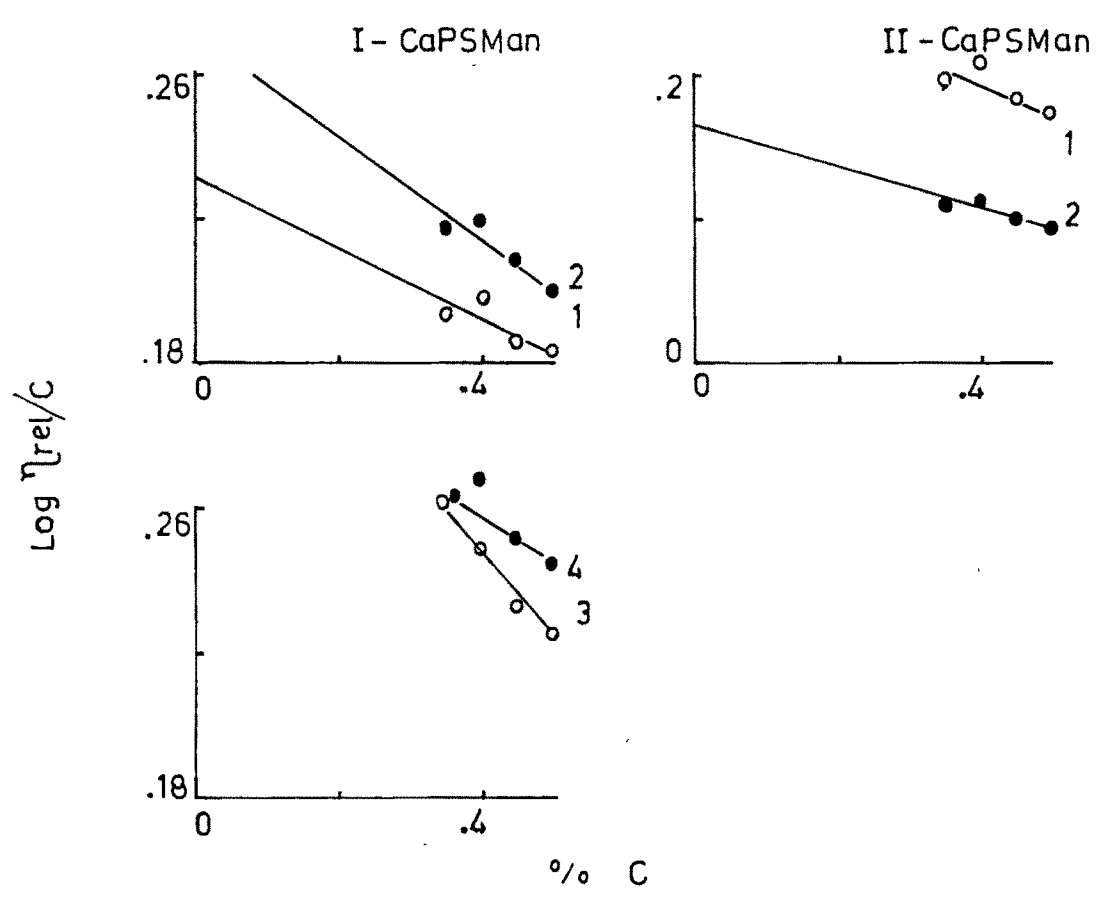
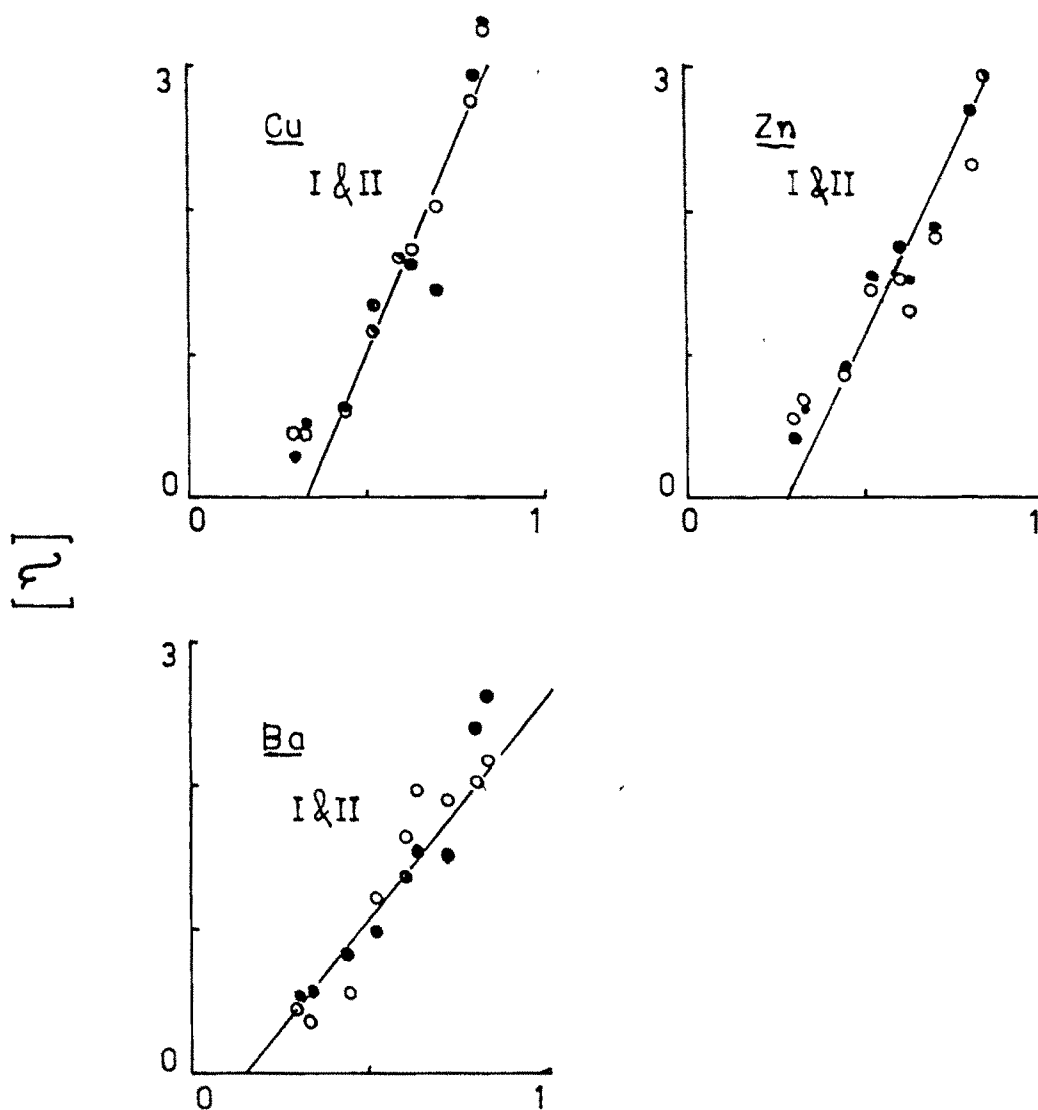


fig.III.35 Plot of $\text{Log } \eta_{\text{rel}}/C$ vs $\% C$ for CaPSMan sets



Mole fraction of Man in PSMan
fig III 36 (for the salts of PSMan)

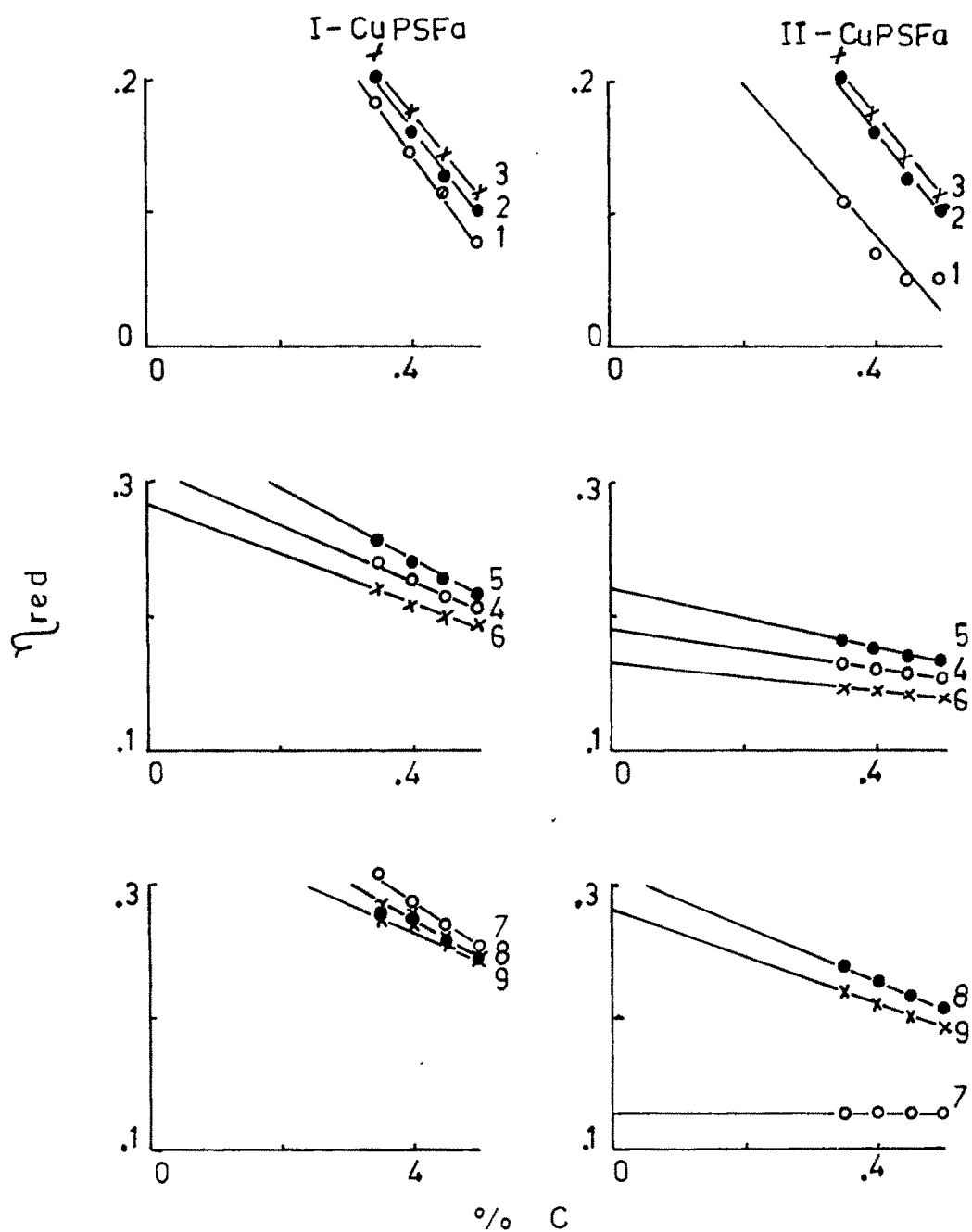


fig.III.38 Plot of η_{red} vs % C
for CuPSFa sets

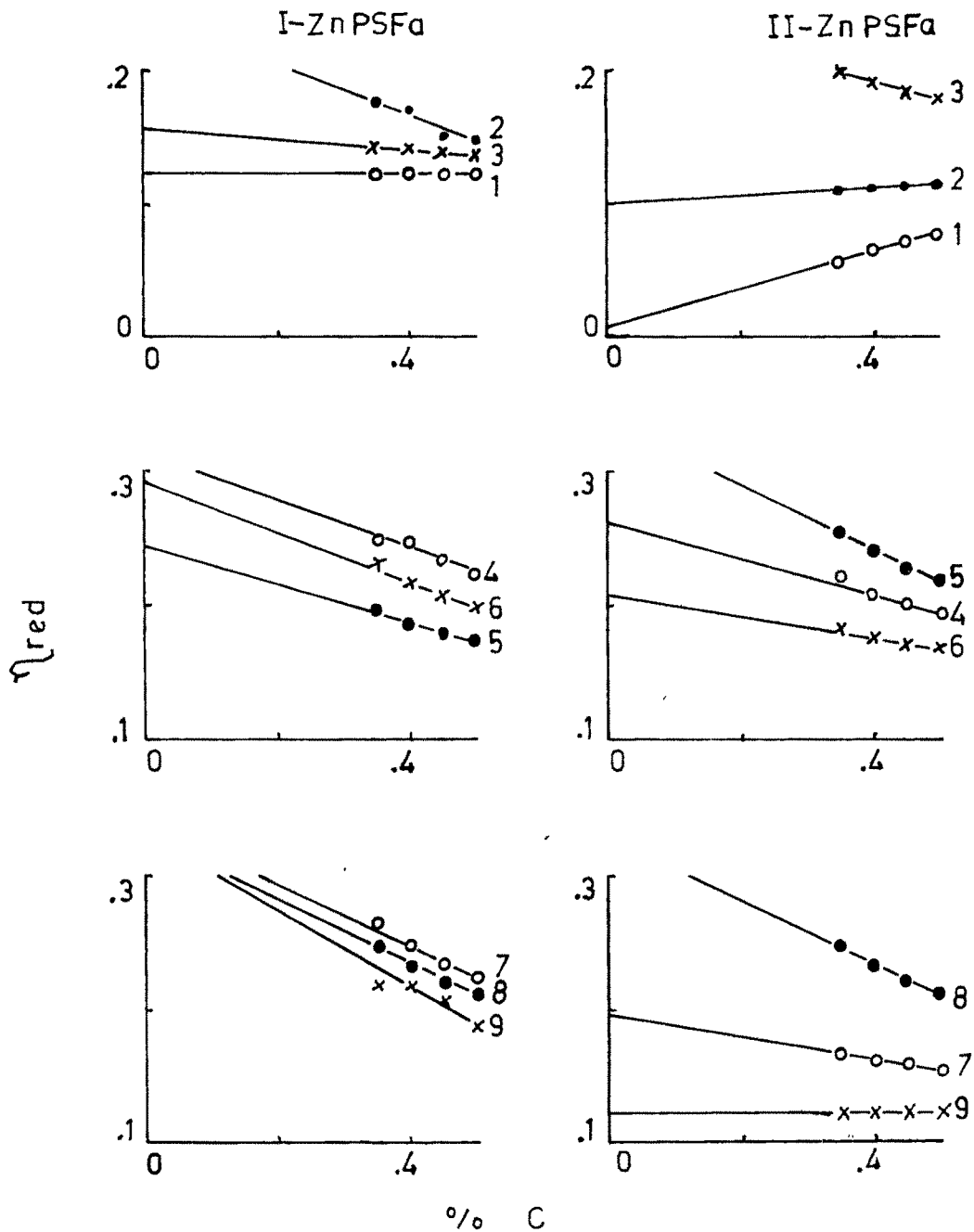


fig.III.39 Plot of η_{red} vs % C
for ZnPSFa sets

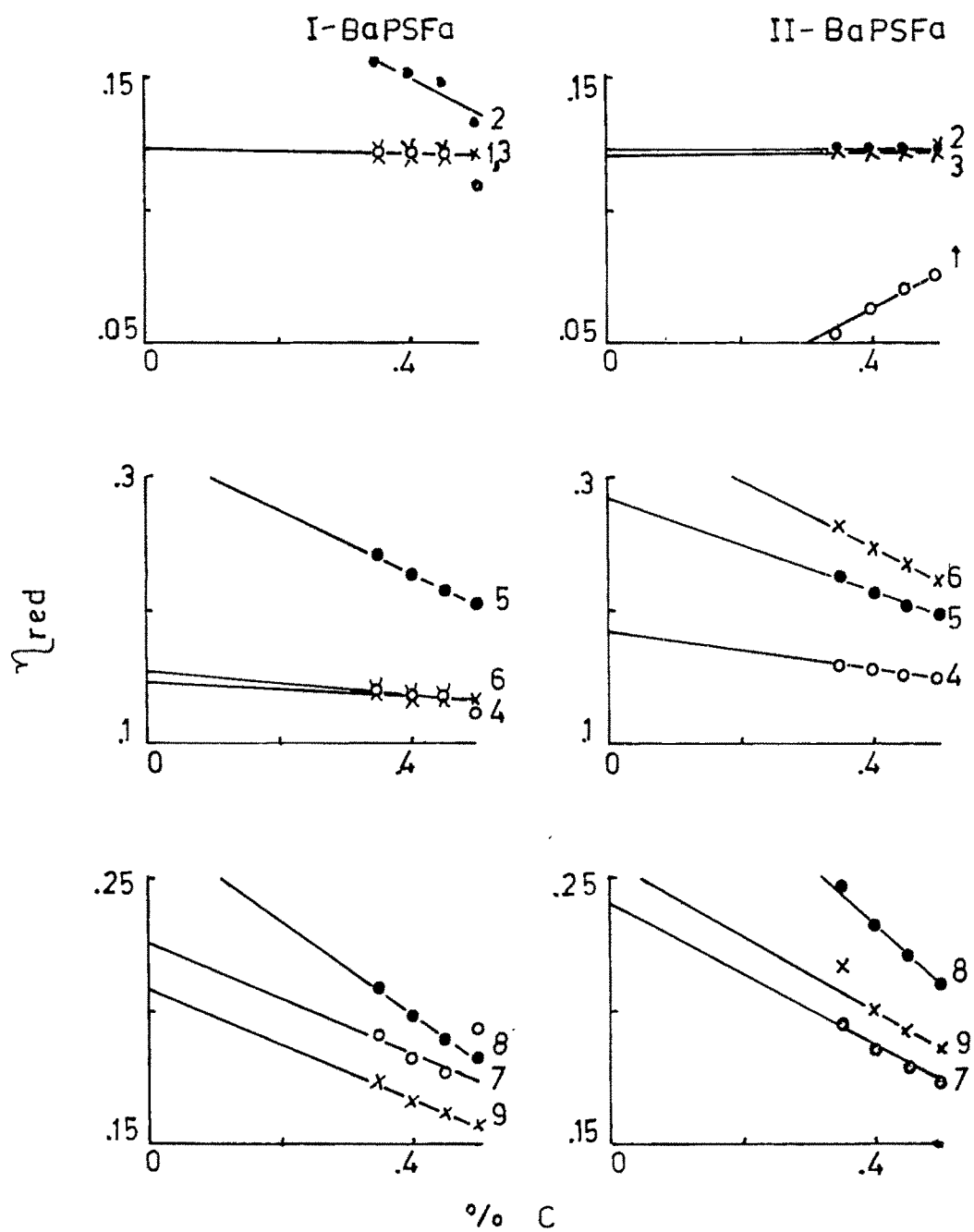


fig.III.40 Plot of η_{red} vs % C

for BaPSFa sets

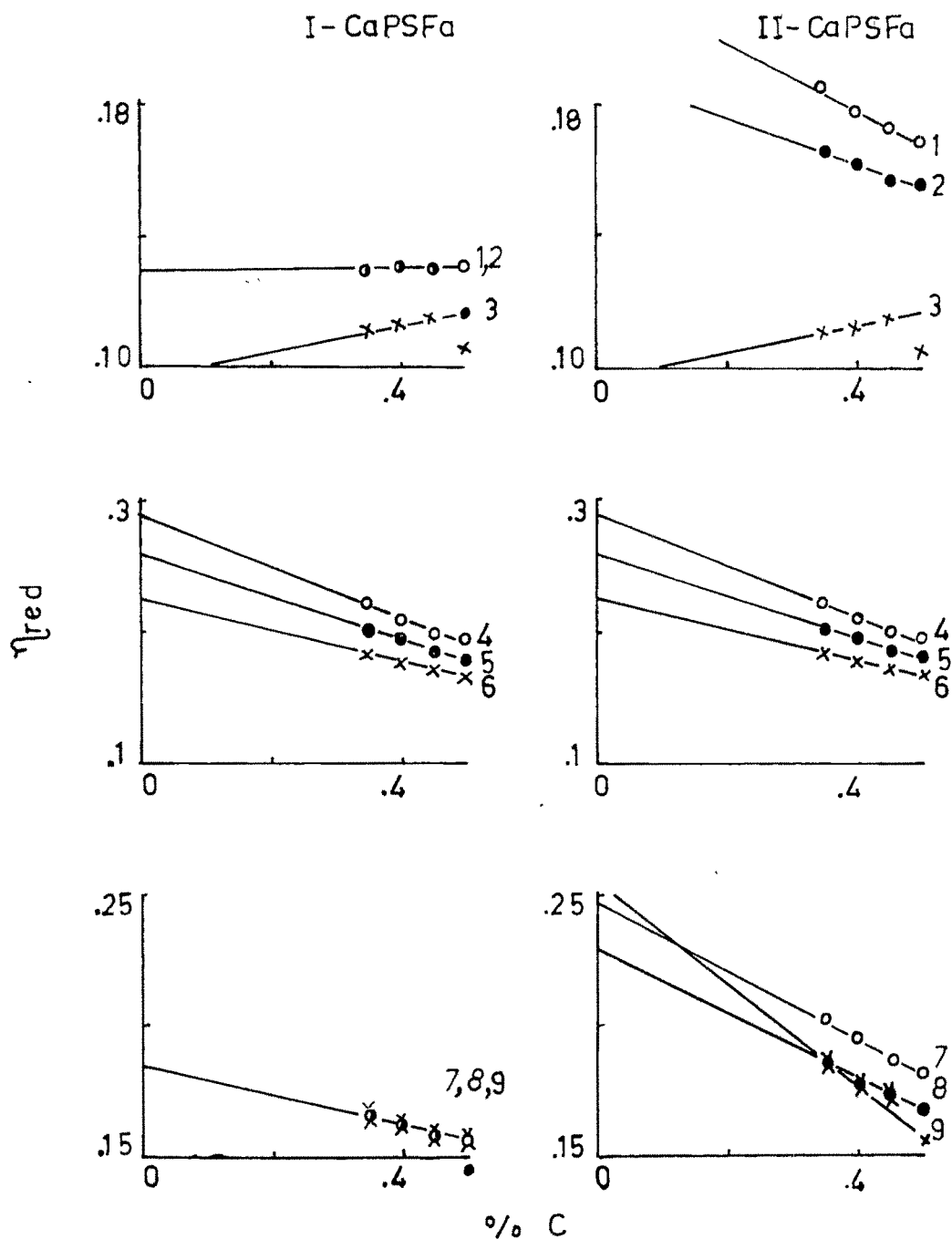


fig.III.41 Plot of η_{red} vs % C
for CaPSFa sets

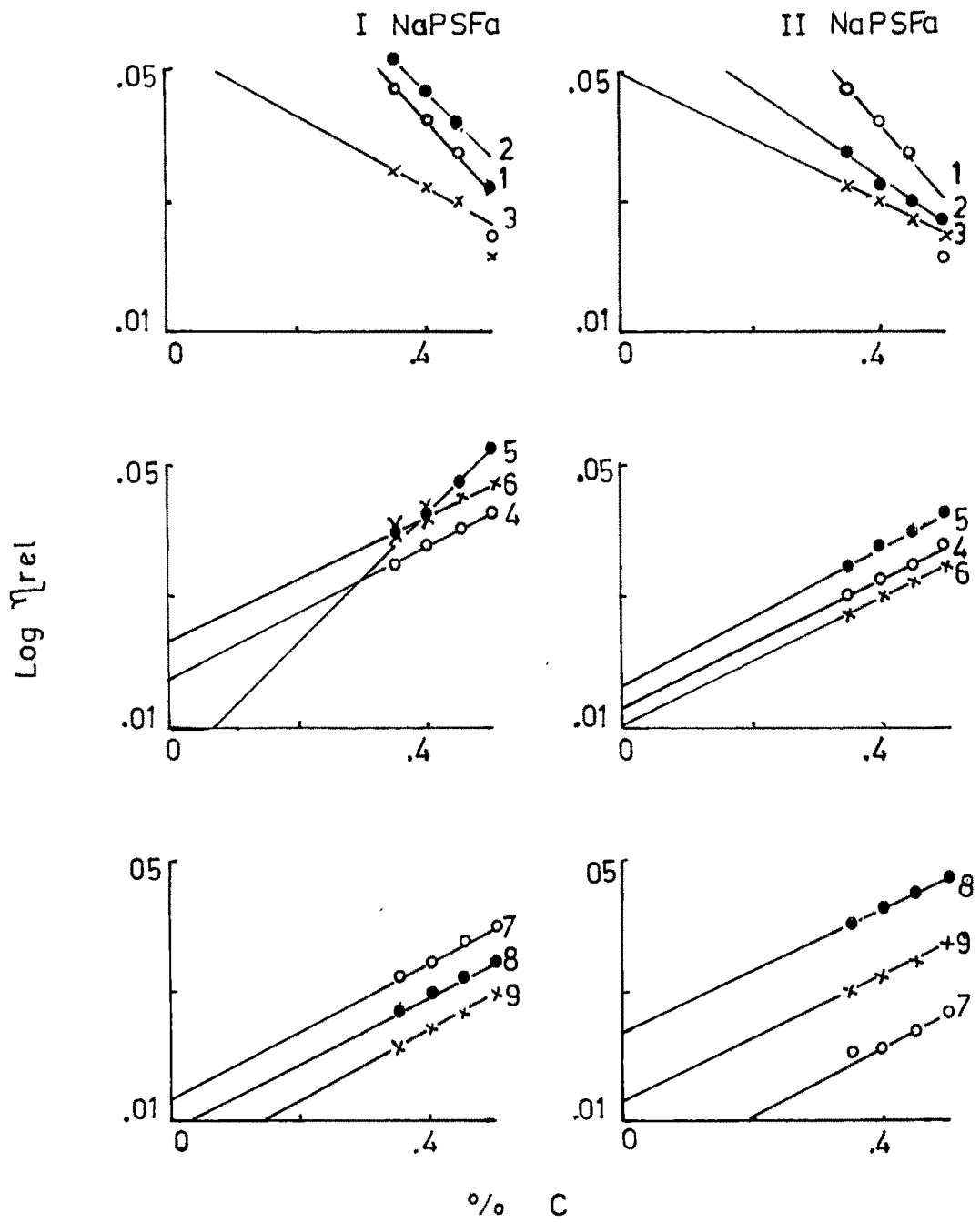


fig.III.42 Plot of $\text{Log } \eta_{rel}$ vs % C for NaPSFa sets

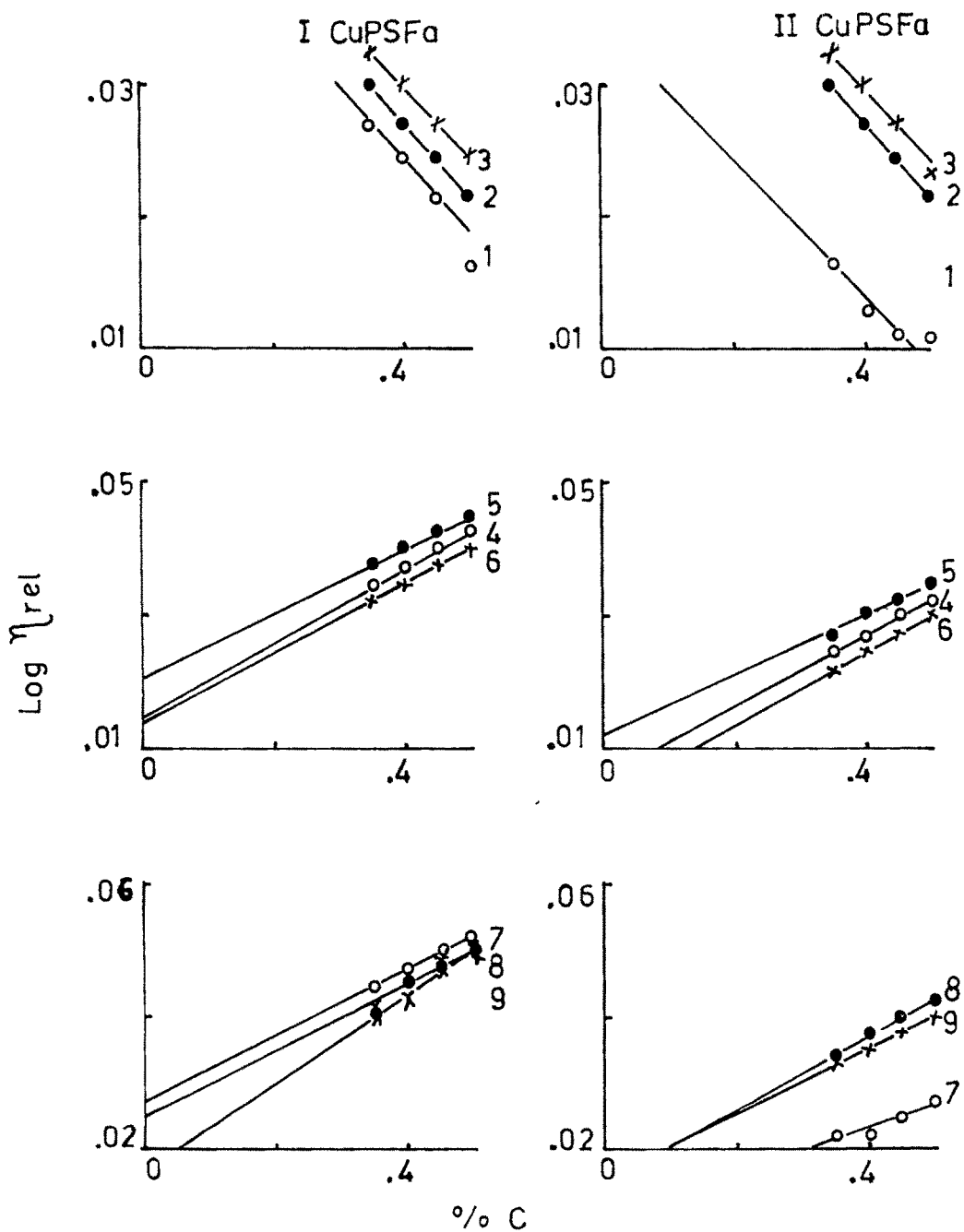


fig.III.43 Plot of $\text{Log } \eta_{\text{rel}}$ vs % C
for CuPSFa sets

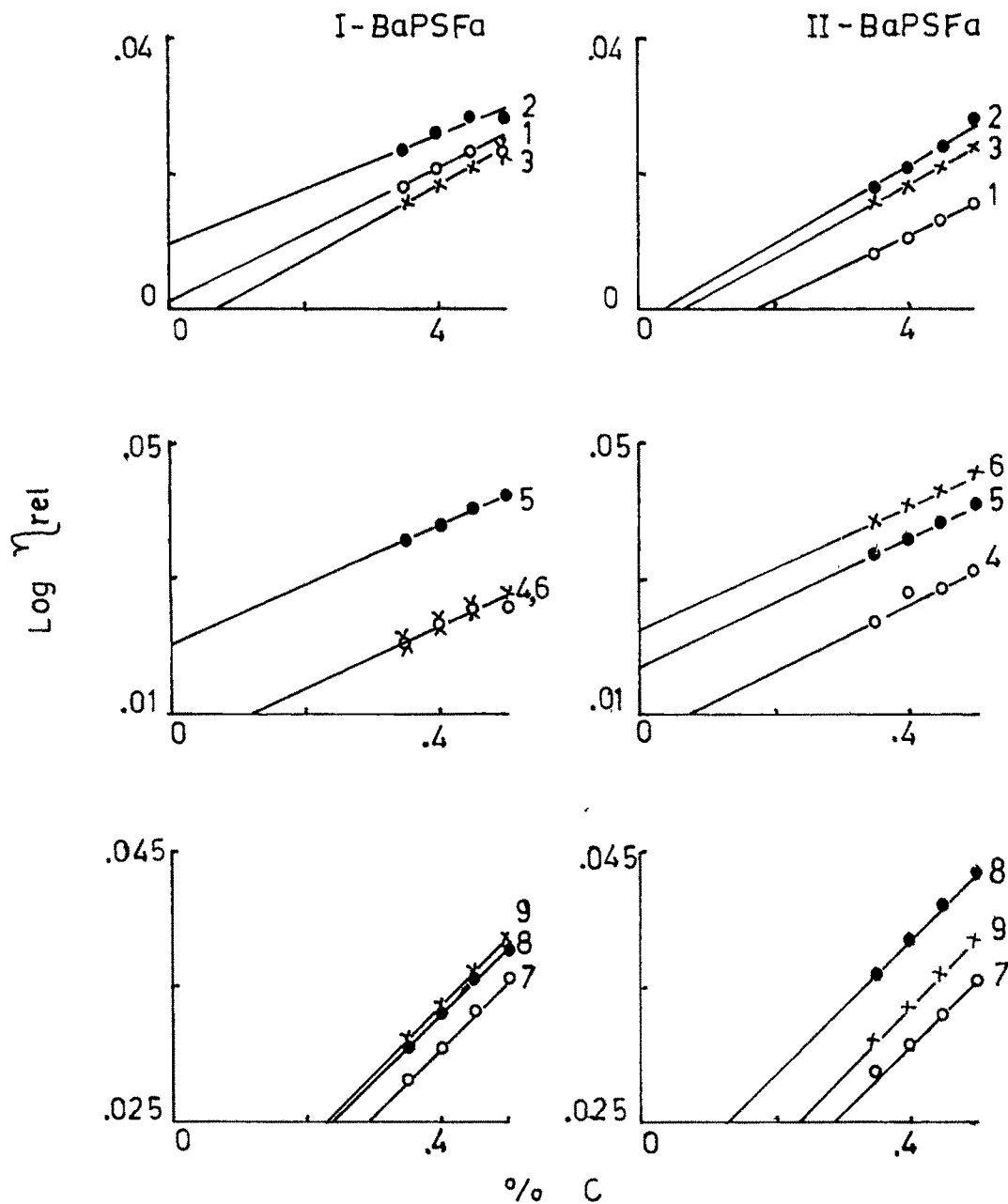


fig III.44 Plot of $\text{Log } \eta_{\text{rel}}$ vs $\% C$
for BaPSFa sets

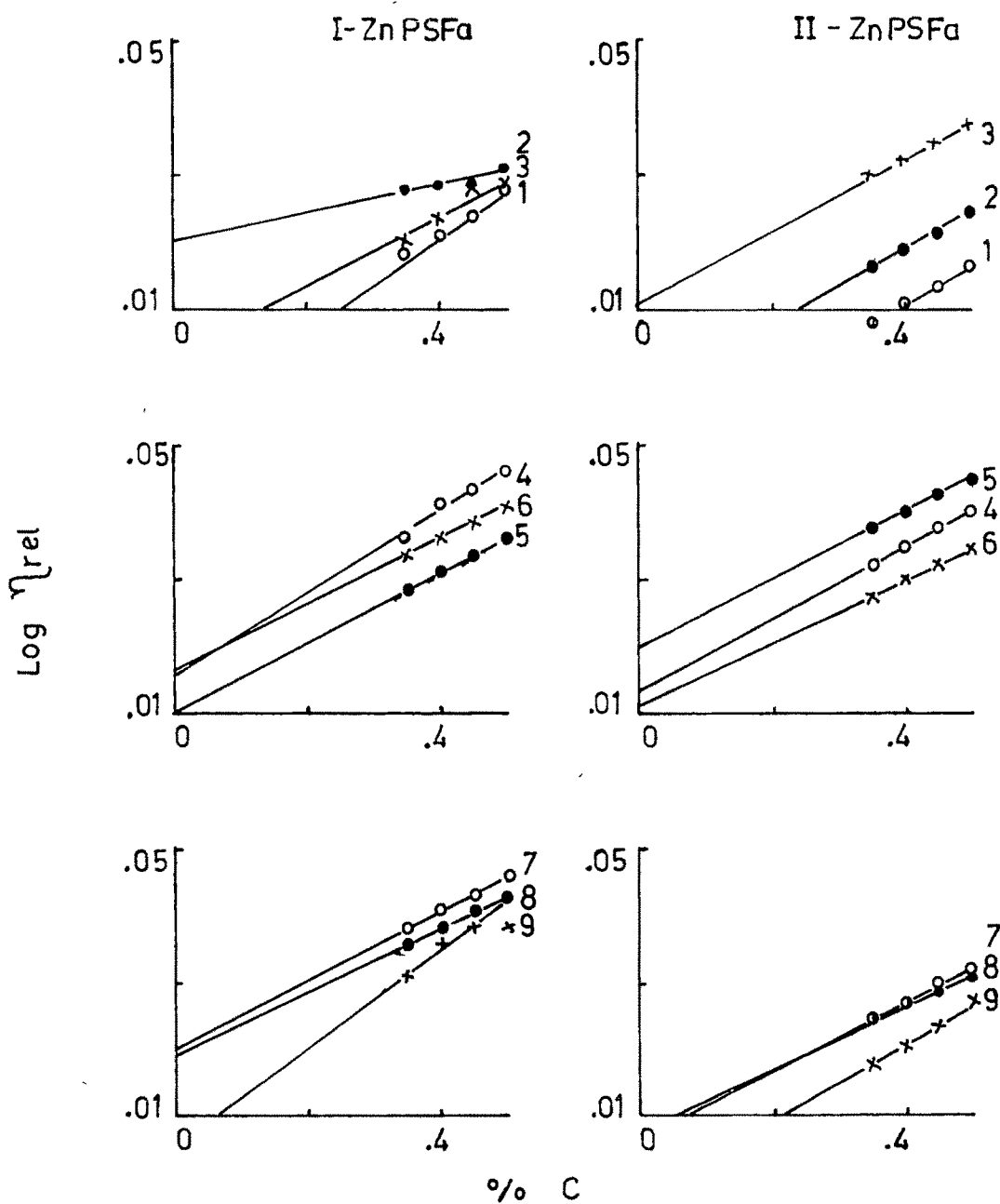


fig III.45 Plot of $\text{Log } \eta_{\text{rel}}$ vs % C
for ZnPSFa sets

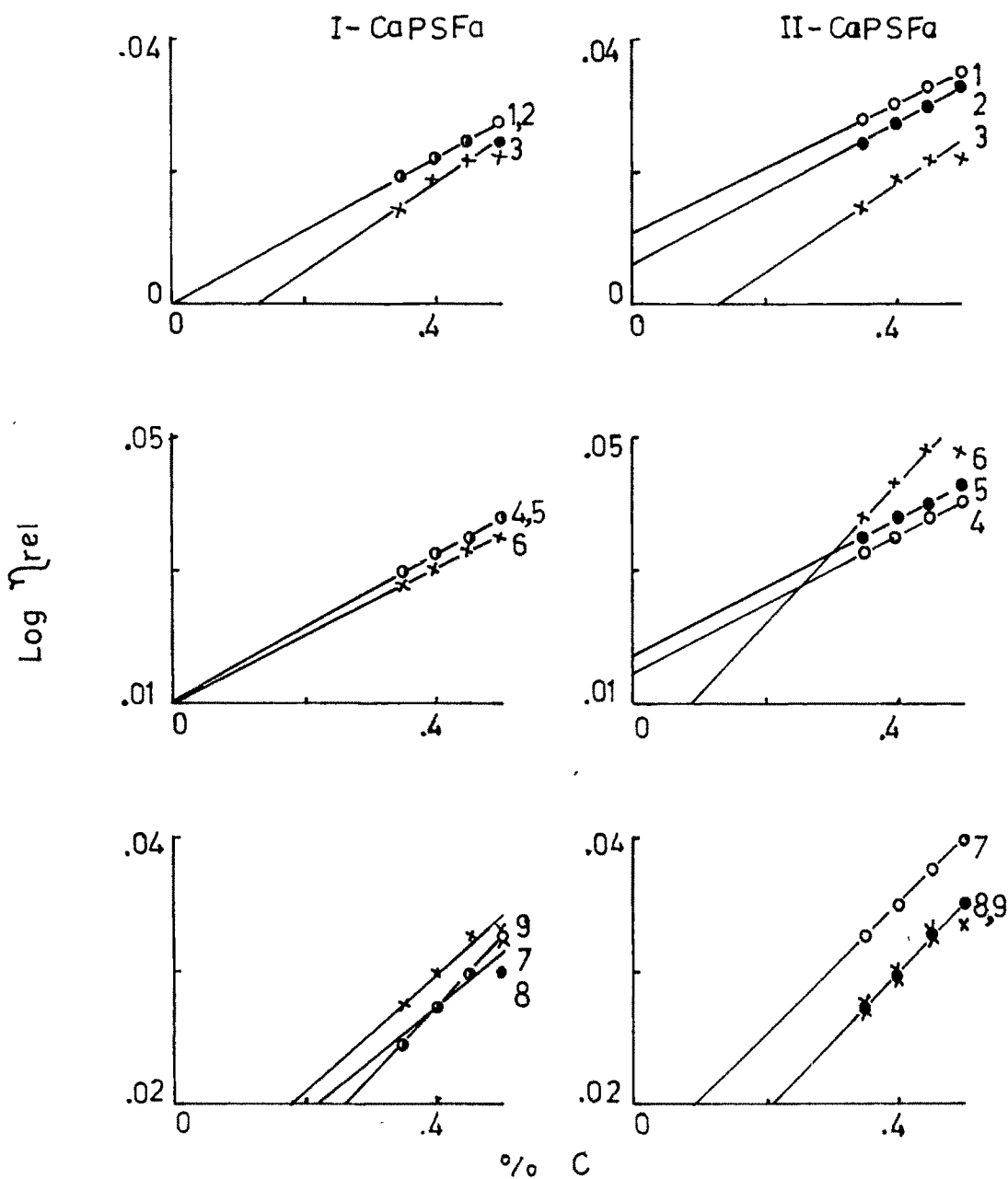


fig.III.46 Plot of $\text{Log } \eta_{\text{rel}}$ vs % C for CaPSFa sets

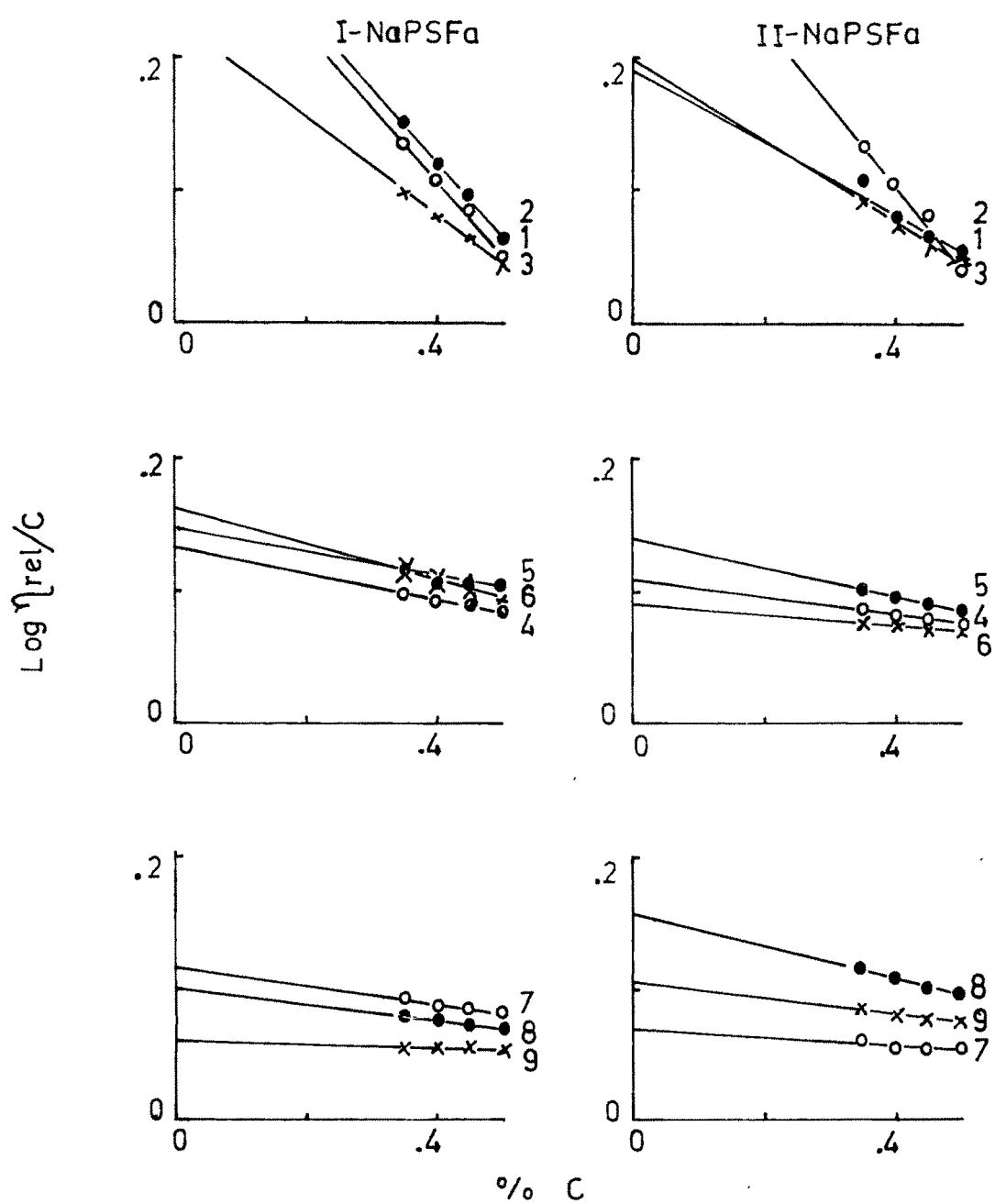


fig.III.47 Plot of $\text{Log } \eta_{\text{rel}}/C$ vs $\% C$ for NaPSFa sets

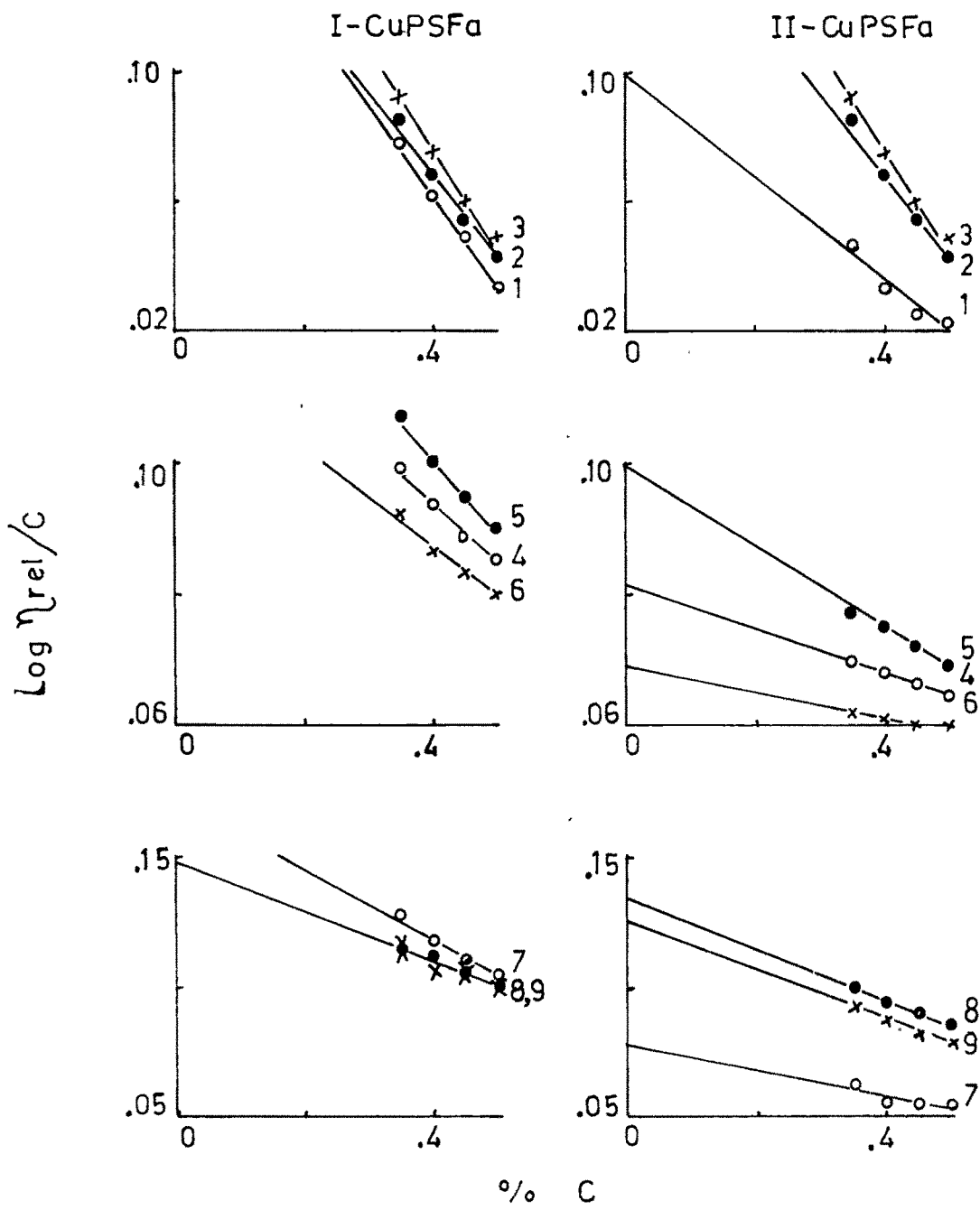


fig.III.48 Plot of $\text{Log } \eta_{rel}/C$ vs $\% C$ for CuPSFa sets

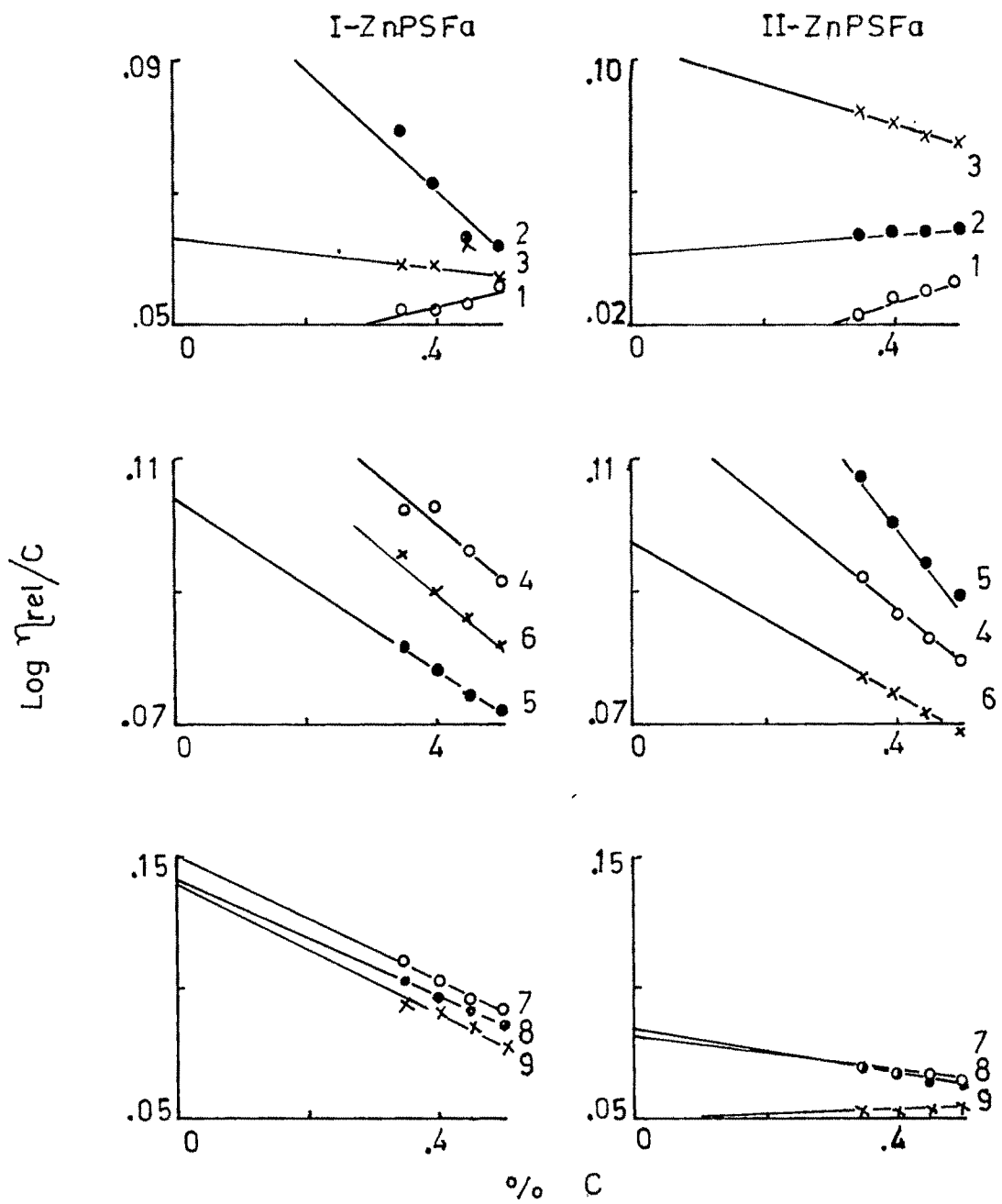


fig. III.49 Plot of $\text{Log } \eta_{\text{rel}}/C$ vs % C for ZnPSFa sets

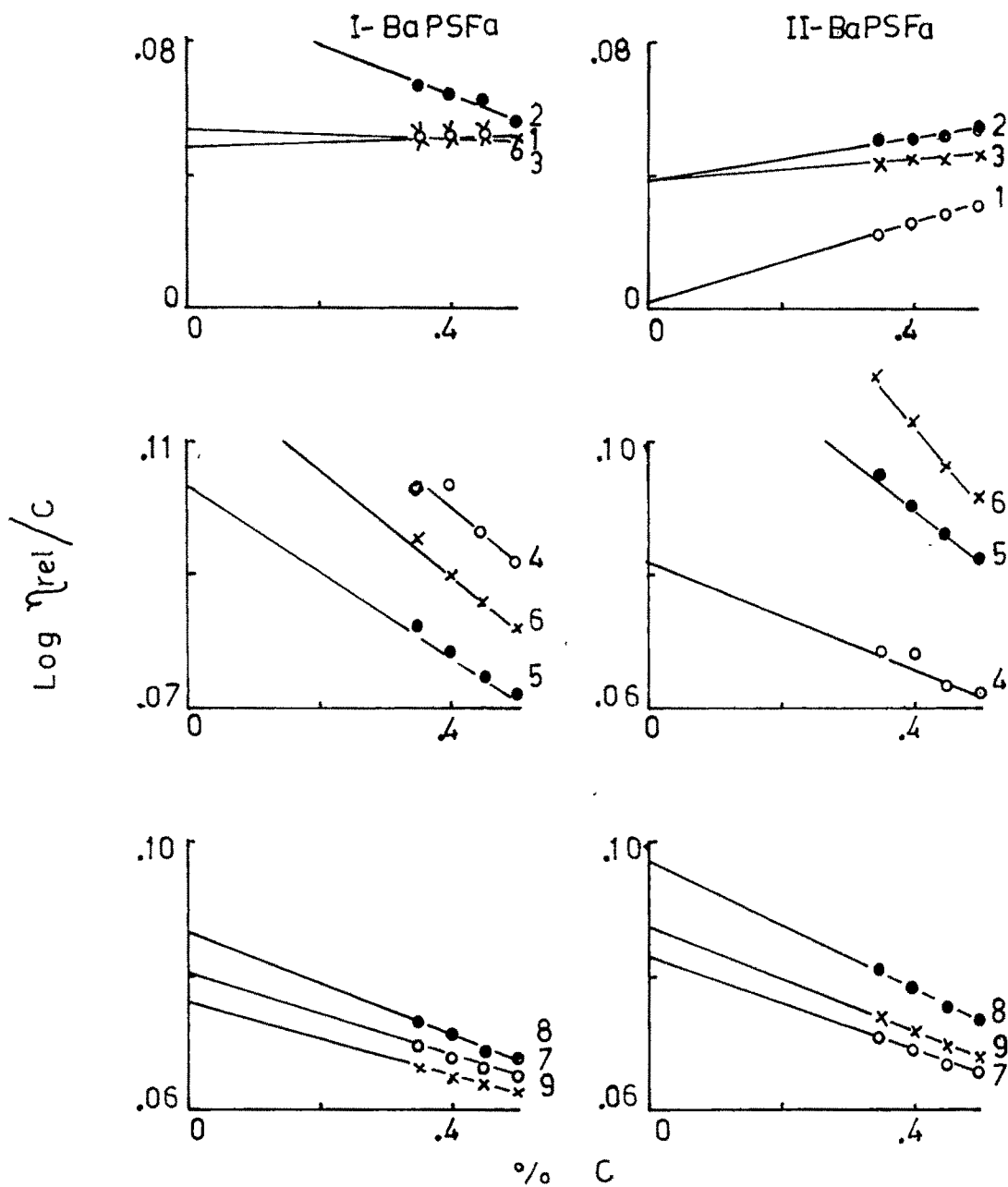


fig.III.50 Plot of $\text{Log } \eta_{rel}/C$ vs % C for BaPSFa sets

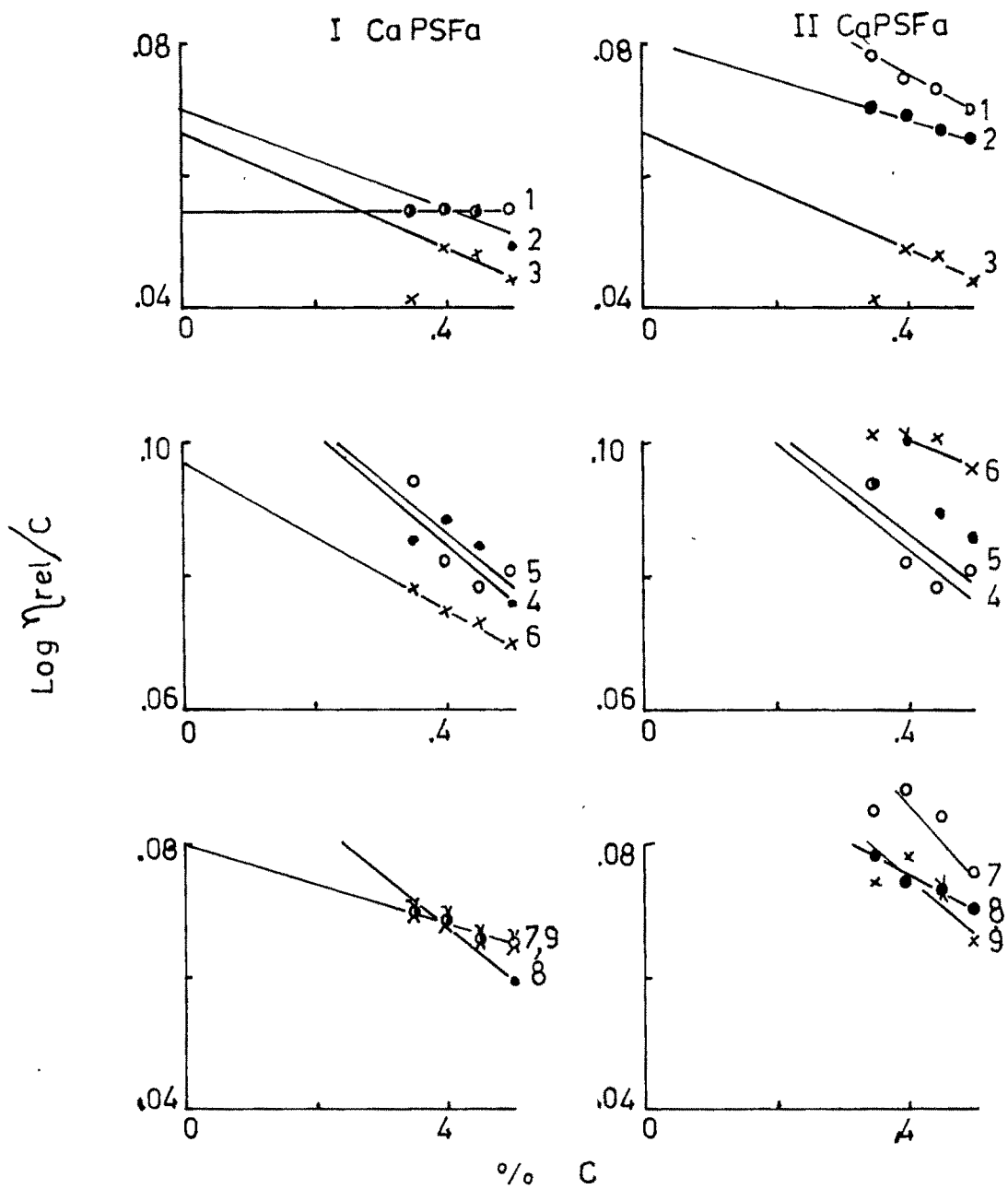
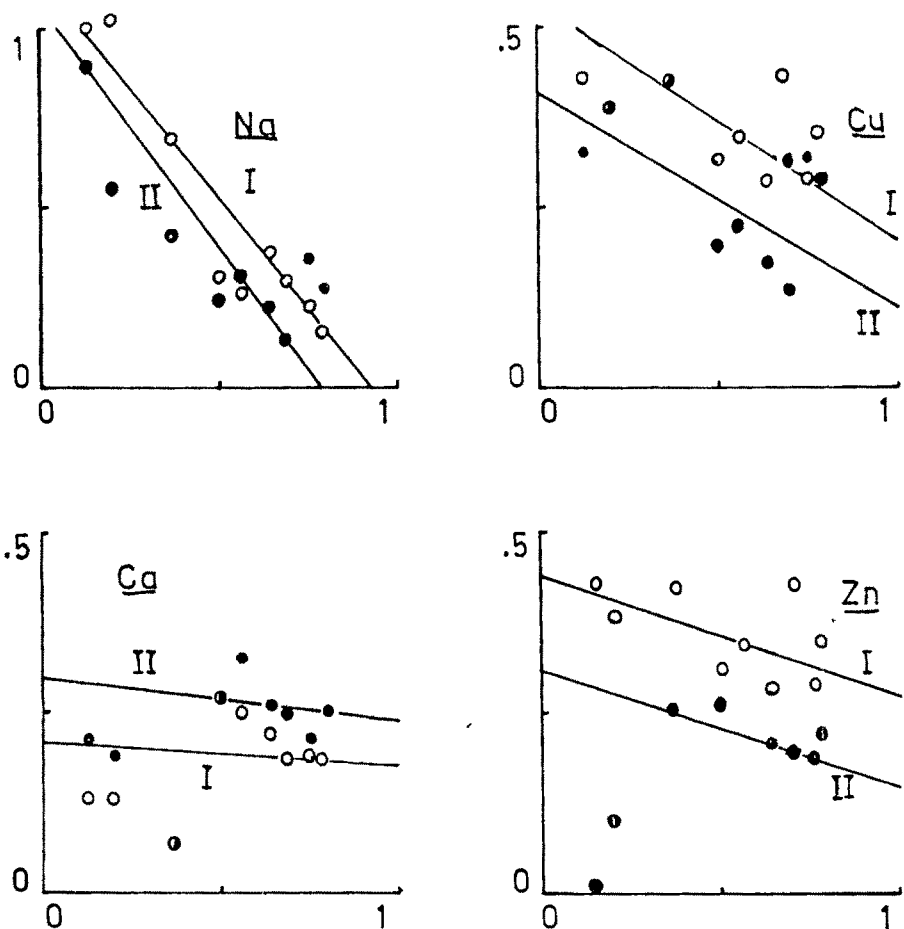


fig.III.51 Plot of $\text{Log } \eta_{rel}/C$ vs % C
for CaPSFa sets

[2]



Mole fraction of Fa in PFa
(for the salts of PFa)

fig.III.52

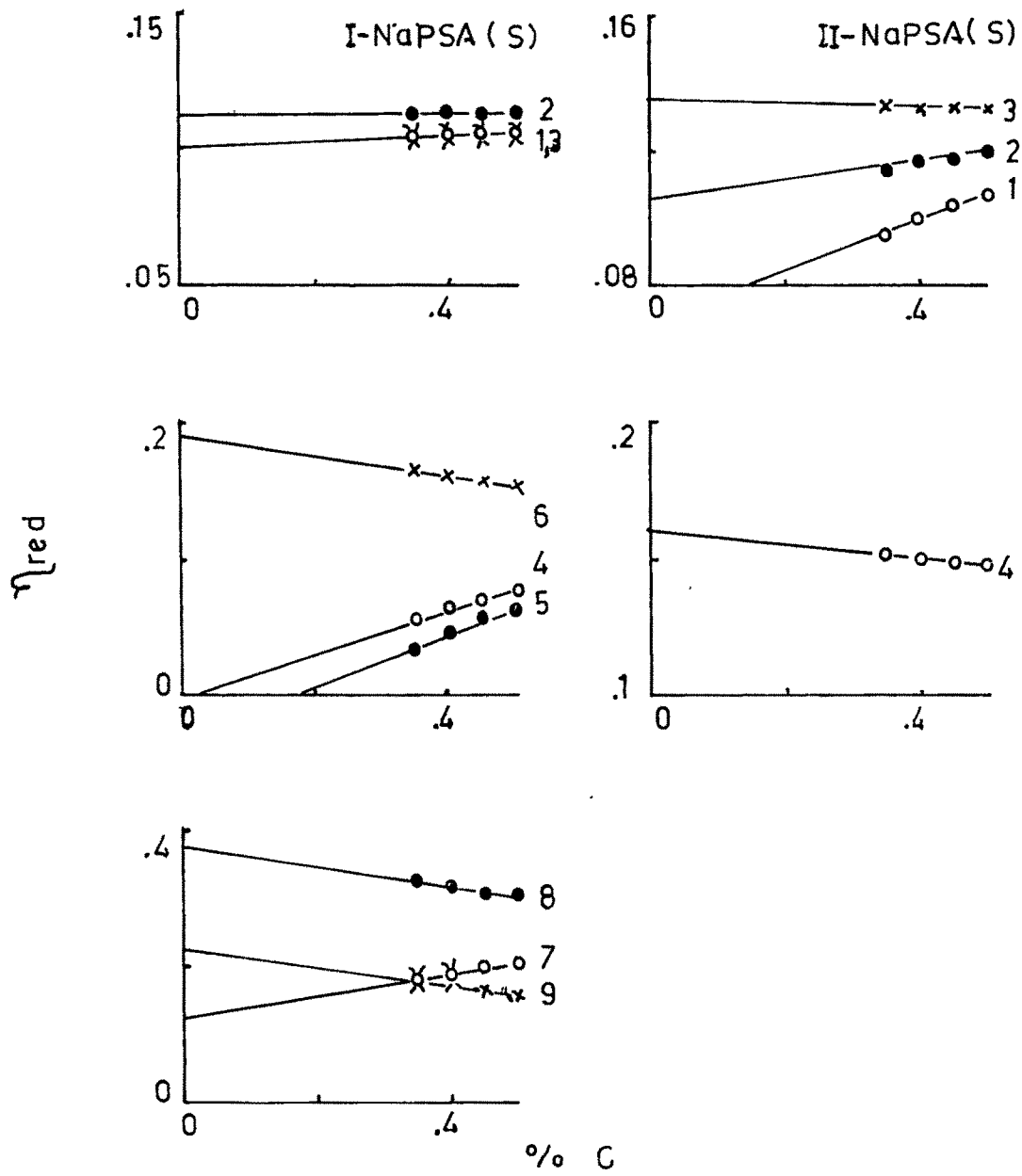


fig.III.53 Plot of η_{red} vs % C
for NaPSA (S) sets

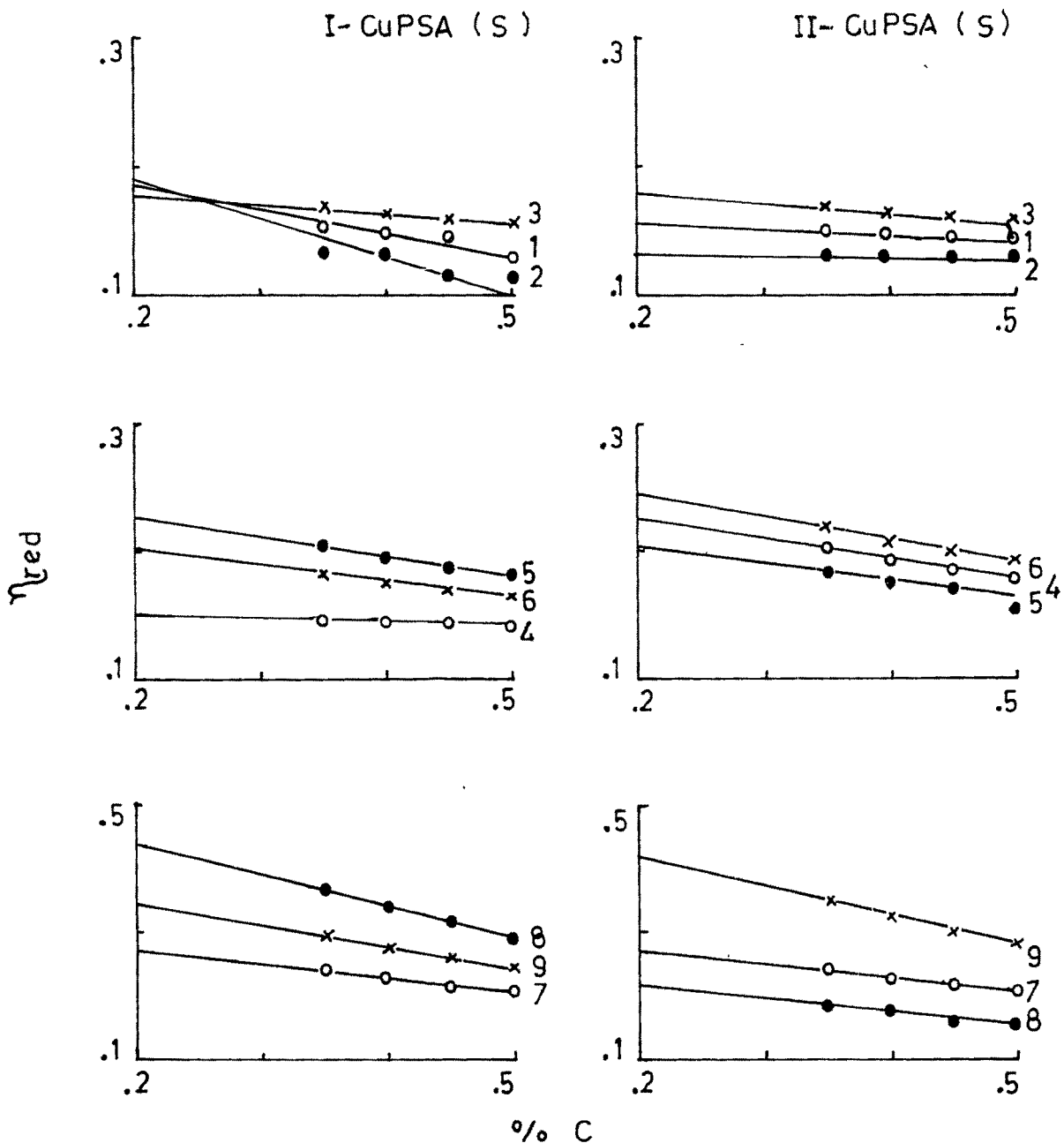


fig.III 54 Plot of η_{red} vs % C
for CuPSA(S) sets

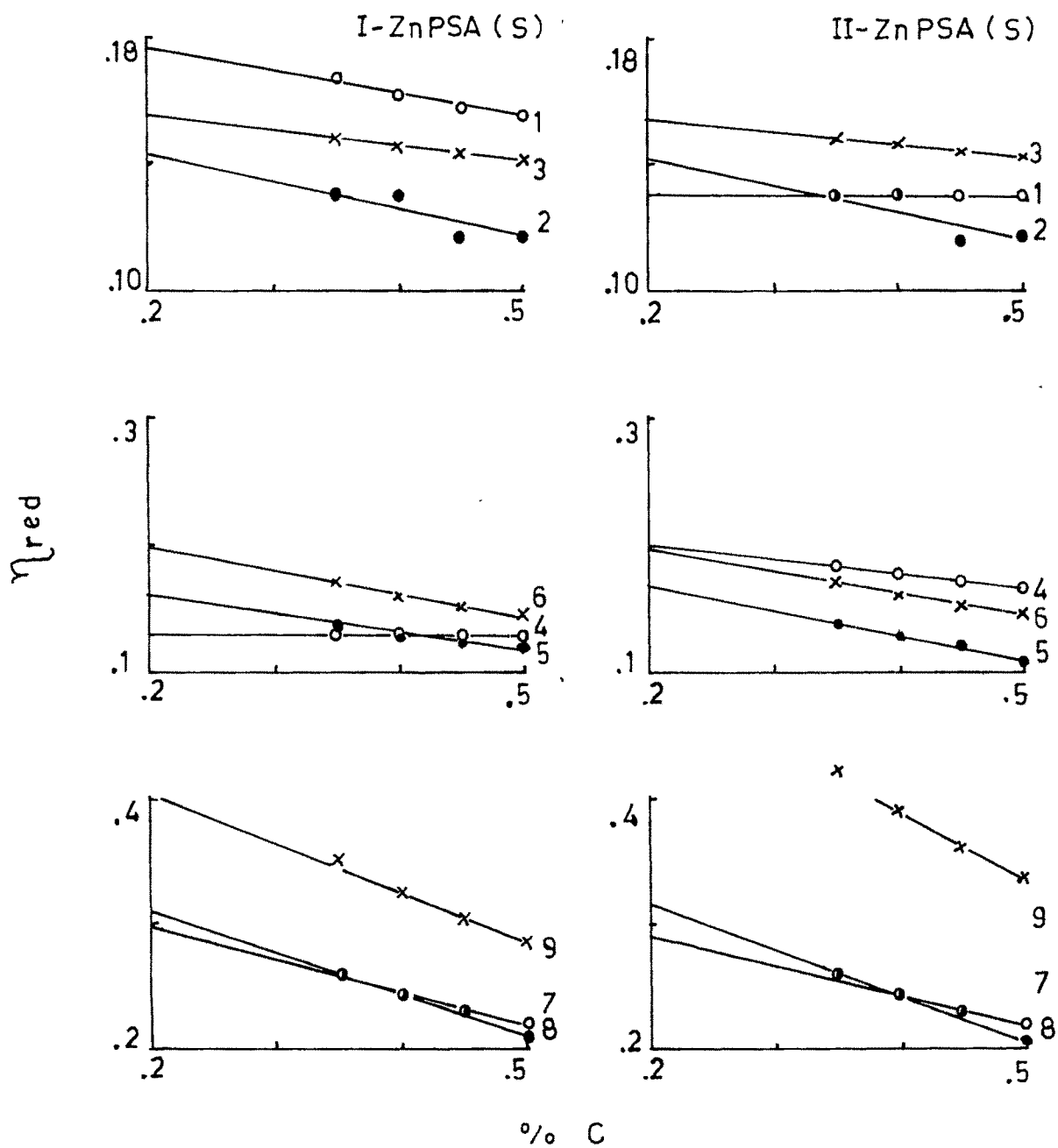


fig.III.55 Plot of η_{red} vs % C
for ZnPSA (S) sets

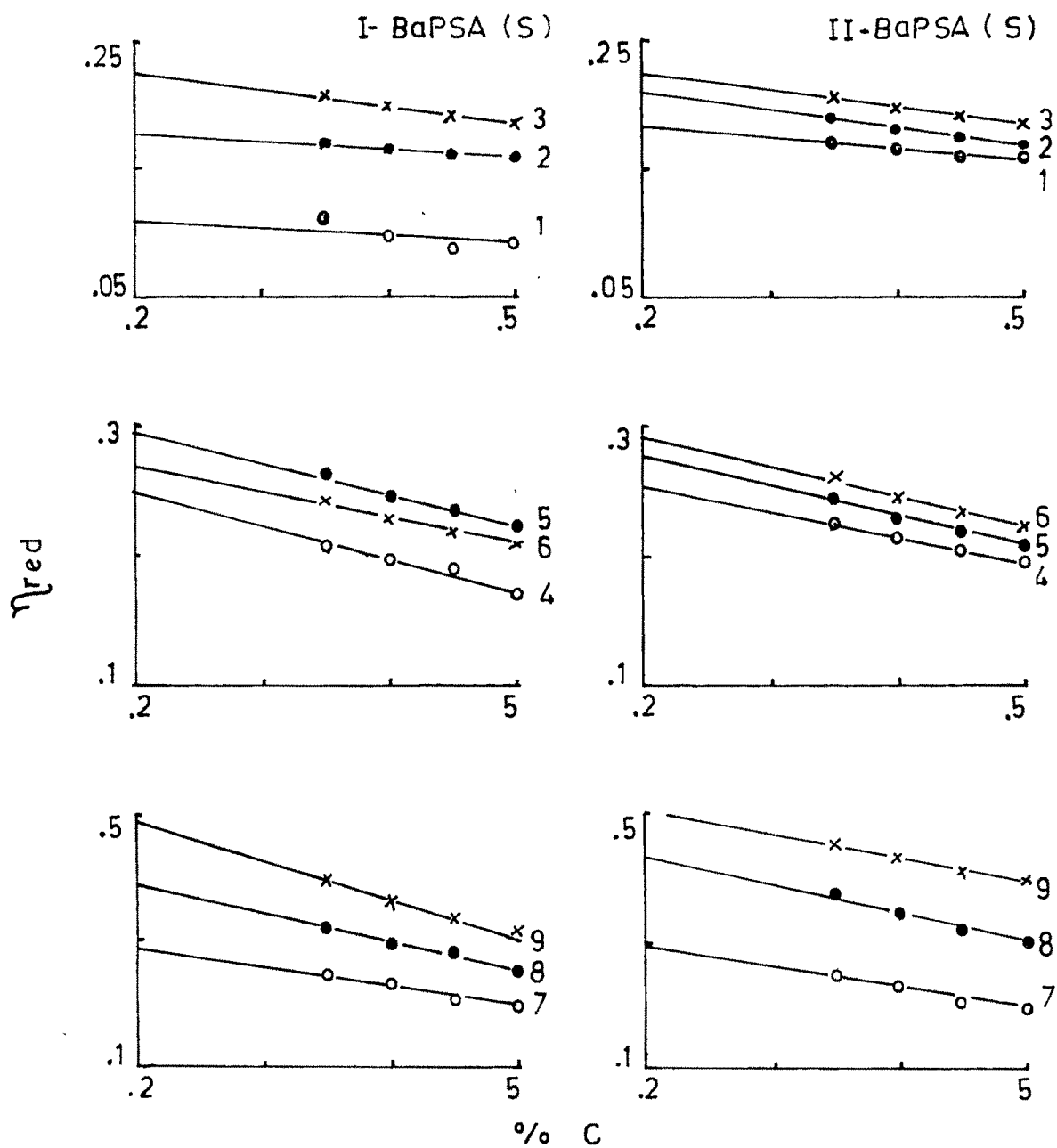


fig.III.56 Plot of η_{red} vs % C
for BaPSA (S) sets

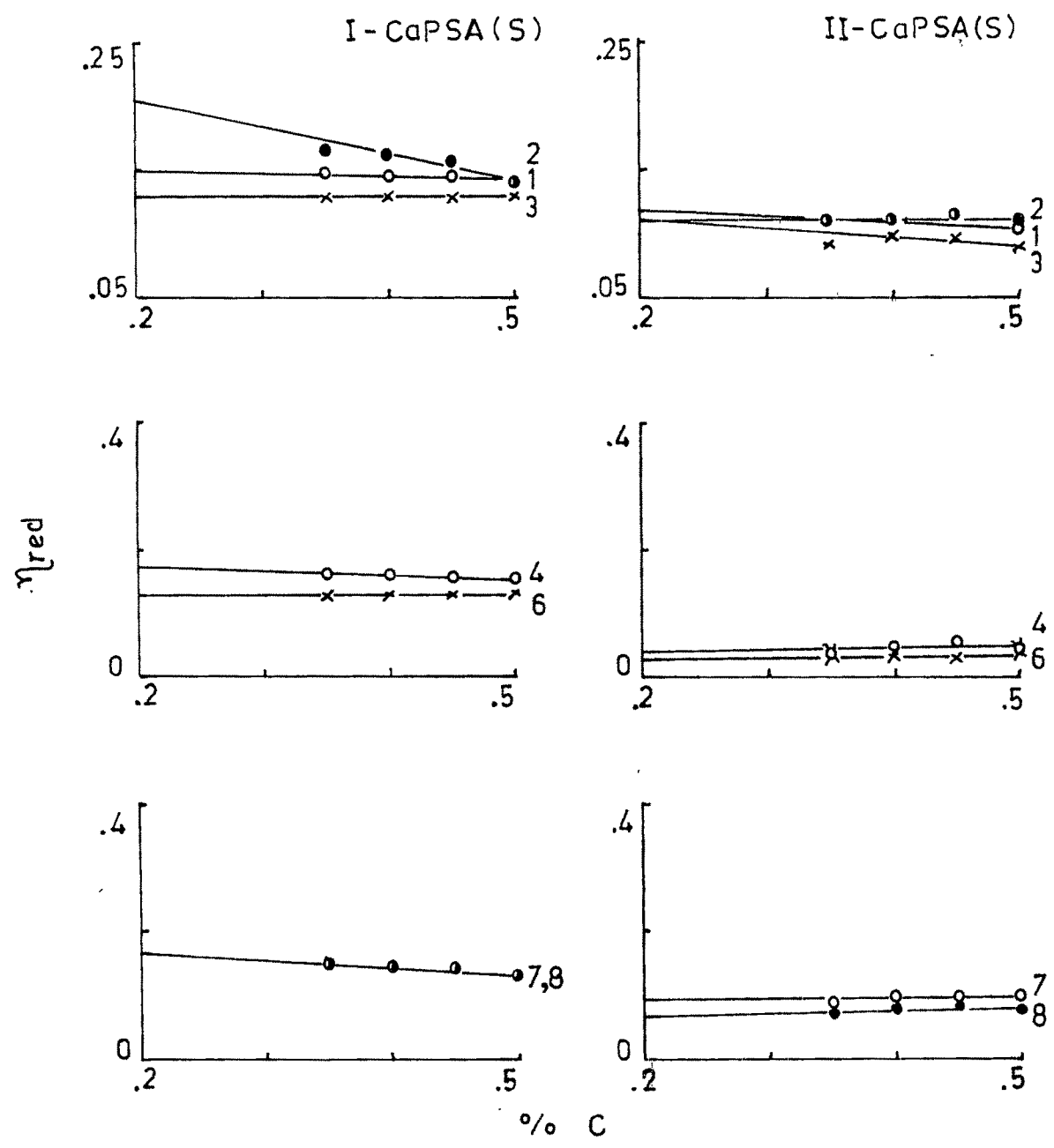


fig III.57 Plot of η_{red} vs % C
for CaPSA(S) sets

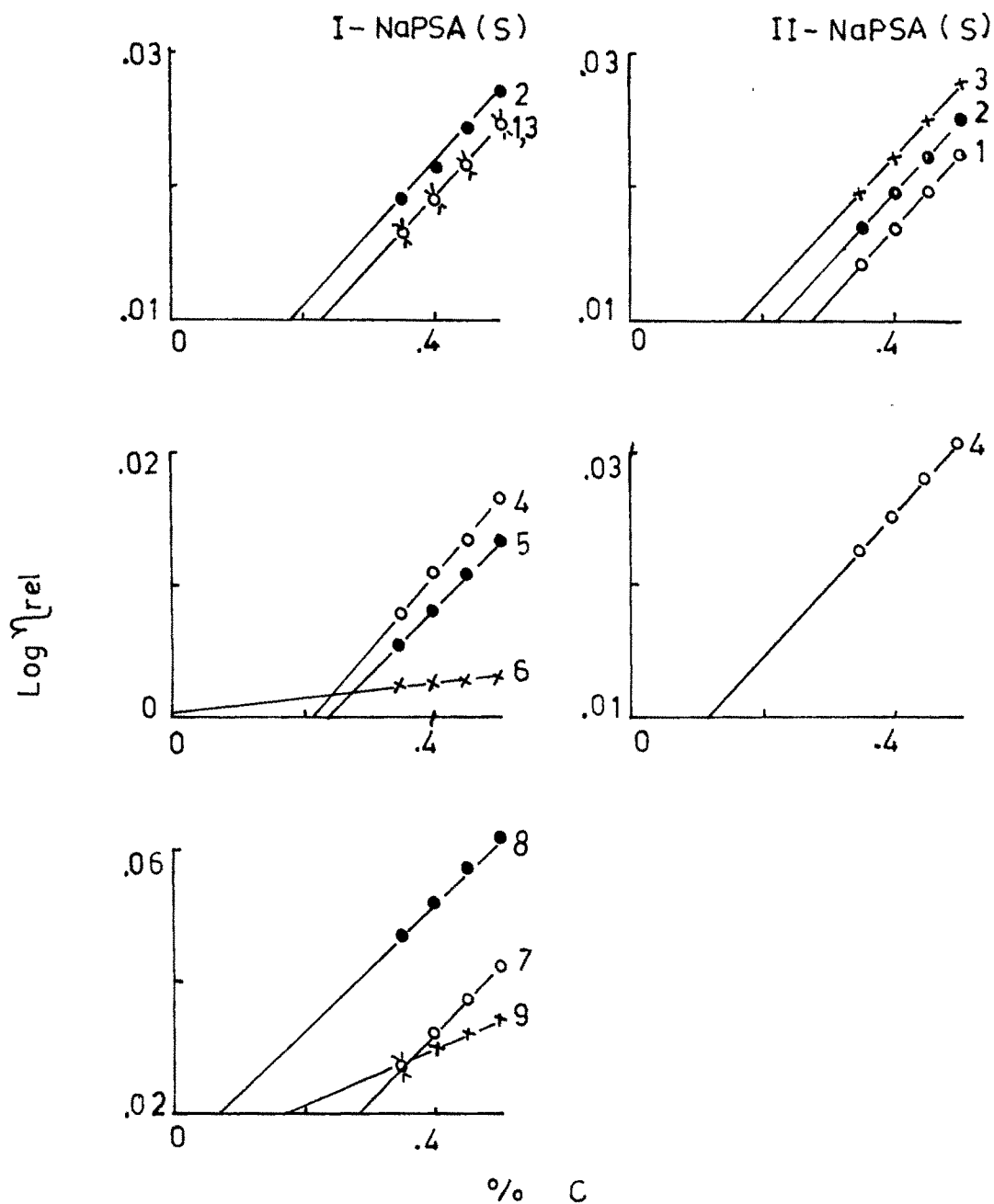


fig.III.58 Plot of $\text{Log } \eta_{\text{rel}}$ vs $\% C$

for NaPSA(S) sets

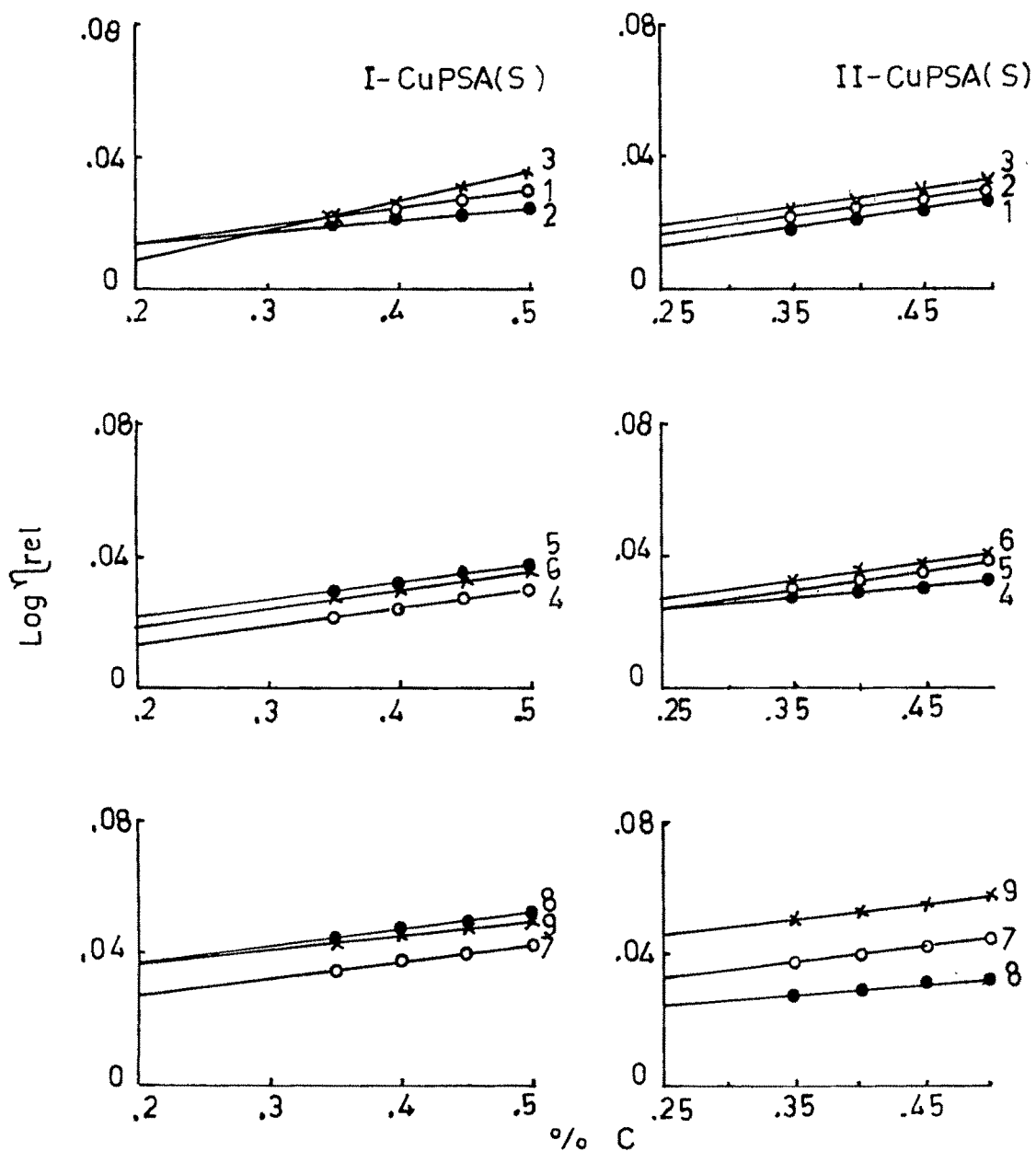


fig. III.59 Plot of $\text{Log } \eta_{\text{rel}}$ vs % C
for the sets of CuPSA(S)

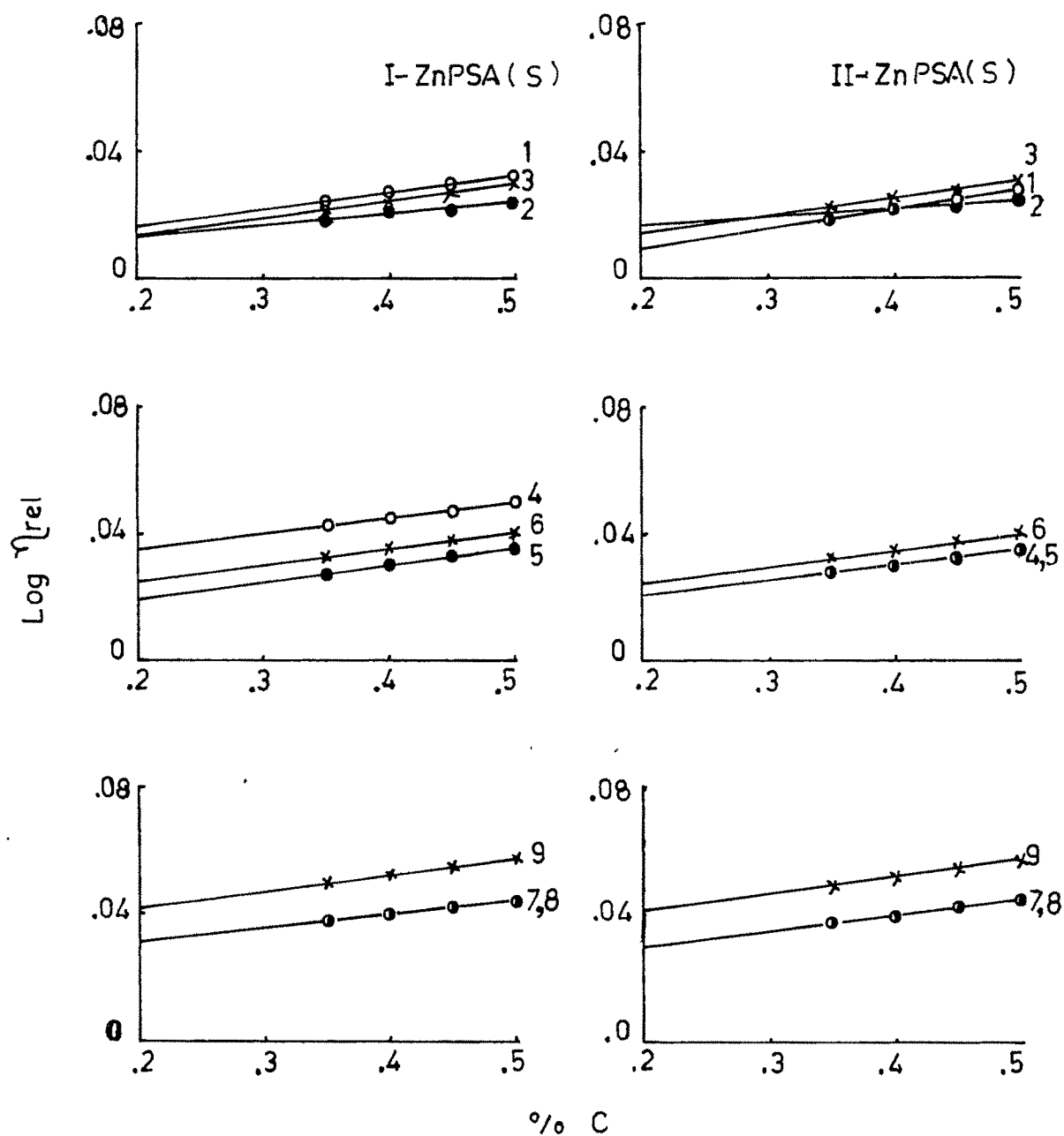


fig.III.60 Plot of $\text{Log } \eta_{\text{rel}}$ vs $\% C$

for the sets of ZnPSA(S)

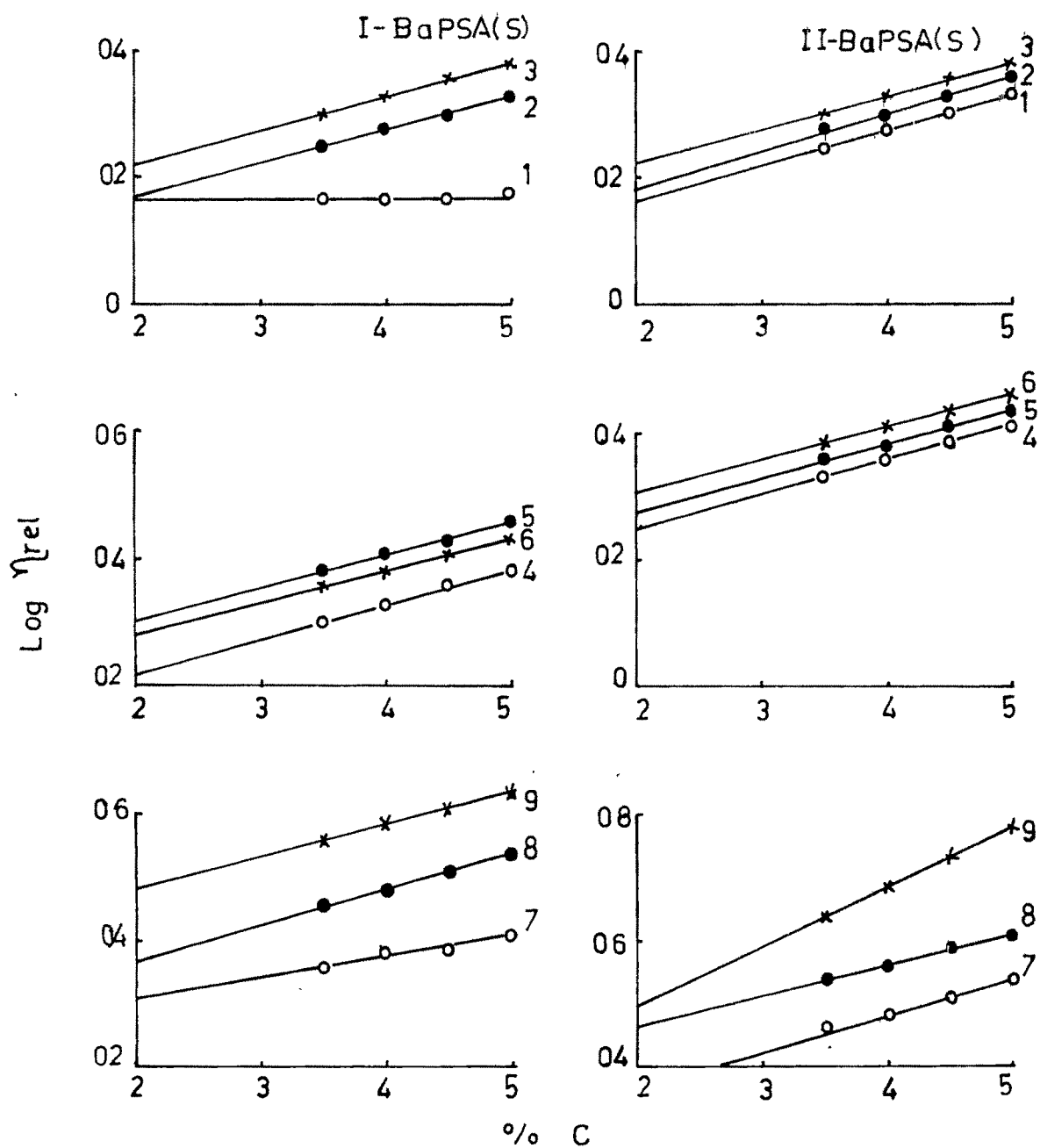


fig. III.61. Plot of $\text{Log } \eta_{\text{rel}}$ vs $\% C$

for the sets of BaPSA(S)

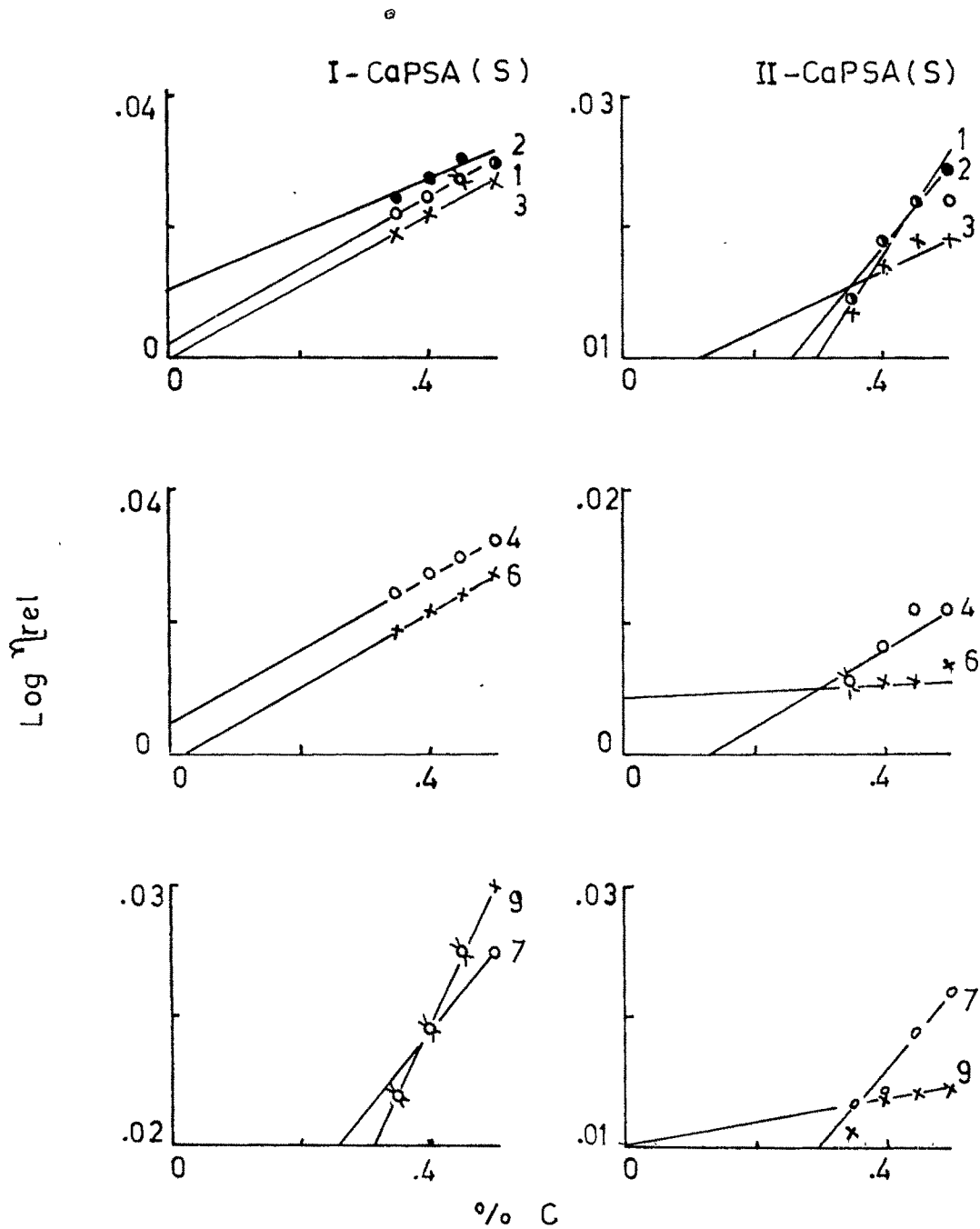


fig.III.62 Plot of $\text{Log } \eta_{\text{rel}}$ vs $\% \text{ C}$
for CaPSA (S) sets

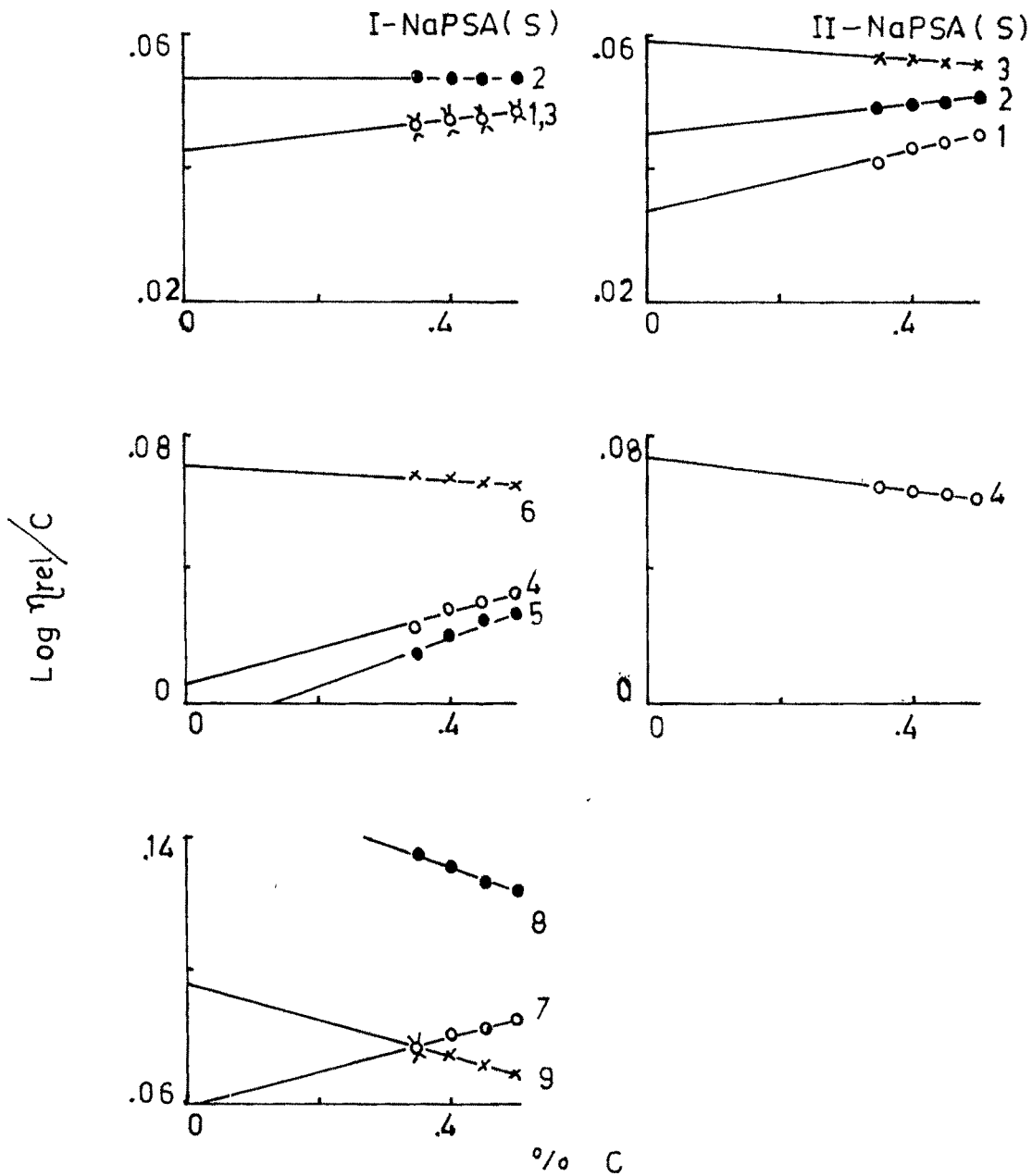


fig.III.63 Plot of $\text{Log } \eta_{rel}/C$ vs $\% C$
for NaPSA(S) sets

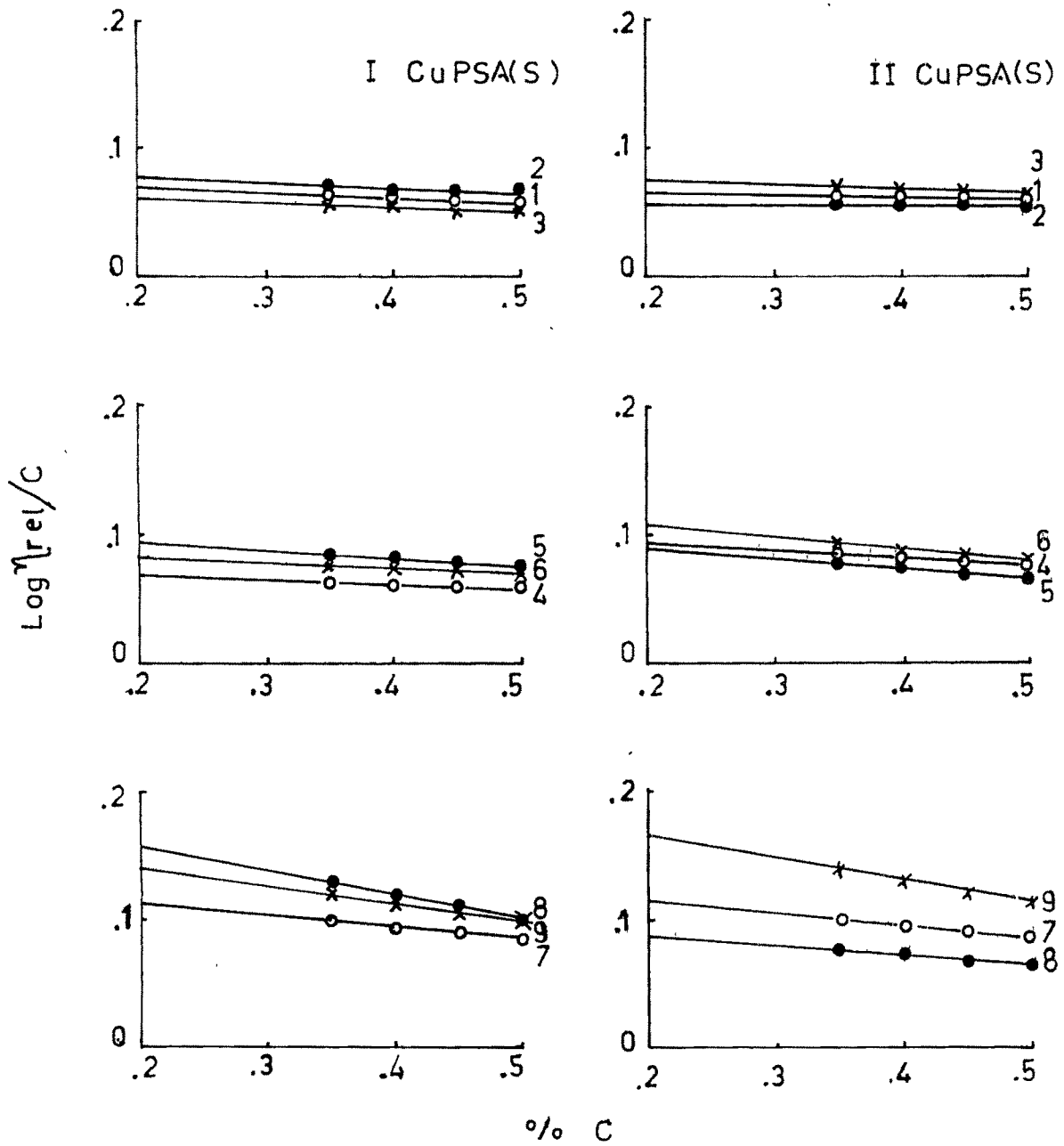


fig. III.64 Plot of $\text{Log } \eta_{\text{rel}}/C$ vs $\% C$
for the sets of CuPSA(S)

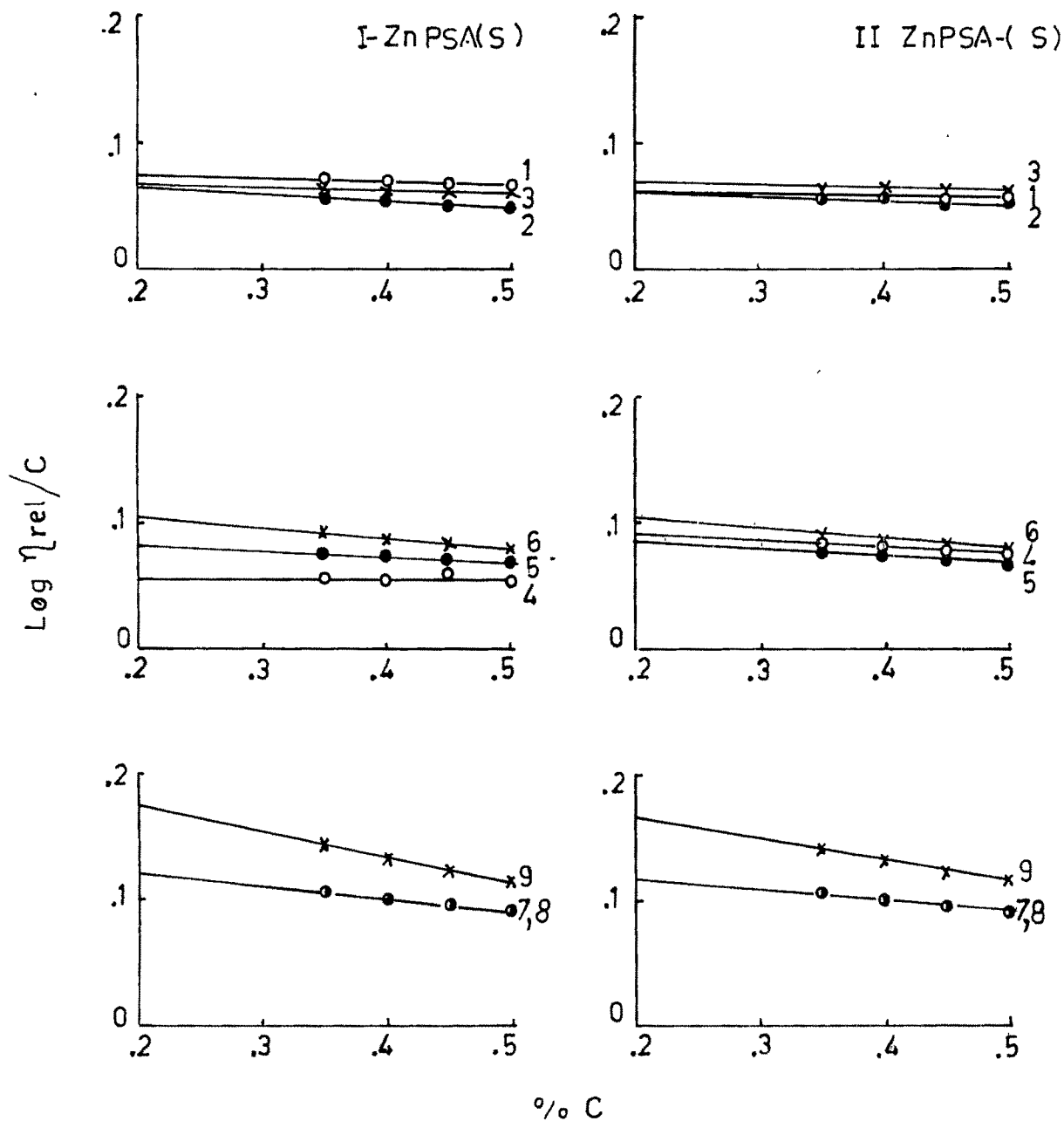


fig.III.65 Plot of $\text{Log } \eta_{\text{rel}}/C$ vs % C for the sets of ZnPSA(S)

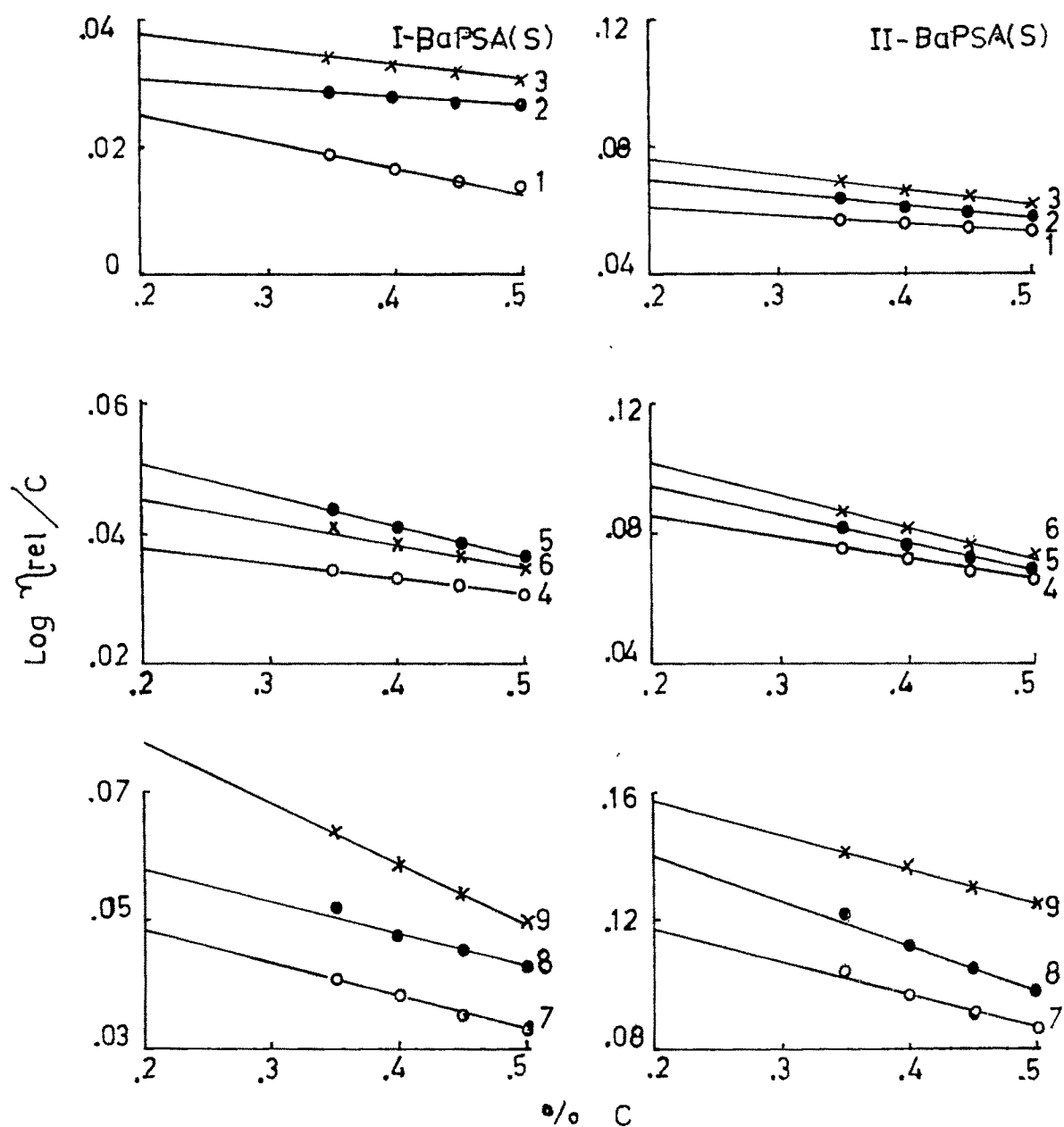


fig. III.66 Plot of $\text{Log } \eta_{rel}/C$ vs $\% C$
for the sets of BaPSA (S)

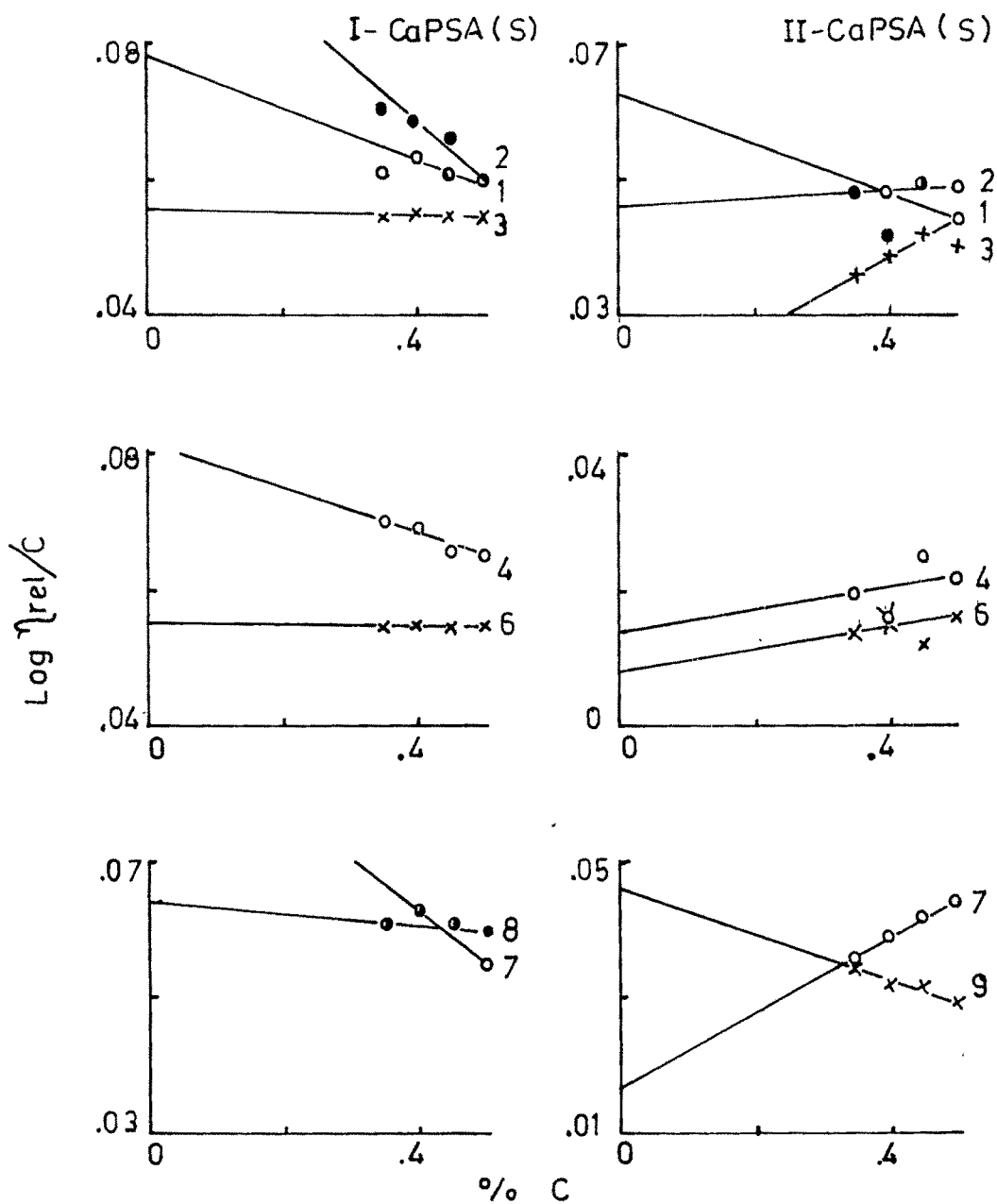


fig.III.67 Plot of $\text{Log } \eta_{rel}/C$ vs $\% C$ for CaPSA (S) sets

of PSMAN higher values are generally observed. It can be attributed to ion-cross-links formed in salts.

It is generally observed that the slopes of the plots are negative for Huggins plots and for Kraemer plots and positive for Martin plots. From the slopes and intercepts, the values of constants k' , k'' and k''' have been calculated. The values of k' vary over a range of -0.2 to -3.2. These values usually increase with increase in the mole fraction of maleic anhydride in PSMAN (in its salts). It also indicates the effect of ion cross-links. Similarly the values of k''' vary from +0.1 to -76.9 and the values of k'' vary from +3.8 to +641.9. Thus the range of variation in the values increases in order.

$$k' < k''' < k''$$

An attempt has been made to calculate Log slope / 2 Log intercept from Martin plots. It was assumed that Log slope = 2 Log intercept and a constant value nearing one would be obtained for the ratio for each series. It has been observed that the value varies (i) From 0.19 to 0.43 for H-form, (ii) from 0.20 to 0.76 for Ca salts (iii) from 0.22 to 0.55 for Zn salt and (iv) 0.26 to 0.51 for Ba salts. The average value can be taken as 0.39. It implies that Martin equation can be better represented as

$$\text{Log } \eta_{\text{rel}} = [\eta'] + k'' [\eta']^a . c$$

An attempt was also made to correlate $[\eta]$ with the degree of substitution (n). The data would not fit the following equations

$$(i) \quad [\eta] = k e^n$$

$$(ii) \quad \text{Log } [\eta] = a + \text{Log } n$$

Salts of PSFa

Intrinsic viscosity $[\eta]$ for all the salts with different degrees of substitution vary with the mole fractions of fumaric acid in the products (fig.III.52). The values of $[\eta]$, $[\eta']$ and $[\eta'']$ increase in order

$$[\eta'] < [\eta''] < [\eta]$$

The slopes of the plots are negative for Huggins plots and for Kraemer plots and generally positive for Martin plots. From the slopes and intercepts, the values of k' , k'' and k''' have been calculated. The values of k' vary over a range of +7.5 to -5.9, the values of k'' vary over a range of -42 to +5000 and the values of k''' vary over a range of -19.2 to +12.5. The range of variation in the values increases in order.

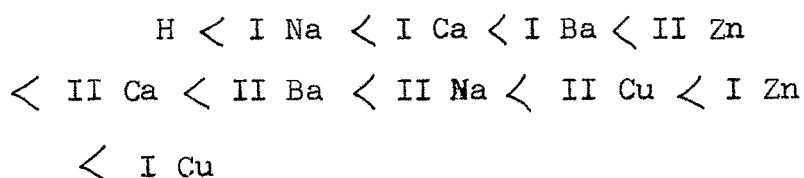
$$k' < k''' < k''$$

An attempt has been made to calculate Log slopes/ 2 Log intercept from Martin plots. If it is assumed that

Log slope = 2 Log intercept the value of the ratio is expected to be nearly 0.21. However, the value obtained vary (i) from 0.18 to 0.45 for H-form (ii) from 0.19 to 0.55 for Na-form, (iii) from 0.24 to 0.49 for Cu-form, (iv) from 0.23 to 0.50 for Zn-form and (v) from 0.19 to 0.44 for Ba form. The average value can be taken as 0.35. It implies that Martin equations be better represented as

$$\text{Log } \eta_{\text{rel}} = [\eta'] + k'' [\eta'']^a c$$

It is observed that the values of $[\eta]$ for the salts are generally higher than those for the corresponding H form of the copolymer set. If PSFa-9 is considered, values of $[\eta]$ increase in order



The order indicates that

(i) the values for 20 % substituted copolymers are lower than those for 50 % substituted copolymers in case of Na, Ca and Ba and (ii) the values for 20 % substituted copolymers are higher than those for 50 % substituted copolymers in case of Cu and Zn. It is suggested that transition metal ions differ in their behaviour in these polymers from alkali and alkaline earth metal ions.

Salts of PSA(s)

Intrinsic viscosity $[\eta]$ for all salts with different degrees of substitution vary with the mole fraction of acrylic acid in the product (fig III.68). The values of $[\eta]$, $[\eta']$ and $[\eta'']$ increase in order.

$$[\eta'] < [\eta''] < [\eta]$$

The slopes of the plots are negative for Huggins plots and for Krammer plots (except for some Na and Ca salts) and positive for Martin plots. From the slopes and intercepts, the values of k' , k'' and k''' are calculated. The values of k' vary from - 0.1 to - 5.6, the values of k'' vary from 30 to 7000, and the values of k''' vary from - 2.8 to -29.4. The range of variation in the values increases in order

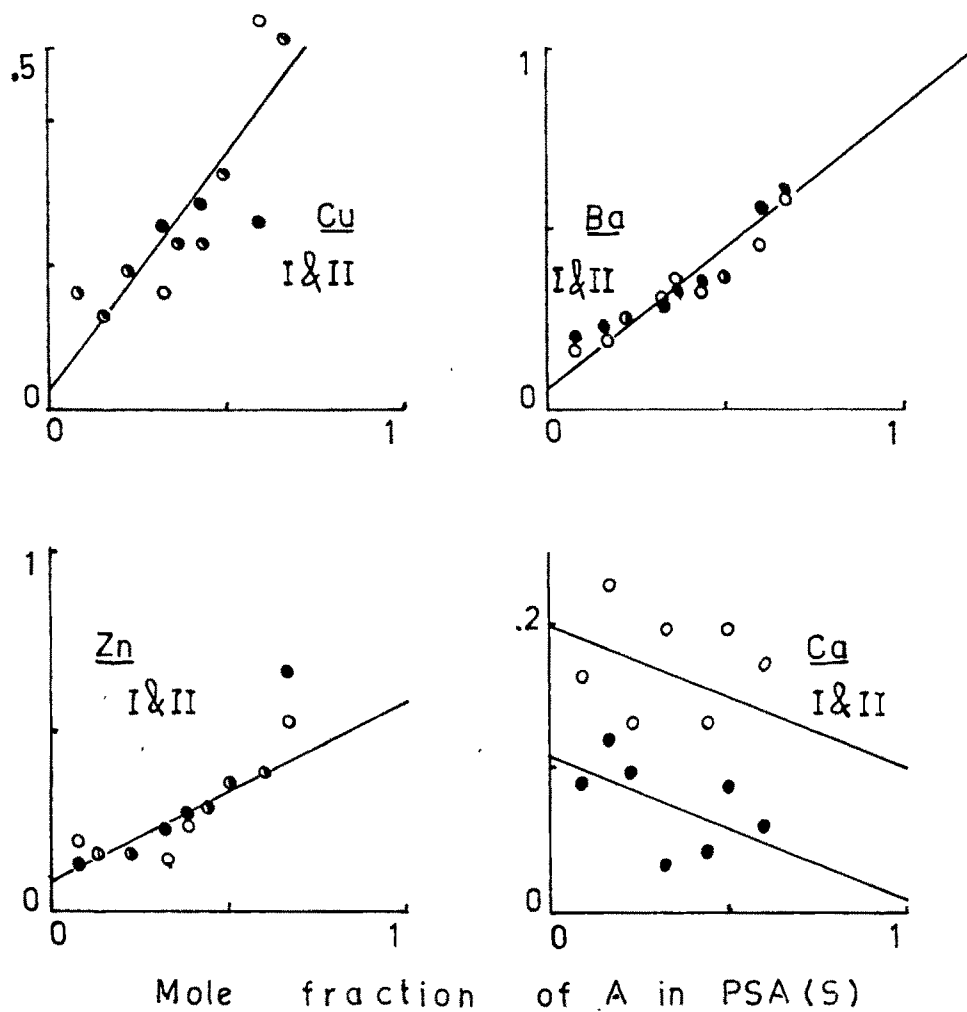
$$k' < k''' < k''$$

It is observed that the values of $[\eta]$ for the salts are generally higher than those for the corresponding H-forms of the copolymer set. If PSA(S)-9 is considered, the values of $[\eta]$ increase in order

$$\begin{aligned} \text{H} < \text{I Cu} < \text{II Cu} < \text{I Zn} < \text{I Ba} < \text{II Ba} \\ < \text{II Zn} \end{aligned}$$

The order indicates that the values for 20% substituted copolymers are lower than those for 50 % substituted ones in case of Cu, Zn and Ba.

[η]



Mole fraction of A in PSA(S)
 [for the salts of PSA(S)]
fig.III.68

III.6. Copolymers of styrene with acrylic acid and their salts

(Bulk polymerization)

6.(a) Copolymers - PSA(B)

A set of nine copolymers of styrene with acrylic acid with varying mole proportions was prepared at 70°C. The yield increased from 84 % to 99 % as the mole % of acrylic acid in the feed increased from 5 % to 66 %. The products are white or pale yellow and soluble in acetone, DMF, etc. The mole fraction of acrylic acid in the product, calculated on the basis of the formula suggested from AVS studies and analytical data, varies from 0.44 to 0.91. If the mole fraction of the acid in the product is plotted vs mole fraction of acid in the feed (fig. III.69) a *curve* is obtained. If these data are compared with the data presented in fig. III.18 it will be observed that mole fraction of acid in the copolymer is much higher in the product formed by bulk polymerization than the product formed by solution polymerization. The products obtained by bulk polymerization may be blocky copolymers (132).

The products show a small variation in melting point. If the melting point is plotted versus mole fraction of acid in the product (fig. III.70) a straight line is obtained.

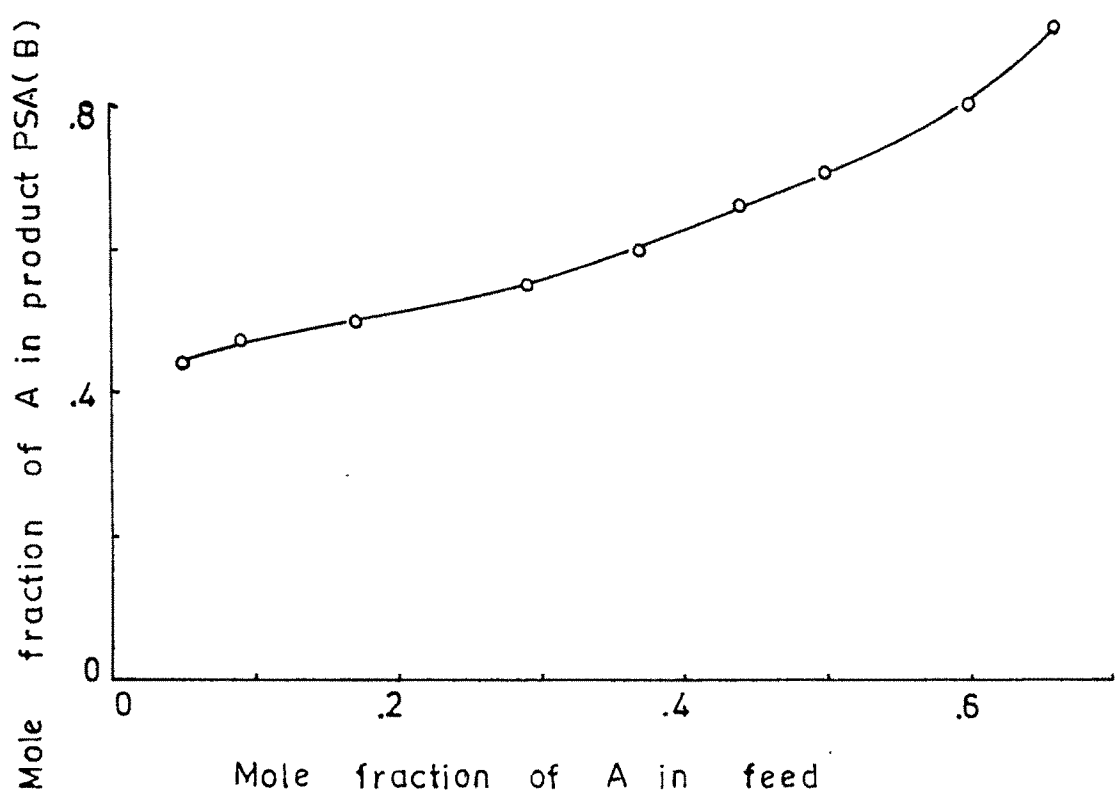


fig. III.69

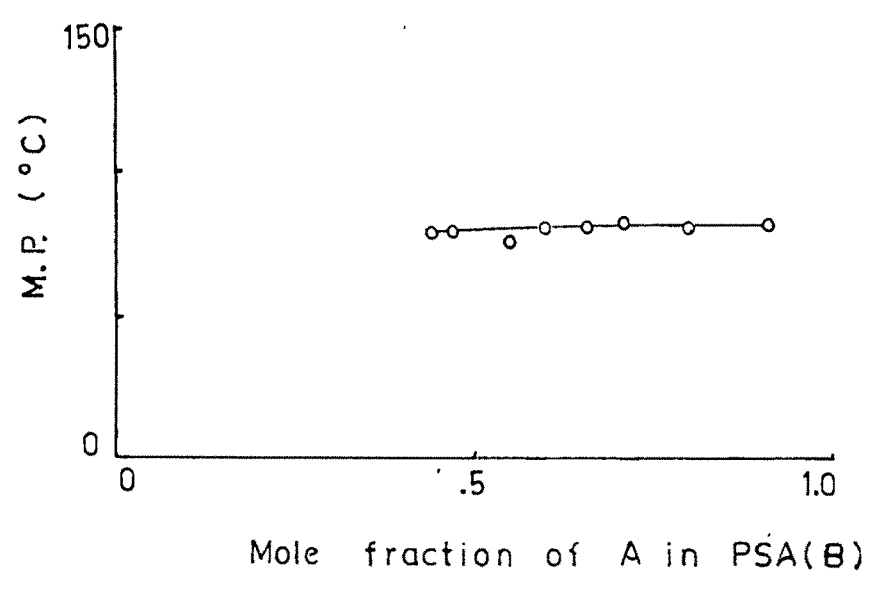


fig. III.70

Studies of the IR spectra of PSA(B)-1,5 and 9 show that absorption band at about 1700 cm^{-1} is somewhat increasing and the absorption band at 695 cm^{-1} is decreasing with the increase in the mole fraction of acid in the products.

Huggins plots, Martin plots and Kraemer plots showing the variation of viscosity with concentration are presented in fig. III.71, 72 and 73 respectively. The values of increase with increasing mole fraction of acid in the product. The values of $[\eta]$, $[\eta']$ and $[\eta'']$ lie in the range of 0.47 to 1.12, 0.016 to 0.059 and 0.135 to 0.45 respectively. Thus

$$[\eta'] < [\eta''] < [\eta]$$

The slopes of the curves are negative for Huggins plots and Kraemer plots and positive for Martin plots. From the values of slopes and intercepts, the value of the constants k' , k'' and k''' are evaluated and are presented in table III.5. It is observed that the values of k' and k''' vary over a small range, while those of k'' vary over a very wide range.

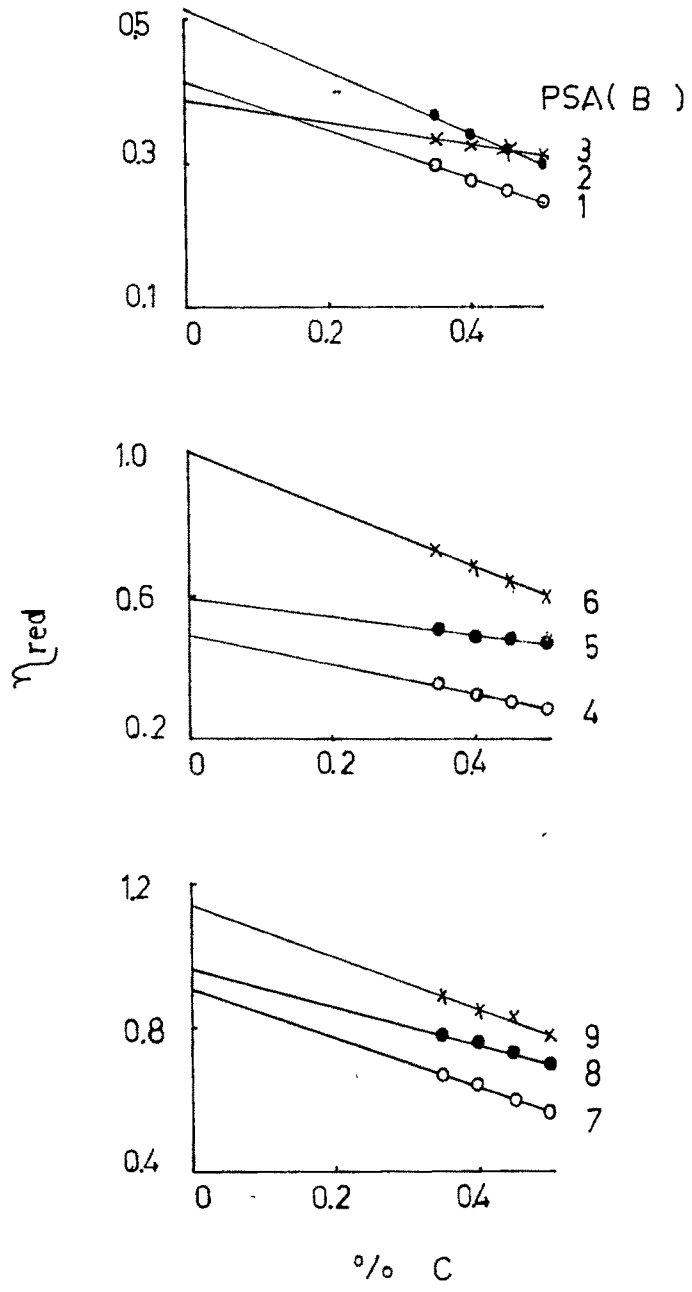


fig. III.71 Plot of η_{red} vs % C
for the set of PSA(B) (H form)

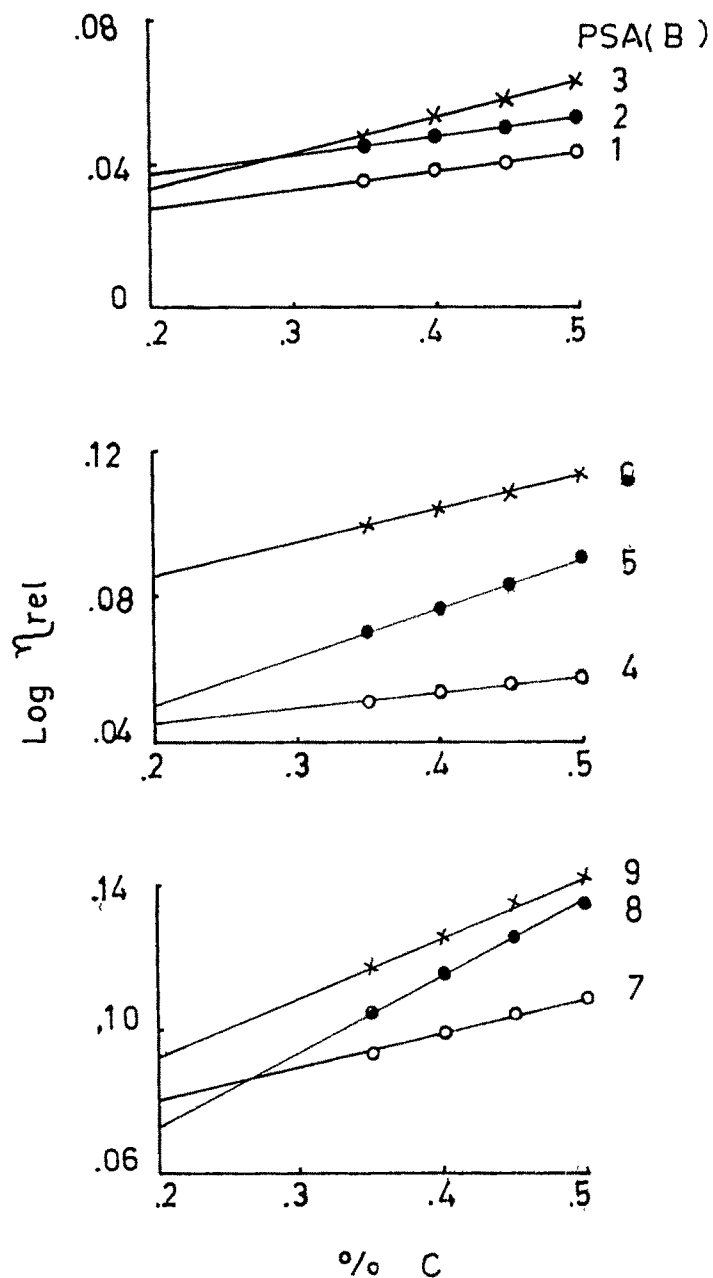


fig. III.72 Plot of $\text{Log } \eta_{\text{rel}}$ vs $\% C$
for the set of $\text{PSA}(B)$ (H form)

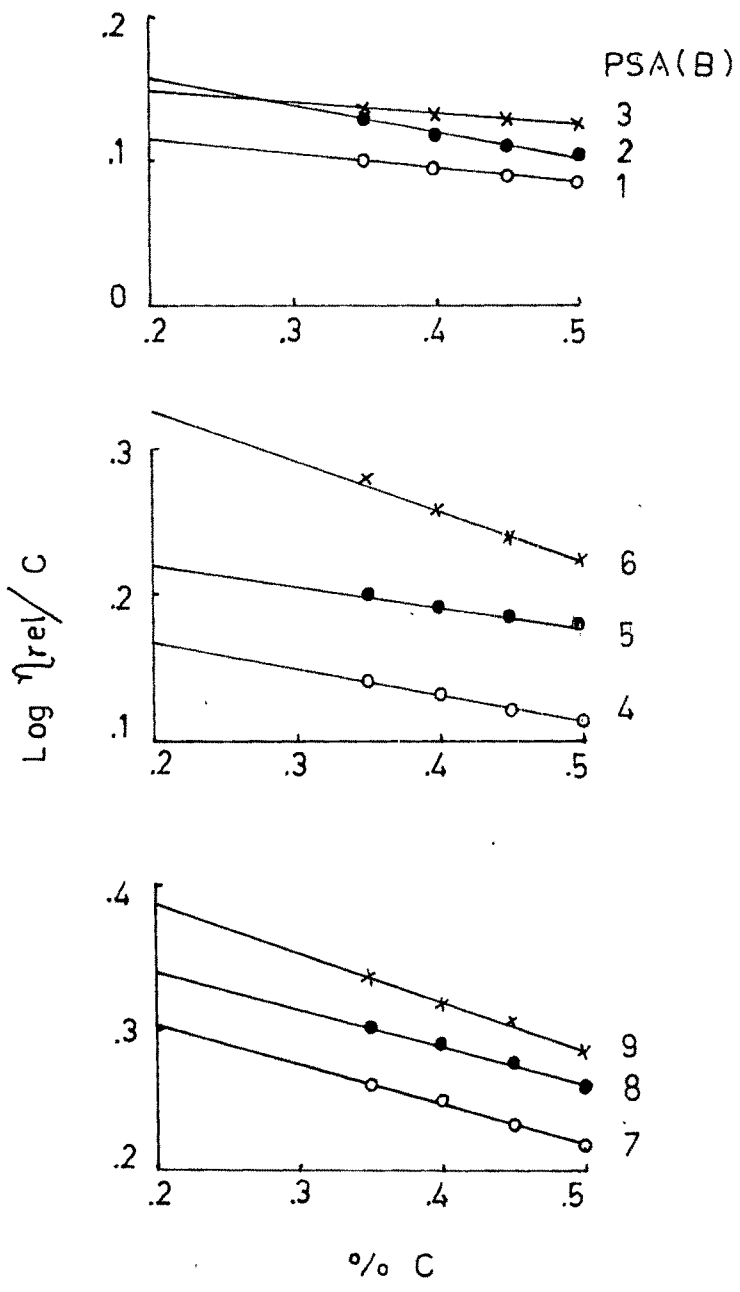


fig. III.73 Plot of $\text{Log } \eta_{\text{rel}}/C$ vs $\% C$
for the set of $\text{PSA}(B)$ (H form)

Table III.5

No	Product	constant		
		k'	k''	k'''
1	PSA(B)-1	- 2.0	210.9	- 5.5
2	PSA(B)-2	- 1.8	704	-25.6
3	PSA(B)-3	- 1.0	3906.3	- 2.83
4	PSA(B)-4	- 1.7	32.1	- 4.4
5	PSA(B)-5	- 0.6	230.9	- 2.6
6	PSA(B)-6	- 0.8	18.6	- 2.1
7	PSA(B)-7	- 0.8	24.5	- 2.2
8	PSA(B)-8	- 0.4	222.2	- 1.7
9	PSA(B)-9	- 0.5	48.0	- 1.6

6(b) Salts of copolymers

To prepare partial salts, available acid content of these copolymers on reaction for 24 hrs was determined. And 20 % and 50 % substitution of the available acidic proton by Na, Cu, Zn, Ba and Ca was carried out. These salts were studied for their viscosity in solution.

Reduced viscosity of these salts in solution was calculated and plotted against % C in figs. III.74, 75, 76, 77 and 78. Plots of $\text{Log } \eta_{\text{rel}}$ vs % C are presented in figs III.79, 80, 81, 82 and 83 and plots of $\text{Log } \eta_{\text{rel}}/C$ vs % C are presented in figs. III 84, 85, 86, 87 and 88. Values of $[\eta]$ increase with the increase in mole fraction of the acid in the copolymeric salts. The values of intrinsic viscosity lie in the range of (i) 0.15 to 1.15 for Huggins plots, (ii) 0.01 to 0.08 for Martin plots and (iii) 0.12 to 0.55 for Kraemer plots. Generally the values increase in order

$$[\eta'] < [\eta''] < [\eta]$$

Increase in the values of intrinsic viscosity with the increase in mole fraction of acid in the product indicates the effects of ion-aggregates and ion cross-links.

Considering the salts of PSA(B)-9, the increasing order for the values of $[\eta]$ can be suggested as follows

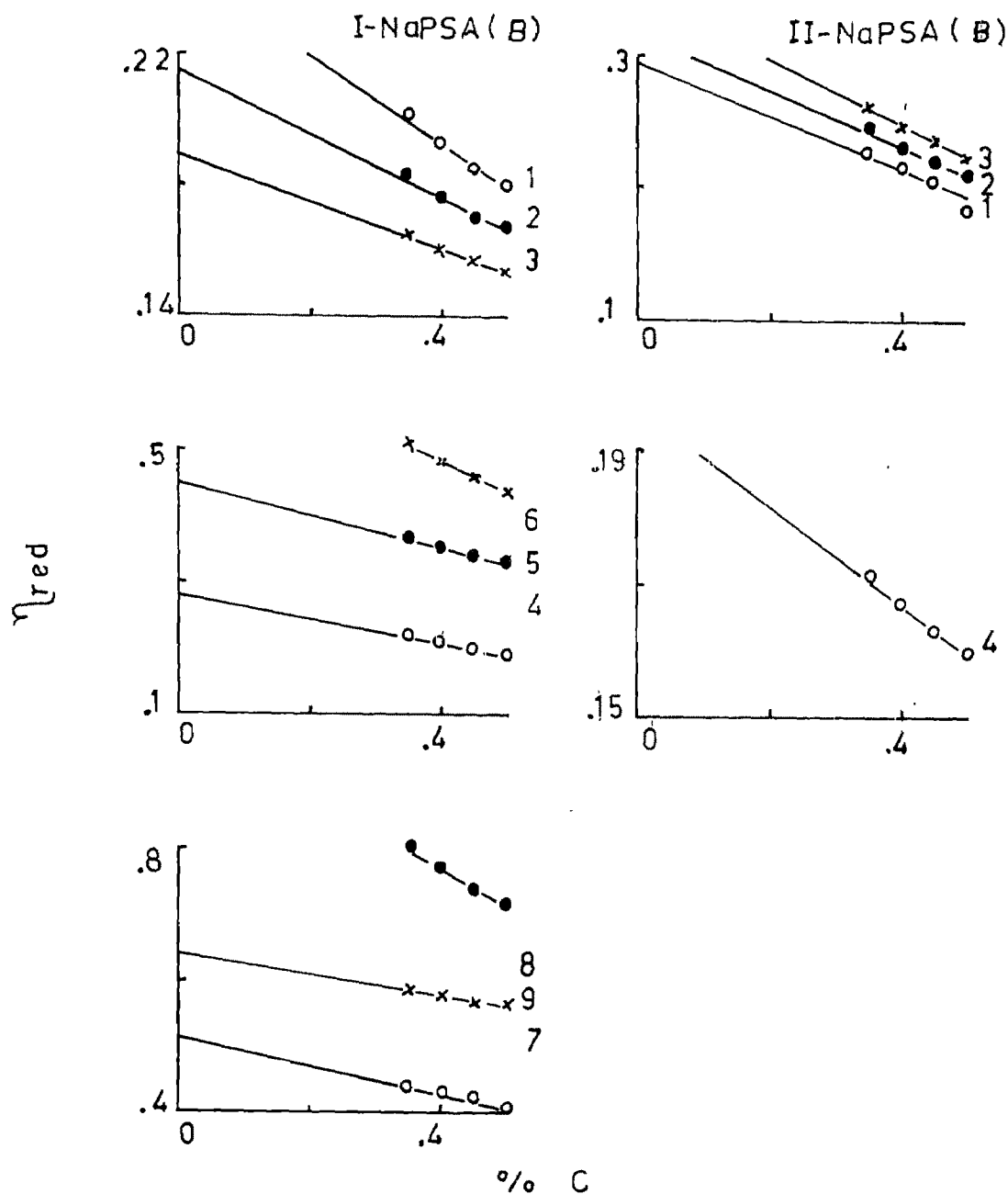


fig. III.74 Plot of η_{red} vs $\% C$
for NaPSA(B) sets

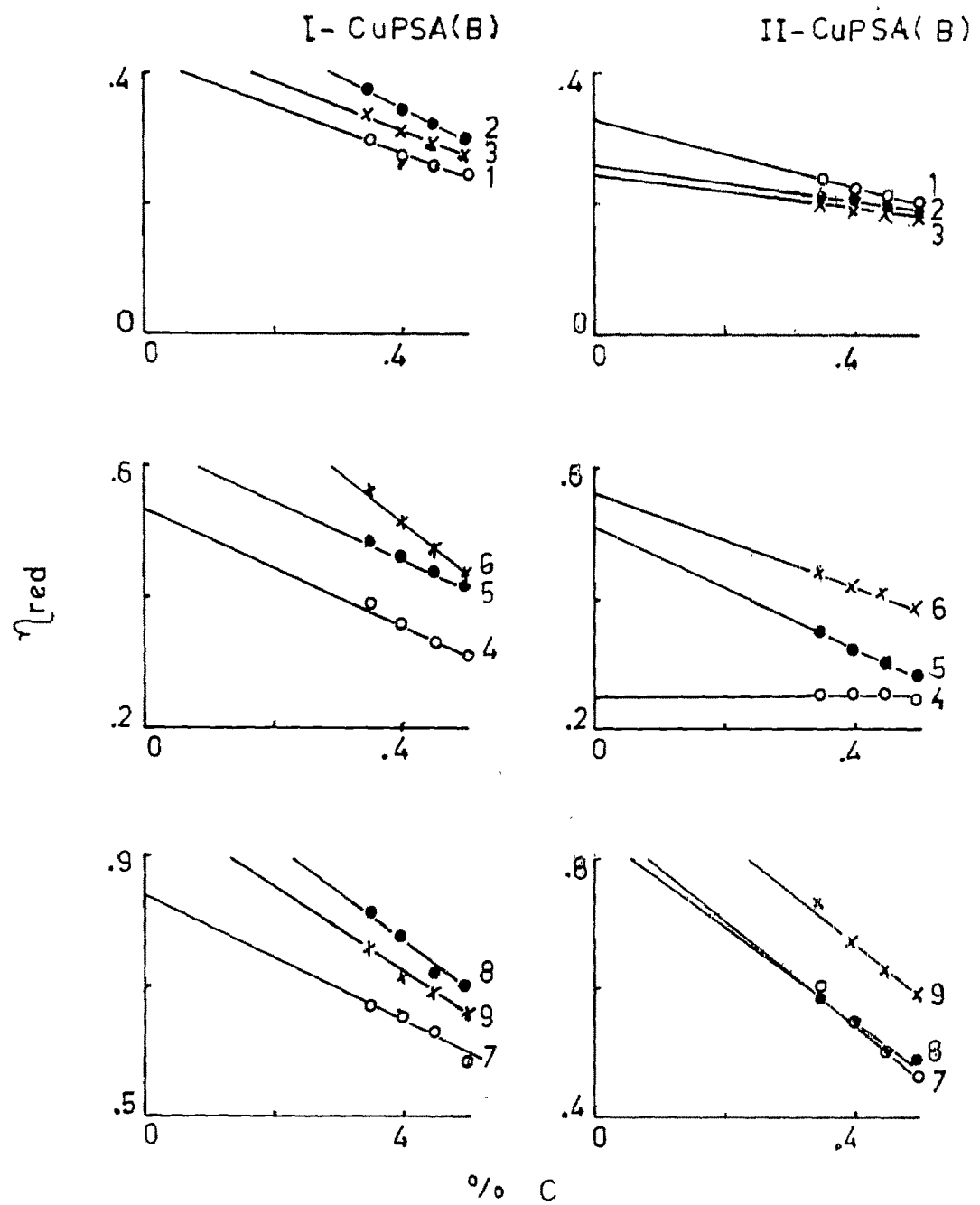


fig.III.75 Plot of η_{red} vs % C
for CuPSA(B) sets

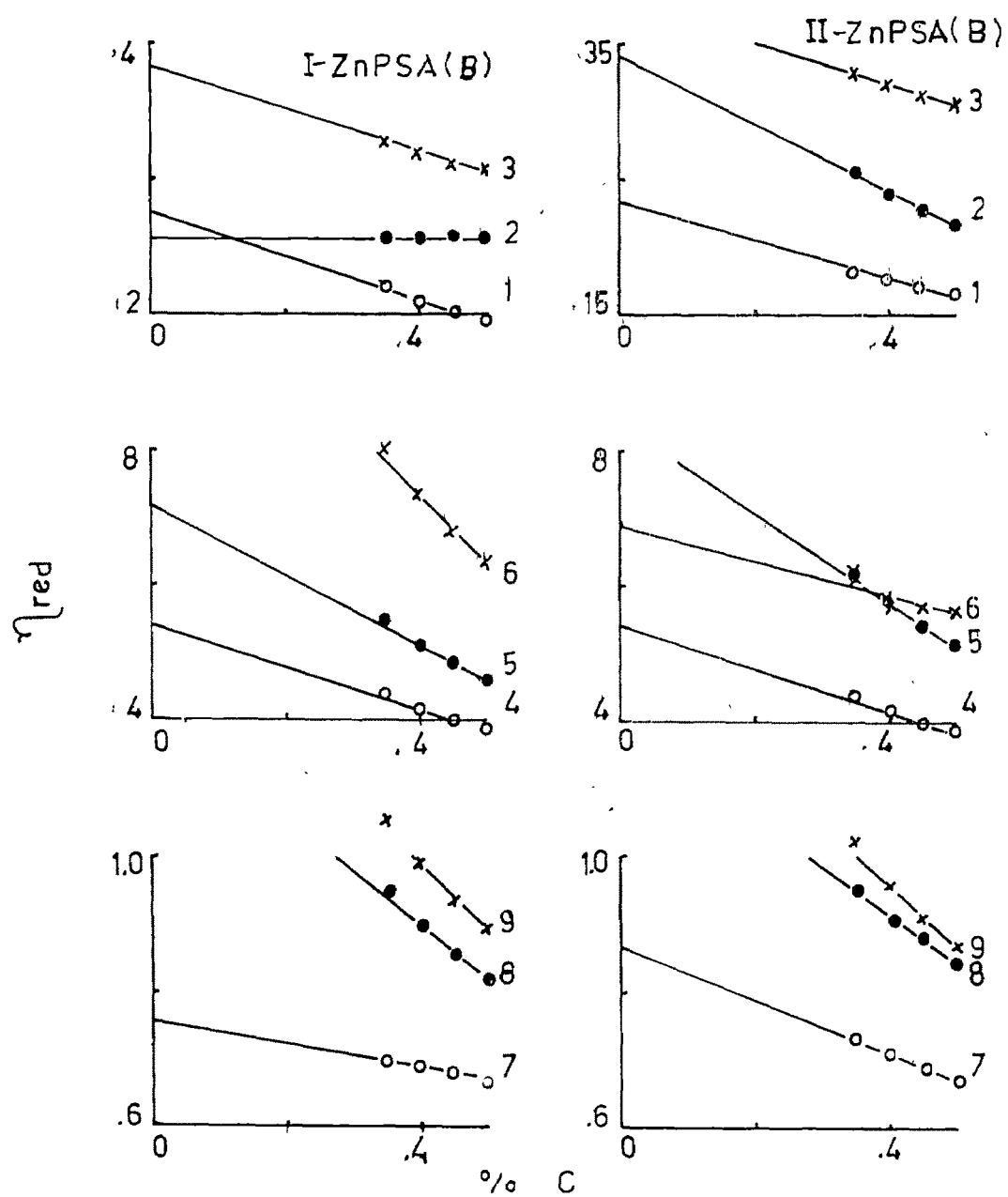


fig. III.76 Plot of η_{red} vs % C
for ZnPSA(B) sets

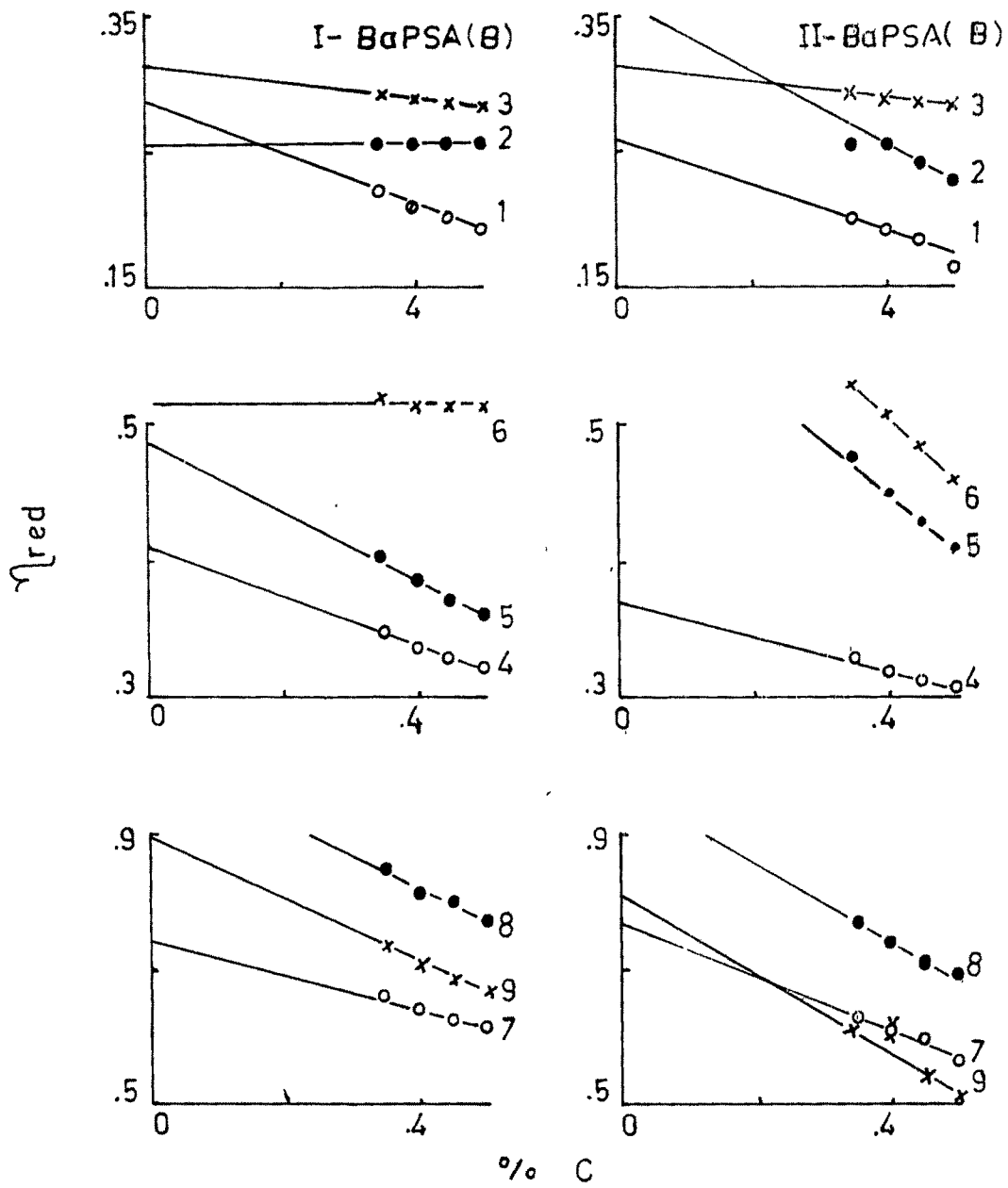


fig. III.77 Plot of η_{red} vs % C
for BaPSA(B) sets

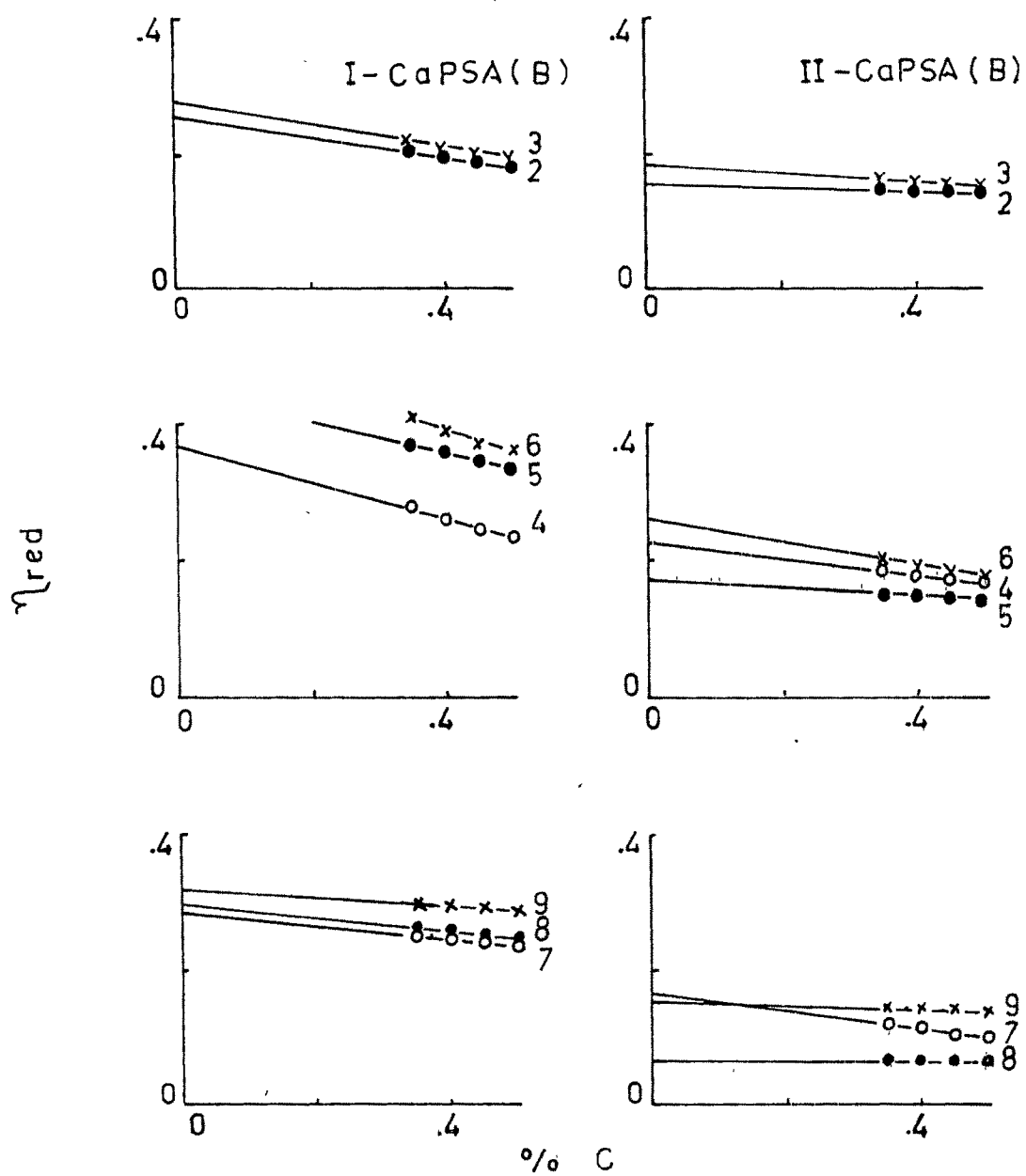


fig. III.78 Plot of η_{red} vs % C
for CaPSA(B) sets

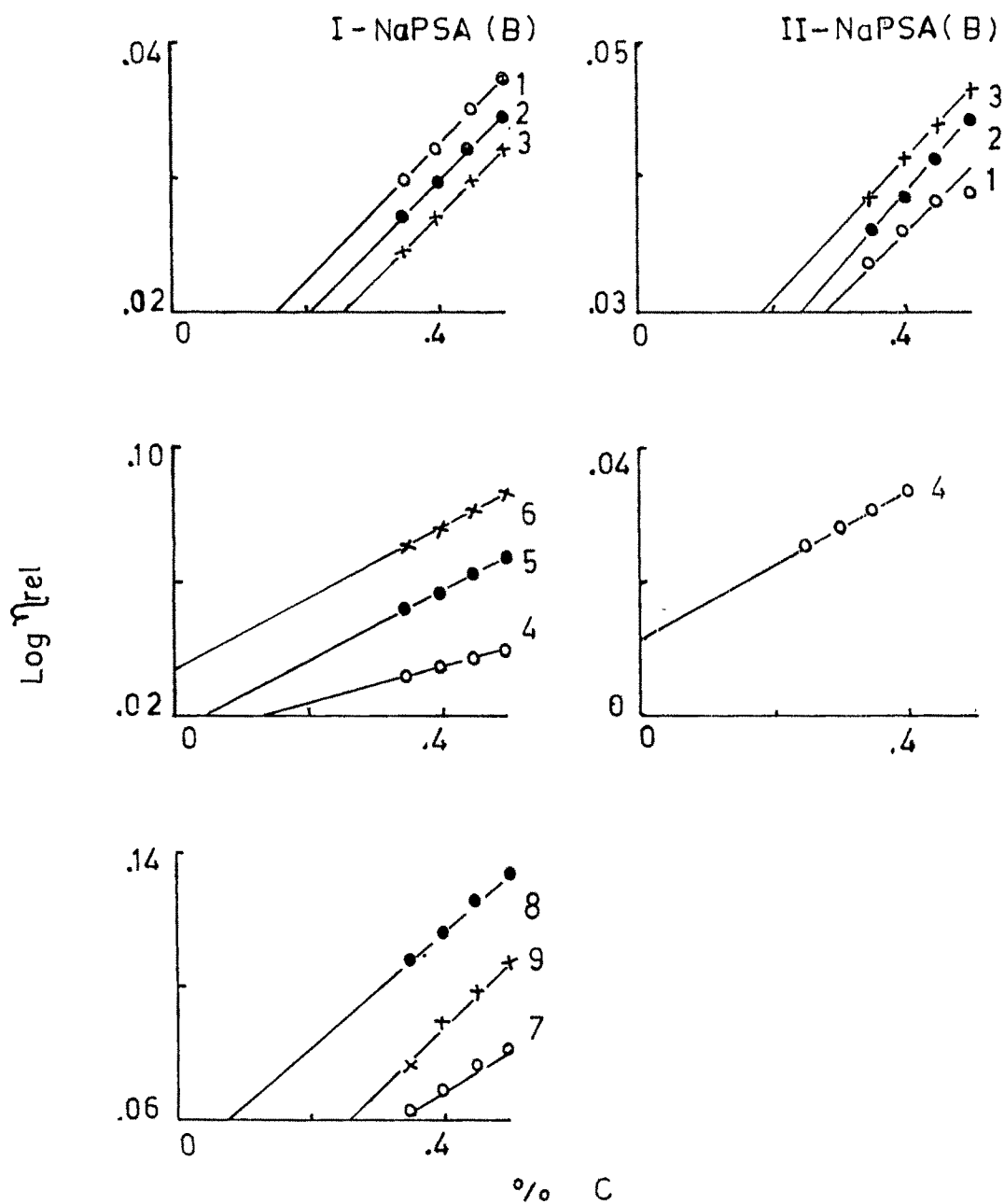


fig.III.79 Plot of $\text{Log } \eta_{\text{rel}}$ vs % C
for NaPSA(B) sets

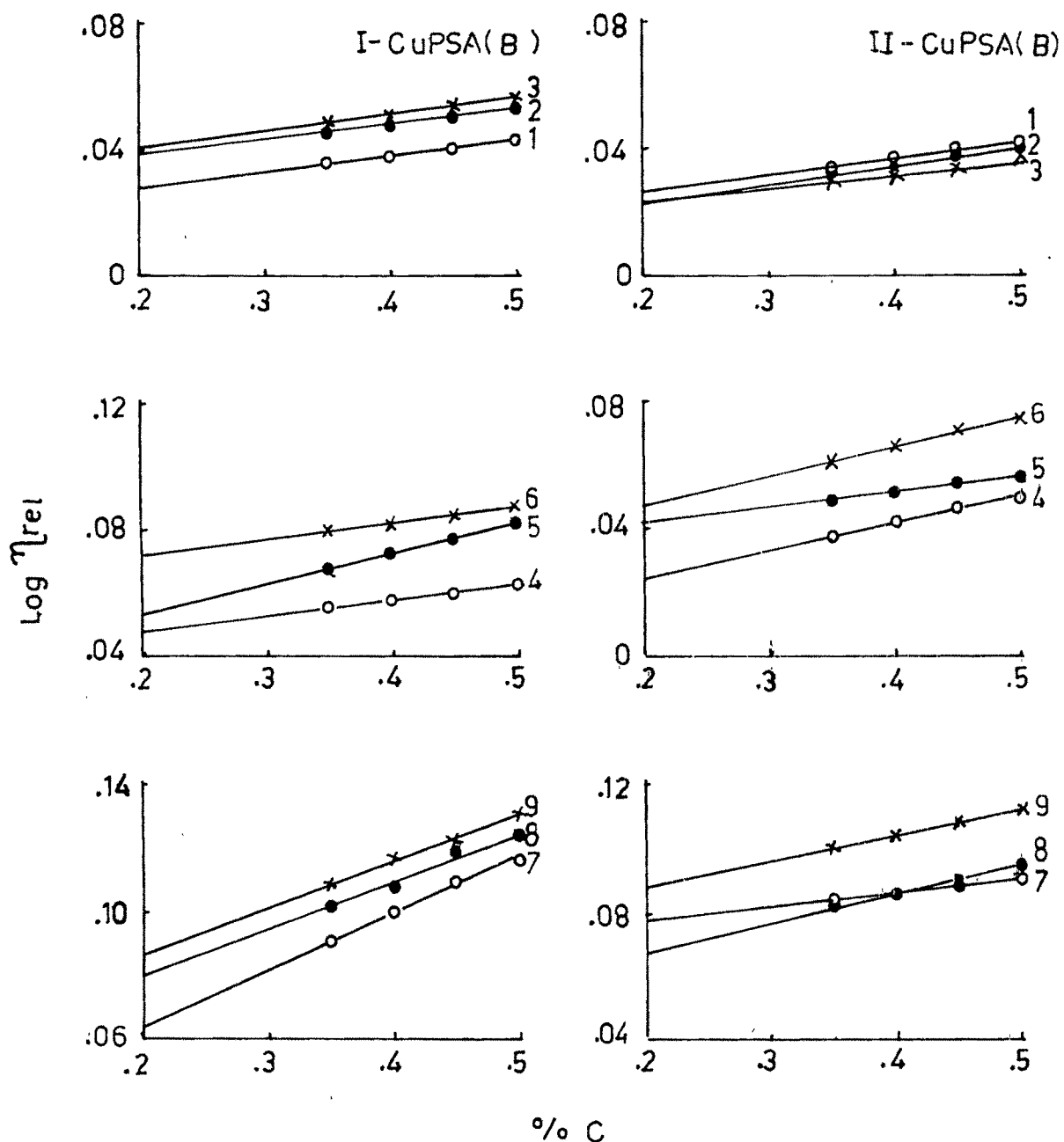


fig. III.80 Plot of $\text{Log } \eta_{rel}/C$ vs $\% C$
for the sets of CuPSA(B)

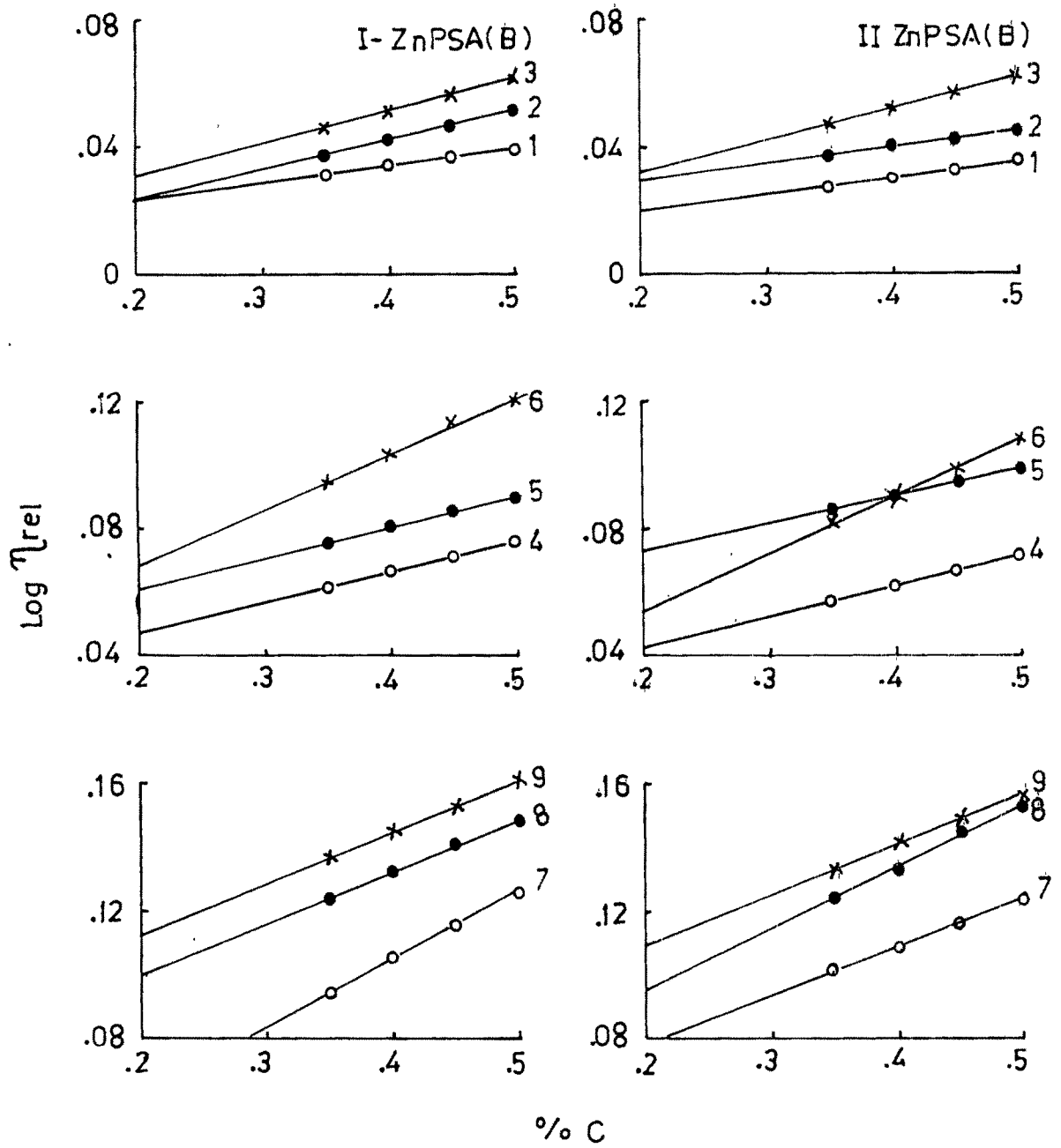


fig.III.81. Plot of $\text{Log } \eta_{rel}$ vs $\% C$ for the sets of ZnPSA(B)

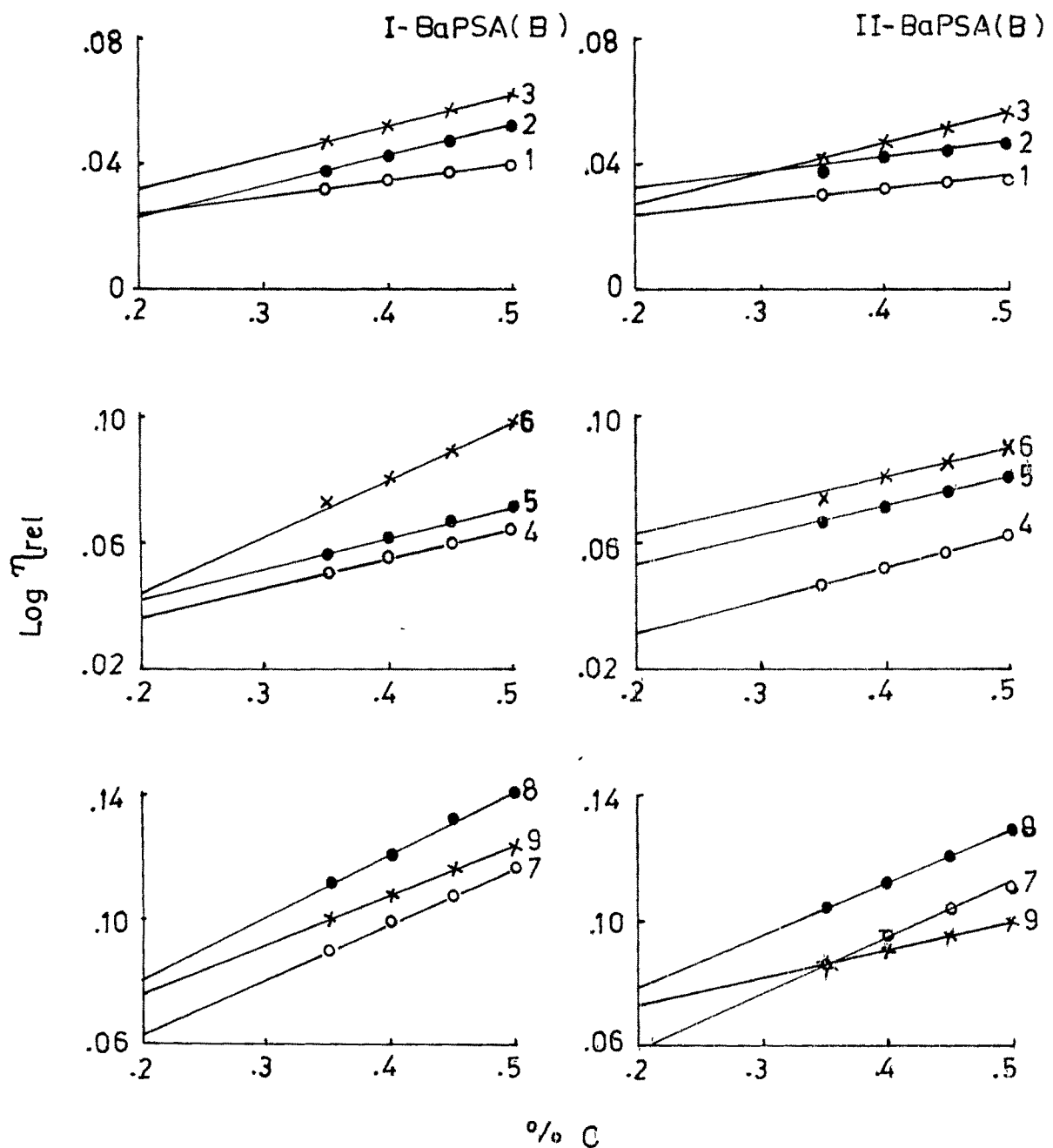


fig. III.82 Plot of $\text{Log } \eta_{rel}$ vs % C
for the sets of BaPSA(B)

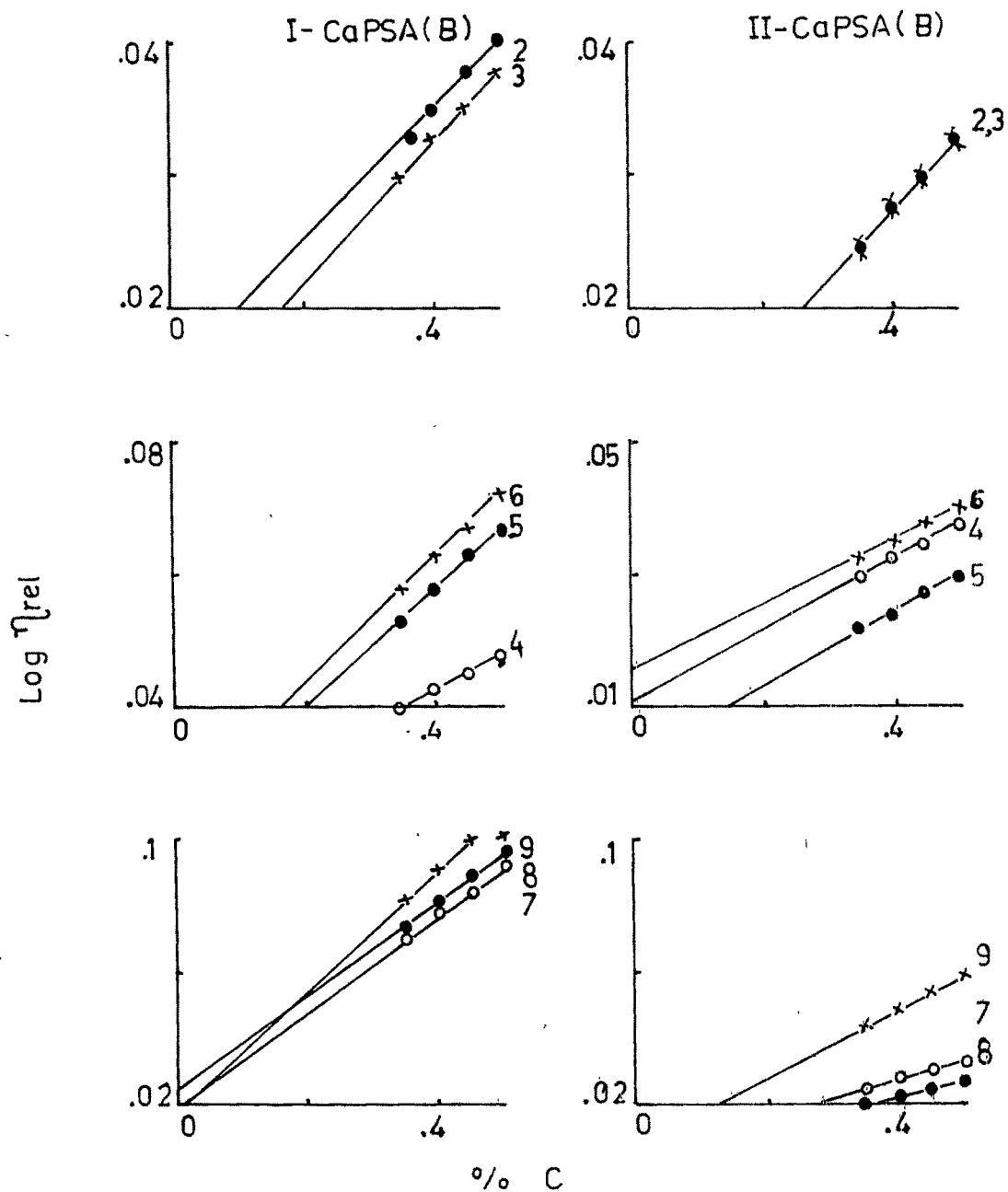


fig.III.83 Plot of $\text{Log } \eta_{\text{rel}}$ vs $\% C$
for CaPSA(B) sets

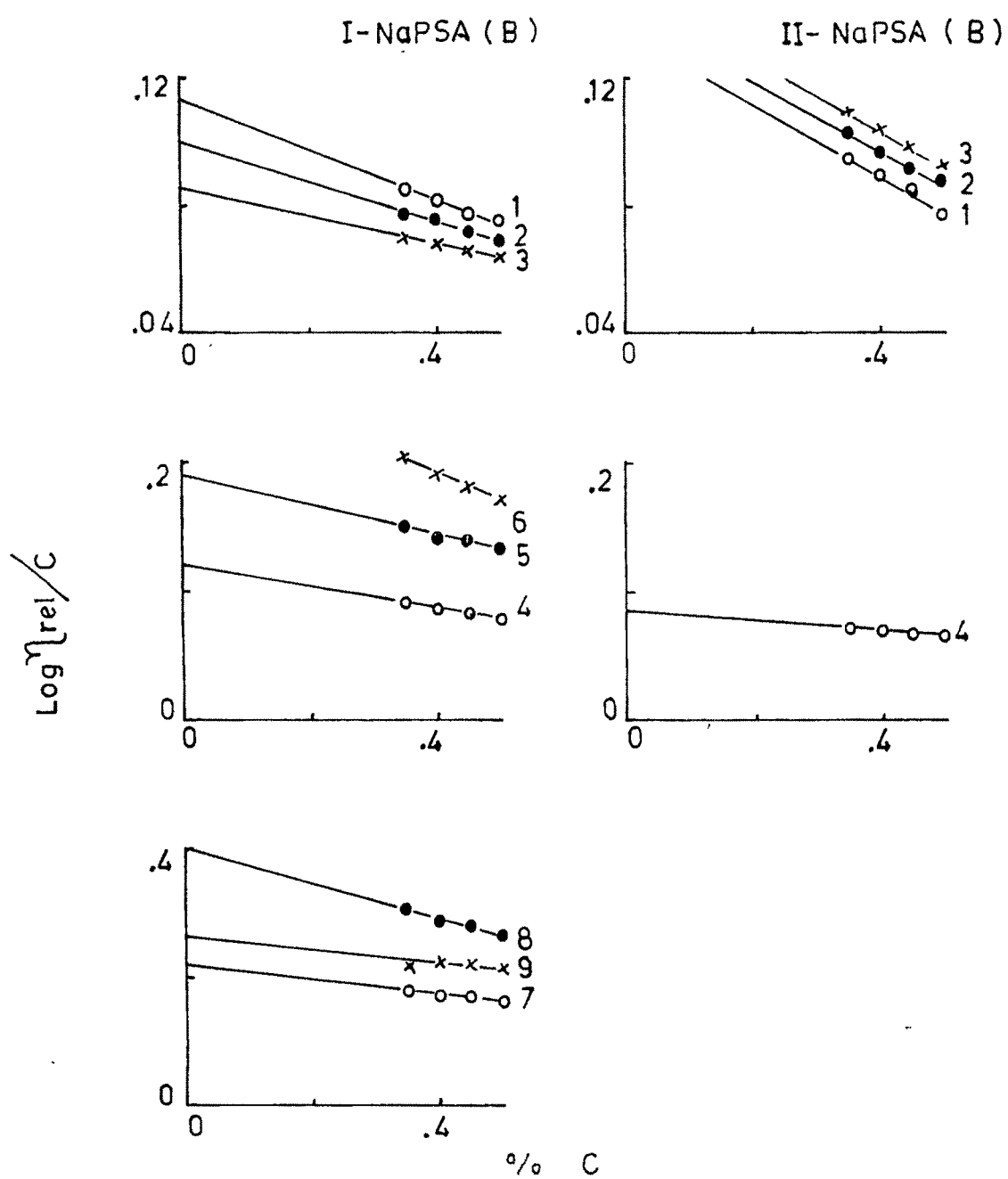


fig.III. 84 Plot of $\text{Log } \eta_{\text{rel}}/C$ vs $\% C$ for NaPSA (B) sets

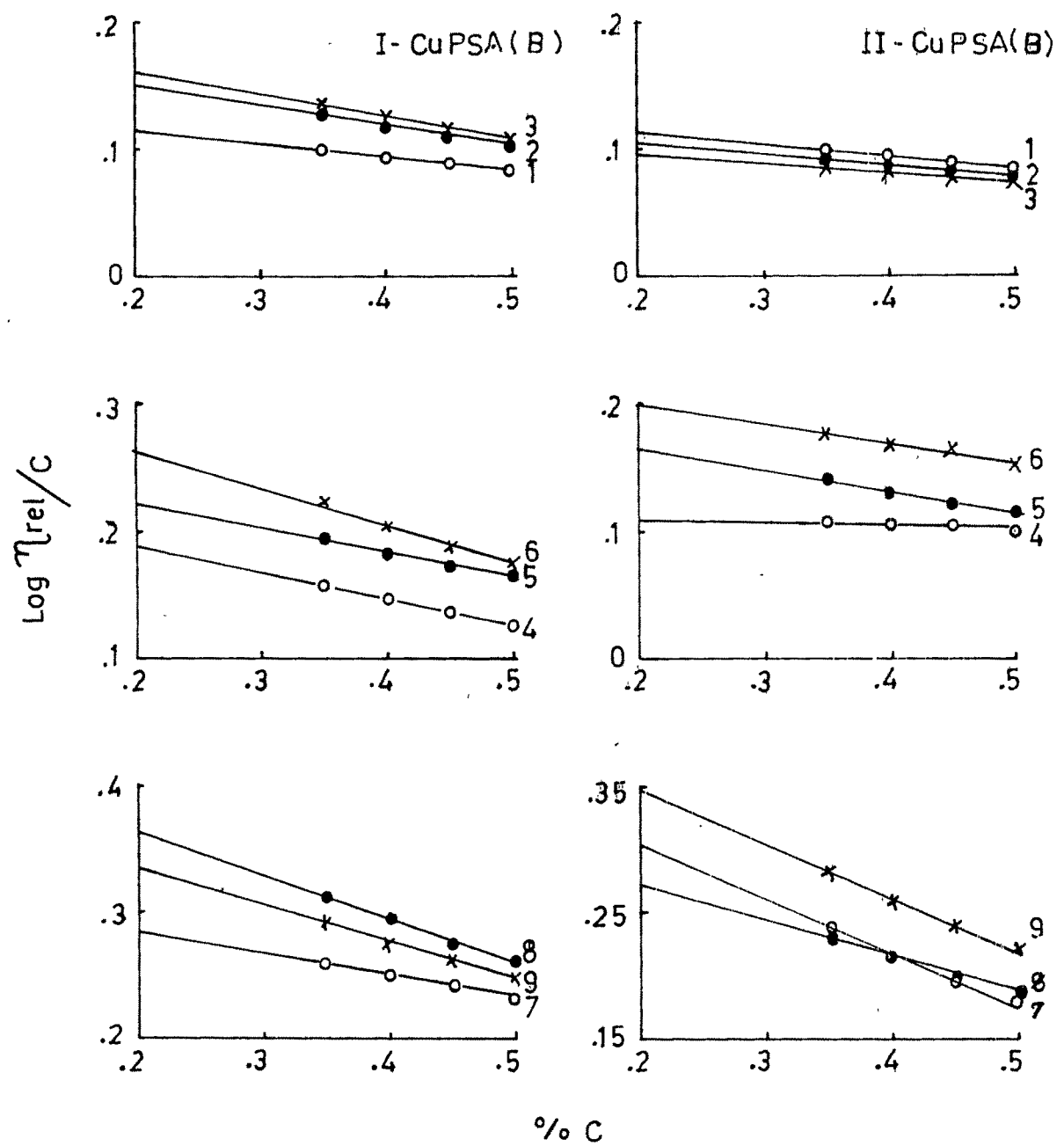


fig.III.85. Plot of $\text{Log } \eta_{rel}/C$ vs $\% C$
for the sets of CuPSA(B)

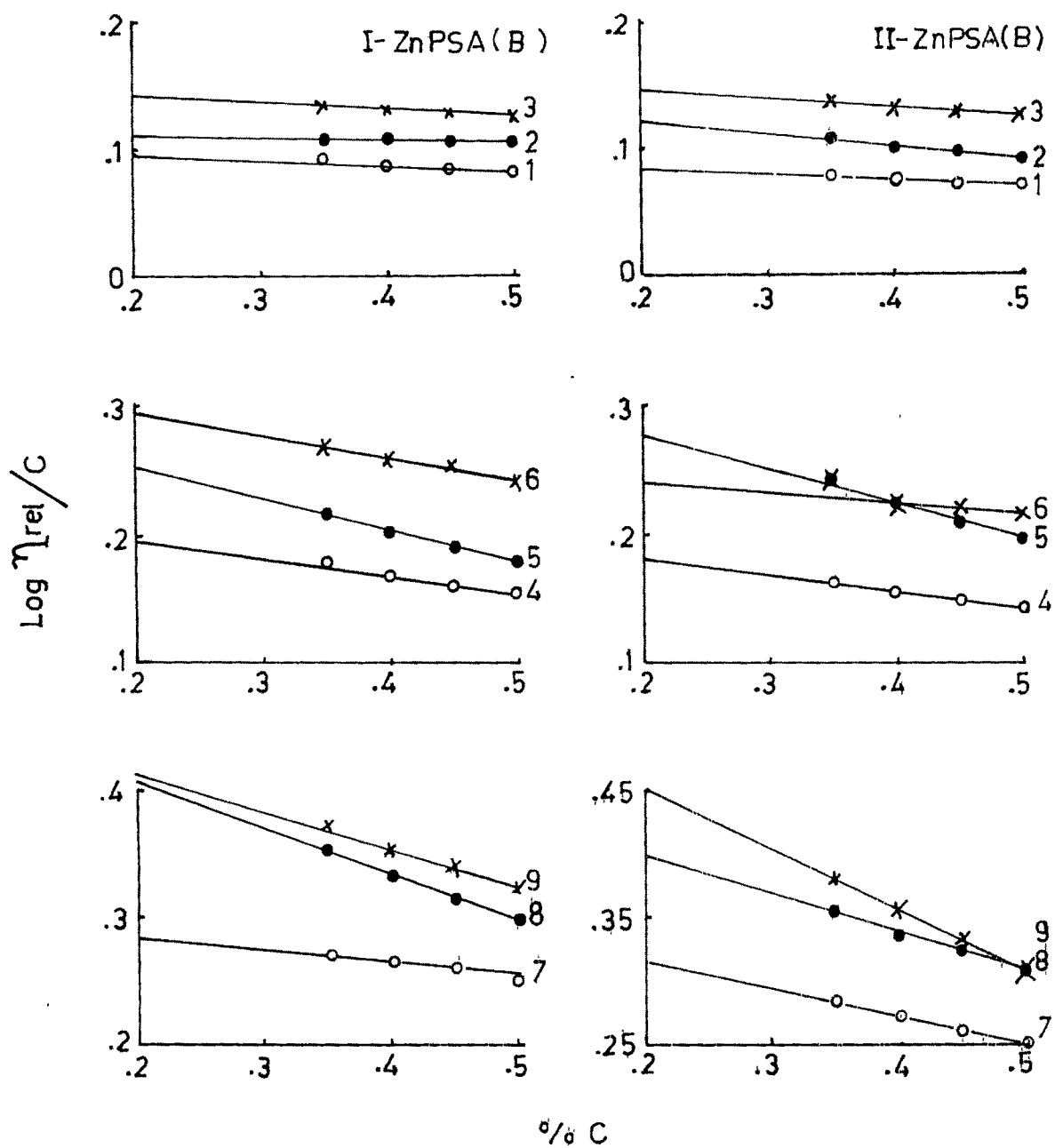


fig.III.86. Plot of $\text{Log } \eta_{\text{rel}}/C$ vs $\% C$
for the sets of ZnPSA(B)

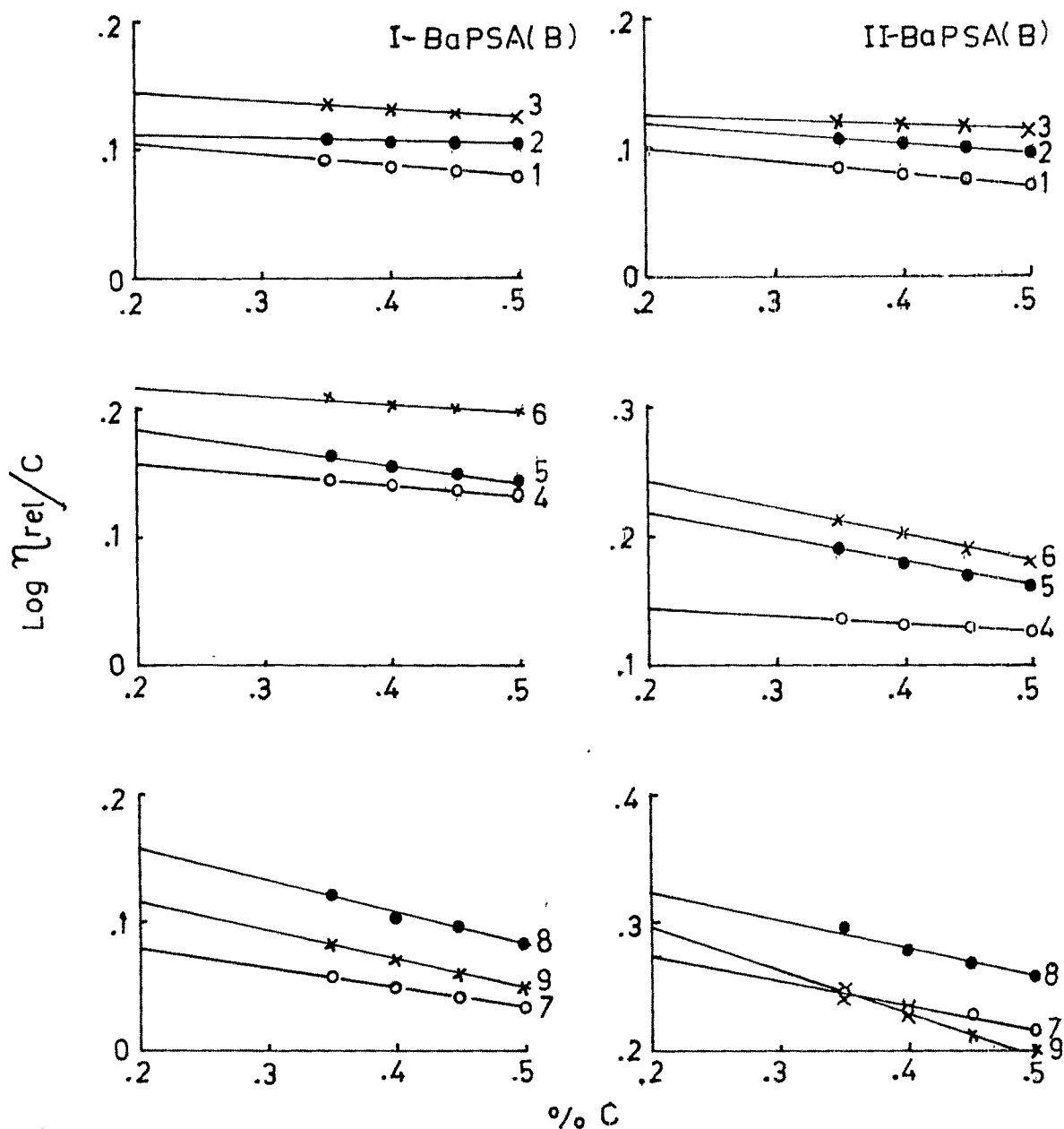


fig. III.87. Plot of $\text{Log } \eta_{rel}/C$ vs $\% C$
for the sets of BAPSA(B)

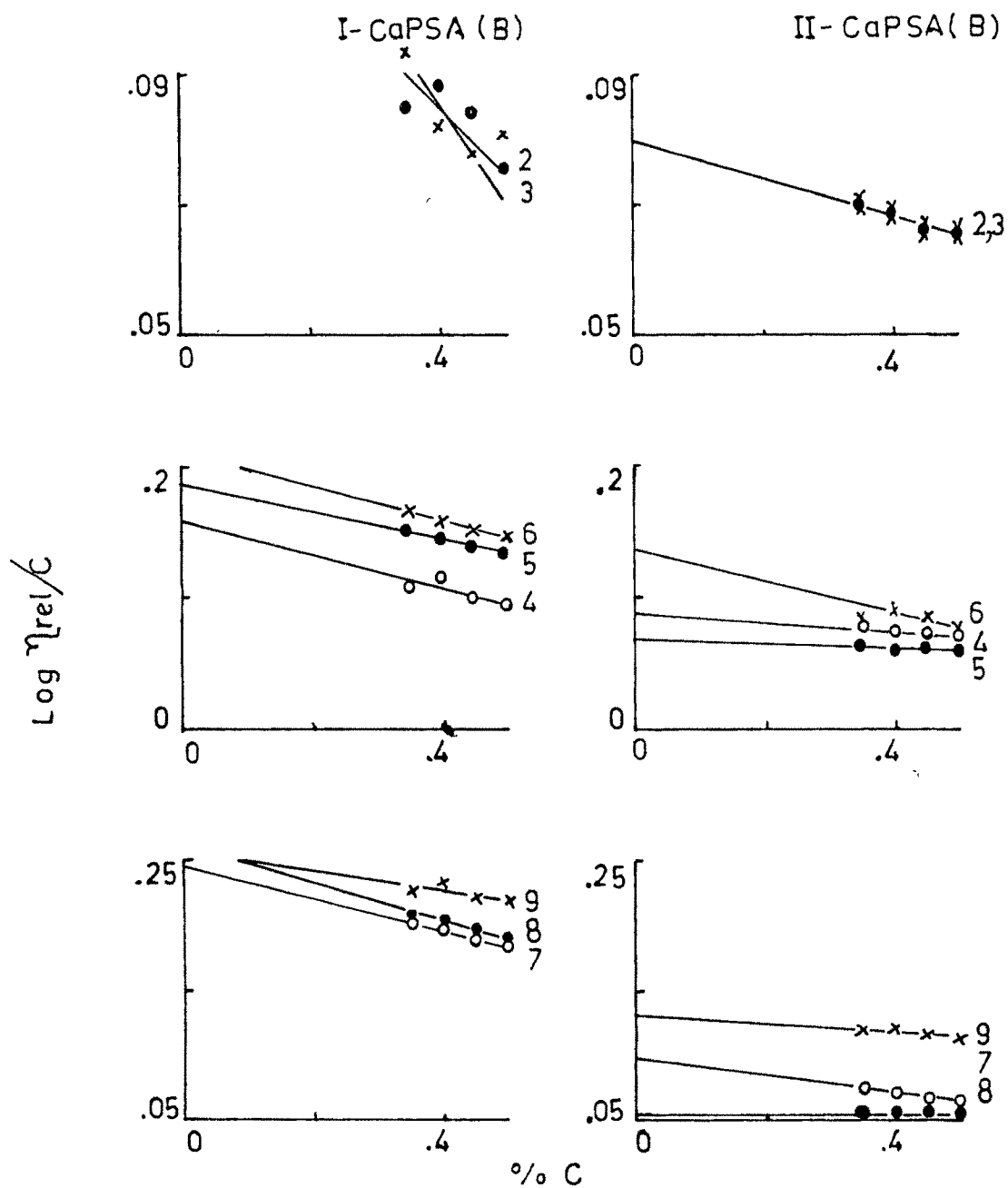
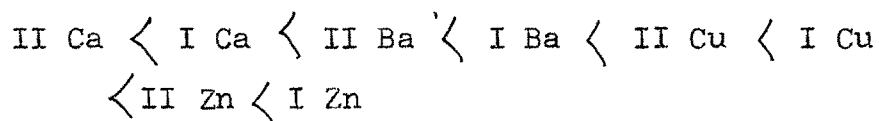
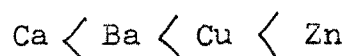


fig.III.88 Plot of $\text{Log } \eta_{rel}/C$ vs % C
for CaPSA (B) sets



The results indicate that the values for 50 % substituted copolymer salts are lower than those for 20 % substituted copolymer-salts and that in terms of metal ions the values are increasing in order



The slopes of the curves are negative for Huggins plots and for Kraemer plots and positive for Martin plots. From the slopes and intercepts, the values of constants k' , k'' and k''' have been calculated. These values generally with the increase in mole fraction of acid in the copolymer salts.

7. Tercopolymers

Tercopolymers were prepared by the solution polymerization of styrene and divinyl benzene with acrylic acid, methacrylic acid or fumaric acid and of styrene and methyl methacrylate with acrylic acid or fumaric acid. Sets were prepared by maintaining definite proportions of styrene and divinyl benzene (or methyl methacrylate) and varying the proportion of acid. Preliminary studies were made to prepare tercopolymers of styrene and divinyl benzene with fumaric acid and acrylic acid. Insoluble products were obtained. Hence their sets were prepared by varying the

relative proportions of styrene and divinyl benzene. However, insoluble products were obtained in all proportions tried. Hence their viscosity studies could not be made and salts were not prepared.

Sets of tercopolymers prepared from styrene, methyl methacrylate and acrylic fumaric acid were found to be soluble in acetone, DMF, etc.

The mole fractions of acid in the products were evaluated from AVS studies. It has been observed that the melting points of PSMmFa increase with increasing mole fraction of acid in the product whereas the melting points of PSMmA show a maximum as the mole fraction of acid in the product is increased.

The IR spectra of PSMmA-1, 3 and 5 and of PSMmFa-3 and 6 have an absorption band at 1720 cm^{-1} increasing in intensity and an absorption at 695 cm^{-1} decreasing in intensity with increase in mole fraction of acid in the products.

Viscosity plots have been presented in figs III 89, 90 and 91 for PSMmA and in figs III 107, 108 and 109 for PSMmFa. The values of $[\eta]$, $[\eta']$ and $[\eta'']$ lie in the range of (i) 0.26 to 0.48, (ii) 0.01 to 0.03 and (iii) 0.11 to 0.20

for PSMmA respectively and (iv) 0.26 to 0.40, (v) 0.00 to 0.02 and (vi) 0.12 to 0.17 for PSMmFa respectively. These results show that

$$[\eta'] < [\eta''] < [\eta]$$

The slopes of the lines are negative for Huggins plot and for Kraemer plots and positive for Martin plots. From the values of slopes and intercepts, the values of the constants, k' , k'' and k''' are calculated. It is observed that values of k' and k''' vary over a small range while those of k'' vary over a very wide range.

Salts of tercopolymers

20 % and 50 % of the available acids proton in the tercopolymers was replaced by Na (I), Cu (II), Zn (II), Ca (II) and Ba (II). The products were studied for their viscosity in solution.

Huggins plots are presented in figs. III. 92, 93, 94, 95 and 96 for the salts of PSMmA and in figs. III. 110, 111, 112, 113 and 114 for the salts of PSMmFa. Martin plots are presented in figs. III. 97, 98, 99, 100 and 101 for the salts of PSMmA and in figs. III. 115, 116, 117, 118 and 119 for PSMmFa. Kraemer plots are presented in figs III 102, 103, 104, 105 and 106 for PSMmA and in figs 120, 121, 122, 123 and

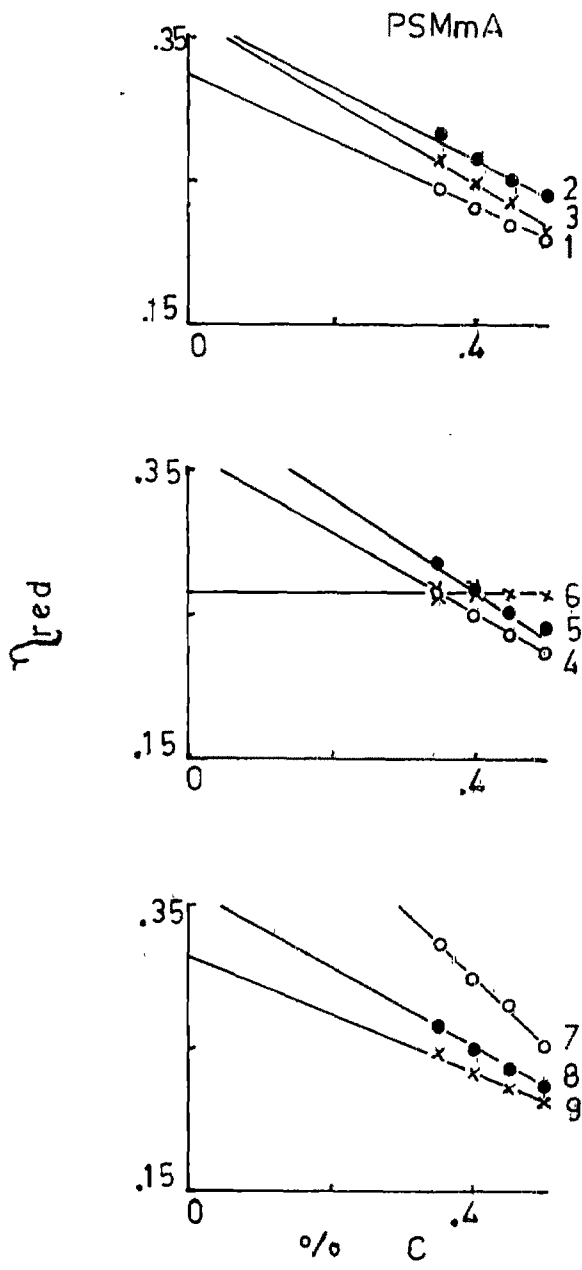


fig.III.89 Plot of η_{red} vs % C
for PSMmA set

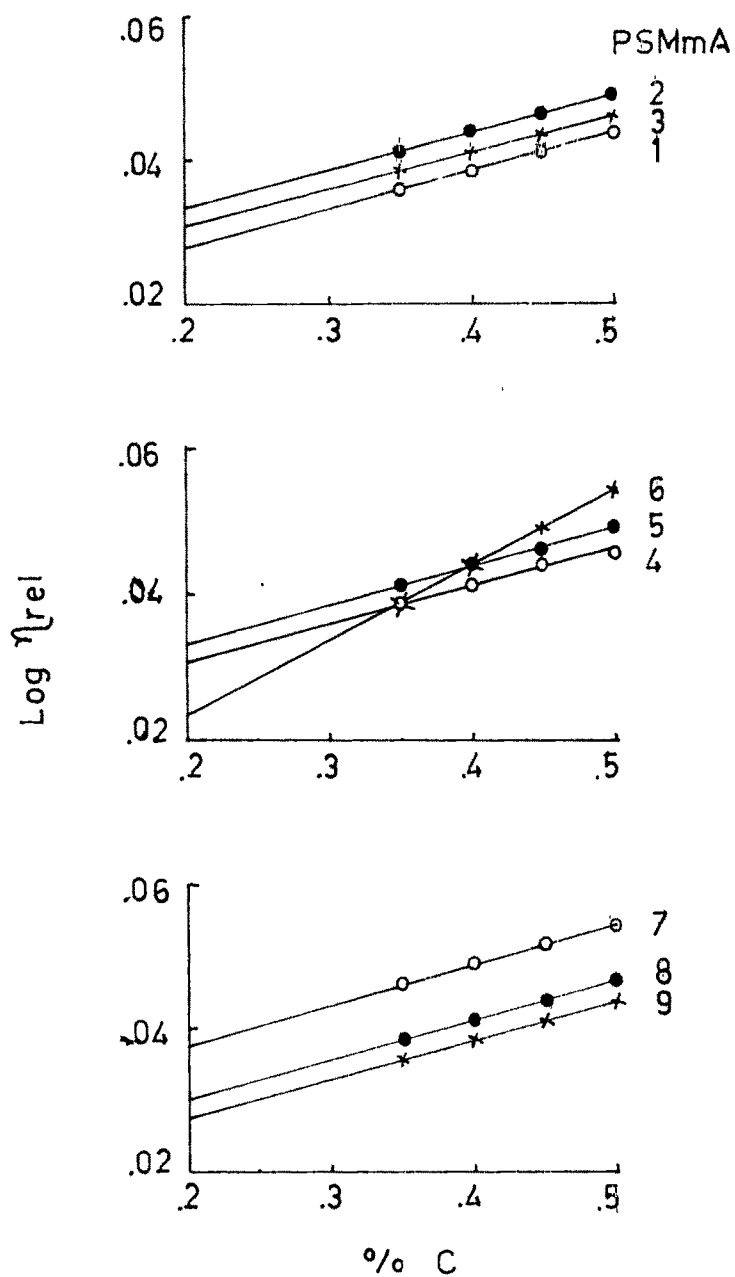


fig. III 90 Plot of $\text{Log } \eta_{rel}$ vs % C
for the set of PSMmA (H form)

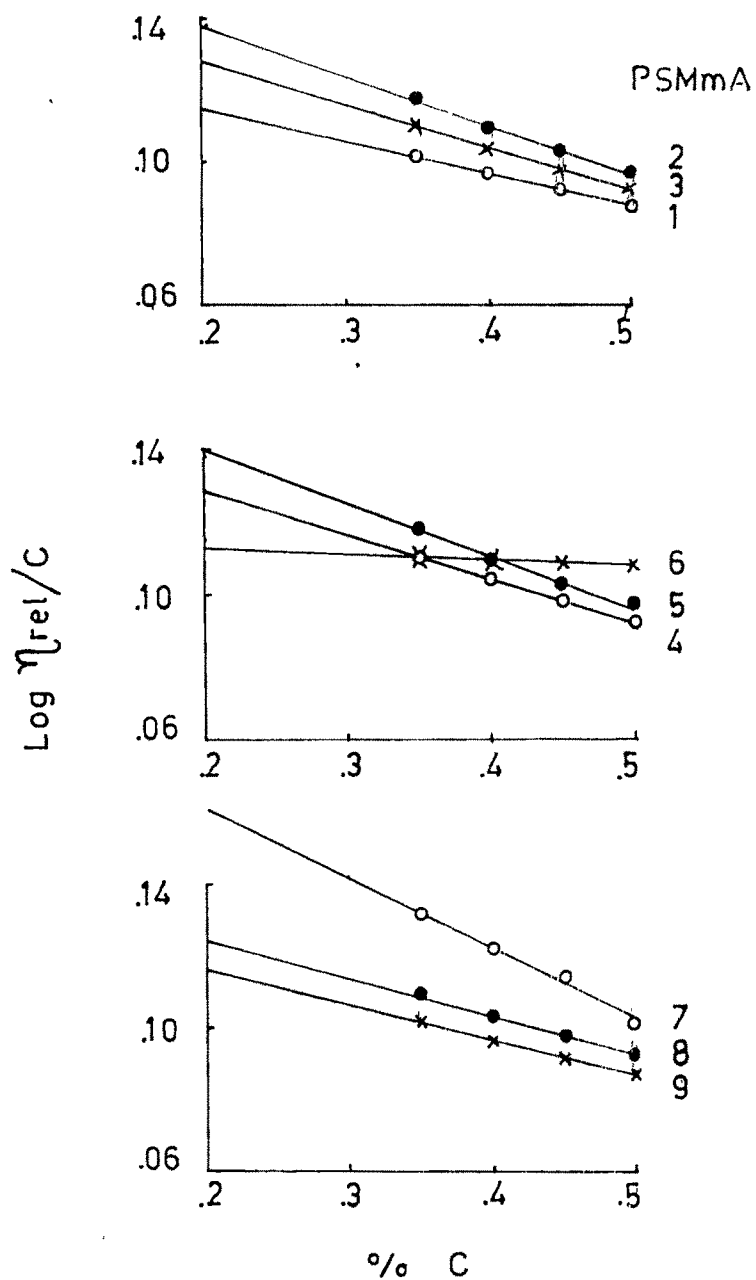


fig.III.91 Plot of $\text{Log } \eta_{rel}/C$ vs % C
for the set of PSMmA (H form)

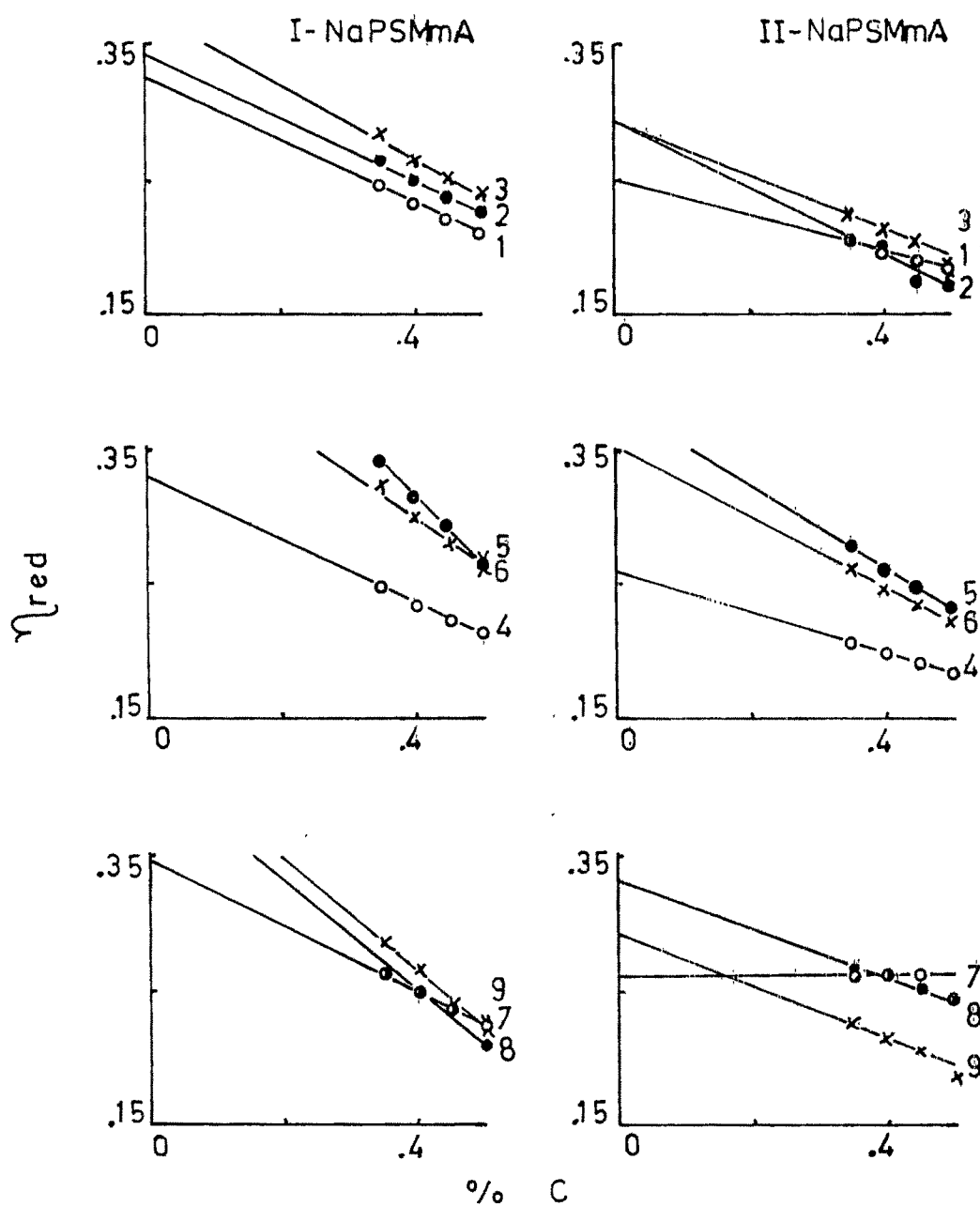


fig.III.92 Plot of η_{red} vs % C
for NaPSMmA sets

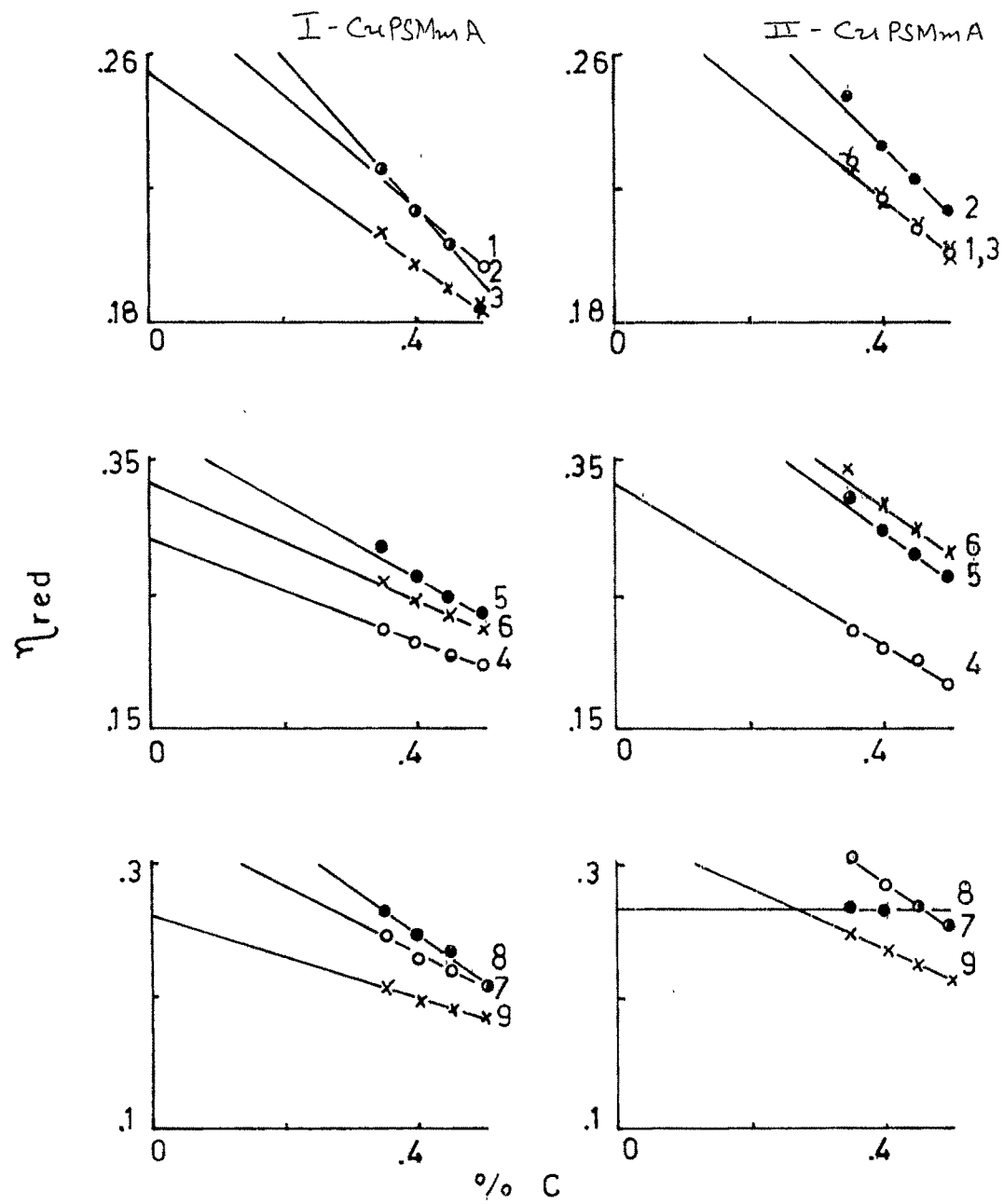


fig.III.93 Plot of η_{red} vs % C for CuPSMmA sets

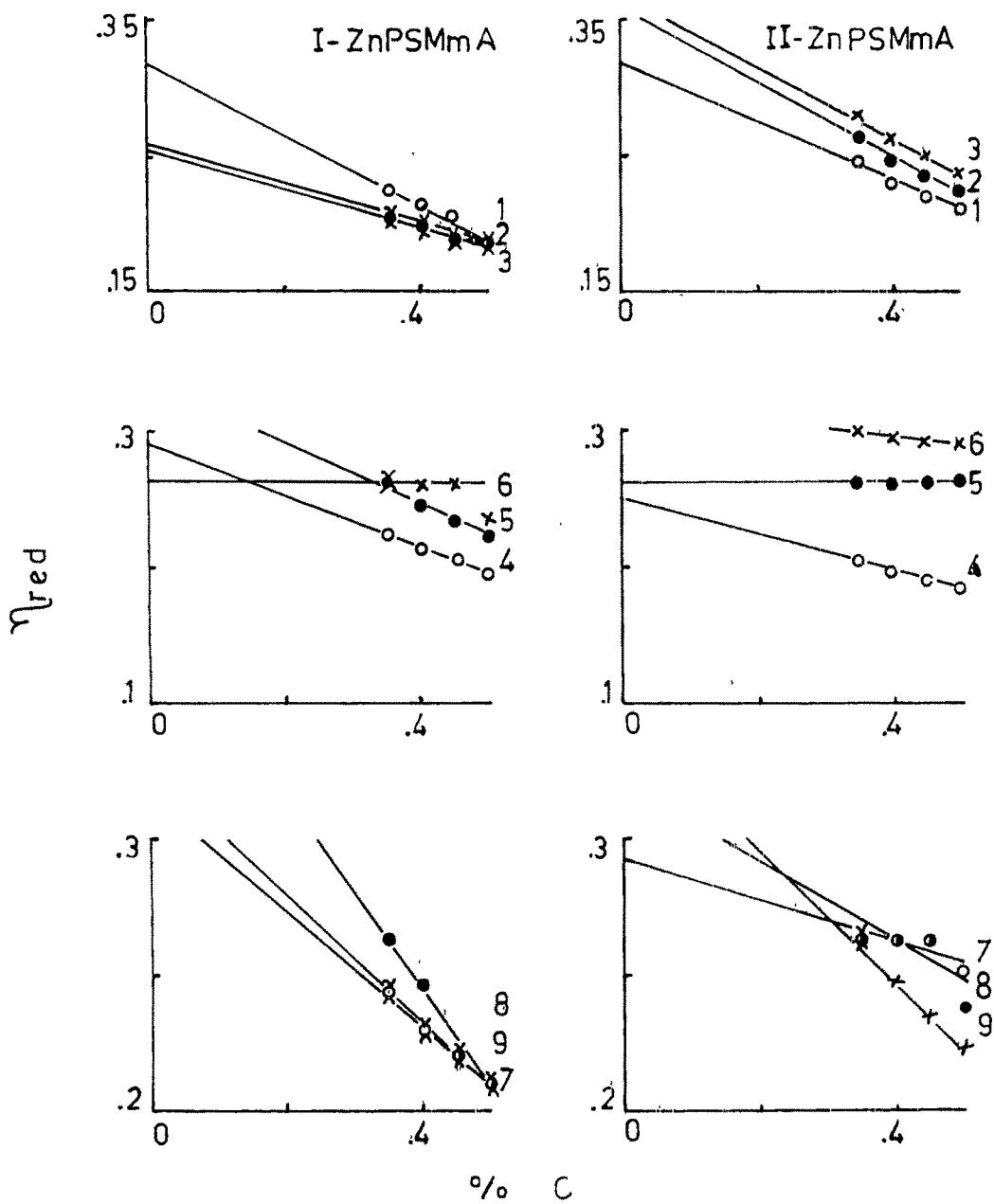


fig.III.94 Plot of η_{red} vs % C for ZnPSMmA sets

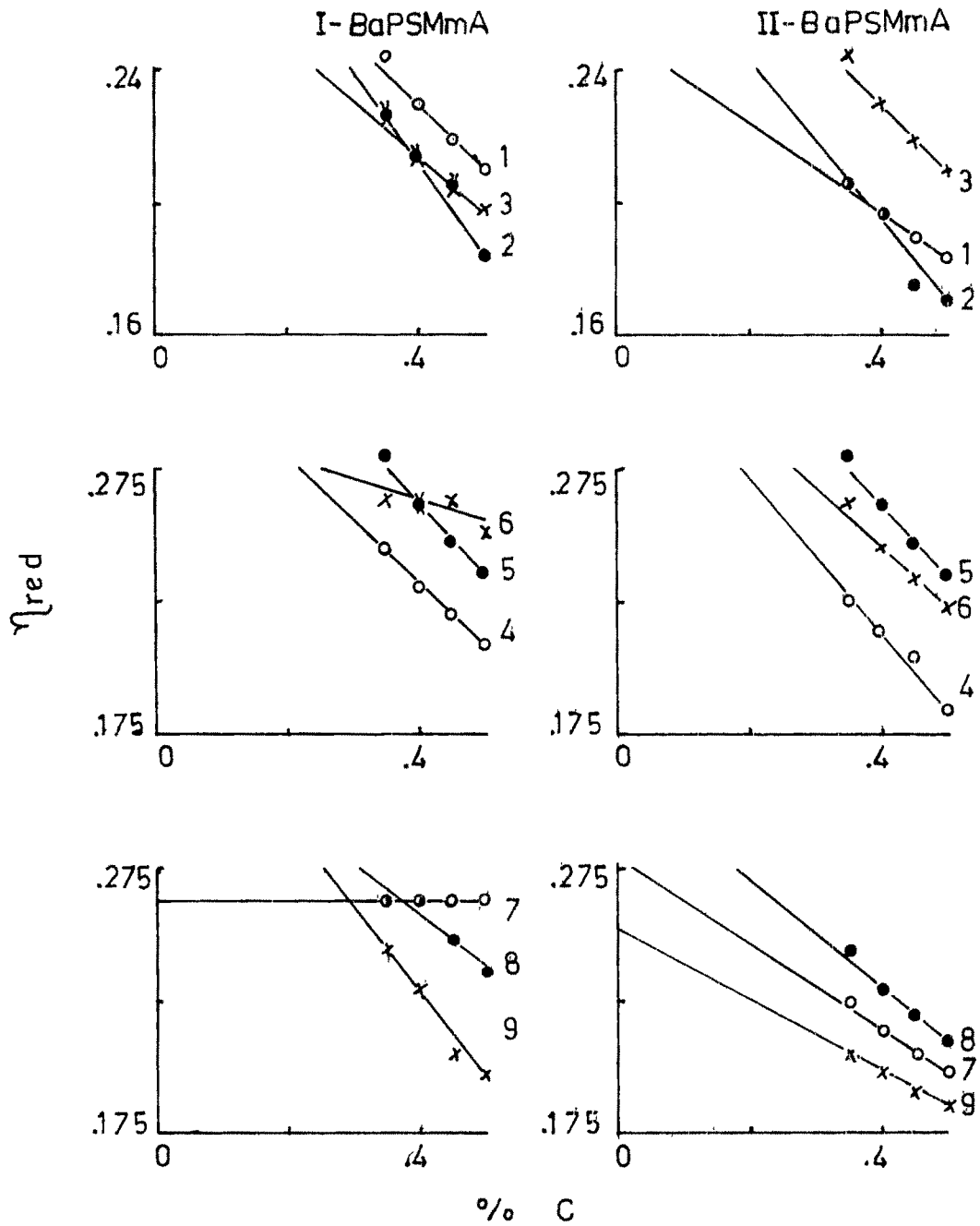


fig.III.95 Plot of η_{red} vs % C for BaPSMmA sets

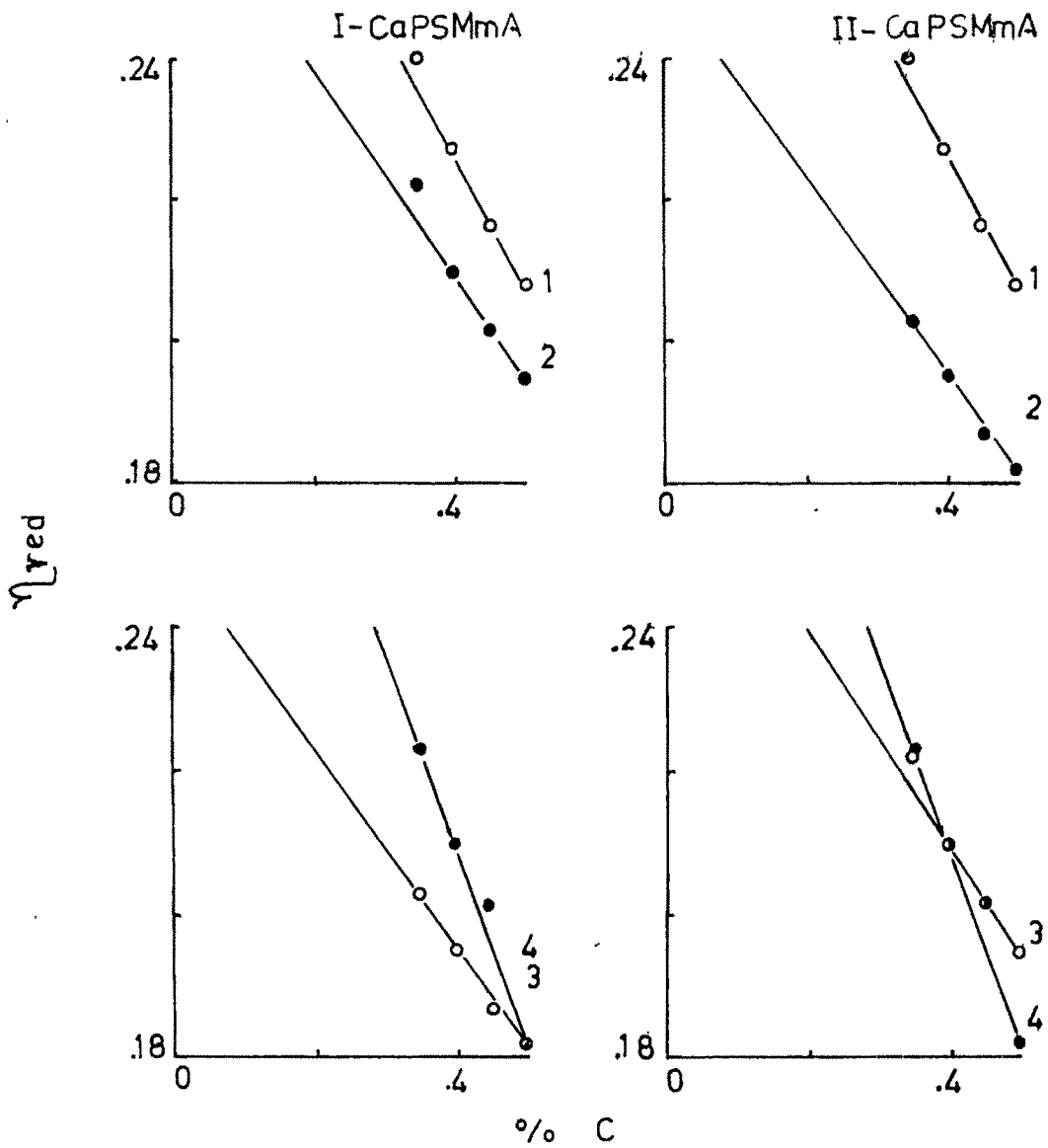


fig.III.96 Plot of η_{red} vs % C
for CaPSMmA sets

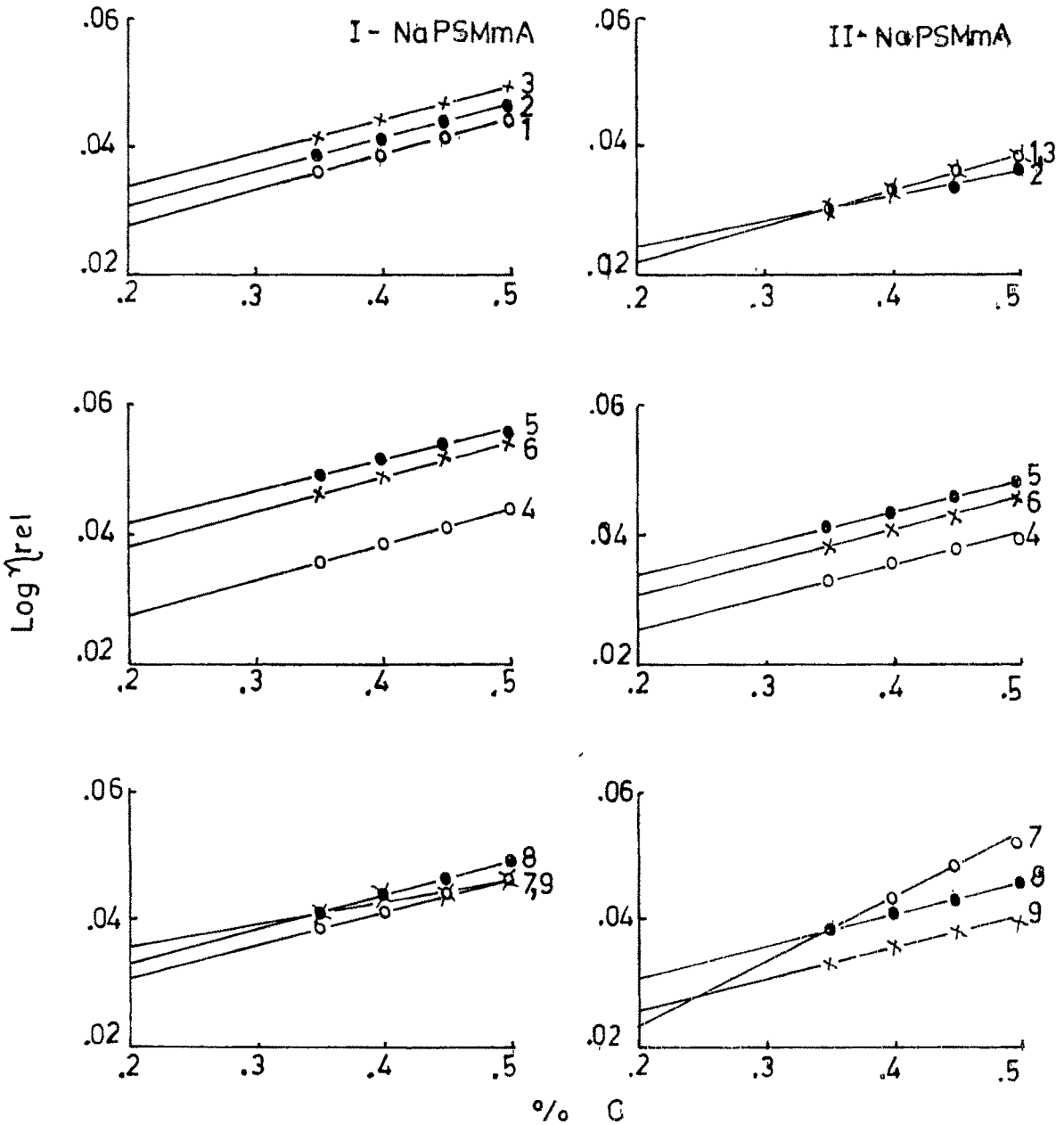


fig.III.97 Plot of $\text{Log } \eta_{\text{rel}}$ vs % C
for the sets of NaPSMmA

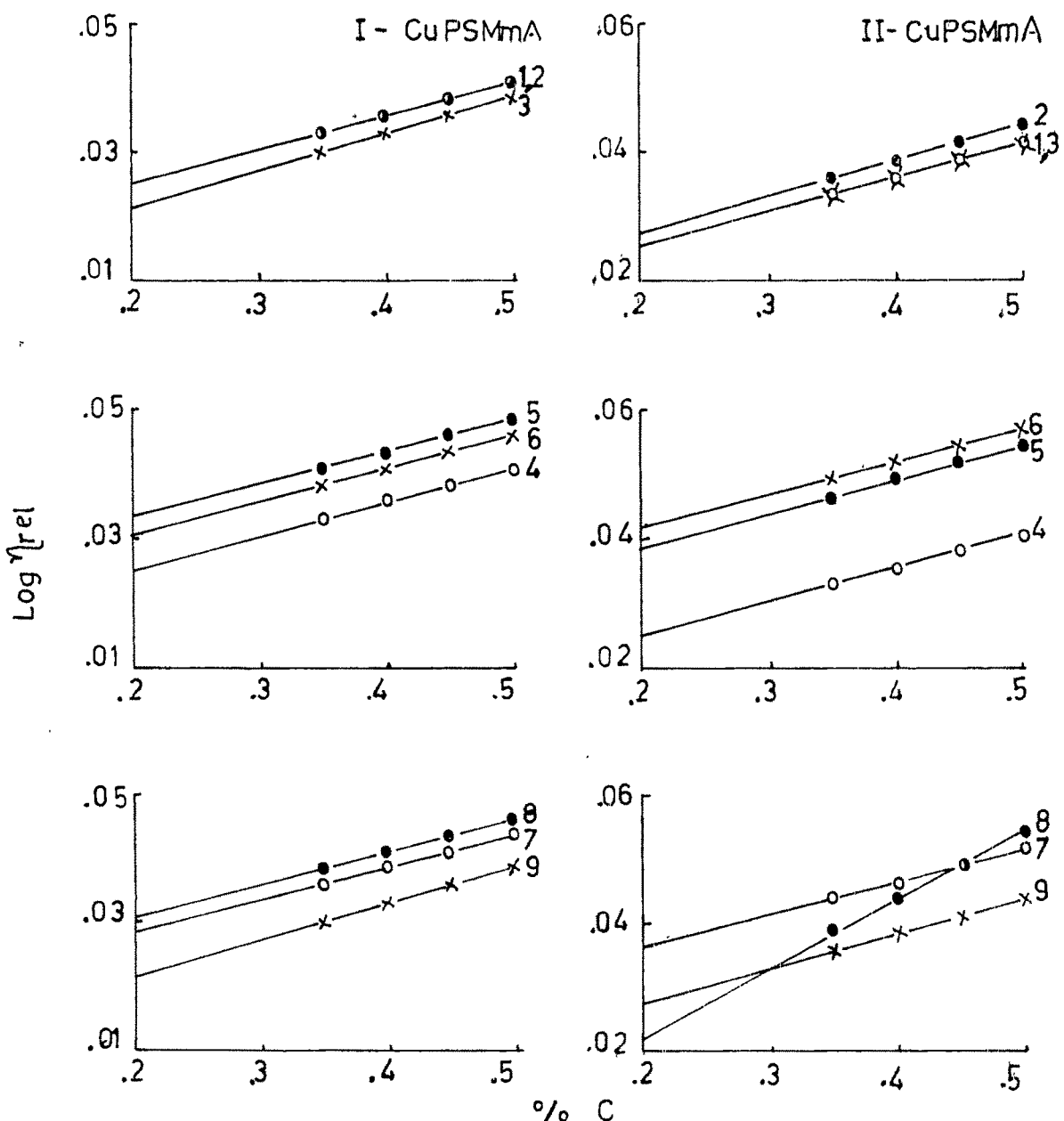


fig.III.98 Plot of $\text{Log } \eta_{\text{rel}}$ vs $\% \text{ C}$
for the sets of CuPSMmA

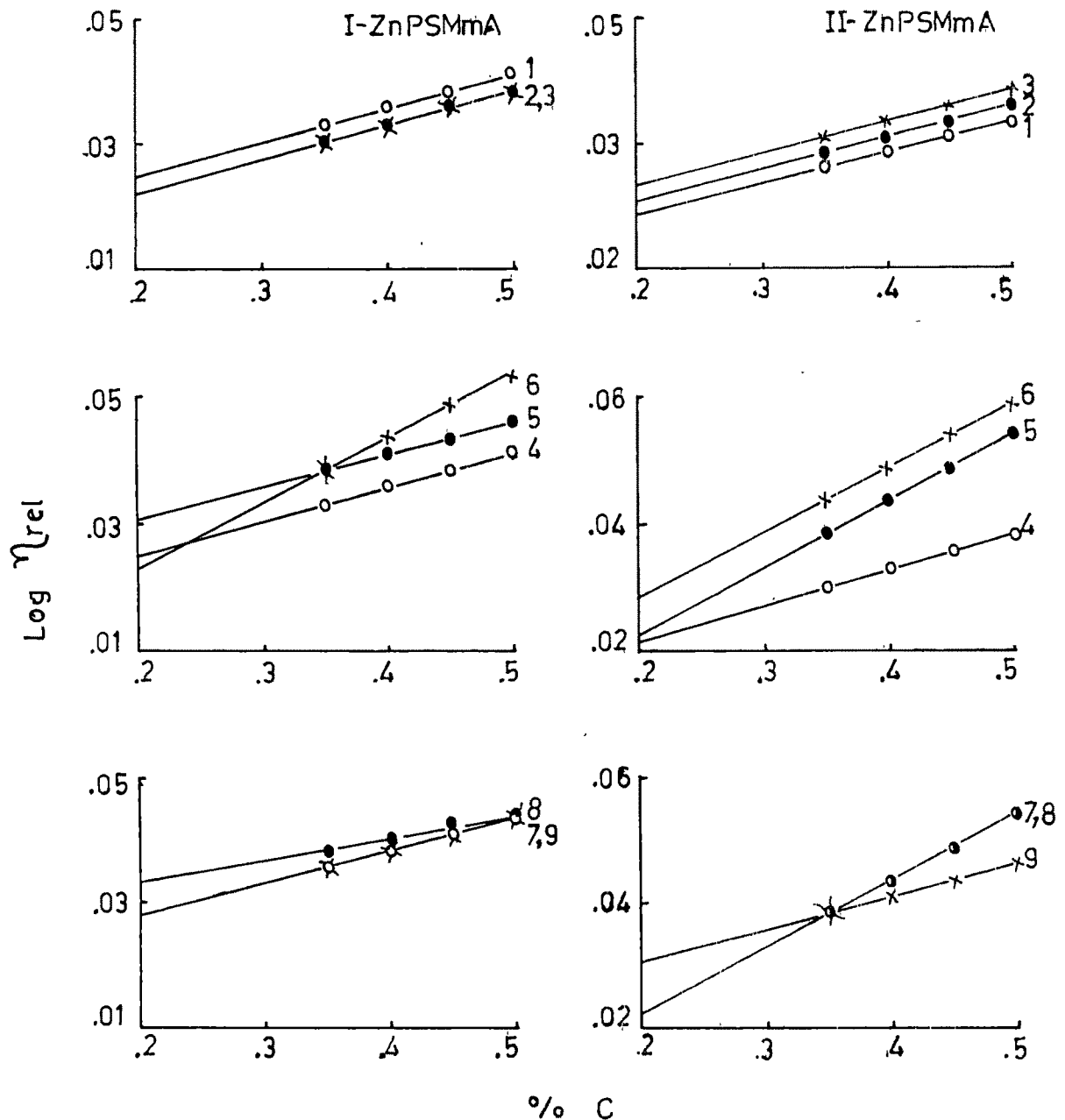


fig.III.99. Plot of $\text{Log } \eta_{\text{rel}}$ vs $\% C$
for the sets of ZnPSMmA

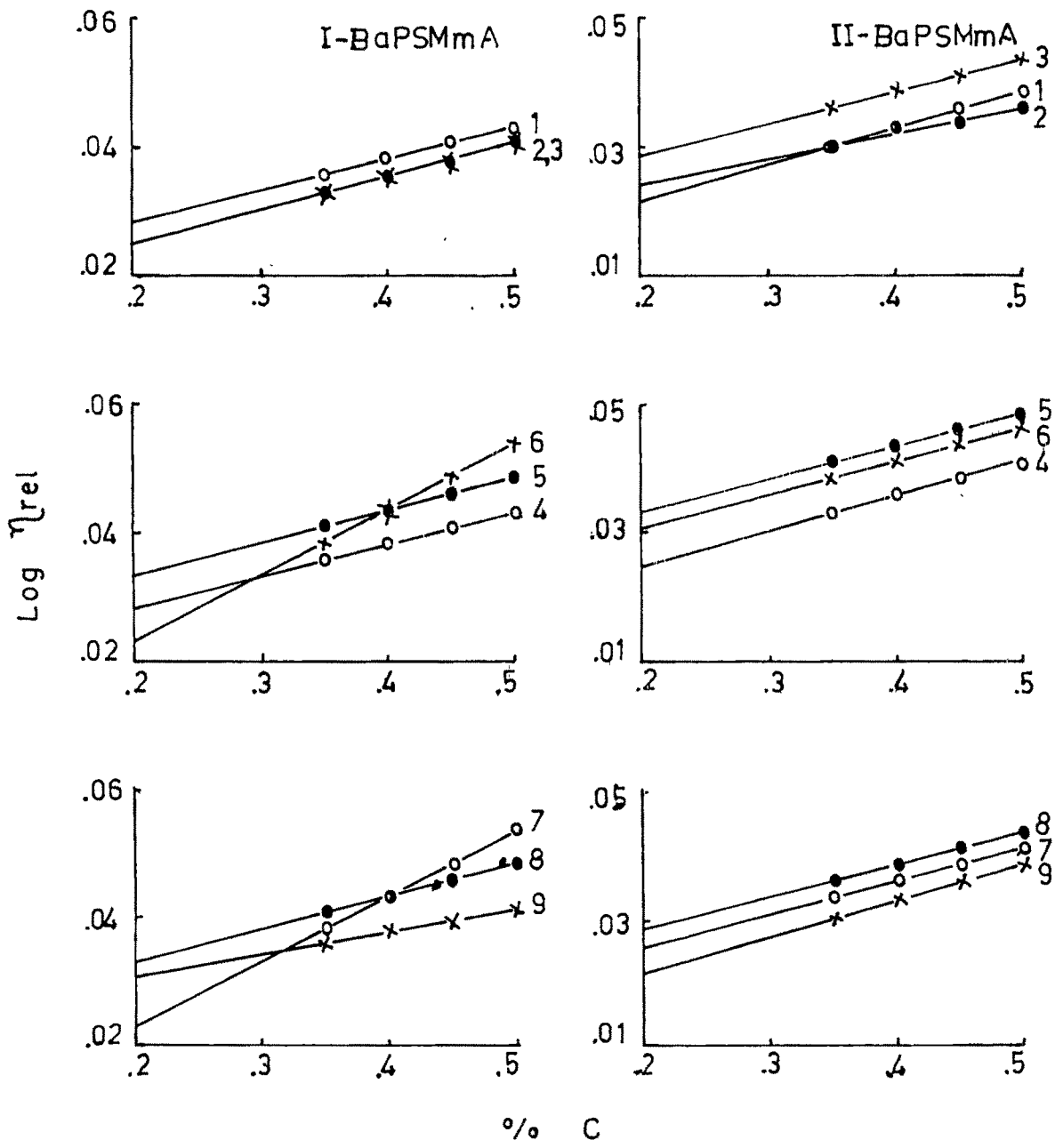


fig. III.100. Plot of $\text{Log } \eta_{\text{rel}}$ vs $\% C$
for the sets of BaPSMmA

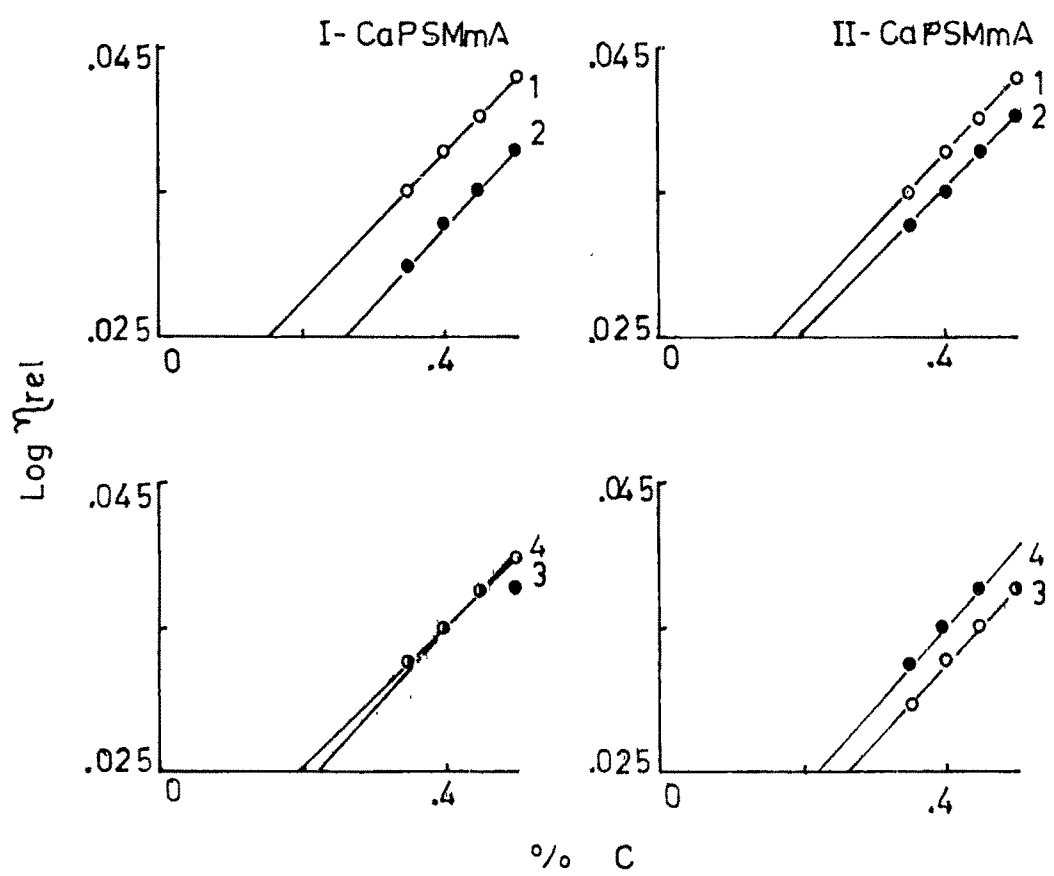


fig.III.101. Plot of $\text{Log } \eta_{rel}$ vs % C
for CaPSMmA sets

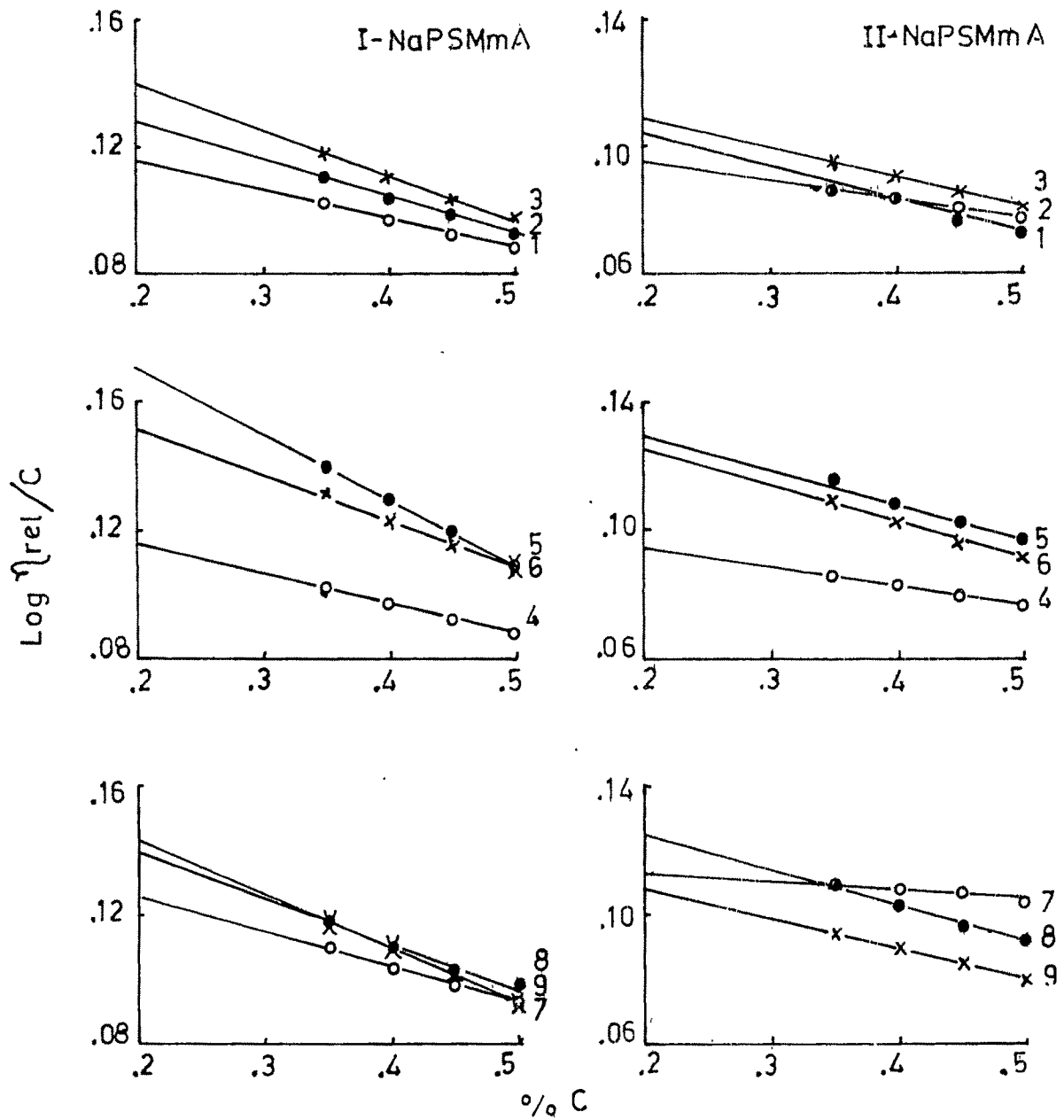


fig.III.102.Plots of $\text{Log } \eta_{\text{rel}}/C$ vs $\% C$
for the sets of NaPSMmA

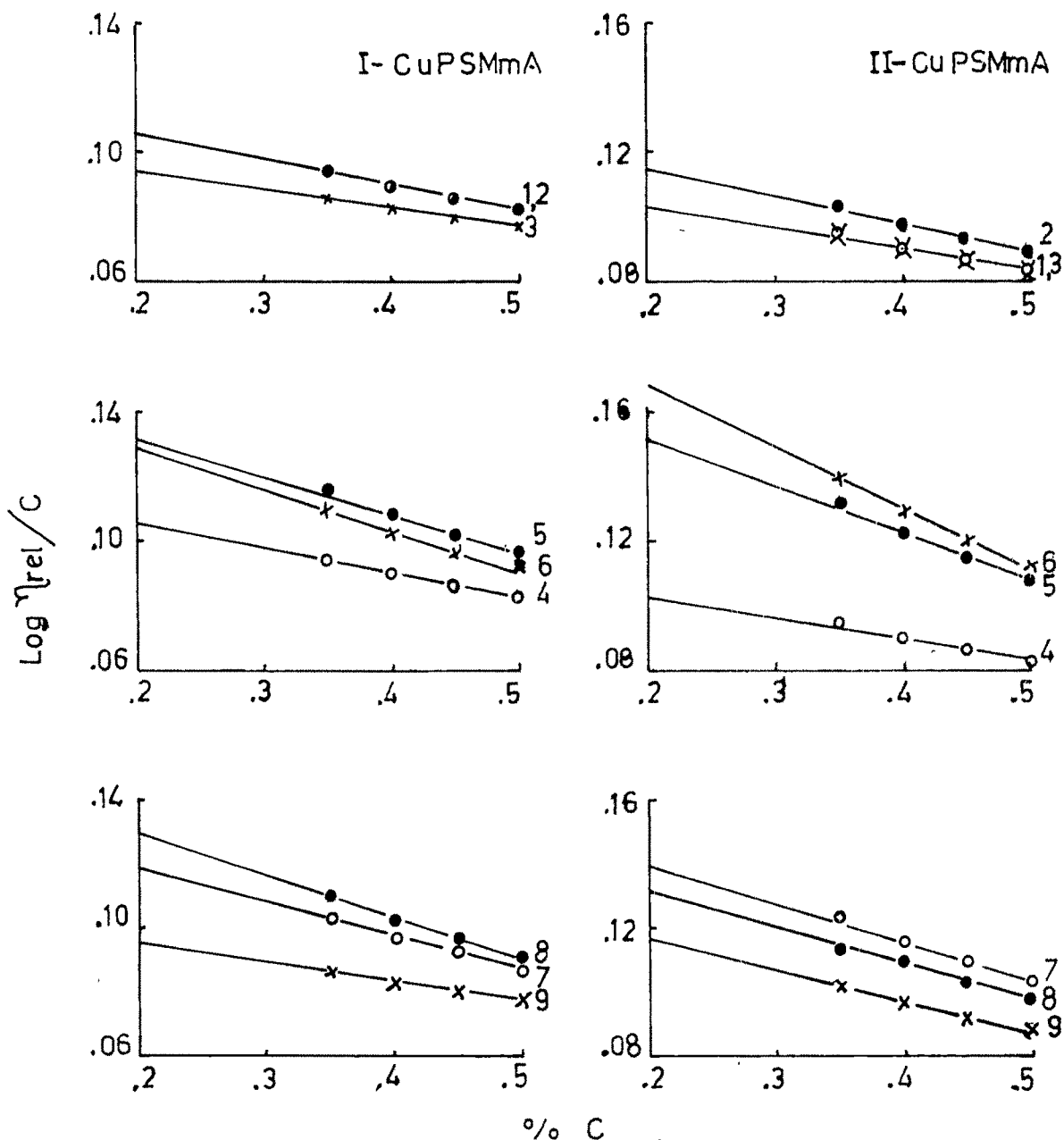


fig.III.103. Plot of $\text{Log } \eta_{rel}/C$ vs $\% C$
for the sets of CuPSMmA

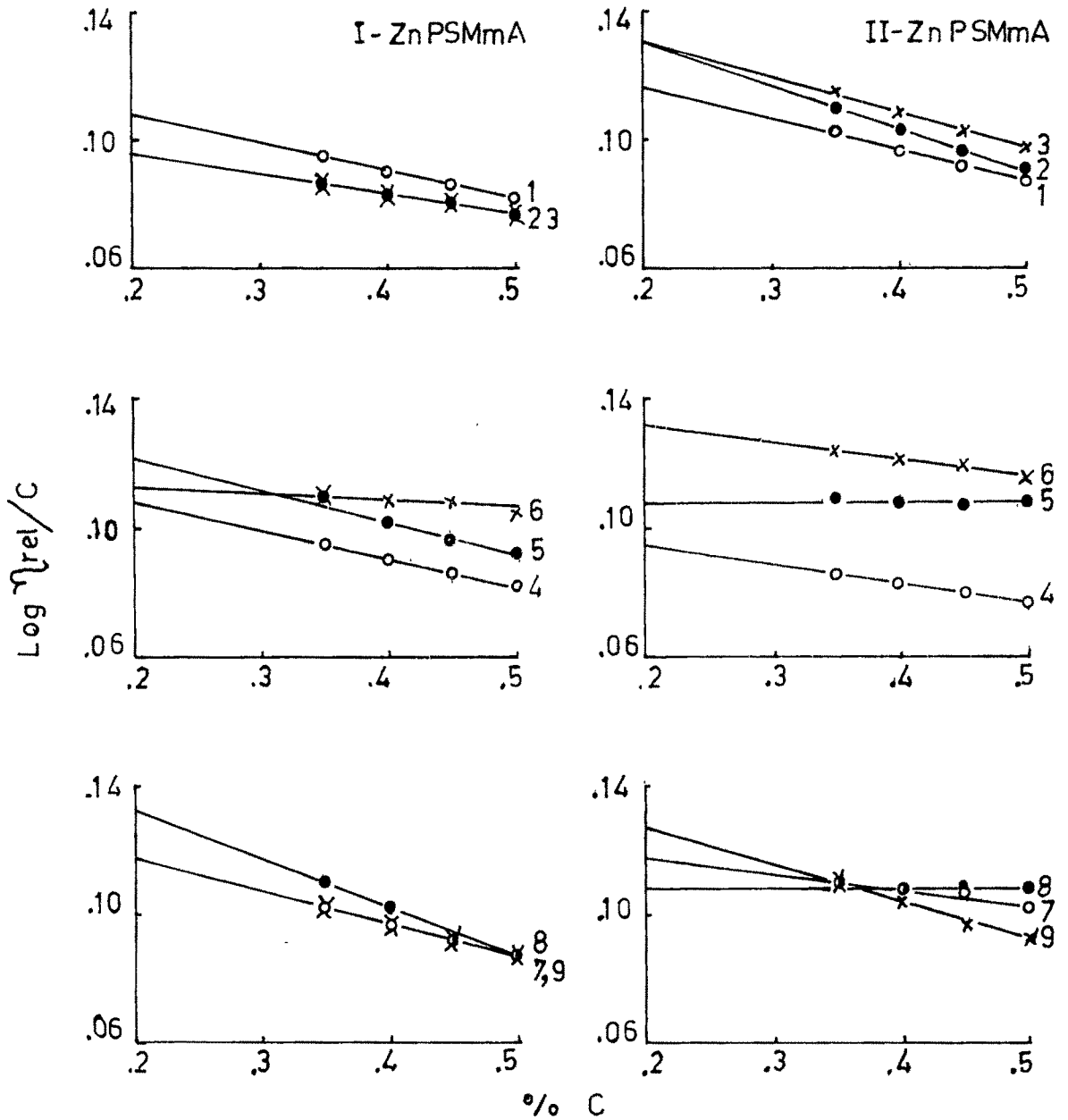


fig.III.104 Plot of $\text{Log } \eta_{\text{rel}}/C$ vs $\% C$
for the sets of ZnPSMmA

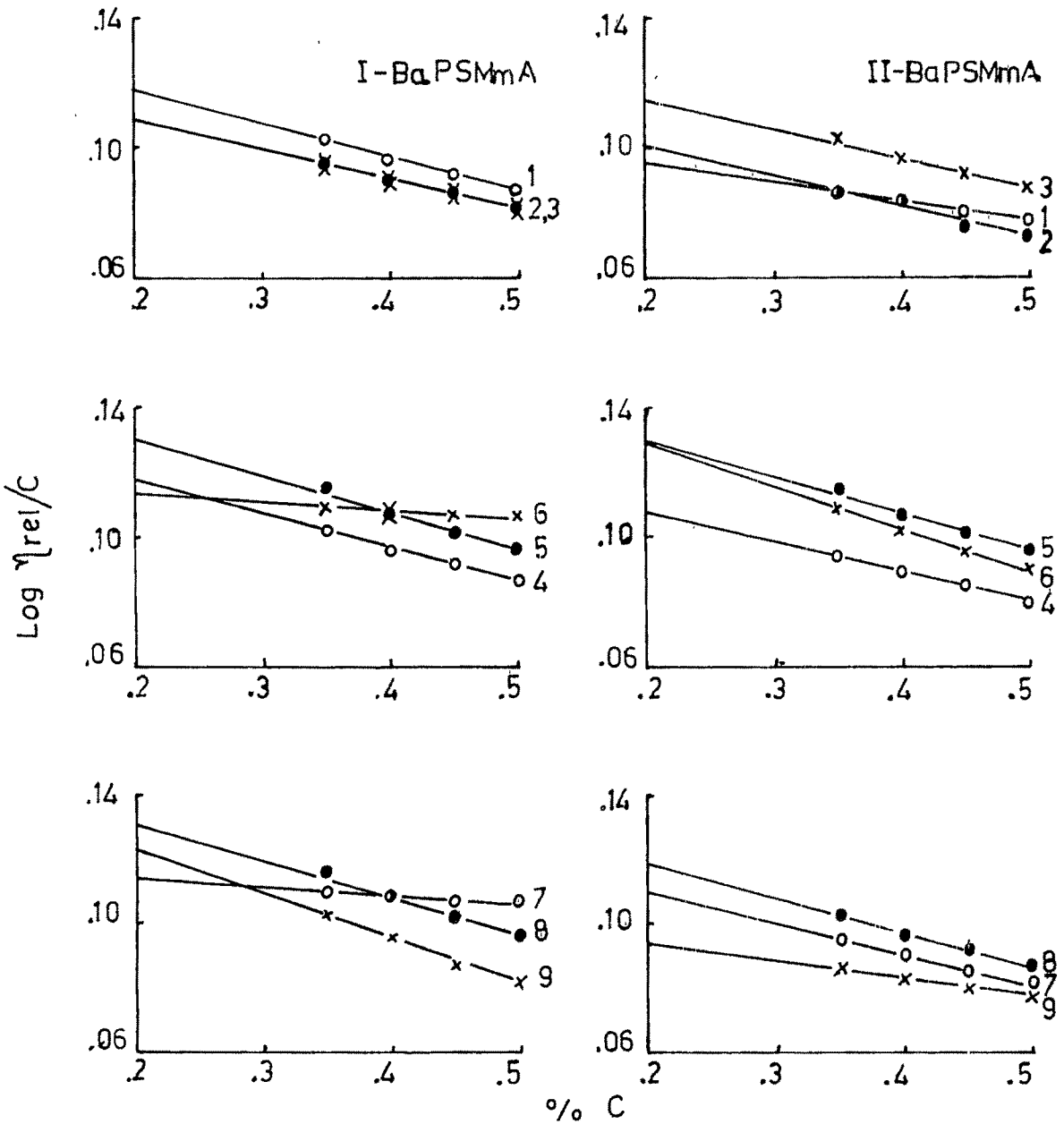


fig. III.105. Plot of $\text{Log } \eta_{rel}/C$ vs $\% C$
for the sets of BaPSMmA

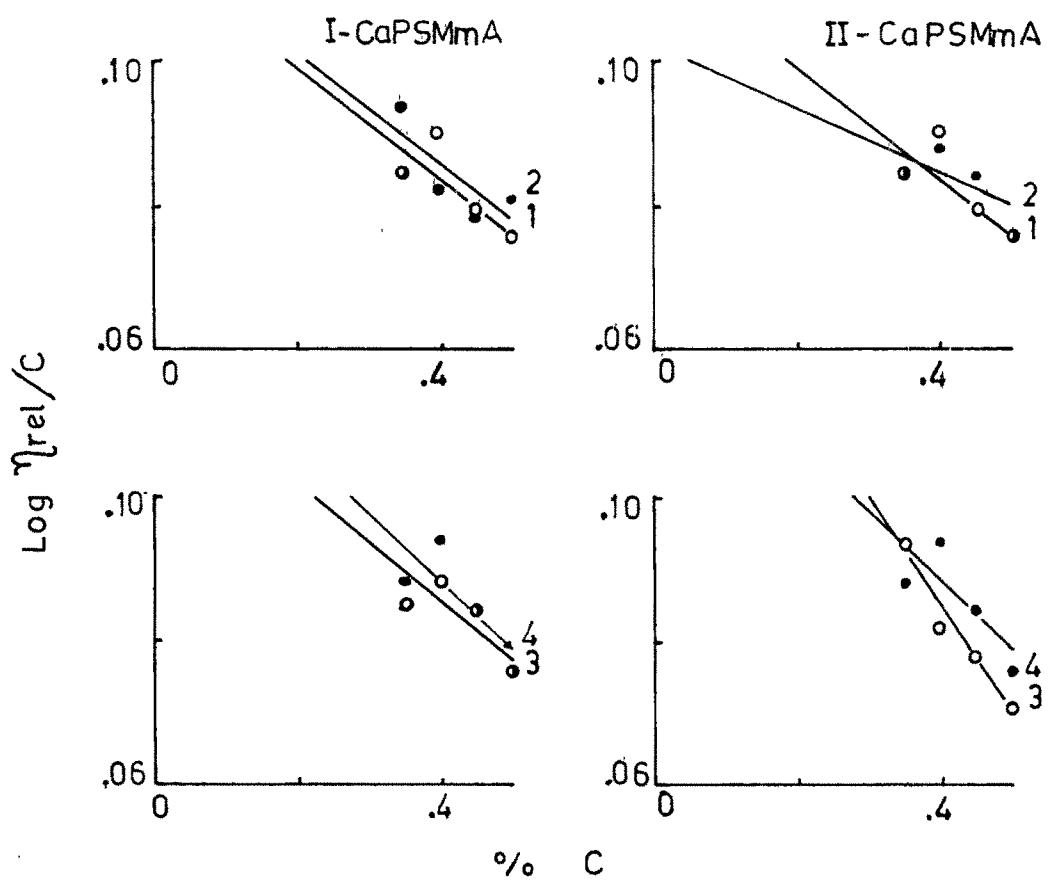


fig.III.106. Plot of $\text{Log } \eta_{\text{rel}}/C$ vs % C
for CaPSMmA sets

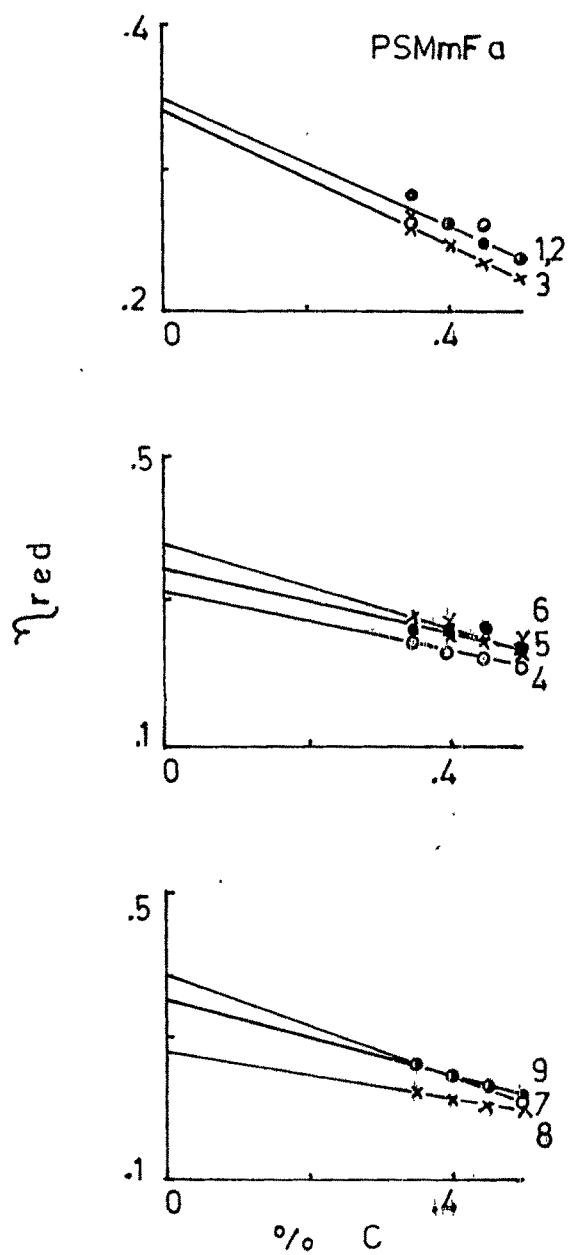


fig.III.107 Plot of η_{red} vs % C
for PSMmFa (H form)

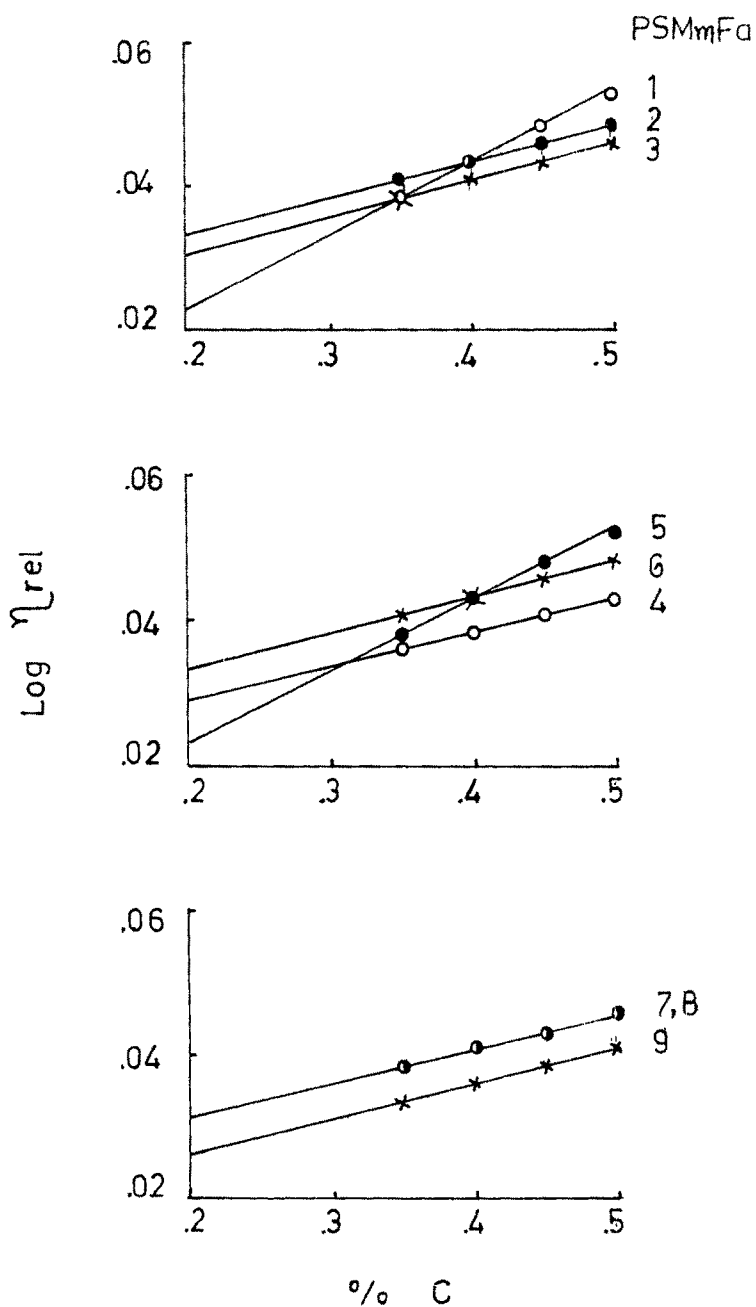


fig. III. 108 Plot of $\text{Log } \eta_{\text{rel}}$ vs $\% \text{ C}$
for the set of PSMmFa (H form)

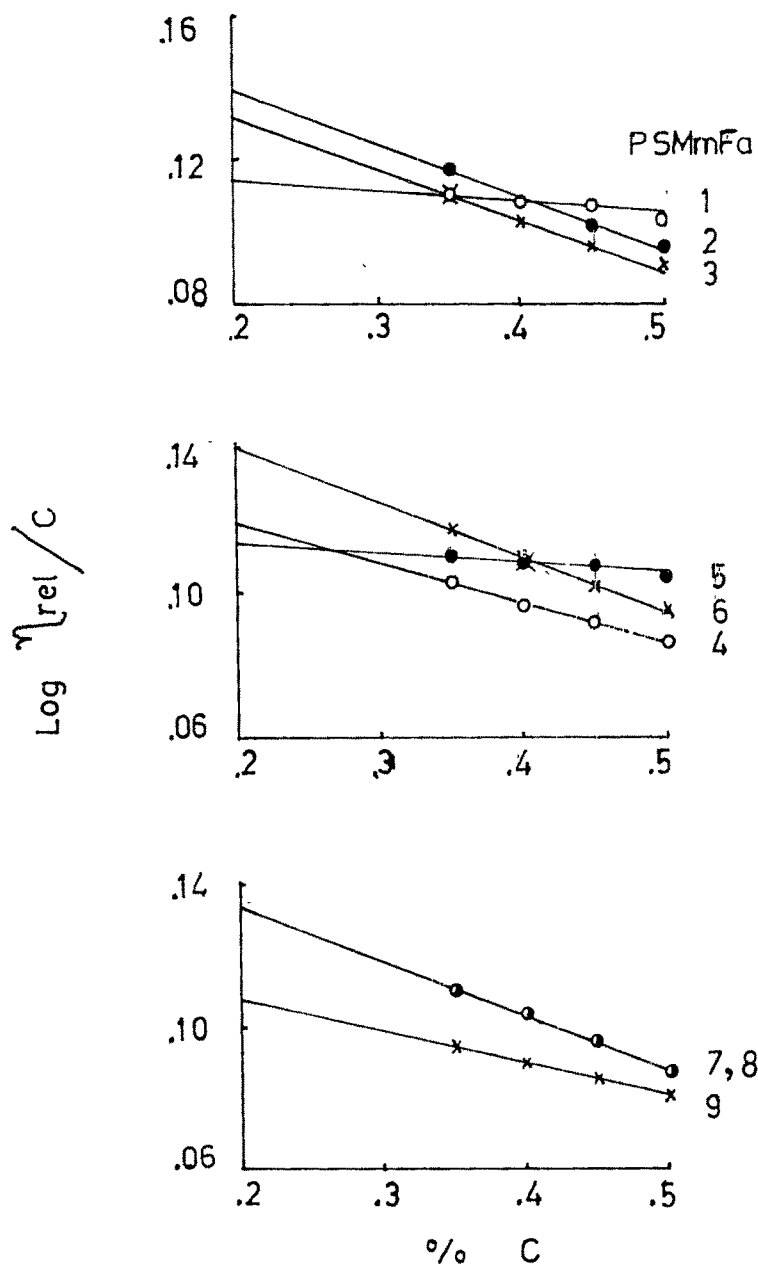


fig. III.109. Plot of $\text{Log } \eta_{\text{rel}}/C$ vs $\% C$
for the set of PSMmFa (H form)

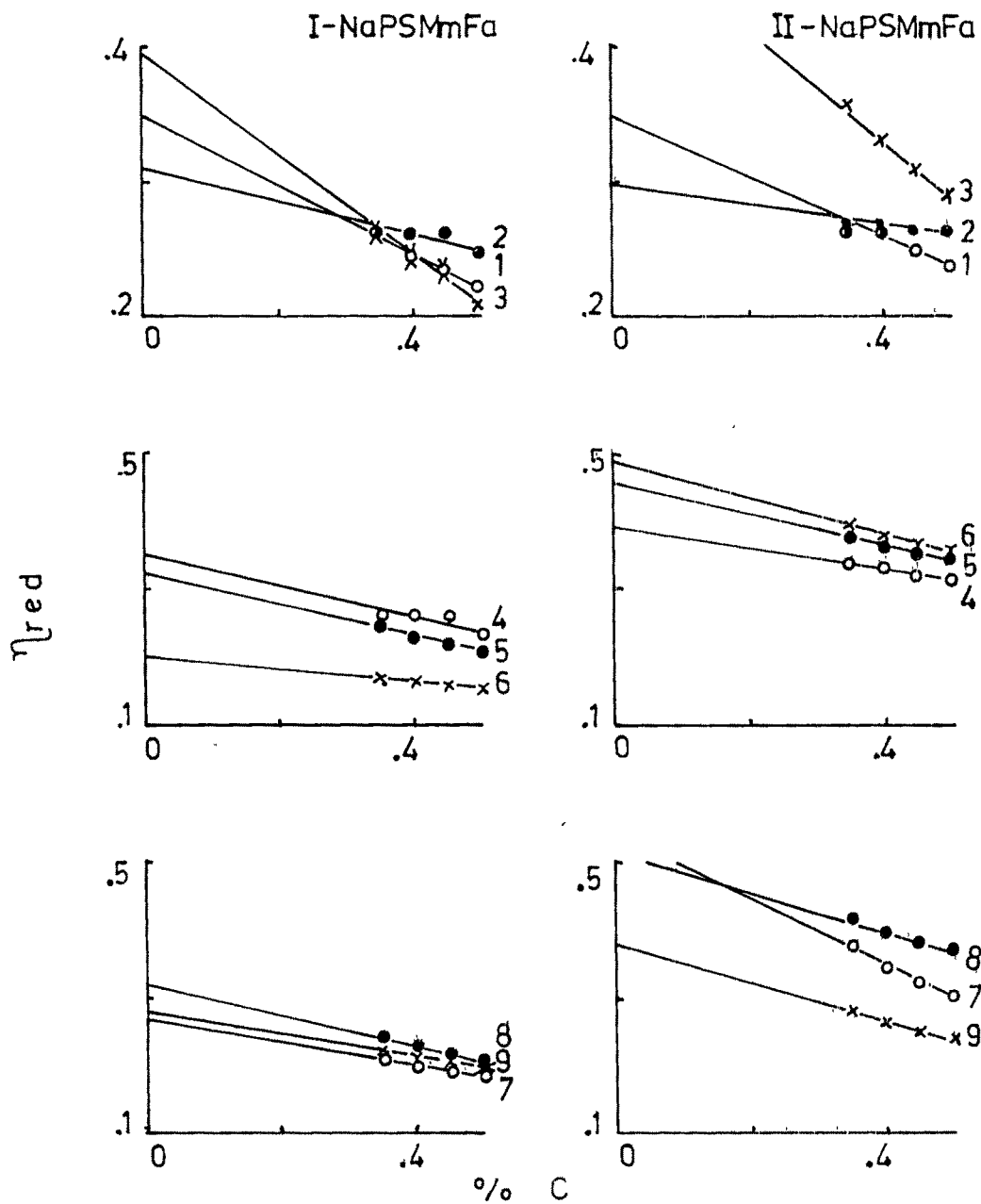


fig.III.110 Plot of η_{red} vs % C
for NaPSMmFa sets

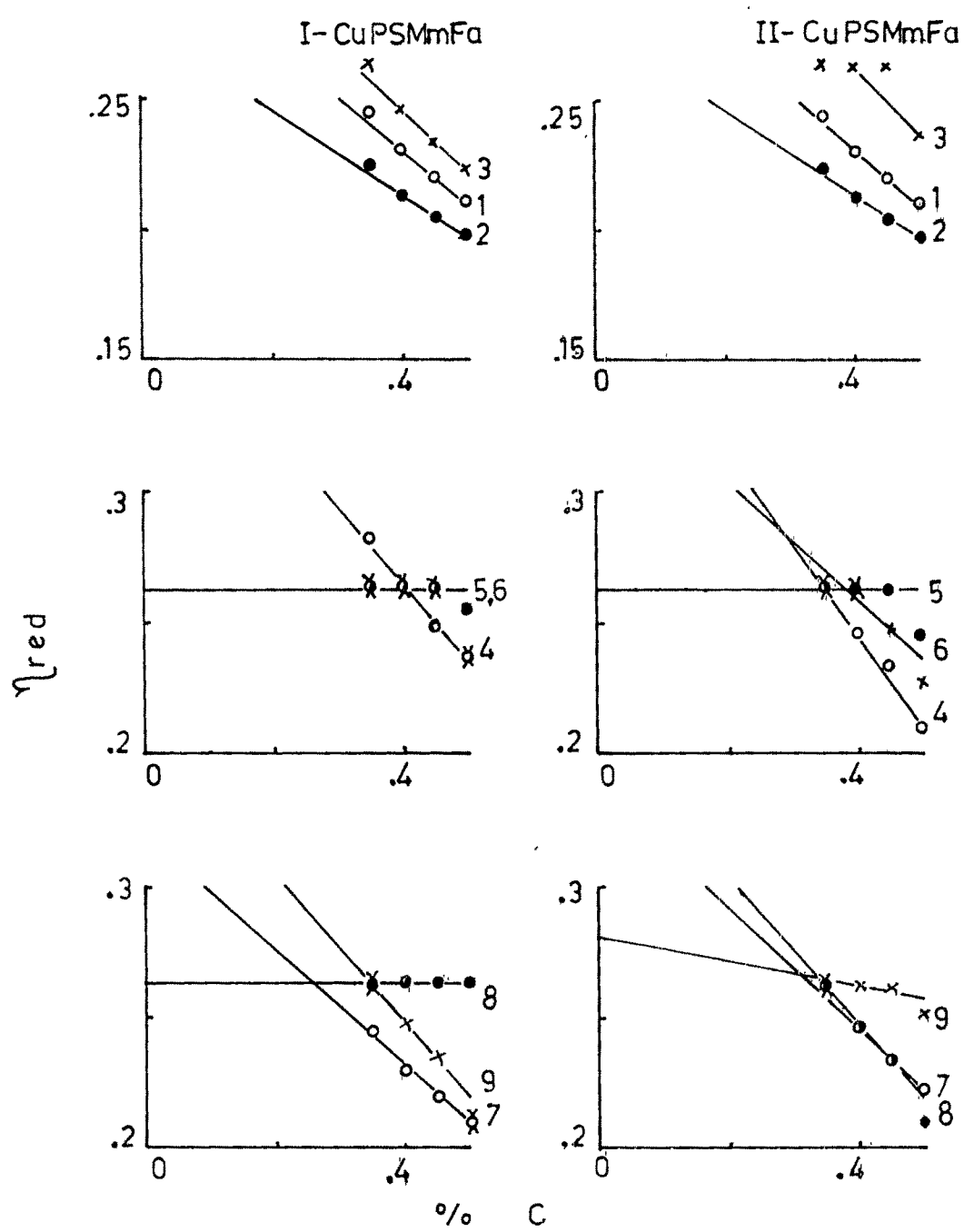


fig.III.111 Plot of η_{red} vs % C
for CuPSMmFa sets

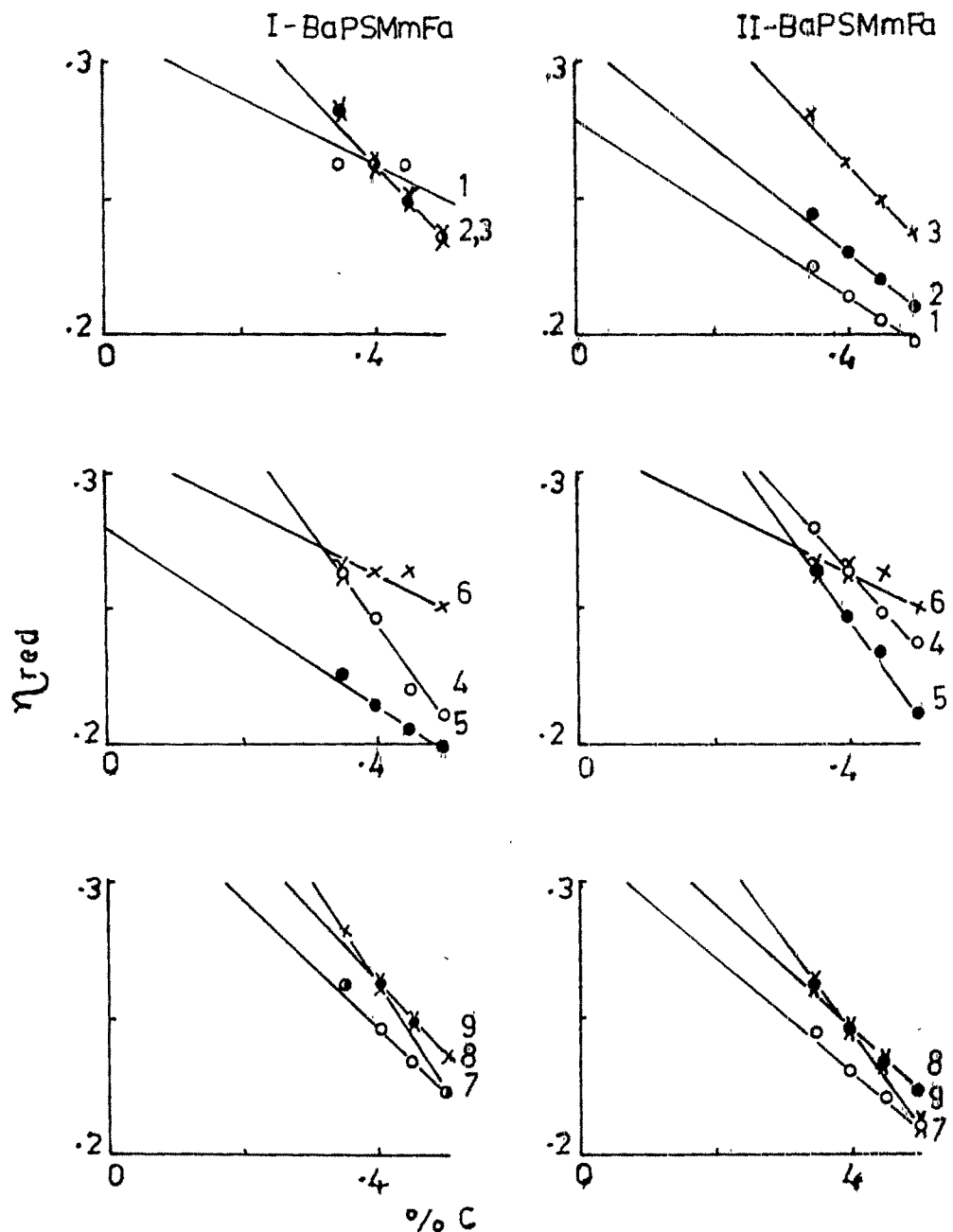


fig.III.113. Plot of η_{red} vs % C for BaPSMmFa sets

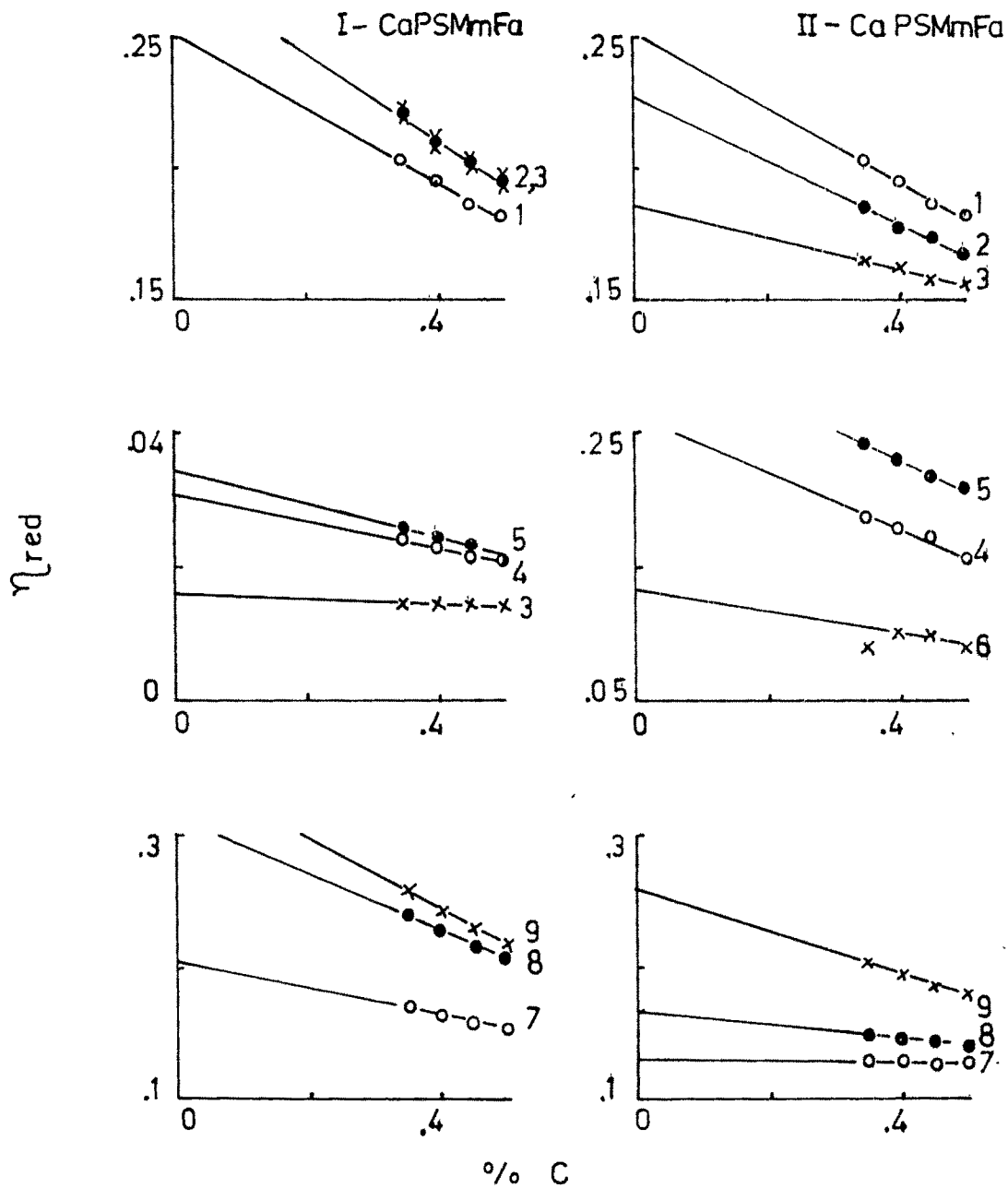


fig. III.114 Plot of η_{red} vs % C for CaPSMmFa sets

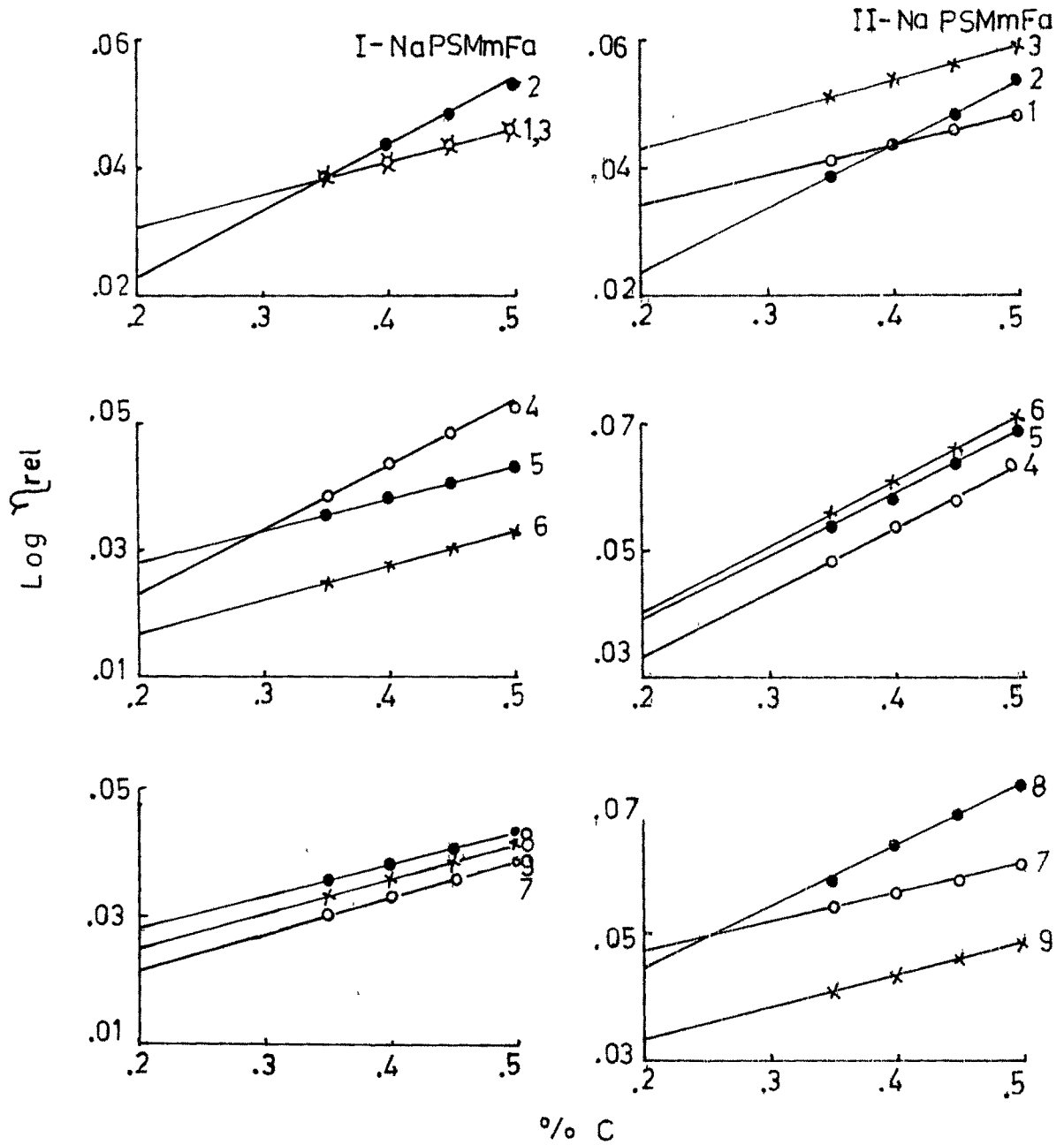


fig. III.115. Plot of $\text{Log } \eta_{\text{rel}}$ vs $\% C$
for the sets of NaPSMmFa

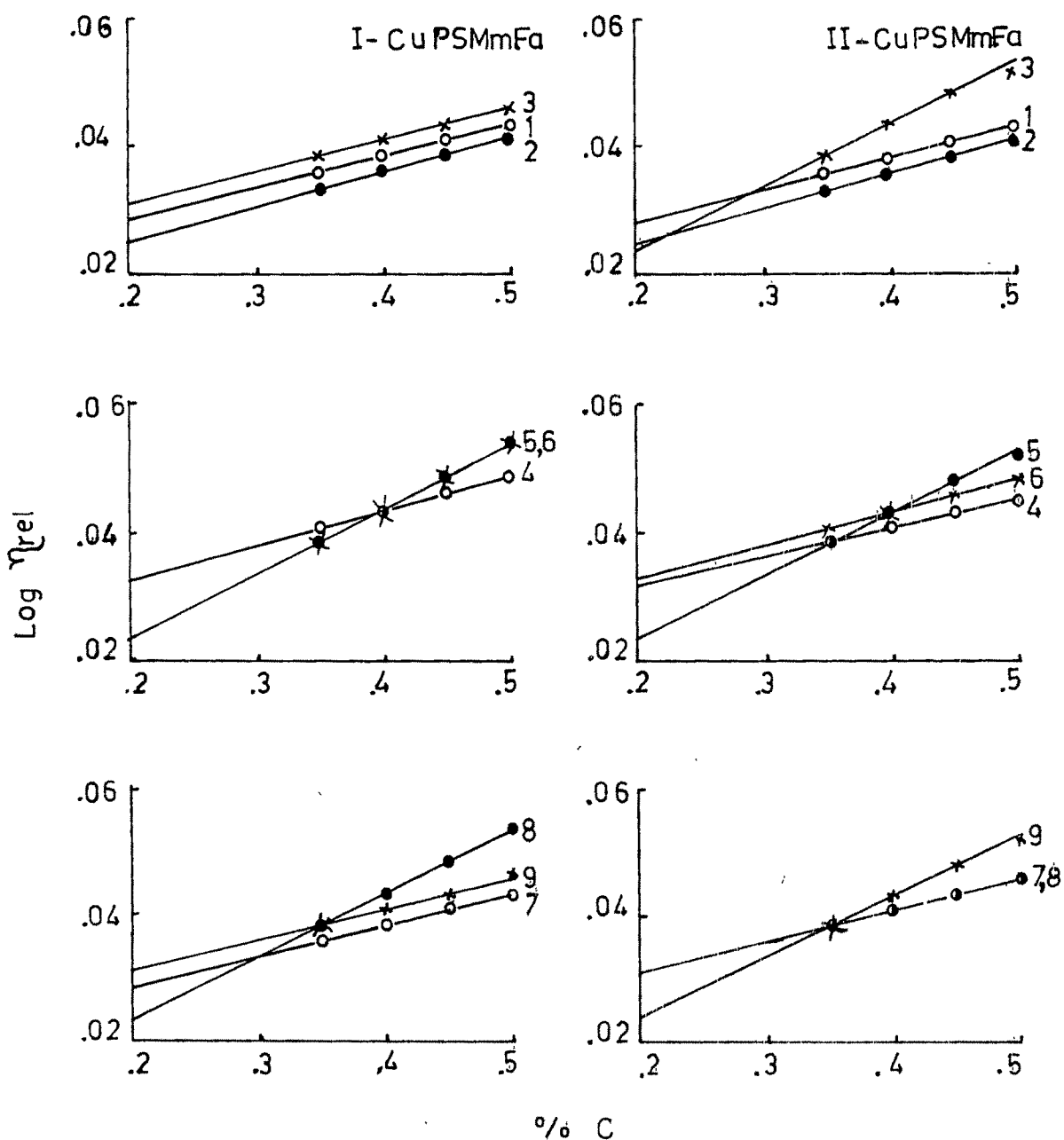


fig.III.116 Plot of $\text{Log } \eta_{\text{rel}}$ vs % C
for the sets of CuPSMmFa

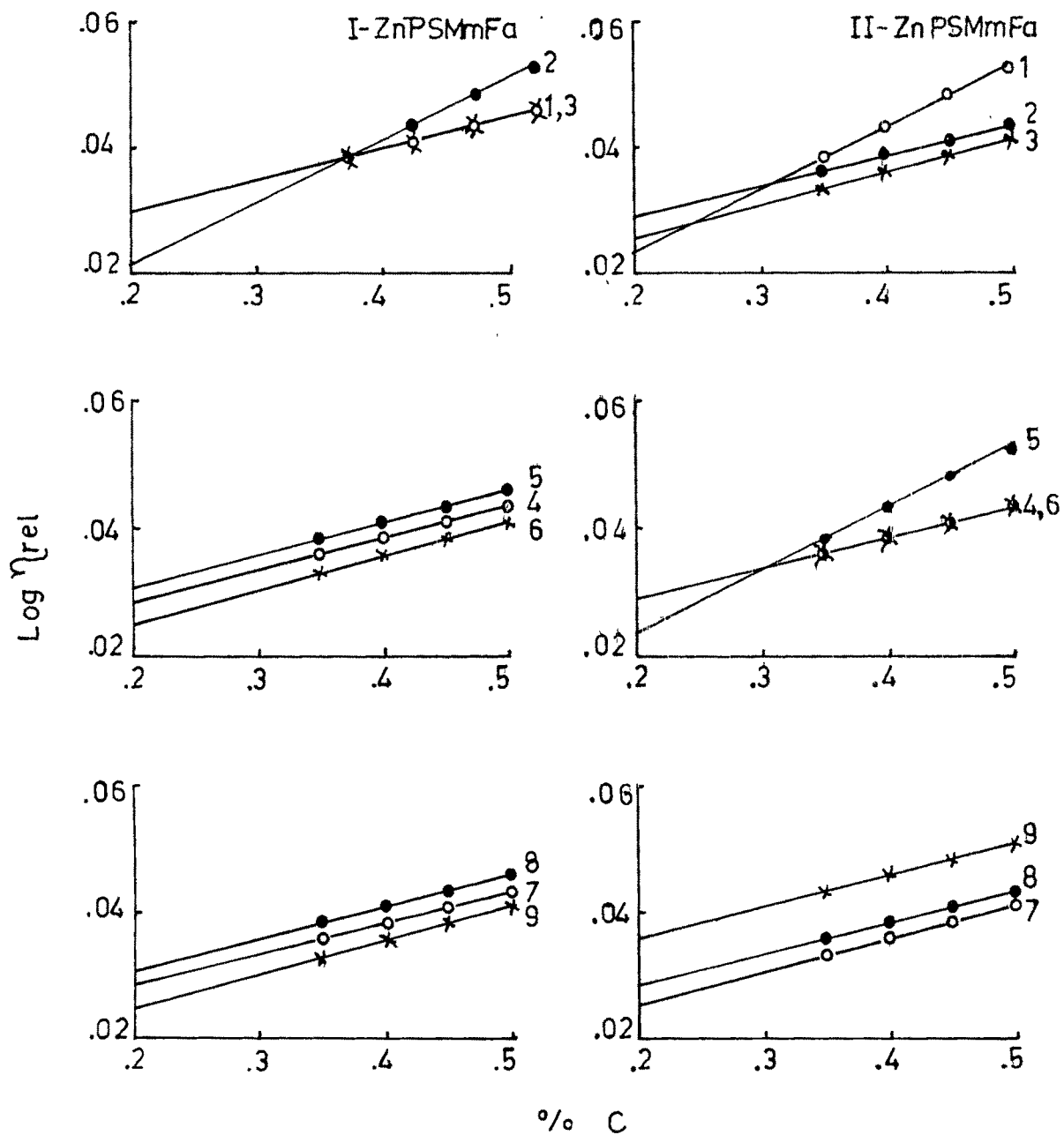


fig.III.117. Plot of $\text{Log } \eta_{\text{rel}}$ vs $\% \text{ C}$
for the sets of ZnPSMmFa

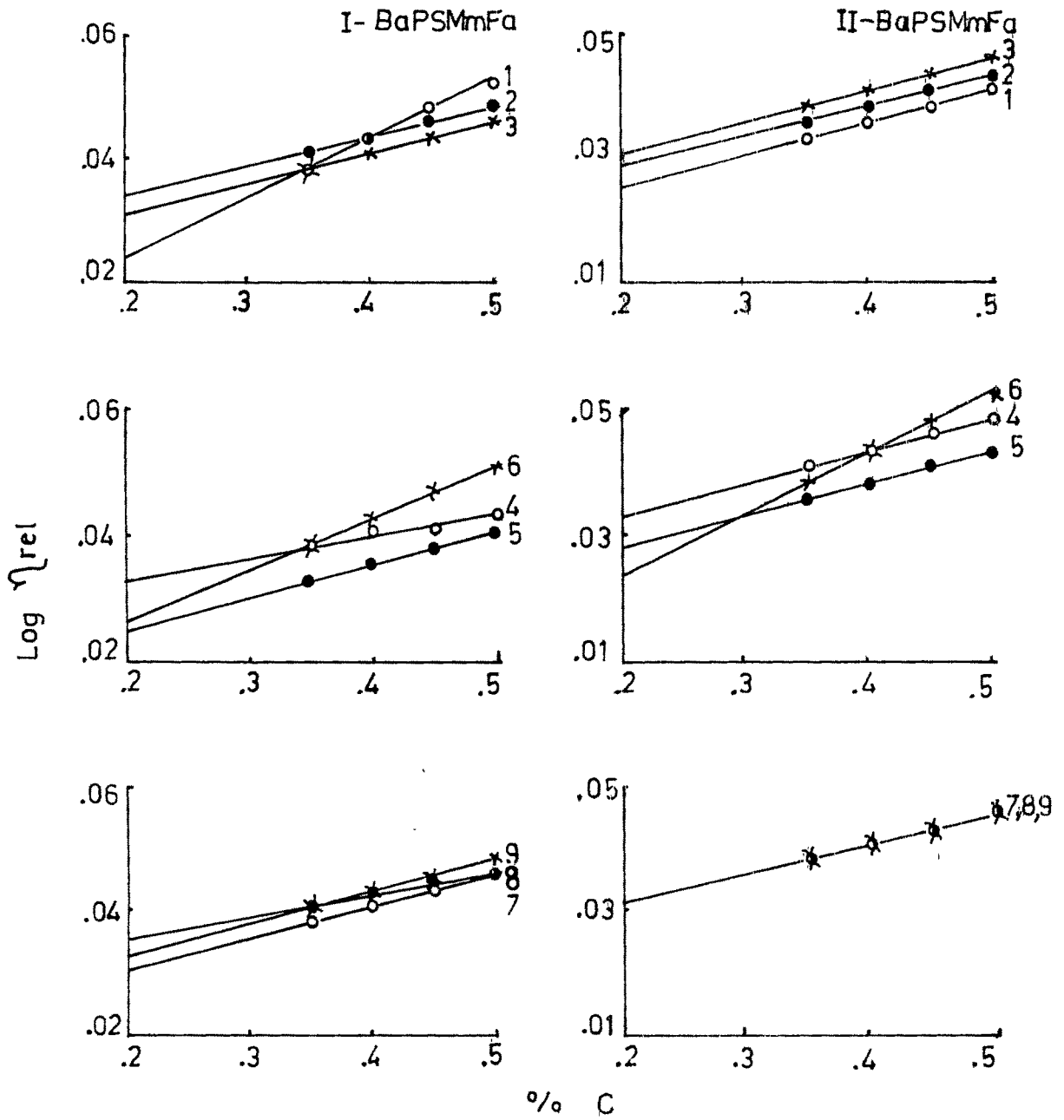


fig.III.118 Plot of $\text{Log } \eta_{\text{rel}}$ vs $\% \text{ C}$
for the sets of BaPSMmFa

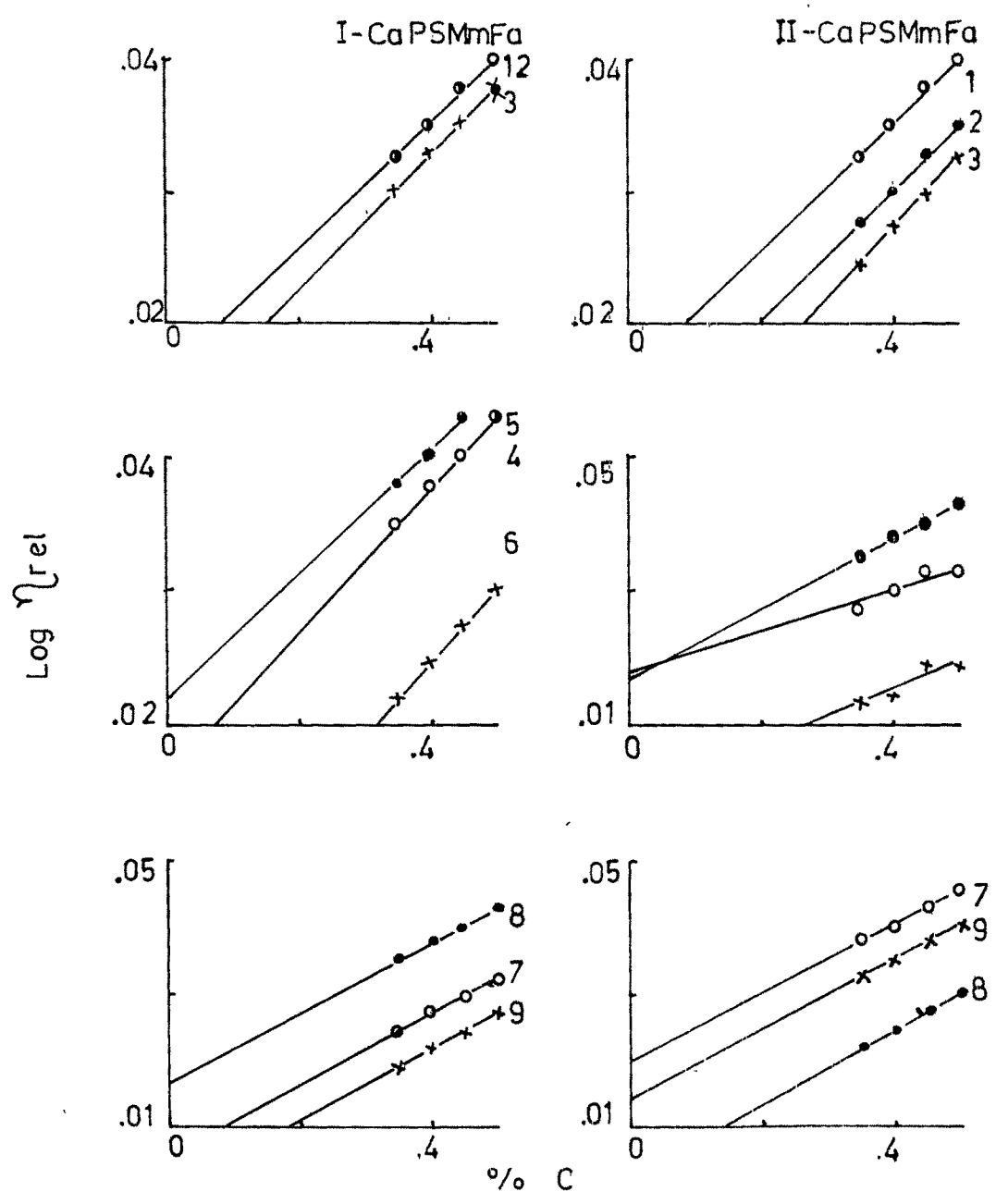


fig.III,119 Plot of $\text{Log } \eta_{\text{rel}}$ vs $\% \text{ C}$
for CaPSMmFa sets

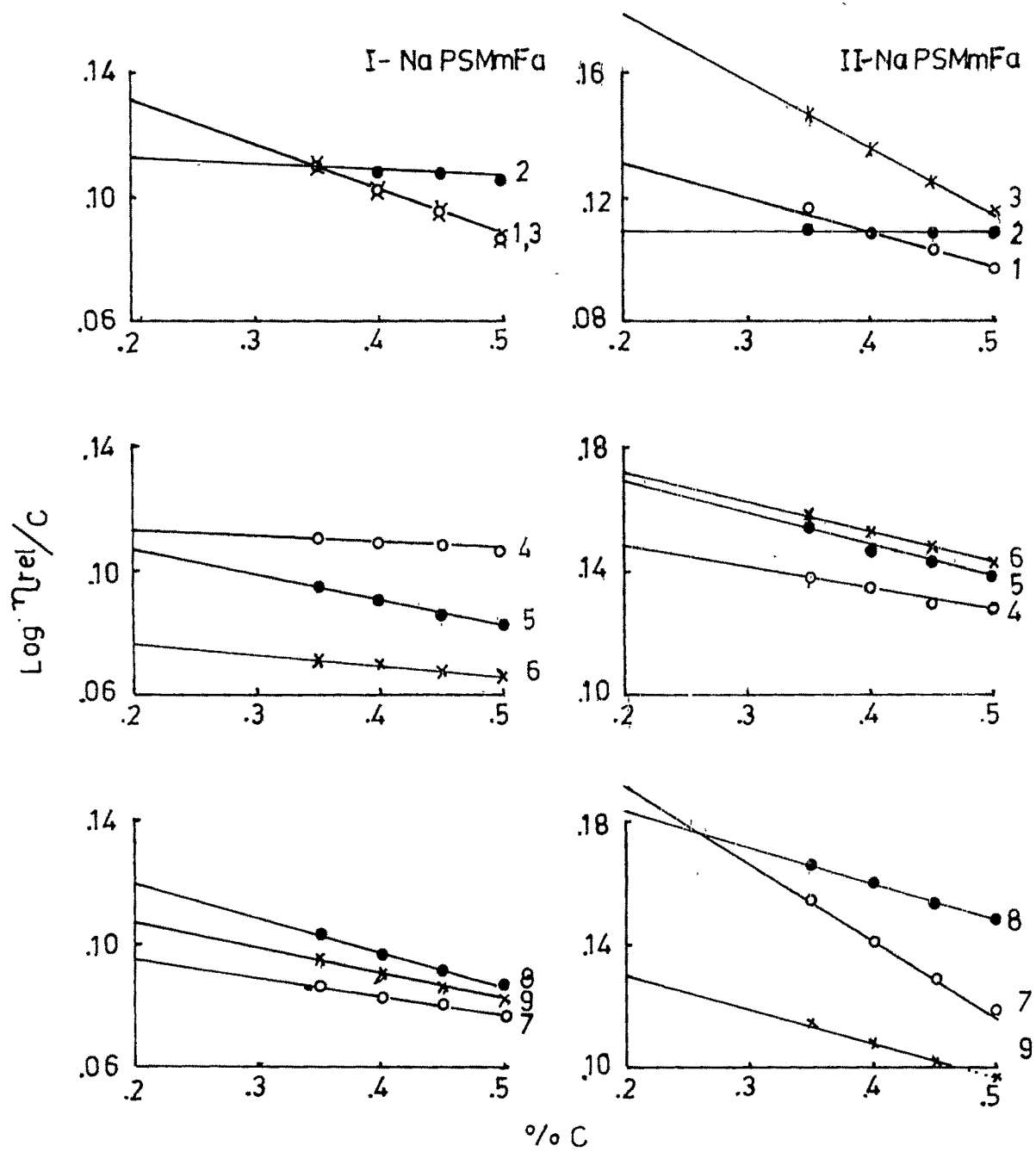


fig.III.120. Plot of $\text{Log } \eta_{rel}/C$ vs $\% C$
for the sets of NaPSMmFa

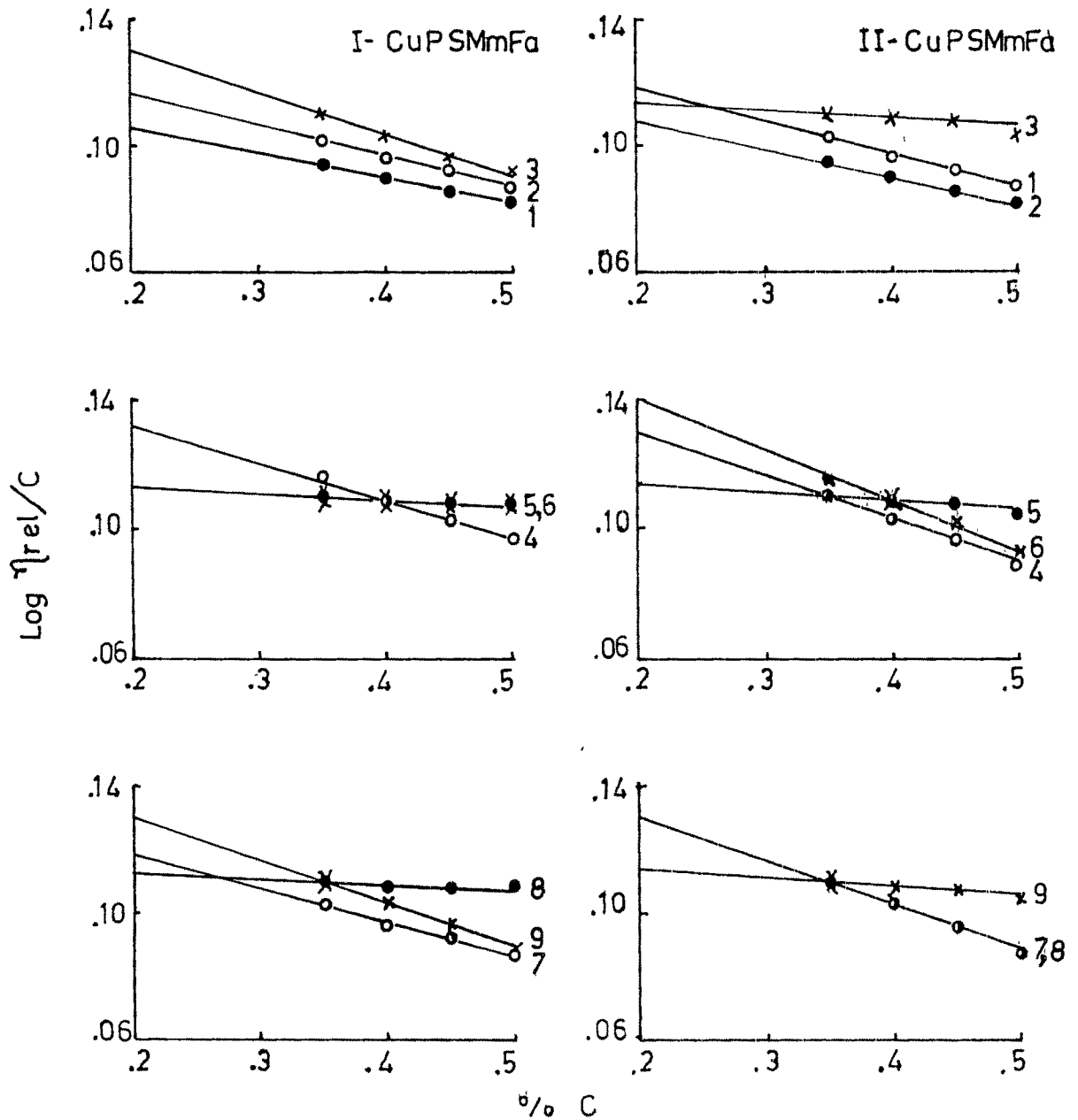


fig.III.121, Plot of $\text{Log } \eta_{rel}/C$ vs % C

for the sets of CuPSMmFa

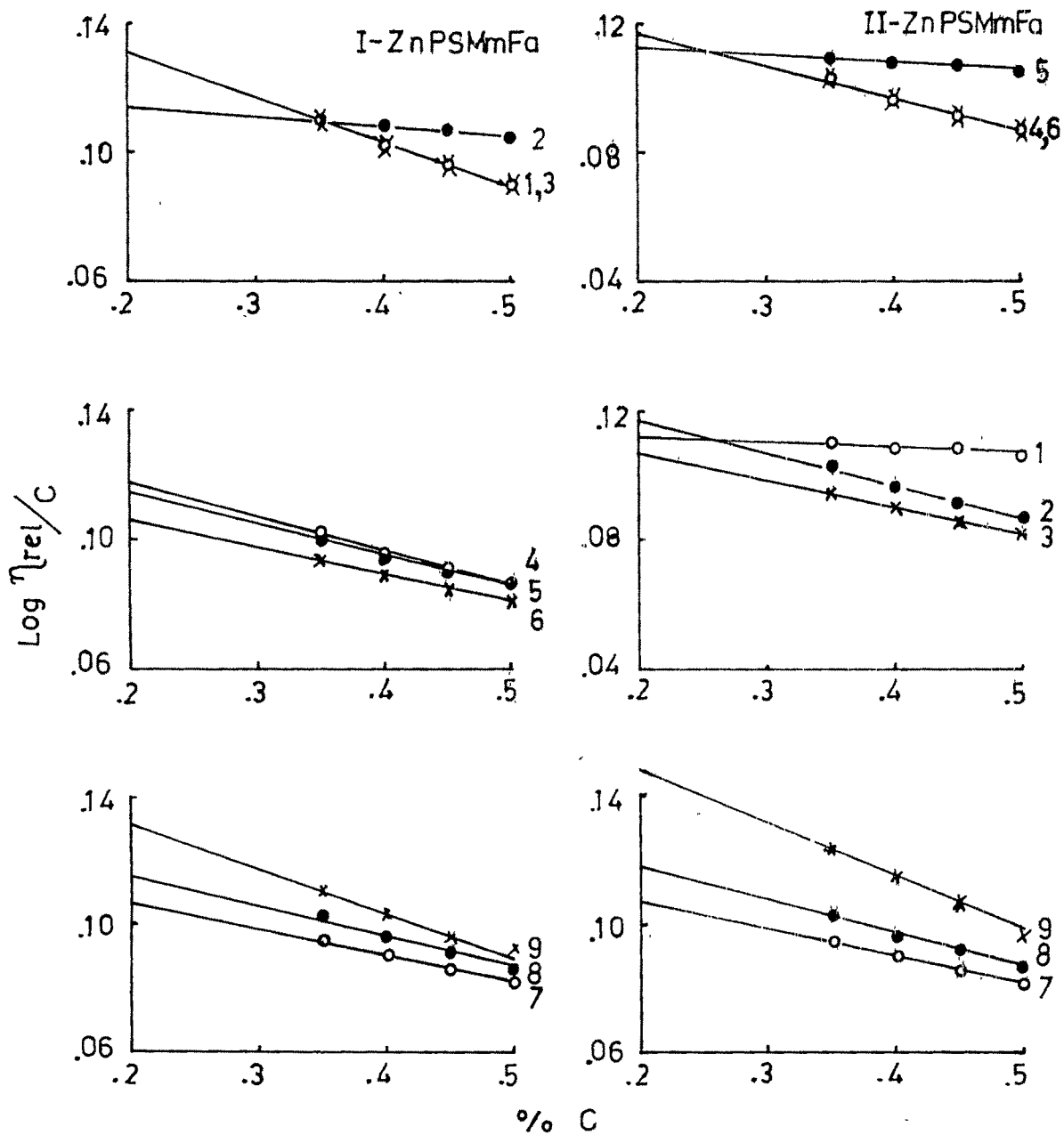


fig.III.122. Plot of $\text{Log } \eta_{\text{rel}}/C$ vs $\% C$
for the sets of ZnPSMmFa

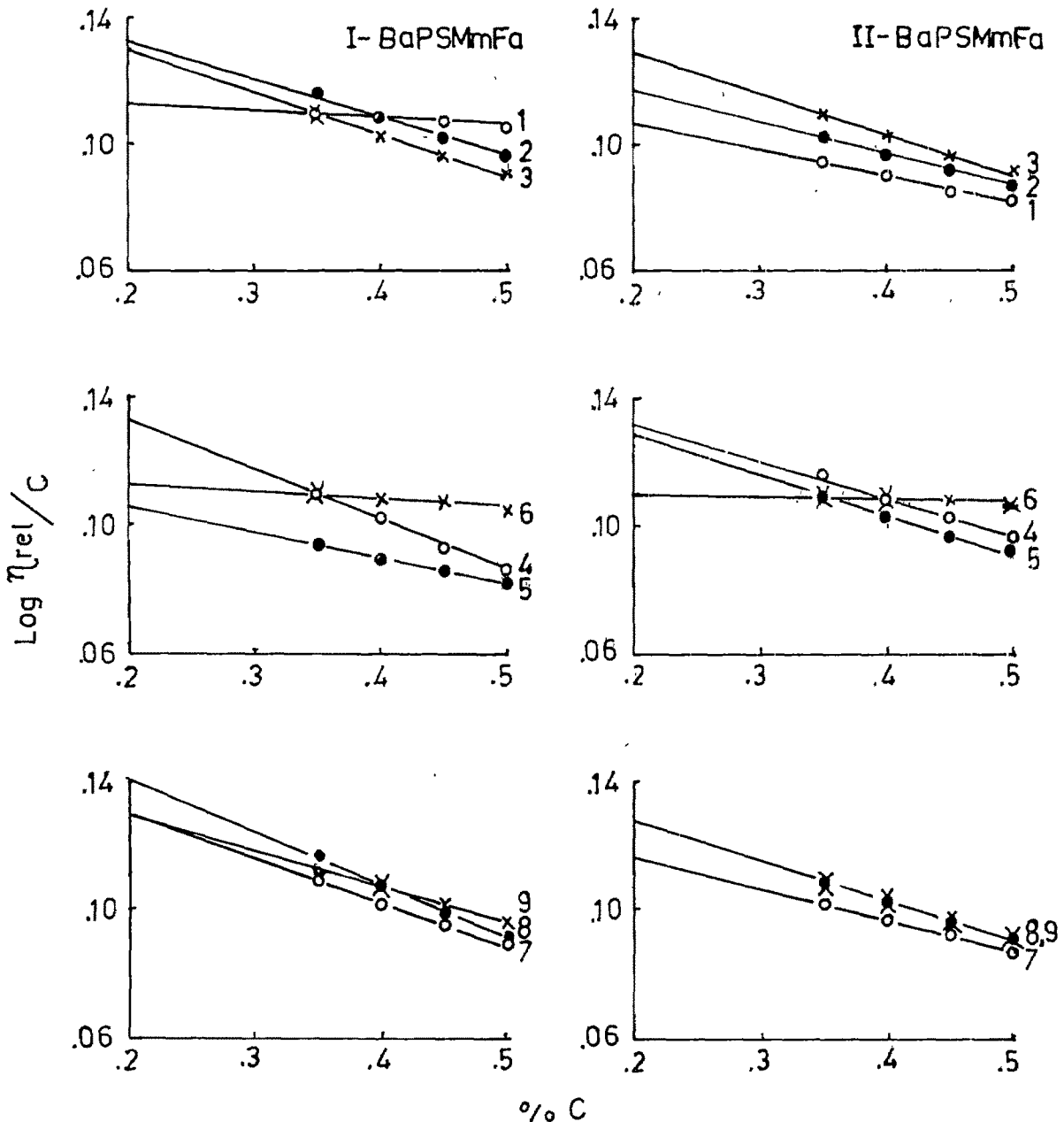


fig.III.123. Plot of $\text{Log } \eta_{\text{rel}}/C$ vs $\% C$
for the sets of BaPSMmFa

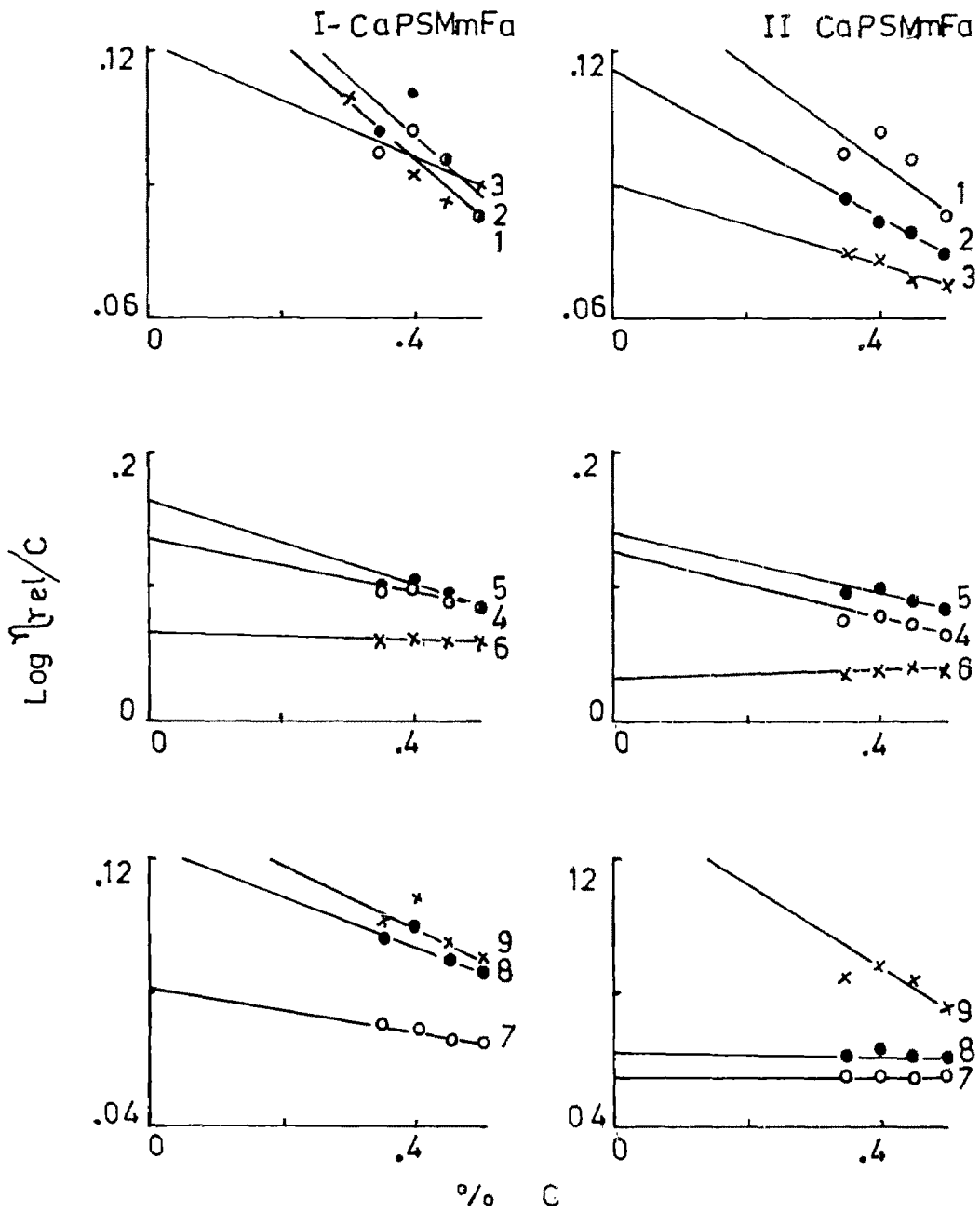


fig.III.124 Plot of $\text{Log } \eta_{\text{rel}}/C$ vs $\% C$ for CaPSMmFa sets

124 for PSMmFa. The values of $[\eta]$ lie in the range of 0.13 to 0.55 for PSMmFa and of 0.25 to 0.51 for PSMmA. The values of $[\eta']$ lie in the range of 0.00 to 0.04 for PSMmFa and of 0.01 to 0.03 for PSMmA. The values of $[\eta'']$ lie in the range of 0.05 to 0.24 for PSMmFa and 0.10 to 0.21 for PSMmA. Thus the values increase in order

$$[\eta'] < [\eta''] < [\eta]$$

The slopes of the curves are negative for Huggins plots and for Kraemer plots and positive for Martin plots. From the slopes and intercepts, the values of constants k' , k'' and k''' are calculated. (tables III. 6 and 7). The values of k' and k''' vary over a small range while the values of k'' vary over a very wide range.

An attempt has been made to calculate $\text{Log slope}/2 \text{ Log intercept}$ from Martin plots on the assumption that $\text{Log slope} = 2 \text{ log intercept}$. It is observed, however, that the value varies from (i) 0.18 to 0.40 for H form, (ii) 0.18 to 0.47 for Na form, (iii) 0.18 to 0.47 for Cu form, (iv) 0.20 to 0.41 for Zn form and (v) 0.21 to 0.47 for Ba form of PSMmFa. The average value can be suggested as 0.32. Thus the Martin equation can be better represented as

$$\text{Log } \eta_{\text{rel}} = [\eta'] + k'' [\eta']^a$$

Table III.6

No	Product	constant		
		k'	k''	k'''
1	PSMmFa-1	- 1.5	2600.0	- 2.1
2	PSMmFa-2	- 2.2	94.5	- 5.1
3	PSMmFa-3	- 2.2	131.6	- 5.5
4	PSMmFa-4	- 2.1	121.6	- 5.6
5	PSMmFa-5	- 0.1	1111.1	- 1.9
6	PSMmFa-6	- 2.1	174.3	- 5.4
7	PSMmFa-7	- 2.5	96.1	- 6.0
8	PSMmFa-8	- 2.0	96.1	- 6.0
9	PSMmFa-9	- 2.3	185.9	- 5.8

Table III.7

No	Product	constant		
		k'	k''	k'''
1	PSMmA-1	- 2.1	184.4	- 5.1
2	PSMmA-2	- 1.9	99.4	- 5.3
3	PSMmA-3	- 2.3	130.0	- 5.1
4	PSMmA-4	- 1.9	130.0	- 5.1
5	PSMmA-5	- 2.7	103.0	- 5.2
6	PSMmA-6	- 0.1	1111.1	- 0.1
7	PSMmA-7	- 2.0	81.3	- 1.0
8	PSMmA-8	- 2.1	154.0	- 5.1
9	PSMmA-9	- 2.1	188.6	- 5.4

III.8 General

The last decade has witnessed an almost explosive growth of research into the properties of ion-containing polymers (140). Some areas such as solid state properties have only recently been receiving extensive attention. Some other areas such as selective plasticization and non-aqueous solution properties are in their infancy.

The primary reason for the great interest in these materials lies in the major changes which can be achieved in the properties of polymers by introducing ions. Among the dramatic effects that have been observed are the changes in glass transition temperatures and in viscosities. Magnesium methacrylate incorporated into polyethylene raises T_g by approximately $10^\circ\text{C}/\text{mole } \%$ of ionic monomer (141) when approximately 13 mole % of LiClO_4 is introduced into low molecular weight propylene oxide, the viscosity rises by a factor of 10^4 (142). An unusual dilute solution property of ion-containing polymers is illustrated by sodium sulphonated polystyrene whose viscosity in xylene solution containing hexanol can increase with temperature (143).

The partially neutralized synthetic styrene-acid copolymers possess weak ionic network character. From a structural point of view, the effect of the incorporation of ions into polymers on their bulk properties can be attributed to the aggregation of ions. The ion pairs form in a medium

of non-ionic hydrocarbon portion of the polymer and of low dielectric constant ; these pairs can coalesce into even larger aggregates, say quartets, sextets and octets. Small angle X-ray (SAXS) and neutron (SANS) scattering provided evidence for ion aggregation in ion-containing copolymers of styrene with acrylic acid or methacrylic acid (144).

The models

In a dilute solution, the long flexible macromolecule curls up into a coil. There are two points of view on the behaviour of such a coil during flow.

According to the free-draining coil model, the coil is regarded as a formation through which the solvent molecules can pass freely. According to the impermeable coil model, the macromolecule in coil retains a definite amount of solvent enclosed by it and moves together with this solvent. Such a coil is a spherical particle impermeable to the rest of the solvents.

The shape of an acidic polymer can easily be changed by changing the degree of dissociation. A poly carboxylic acid is weakly dissociated in solution, contains a small number of charges along their chains and therefore their chains curl up into coils. Na salts of the poly acid

dissociate well, so that a large number of negative charges form along their chains at fairly close spacing and electrostatic repulsion arises between these charges which tends to straighten the chain. Ca and Ba ions behave similarly in their salts. Transition metal ions like Cu and Zn differ from alkali metal ions in that they may involve coordination covalencies.

The ratio $[\eta]_{\text{metal}} / [\eta]_{\text{H}}$ can represent the degree of uncoiling of the chains. It has been observed that the values of the ratio depends not only on the nature of metal ion and its valency and coordination behaviour, but also on the nature and mole fraction of acid in the copolymer, and the degree of neutralization of the acid. Cluster formation of the ions is favoured by the increase in ionic charges on the chain.

An empirical equation

$$\frac{\eta_{\text{sp}}}{c \cdot \eta_{\text{rel}}} = [\eta] - k [\eta] \left(\frac{\eta_{\text{sp}}}{\eta_{\text{rel}}} \right)$$

suggested by Chen (145) has been considered for these salts but no generalization can be made. Similarly the equation relating viscosity exponentially with the degree of neutralization was also studied, but good fit of the data was not observed.

The solvent used has a high dielectric constant and its polar nature will introduce polymer-solvent interactions. The effect of this has not been evaluated.

Numerous calculations were made regarding the slopes and intercepts and the values of $[\eta]$ and k' , k'' or k''' for these salts, of copolymers and tercopolymers. These data have been used for generalizations but not presented in tables.

Martin equation can be better expressed by the relation

$$\text{Log } \eta_{\text{rel}} = [\eta'] + k'' [\eta]^a C$$

where 'a' and k'' are constants.

Generally, k''' is negative and smaller in magnitude than k' . Hence $(\text{Log } \eta_{\text{rel}})/C$ changes less rapidly with % C than does η_{red} . For this reason extrapolation of $(\text{Log } \eta_{\text{rel}})/C$ can be preferred over extrapolation of η_{red} .